UNIVERSIDADE DO VALE DO TAQUARI

PROGRAMA DE PÓS-GRADUAÇÃO *STRICTO SENSU*

DOUTORADO EM BIOTECNOLOGIA

PROTEÔMICA DO EPIDÍDIMO SUÍNO: USO DO MODELO IMUNOCASTRADO NA IDENTIFICAÇÃO DE MARCADORES MOLECULARES PARA A QUALIDADE SEMINAL

Ana Paula Binato de Souza

Lajeado

Ana Paula Binato de Souza

PROTEÔMICA DO EPIDÍDIMO SUÍNO: USO DO MODELO IMUNOCASTRADO NA IDENTIFICAÇÃO DE MARCADORES MOLECULARES PARA A QUALIDADE SEMINAL

Tese apresentada ao Programa de Pós-Graduação em Biotecnologia, da Universidade do Vale do Taquari, como exigência para obtenção do grau de Doutora em Biotecnologia.

Orientador:

Prof. Dr. Ivan Cunha Bustamante Filho

Lajeado

UNIVERSIDADE DO VALE DO TAQUARI
PROGRAMA DE PÓS-GRADUAÇÃO EM BIOTECNOLOGIA

ATA 007/2020 – DEFESA DE TESE

A tese da doutoranda **ANA PAULA BINATO DE SOUZA** sob título "PROTEÔMICA DO EPIDÍDIMO SUÍNO: USO DO MODELO IMUNOCASTRADO NA IDENTIFICAÇÃO DE MARCADORES MOLECULARES PARA A QUALIDADE SEMINAL", foi defendida em sessão pública no dia 04 de setembro de 2020, às 13h30min, tendo sido considerada **APROVADA** pela Banca Examinadora, abaixo assinada, conforme pareceres individuais anexos, parte integrante desta ata, estando apta a receber o diploma de Doutora em Biotecnologia. Fica consignada a participação dos membros Prof. Dr. Ivan Cunha Bustamante Filho; Profa. Dra. Verônica Contini; Prof. Dr. Arlindo de Alencar Araripe Noronha Moura e Prof. Dr. Carlos Augusto Rigon Rossi e da doutoranda Ana Paula Binato de Souza por meio de videoconferência - medida excepcional adotada em virtude da Covid-19 (Novo Coronavírus).

Banca Examinadora		
Membros		**Assinatura**
Orientador	Prof. Dr. Ivan Cunha Bustamante Filho	(videoconferência)
2° Membro	Profa. Dra. Verônica Contini	(videoconferência)
3° Membro	Prof. Dr. Arlindo de Alencar Araripe Noronha Moura	(videoconferência)
4° Membro	Prof. Dr. Carlos Augusto Rigon Rossi	(videoconferência)

Obs.: O aluno deverá encaminhar no prazo de 30 (trinta) dias, a contar da data da defesa, o protocolo de Colação de Grau, conforme normas definidas pelo PPGBiotec.

Ciente do(a) doutorando(a):	(videoconferência)

Jenifer Tais de Souza
Secretária de Pós-Graduação *Stricto Sensu*

AGRADECIMENTOS

Obrigada Deus pela proteção em todos os dias que me fizeram chegar aqui. Com muito carinho agradeço as pessoas que conheci nesta trajetória de Univates, colegas de laboratório, aula, corredor, do sagrado café. Muitos desses momentos foram marcados por pessoas especiais ao meu lado, por isso agradeço imensamente aos amigos que conquistei, que me apoiaram em muito momentos, tirando dúvidas e amenizando as dificuldades. Aos colegas do grupo de pesquisa em reprodução animal, aprendi com vocês desde o primeiro dia de laboratório, não seria tão bom passar dias na bancada se não fosse por vocês, tornando agradável a nossa convivência. Agradeço ao programa de Pós Graduação em Biotecnologia, aos professores que disponibilizaram seu conhecimento e contribuíram para minha formação. Meu agradecimento especial àquele que me orientou. Ivan, gratidão por tudo que me ensinou, a disponibilidade em todos os momentos que precisei, as revisões de texto, artigo, apresentações, em fim todo teu apoio como orientador foi essencial. Muito além disto é um grande amigo, sempre ouviu minhas angústias e aconselhou em difíceis momentos com a maternidade. Obrigada por todo teu apoio.

Aos pesquisadores Lucelia Santi e Walter Beys da Silva que disponibilizaram seu conhecimento em análises proteômicas e contribuições desde o projeto deste trabalho.

Agradeço a minha família, pela vida, cuidados e incentivo em todos os momentos. Meu esposo Mairo, sem palavras por todo teu apoio e companheirismo, apesar de distante um do outro me deu toda a motivação para continuar. Oportunizou-me ser mãe da Joana, por ela cheguei até aqui.

Muito Obrigada.

RESUMO: O epidídimo é um órgão especializado responsável pela maturação de células espermáticas pós-testiculares, dando a ele motilidade e capacidade de fertilização. A passagem dos espermatozoides pelo epitélio epididimal promove interações entre as secreções ao longo das três principais regiões cabeça, corpo e cauda. Cada região tem um perfil proteico garantindo diferentes funções em cada etapa da maturação e armazenamento epididimário. Entretanto este processo é dependente de diversos fatores contribuem na qualidade seminal e estes podem estar relacionados ao sistema androgênico e condições patológicas de cada individuo. Deficiência androgênica causada por uma desregulação endócrina altera a síntese e secreção de proteínas envolvidas em importantes processos celulares da reprodução. A infertilidade masculina é associada a interrupção do eixo hipotálamo-hipófise-gônadas a secreção de hormônio liberador de gonadotrofinas-GnRH que caracterizam o hipogonadismo secundário. Esta patologia altera o perfil proteíco e permite identificar, utilizando abortagens proteômicas, grande numero de proteínas candidatas a marcadores proteicos de fertilidade. A presente tese tem por objetivo avaliar as alterações proteômicas nos espermatozoides (CESperm) e no fluído da cauda do epidídimo (CEF) de suínos imunizados contra GnRH sendo este um modelo para hipogonadismos secundário. Foram obtidos tecidos reprodutivos de 10 suínos machos reprodutores saudáveis e 10 de animais previamente imunizados contra GnRH Vivax (Pfizer). Espermatozoides foram coletados da cauda do epidídimo por dissecação e lavagem, o fluído foi retirado e centrifugado para remoção de resíduos celulares. Após dosagem de proteína total, pools com as amostras do grupo controle e imunizado foram realizadas utilizando 300ug de proteína cada grupo e realizada proteômica utilizando a técnica de MudPIT, composto de separação dos peptídeos por HPLC Agilent 1100, seguido por identificação dos peptídeos por espectrometria de massa utilizando LTQ Orbitrap XL. Analises de bioinformática foram realizadas para categorizar as proteínas em relação a Gene Ontology, vias metabólicas por KEGG, mapeamento funcional e identificação dos genes que codificam proteínas especificas de cada condição e estratégias de validação dos resultados obtidos na proteômica. Além disso foram analisadas a expressão genica, por qPCR, no testículo e três regiões epididimárias de genes associados a proteínas que foram diferencialmente expressas em espermatozoides e fluído epididimário de ambos os grupos. A imunização com GnRH dobrou o número de proteínas no CEF, com 417 proteínas sendo encontradas exclusivamente em amostras de suínos imunizados com GnRH. O CEF de machos imunizados com GnRH apresentou aumento no número de proteínas relacionadas a processos celulares e metabólicos, com afinidade por compostos orgânicos cíclicos, pequenas moléculas e compostos heterocíclicos, além de alterar o perfil enzimático. O aumento significativo no número de proteínas associadas ao sistema ubiquitina-proteassoma foi identificado no CEF de animais imunizados com GnRH. Em espermatozoides (CESperm) foram identificados 1.322 proteínas, com abundancia de proteínas envolvidas no metabolimo dos espermatozoides (enolase, piruvato desidrogenase), reação do acrossomo e capacitação (oxoprolinase, proteína acrossomal SP-10, diidrolipoil desidrogenase) e interações espermatozoides-oócitos (proteína de ligação à zona pelúcida, zonadesina, molécula de adesão de espermatozoides 1). Além disso, a abundância de proteínas mitocondriais foi severamente afetada, com alterações significativas nas proteínas dos Complexos I e II, bem como na ATPase da cadeia de fosforilação oxidativa. Esses resultados trazem fortes evidências do impacto do hipogonadismo secundário no ambiente epididimário, responsável pela maturação e armazenamento dos espermatozoides antes da ejaculação. Finalmente, as proteínas expressas de forma diferente no CEF e CESperm são candidatos a biomarcadores seminais para distúrbios testículares e epididimários causados por hipogonadismo secundário.

Palavras-chave: epidídimo, fertilidade, hipogonadismo, proteômica.

ABSTRACT: The epididymis is a specialized organ responsible for the maturation of post-testicular sperm cells, giving it motility and fertilization capacity. The passage of sperm through the epididymal epithelium promotes interactions between secretions along the three main head, body and tail regions. Each region has a protein profile guaranteeing different functions at each stage of maturation and epididymal storage. However, this process is dependent on several factors that contribute to seminal quality and these may be related to the androgenic system and pathological conditions of each individual. Androgen deficiency caused by endocrine disruption alters the synthesis and secretion of proteins involved in important reproductive processes. Male infertility is associated with an interruption of the hypothalamic-pituitary-gonadal axis to the secretion of gonadotropin-releasing hormone-GnRH that characterize secondary hypogonadism. This pathology alters the protein profile and allows the identification, using proteomic abortions, of the large number of candidate proteins for protein fertility markers. This study aims to evaluate how proteomic changes in sperm (CESperm) and epididymis tail fluids (CEF) of swine immunized against GnRH are a model for secondary hypogonadism. Reproductive tissues were collected from 10 healthy male breeding pigs and 10 animals previously immunized against GnRH Vivax (Pfizer). Sperm were collected from the tail of the epididymis by dissection and washing, the fluid was removed and centrifuged to remove cell debris. The dosage of total protein, pools with the control and immunized groups were performed using 300ug of protein each group and proteomics was performed using MudPIT technique, compound of peptide separation by HPLC Agilent 1100, followed by identification of the peptides by mass spectrometry using LTQ Orbitrap XL. Bioinformatics analyzes were carried out to categorize proteins in relation to a Genetic Ontology, metabolic pathways by KEGG, functional mapping and identification of the genes encoding specific proteins for each condition and clinic for validating the results requested in proteomics. In addition, gene expression was analyzed by qPCR in the testis and three epididymal regions of genes associated with proteins that were differentially expressed in sperm and epididymal fluid from both groups. GnRH immunization doubled the number of proteins in the CEF, with 417 proteins being evaluated exclusively in pigs immunized with GnRH. The CEF of males immunized with GnRH shows an increase in the number of proteins related to cellular and metabolic processes, with affinity for organic compounds, small molecules and heterocyclic compounds, in addition to altering the enzymatic profile. The significant increase in the number of proteins associated with the ubiquitin-proteasome system was identified in the CEF of animals immunized with GnRH. In spermatozoa (CESperm), 1,322 proteins were identified, with abundance of proteins involved in the metabolism of sperm (enolase, pyruvate dehydrogenase), acrosome reaction and capacity building (oxoprolinase, acrosomal protein SP-10, dihydrolipoil dehydrogenase) and sperm-oocyte interactions (protein binding to the pellucid zone, zonadesin, sperm adhesion molecule 1). In addition, the abundance of mitochondrial proteins was severely affected, with significant changes in the proteins of Complexes I and II, as well as in the ATPase of the oxidative phosphorylation chain. These results provide strong evidence of the impact of secondary hypogonadism on the epididymal environment, responsible for the maturation and storage of sperm before privacy. Finally, as proteins expressed differently in CEF and CESperm they are candidate seminal biomarkers for testicular and epididymal disorders caused by secondary hypogonadism.

Keywords: epididymis, fertility, hypogonadism, proteomics.

SUMÁRIO

CAPÍTULO I

1. INTRODUÇÃO

O epidídimo já foi considerado o órgão do sistema reprodutor masculino com relevância marginal para a fertilidade no homem e em animais domésticos, sendo associado apenas ao armazenamento dos espermatozoides. Contudo, a partir dos anos 1960, novos dados evidenciaram a importância do epidídimo para a formação de um espermatozoide apto a fertilizar (SULLIVAN et al.,2016).

O espermatozoide na sua trajetória pelo epidídimo interage com as secreções que desempenham o papel fundamental para a maturação (CORNWALL et al., 2009; BELLEANNÉE et al., 2012). Cada região do epidídimo é organizada em lóbulos separados por tecido conjuntivo que serve tanto como suporte interno para o órgão, mas também como uma separação funcional, que permite expressão seletiva de genes e proteínas dentro cada lóbulo individual (ROBAIRE et al., 2006; TURNER et al., 2003). A secreção de proteínas na região da cabeça, corpo e cauda representa 83, 16 e 1% respectivamente, da secreção geral do epidídimo. Cada tipo celular do epitélio epididimário contribui para o estabelecimento e regulação de um ambiente promissor para a concentração, maturação, armazenamento e viabilidade do espermatozoide. Ao final do processo de maturação os espermatozoides são armazenados na cauda e mantidos em baixa atividade metabólica (ZHOU et al., 2018). Este ambiente, composto de secreções advindas do testículo e epidídimo possui papel fundamental na manutenção da viabilidade celular, podendo ser considerado um meio natural de preservação dos gametas.

Diversas patologias que afetam a fertilidade masculina estão relacionadas a desregulações endócrinas e distúrbios hormonais (AGARWAL et al., 2008). O hipogonadismo é uma destas condições e esta associado entre 30 a 70% dos casos de infertilidade no homem (HOTALING et al., 2014). Esta condição resulta da incapacidade dos testículos produzirem níveis fisiológicos de testosterona e espermatozoides devido a falhas no eixo hipotálamo-hipófise-testículo (BHASIN et al., 2006). A compreensão dos mecanismos

fisiológicos associados ao hipogonadismo secundário pode auxiliar no desenvolvimento de ferramentas que auxiliam na predição da qualidade seminal.

Os critérios que baseiam a avaliação da fertilidade masculina inclui o estudo da qualidade do espermatozoide no ejaculado, destacando-se como os parâmetros seminais mais importantes a concentração, motilidade e morfologia espermáticas (JODAR et al., 2017). Porém, mecanismos moleculares que podem estar envolvidos nas causas de infertilidade não são avaliados rotineiramente, sendo estas de origem genética, epigenética e principalmente de ambiente. Para isso, as técnicas como a proteômica são exploradas de modo a fornecer informações sobre os mecanismos moleculares básicos da produção e maturação dos espermatozoides bem como sobre a causa da infertilidade masculina.

As consequências testiculares e epidimárias do hipogonadismo no homem são de difícil investigação devido à impossibilidade de avaliação *in situ* sem comprometer os órgãos. Desta forma, há uma necessidade de estabelecimento de um modelo animal que permita o desenvolvimento de estudos envolvendo processos celulares e moleculares intra-tubulares (tubulos seminíferos e epididimários). Os trabalhos de Schorr-Lenz et al. (2016) e Weber et al. (2018) foram os primeiros a utilizar o macho suíno imunizado contra o GnRH como modelo para o hipogonadismo secundário no homem. A imunização, denominada imunocastração, é uma prática de rotina zootécnica que visa diminuir a produção de andrógenos pelos testículos, e consequentemtne reduzir o odor do macho, característica indesejada na produção de carne suína (ZAMARATSKAIA et al., 2008). Estes estudos pioneiros evidenciaram alterações importantes na expressão de proteínas da família das proteina dissulfeto isomerase e beta-defensinas nos animais com bloqueio hormonal. Estes resultados apontaram para a necessidade de se compreender mais as consequências da imunização anti-GnRH na síntese de proteínas epididimárias e correlação com a qualidade espermártica. Assim, o estudo do perfil proteômico diferencial do fluído e espermatozoide epididimários de animais imunizados e não-imunizados pode fornecer informações valiosas para compreender quais são as reais alterações bioquímicas e fisiológicas que ocorram no epidídimo em caso de deficiência androgênica induzida por bloqueio da ação do GnRH.

Outra oportunidade que se apresenta com o presente estudo é compreender com maiores detalhes os processos fisiológicos da maturação epididimária dos espermatozoides em suínos e o papel da regulação endócrina em eventos envolvidos. O epidídimo é intrinsecamente influenciado por hormônios esteroides, em especial aqueles oriundos do fluido testicular. De

fato, a presença de receptores de andrógenos e estrógenos e outros estudos realizados com ligaduras de segmentos epididimários confirmaram esta influência (HESS et al., 1997). A melhor compreensão de como a secreção proteica epididimária é regulada endocrinamente pode abrir portas para identificação de marcadores proteicos seminais associados a puberdade em suínos em centrais de produções de doses para inseminação artificial.

A proteômica tem sido empregada para a detecção de marcadores bioquímicos da fertilidade, congelabilidade do sêmen e sexagem em especies de interesse zootécnico e alto valor econômico (STRZEZEK et al., 2005; KILLIAN et al., 1993; MOURA et al., 2006). Técnicas moleculares de análise de sêmen correlacionam parâmetros de qualidade seminal e desempenho na IA, auxiliam na seleção dos machos de maior fertilidade, sub-férteis, até mesmo determinar a resistência de um ejaculado a diferentes métodos de preservação seminal (SANCHO & VILLAGRAN, 2013). Associações significativas entre a expressão de proteínas seminais e a fertilidade dos machos já foram avaliadas, tanto *in vivo* quanto *in vitro* (PEDDINTI et al., 2008; RODRIGUEZ-VILLAMIL et al., 2016). Em mamíferos, um número pequeno de proteínas representam 80-90% do conteúdo total de proteínas epididimárias intraluminais, incluindo clusterina, prostaglandina D sintase, glutationa S-transferase, lipocalina (DACHEUX et al ., 2006 , 2009). Tais marcadores já são realidade em outras espécies, e tem-se apresentado de grande importância na biotecnologia da reprodução animal.

Frente ao exposto, a presente tese busca compreender, através de técnicas de *shotgun proteomics*, bioinformática e biologia molecular, os efeitos da imunização contra GnRH no fluído e espermatozoides da cauda do epidídimo de suínos, com enfase nas mudanças de processos bioquímicos e rotas de sinalização celular que possam estar relacionadas com redução da fertilidade.

2. OBJETIVO

2.1.1. Geral

Identificar proteínas que possam ser utilizadas como marcadores moleculares para a qualidade seminal através do estudo proteômico do espermatozoide e fluído retirado da cauda do epidídimo de animais com deficiência androgênica por imunização contra GnRH.

2.1.2. Específicos

- Realizar uma revisão de literatura sobre o papel do epidídimo na função espermática e fertilidade em espécies domésticas, com foco em estudos proteômicos.
- Analisar o proteôma diferencial do fluído e espermatozoide da cauda do epidídimo de animais sadios e imunocastrados e identificar proteínas associadas a estas condições.
- Realizar analises de bioinformática, correlacionando os dados de proteômica diferencial do fluido e espermatozoides da cauda do epidídimo com funções moleculares e vias metabólicas e de sinalização afetadas pela imunização contra GnRH.
- Verificar a expressão gênica de proteínas diferencialmente expressas validando os possíveis marcadores moleculares no testículo e ao longo do epidídimo de animais sadios e com deficiência androgênica.

3. REFERENCIAL TEÓRICO

3.1 Epidídimo

Aparentemente o epidídimo exibe uma estrutura única de um tubo longo em espiral que compõe o aparelho reprodutor masculino. No entanto, estudos fisiológicos, bioquímicos e moleculares realizados neste órgão durante décadas, revelam uma complexidade estrutural e funcional. A fisiologia do epidídimo depende de fatores como a concentrações de andrógenos circulantes que regulam a transcrição gênica e a secreção de proteínas, influenciando diretamente na composição do fluido epididimário e consequentemente a qualidade espermática (ROBAIRE & VIGER, 1995; PRIMIANI et al., 2007; HAMZEH e ROBAIRE, 2009; BELLEANNÉE et al. 2012).

O epidídimo é responsável por fornecer um ambiente que promove a transformação funcional e armazenamento das células espermáticas. Espermatozoides produzidos pelos testículos, através do ducto eferente, chegam ao ambiente epididimário imóveis e imaturos. Sob controle de andrógenos, o epitélio epididimário possui seis categorias celulares distintas que secretam proteínas e criam um ambiente complexo em torno dos espermatozoides (HERMO et al., 1994, 2004; SULLIVAN et al., 2004). Dessa forma o ambiente epididimário permite a concentração e maturação dos espermatozoides, devido as interações lumiais.

Além disso, o epidídimo possui a capacidade de transportar e armazenar as células espermáticas até a ejaculação. A membrana plasmática do espermatozoide rica em Ácidos Graxos Polinsaturados, são alvo das espécies reativas de oxigênio, dessa forma o epidídimo desenvolve estrategias para proteger os espermatozoides das reações de oxidação e de agentes bacterianos (ROBAIRE et al., 2006; GATTI et al., 2004) mantendo-os ativos.

Anatomicamente, o epidídimo é altamente especializado, formado por um ducto único, alongado e contorcido, possui septos de tecido conjuntivo que são projetados para o interior do órgão, dividindo-o em segmentos (TOSHIMORI, 1998; ROBAIRE & HINTON, 2002; PRIMIANI et al., 2007). Esses segmentos variam de acordo com a espécie estudada, apresentando geralmente quatro regiões denominadas de segmento inicial, cabeça, corpo e cauda (SULLIVAN et al., 2005; ROBAIRE et al., 2006; HAMZEH & ROBAIRE, 2009). Desta forma, estudos consideram que o epidídimo exibe características altamente

regionalizadas. Cada região apresenta perfil de expressão gênica diferente, a qual desencadeia secreções de proteínas específicas no líquido luminal portanto, formando microambientes para cada etapa da maturação espermática (GATTI et al., 2004; DACHEUX et al., 2006 COOPER, 2007).

A complexidade do organismo em formar estruturas tubulares como o epidídimo é seguida por eventos morfogênicos importante. No início do epidídimo à formação de um tubo simples, posteriormente, é necessário o alongamento e enovelamento para a armazená-lo em um espaço muito pequeno como a cauda. Para que ocorra o alongamento e enrolamento, os andrógenos produzidos tem papel importante, podendo atuar diretamente na manutenção do epitélio celular (HINTON et al., 2011).

O segmento inicial é responsável por fazer a troca do fluido que acompanha os espermatozoides vindos dos testículos, assim como secreta novas substâncias. Posteriormente, as regiões da cabeça e corpo são as que mais sintetizam, chegando a 80% dos componentes do fluido, em que ocorre maior numero de interações para aquisição da motilidade espermática e capacidade de fertilização (TURNER, 1995). Finalmente, a cauda é caracterizada por um lúmen relativamente grande e suas células epiteliais exibem forte atividade de absorção (ROBAIRE et al., 2006). Nela ocorre a manutenção dos componentes do fluido epididimário, e permanece ocorrendo a troca ativa de substâncias para o armazenamento adequado dos espermatozoides durante dias, em condições que preservam sua fertilidade (JONES & MURDOCH 1996; ROBAIRE & VIGER, 1995; GATTI et al., 2004).

De acordo com as regiões descritas e as diferentes atividades secretórias já é de conhecimento que existem alterações histológicas que compõe as regiões epididimárias (BRIZ et al., 1993). O epitélio é mais espesso na porção inicial e vai se tornando mais fino até chegar a cauda, enquanto a espessura da camada muscular e o diâmetro luminal aumentam da cabeça para a cauda. O formato luminal também varia, sendo oval nas porções inicias e estrelado na porção caudal (DACHEUX et al., 2005).

As células epiteliais epididimárias, bem como as células de Sertoli testiculares, formam uma barreira sanguínea, provendo assim permeabilidade seletiva local. Esta diferenciação além de ser anatômica e fisiológica, devido a modificações celulares e nos seus mecanismos de sinalização e transporte celular, é também imunológica, devido a alterações

nos padrões de resposta a estímulos (HINTON, 2000; MITAL et al., 2011; CHENG e MRUK, 2012; GREGORY & CYR, 2014).

A composição do ambiente intra-luminal é definido pelo epitélio pseudoestratificado composto por seis tipos de células possuindo funções fisiológicas distintas: células principais, células estreitas, células apicais, células claras, células basais, células de halo e células dendríticas. Estes tipos celulares são responsáveis por funções de secreção e absorção epididimária, pela manutenção do ambiente luminal e, consequentemente, pela maturação espermática. Encontrados em todas as porções do epidídimo podendo apresentar diferenças nas suas atividades, dependendo do local (ARRIGHI, 2014; ROBAIRE & HINTON, 2015).

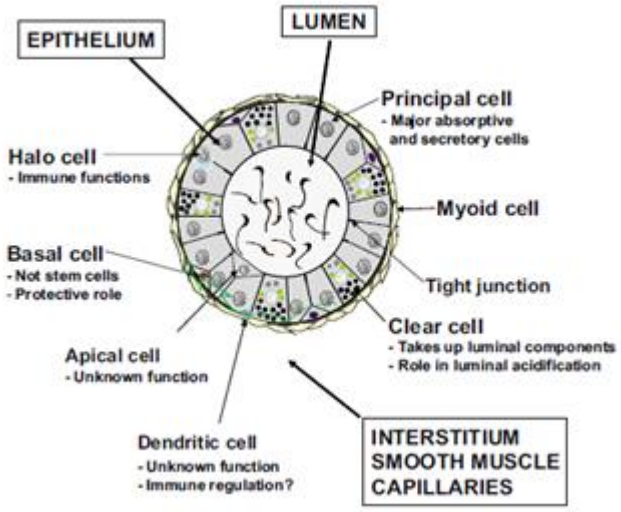

Figura 1 Organização esquemática dos principais tipos de células em uma seção transversal do epidídimo observado no microscópio óptico. A posição, distribuição e função principal (s) associada (s) a cada tipo de célula é também identificada.

Fonte: ROBAIRE & HINTON, 2015

As células principais atuam no transporte de metabólitos através do epitélio, possuem grande aparato secretório refletindo na alta capacidade de promover exocitose (exocitótica), principalmente nas porções proximais (cabeça e corpo). Já na porção distal (cauda) do epidídimo sua função passa a ser endocitótica reabsorvendo componentes do fluído epididimário (HERMO et al., 2002; DACHEUX et al., 2009). As células basais e as células

claras são piramidais e isodiamétricas, respectivamente, em contato com a lâmina basal do epitélio, mas não alcançam sua superfície livre, isto é, o lúmen (BRIZ et al., 1993). As células basais expressam antígenos inerentes aos macrófagos (YEUNG et al., 1994, SEILER et al., 1999), bem como diferentes enzimas tais como glutationa-S-transferase (VERI et al., 1993) e superóxido dismutase (SOD) (NONOGAKI et al., 1992). Seu papel é controverso, mas eles são principalmente relacionadas à atividade fagoctica e à proteção imune e oxidativa do espermatozoide (BASSOLS et al., 2006b). As células claras apresentam elementos necessários para acidificação do ambiente luminal destacando seu papel de regulação do pH epididimal (BROWN et al., 1997).

Portanto, cada região do epidídimo permite para expressão seletiva de genes e proteínas dentro cada lóbulo individual (ROBAIRE et al., 2006; TURNER et al., 2003). Embora essas moléculas estejam em todo o ambiente e seguimento epididimal elas possuem um grau de regionalização, que reflete na atividade diferencial das células epiteliais (ZHOU et al., 2018) sob controle dos andrógenos e outros fatores de origem testicular, contribuindo para maturação, proteção e armazenamentos dos espermatozoides.

3.2 Secreção de proteínas no epidídimo

As atividades das células secretórias e absortivas combinadas com células epiteliais epididimárias criam microambientes altamente especializados que compõem o fluido luminal do epidídimo. Dessa maneia o fluido epididimário é caracterizado por uma complexa paisagem molecular que engloba fatores solúveis, matrizes amilóides não patológicas e vesículas extracelulares denominadas epididimossomas. Estes últimos estão sob crescente estudo devido ao seu potencial para facilitar a transferência de proteínas e pequenos RNA não codificantes, além de comunicar-se com as células espermáticas em amadurecimento (ZHOU et al., 2018). A Cysteine- Rich Secretory Protein 1 (CRISP1) já descrita como uma proteína essencial para a fertilização, envolvida na fusão de espermatozoide e oócito, esta presente exclusivamente nos epididimossomas que circundam as células espermáticas ao longo do epidídimo em humanos. A alfa-manosidase foi descrita em suínos em 1995, pelo grupo Dacheux, secretado por diferentes regiões epididimárias (OKAMURA et al., 1995). Essa proteína está localizada no acrossoma ou integrada no espermatozoide da membrana, estando relacionada à interação espermática de oócitos (KUNO et al., 2000). Nos equinos, essa

proteína está relacionada à aquisição de motilidade e fertilidade, além da interação direta dos espermatozoides com a zona pelúcida (RETAMAL et al., 2012). Esses achados, reforçam a ideia de que o epidídimo fornece proteínas importantes para a fertilização. (JODAR et al, 2017; DA ROS et al., 2015).

A síntese e secreção de proteínas envolvidas na maturação espermática no epidídimo é influenciada diretamente pela testosterona produzida pelas células de Leydig, por conseguinte, afeta o metabolismo, transporte iônico e armazenamento dos espermatozoides (BILINSKA et al., 2006). O controle androgênico pode agir positiva ou negativamente, dependendo dos níveis variáveis de sensibilidade (TEZON et al., 1985; ELLERMAN et al., 1998; DACHUEX et al., 2005; ROBAIRE & HENDERSON, 2006). Em suínos as proteínas secretadas ao longo do epidídimo são altamente regionalizadas e a idade púbere dos animais determina a manutenção dessas regiões, devido aos níveis de testosterona e outros andrógenos circulantes (SYNTIN et al., 1999, TOSHIMORI, 2003).

Algumas das condições patológicas que afetam o epidídimo como epididimite, infecções bacterianas, traumas e distúrbios endócrinos tornam o epidídimo um local inadequado para a preservação do espermatozoide. Já é descrito a influência da orquiectomia e da ligadura do ducto eferente no epidídimo, com mudanças drásticas na morfologia e função da célula espermática (TURNER et al., 2007a; TURNER et al., 2007b). Portanto, há uma dependência comprovada nos fatores testiculares e circulantes para função epididimária adequada (BELLEANNEE et al., 2011).

3.3 Espermatogênese e regulação endócrina

Os espermatozoides constituem um dos tipos celulares mais diferenciados do corpo e são produzidos dentro dos túbulos seminíferos do testículo durante a espermatogênese, um processo complexo e fortemente regulado, com duração e torno de 2,5 meses em humanos e 7 semanas em ratos (HELLER & CLERMONT, 1964; CLERMONT, 1972). A duração total da espermatogênese baseada em 4,5 ciclos espermatogênicos é de aproximadamente 30-75 dias em mamíferos (RUSSELL et al., 1990; FRANÇA & RUSSELL, 1998; SHARPE, 1993) e está sob o controle do genótipo da célula germinativa (FRANÇA et al., 1998). O processo espermatogênico em suínos, assim como em outros mamíferos, é composto por três fases que

são distintas funcional e morfologicamente: 1- espermatogonial (proliferativa ou mitótica); 2- espermatocitária (meiótica) e 3- espermiogênica (diferenciação) (ROOIJ E RUSSELL, 2000).

Em cachaços, cada ciclo espermatogênico dura em média 8,6 – 9,0 dias, onde a duração total da espermatogênese é de cerca de 40 dias (FRANÇA & CARDOSO, 1998). No reprodutor suíno, a puberdade, se inicia quando as primeiras células espermáticas maduras são encontradas na cauda do epidídimo, em torno de 120 dias de idade. Este momento é marcado também pela estabilização das concentrações plasmáticas de testosterona (FRANÇA et al., 2000).

A espermatogênese e a secreção de hormônios são reguladas por componentes endócrinos constituídos por um sistema integrado entre hipotálamo, hipófise e testículos (FRAIETTA et al., 2013). O hormônio liberador de gonadotropina (GnRH), sintetizado pelo hipotálamo, estimula a liberação do hormônio folículo-estimulante (FSH) e o hormônio luteinizante (LH), secretados sintetizados pela glândula hipófise (SENGER, 2003). O LH estimula as células de Leydig a produzir andrógenos, convertendo o colesterol em testosterona. A síntese de testosterona é estimulada pela ação do LH, através do controle da funcional de receptores de andrógenos, e FSH, que estão presentes respectivamente nas células de Leydig e células de Sertoli (ZIRKIN, 1998, FRAIETTA et al., 2013). Assim, estas estimulam a proliferação e a diferenciação de espermatogônias á espermatozoides (GARTNER, 1999).

Este grupo de hormônios inclui uma variedade diversificada e heterogênea de substâncias químicas naturais e sintética, suscetíveis a ter efeitos adversos sobre o organismo através de atividades anti-androgênicas, interferindo no desenvolvimento e função das gônadas (FRAIETTA et al., 2013).

3.4 Hipogonadismo

A infertilidade masculina é cerca de 40% da causa de todos os casos de infertilidade em casais humanos (HIRSH et al.,2003), esta mesma porcentagem esta associada a falhas na reprodução na indústria animal (PARK et al., 2013).

O hipogonadismo é caracterizado como função gonadal inadequada, manifestada por deficiência na gametogênese e/ou secreção de hormônios gonadais (PETAK et al., 2002).

Tais alterações no eixo hipotálamo-hipófise-testículo estão associadas a patologias ou a exposição de toxinas ambientais, decorre em consequências diretas na qualidade do espermatozoide sendo capaz de causar infertilidade ou subfertilidade (DOHLE et al., 2015). Além disso, até 40% dos homens inférteis exibem infertilidade idiopática que pode refletir distúrbios durante a maturação do espermatozoide (CORNWALL et al., 2009; SULLIVAN et al., 2004).

Classificado de acordo com a localização anatômica do órgão afetado, o hipogonadismo leva à falha funcional do testículo. O hipogonadismo primário é causado por defeitos inerentes nos testículos e normalmente não responde a tratamento de suplementação hormonal. O hipogonadismo secundário ou hipogonadotrópico é caracterizado por níveis baixos de testosterona, combinados com níveis plasmáticos normais ou baixos de FSH e LH devido a um comprometimento da função hipofisária (GRANDE et al., 2019).

O hipogonadismo secundário é uma consequência de doenças congênitas ou adquiridas que afeta o hipotálamo e/ou a hipófise prejudicando a secreção de GnRH (DARBY, 2005). Em humanos esta condição é sub-diagnosticada e subtratada (KATZ, 2012), devido principalmente ao diagnóstico molecular impreciso.

3.5 Imunocastração

Em suínos a imunocastração é uma alternativa utilizada à prática comum de castração cirúrgica. Consiste na imunização contra o hormônio liberador de gonadotrofinas (GnRH), também conhecido como castração imunológica. O modo de ação da vacina é provocar uma resposta imune ao endógeno GnRH, um neuropeptídeo que estimula a liberação do hormônio luteinizante (LH) e do hormônio folículo-estimulante (FSH) (ZAMARATSKAIA et al., 2008).

O protocolo de inibição é alcançado mediante a administração de duas doses de um análogo sintético do GnRH conjugado a uma proteína transportadora (Improvac®) (ZOETIS, 2015), com pelo menos 4 semanas de intervalo entre as doses e a última com no mínimo 4 semanas antes do abate (EINARSSON, et al. 2011).

A imunocastração induz a formação de anticorpos contra o GnRH, que se ligam ao GnRH endógeno e o impedem de estimular a secreção de LH e FSH pela glândula pituitária suprimindo o crescimento testicular e a formação de testosterona, que, por sua vez, reduz os

níveis séricos de androstenona e escatol, indesejáveis na produção de carne suína (DUNSHEA et al., 2001; ABCS, 2014).

As concentrações de testosterona, medidas no plasma sanguíneo periférico de suínos, são drasticamente reduzidas quando os animais são imunizados (0,04 e 0,05 ng / mL) em comparação com os controles (1,4 ng / mL). Além disso, o número de espermatozoides normais reduz drasticamente de 71% para 5% quando imunizados (EINARSSON et al., 2011). Consequentemente os níveis reduzidos de testosterona circulante ocasiona a redução concomitante no tamanho dos testículos e das glândulas bulbouretrais, bem como os efeitos na espermatogênese nos animais imunocatrados.

Através deste protocolo obtêm-se o suíno com hipogonadismo secundário, modelo animal utilizado nesta pesquisa, o qual pode ser uma alternativa segura para estudar a disfunção que, em homens, causa inúmeras dúvidas em relação à infertilidade e qualidade do sêmen.

3.6 Proteômica na andrologia

Compreender o mecanismo para seleção de espermatozoides no trato feminino e identificar subpopulações de espermatozoides com atributos relevantes para a fertilização são necessidades atuais para o desenvolvimento de futuras tecnologias de avaliação do espermatozoide (HOLT et al., 2004). Para tanto o estudo do proteôma seminal pode indicar potencial reprodutivo no que diz respeito às avaliações, muitas vezes subjetivas, para a qualidade seminal.

Alterações na expressão de proteínas esta associadas a parâmetros relacionados à fertilidade, a análise proteômica do plasma seminal (SP) e dos espermatozóides emergiu como uma ferramenta muito importante para a identificação de possíveis biomarcadores de fertilidade (revisado por CABALLERO et al., 2012).

As proteínas possuem várias funções no organismo, elas atuam no controle da maior parte dos processos celulares que ocorrem em grande diversidade, podendo atuar como enzimas, anticorpos, hormônios, componentes estruturais e sinalizadores celulares (MANN, 2003). Assim, a proteômica baseia-se em princípios bioquímicos, biofísicos e de bioinformática para quantificar e identificar as proteínas expressas, pois elas se modificam de

acordo com o desenvolvimento de um organismo bem como em resposta aos fatores ambientais (ANDERSON, 1996; WILKINS et al., 1996). Através da pesquisa proteômica é possível identificar e caracterizar marcadores biológicos, ou seja, moléculas endógenas ou exógenas específicas de um determinado estado patológico. Em relação à reprodução animal essa técnica tem sido empregada principalmente para a detecção de marcadores bioquímicos de fertilidade.

O espermatozoide sofre alterações ao longo do epidídimo que determinam a sua natureza proteica, através da remoção e transformação de muitas proteínas superficiais e adicionam proteínas importantes para função espermática (COWAN & MYLES, 1993; DACHEUX et al., 2005). As alterações pós traducionais sofridas pelo espermatozoide, como a fosforilação e glicolisação, podem alterar a composição proteica espermática, sendo necessário assim que as metodologias utilizadas para análise proteômica incluam modificações pós traducionais, como a técnica de MudPIT (BAKER, 2016).

A análise proteômica já é realidade em diversas espécies porem com um fator limitante de técnicas para este mapeamento. Um dos primeiros trabalhos a caracterizar de forma abrangente a composição proteica do plasma seminal suíno foi desenvolvido por Gonzalez-Cadavid (2014). Por 2D SDS-PAGE, foram identificadas 39 proteínas diferentes. Cristina Perez-Patiño et al. (2016) encontrou o maior número de proteínas (406) já descritas no plasma seminal (PS) de suínos e forneceu um panorama dos potenciais biomarcadores da função espermática. Mais recentemente, utilizando abordagem shotgun, Perez-Patiño et al. (2018), expandiram este valor para 872 proteínas, sendo 390 pertencendo especificamente á taxonomia *Sus scrofa*.

Na análise proteômica pelo método de MudPIT uma coluna microcapilar bifásica de fase reversa e troca forte de cátions com uma cromatografia líquida de alta eficiência (HPLC) é carregada com uma mistura de peptídeos complexa gerada a partir de uma amostra biológica. A coluna microcapilar bifásica é interfaceada com uma bomba de HPLC quaternária que atua como fonte para o espectrômetro de massa acoplado a ela. Os peptídeos são eluídos da coluna microcapilar bifásica e diretamente ionizados e analisados no espectrômetro de massa em tandem (MS/MS). Os dados de espectrometria de massa em tandem resultantes são pesquisados utilizando o algoritmo SEQUEST, que interpreta os espectros de massa gerados e identifica a sequência peptídica a partir da qual foi gerada,

resultando na determinação quantitativa de proteína da amostra original (ENG et al., 1994; WASHBURN et al., 2001; WOLTERS et al., 2001).

Comparando plasma seminal de touros de alta e baixa fertilidade, Viana et al., (2018) identificou 1159 proteínas o que contribuiu para o perfil proteômico na espécie *Bos taurus*. Além disso, identificou-se proteínas seminais específicas com diferentes perfis de expressão em touros com fenótipos contrastantes e fertilidade determinada *in vivo*.

A reprodução animal necessita destes métodos avançados para mapear proteínas que podem estar envolvidas na fertilidade e serem candidatas a marcadores moleculares. Assim, o epidídimo como alvo para análise proteômica é relevante já que é neste órgão que as células espermáticas sofrem maturação, tornando-o apto para fertilização.

De acordo com Bassols e colaboradores, (2007) o perfil proteômico é alterado com os tipos de células epididimárias que se modificam devido às secreções ao longo das diferentes regiões do epidídimo. Esses mesmo autores estabeleceram um procedimento bem-sucedido para a cultura in vitro de células epididimárias, em vários estágios (cabeça, corpo e cauda). Os autores concluíram que, à medida que a cultura *in vitro* progredia, os perfis proteicos foram alterados nos vários tipos de células epididimárias que, no entanto, mostraram perfis diferentes em consequência da região a partir da qual a cultura primária foi iniciada, coincidindo com estudos preliminares no nível do transcriptoma.

Belleannee et al,. (2011) monitoraram proteínas da superfície espermática durante os diferentes estágios de maturação no epidídimo. Os autores estabeleceram um método capaz de separar proteínas associadas á membrana e proteínas integrais. Verificou-se que várias proteínas diminuíram em abundância como consequência da maturação dos espermatozoides, incluindo ACE (enzima de conversão da angiotensina), proteínas de choque térmico HSPA4L e HSPA2, ALDR2 (aldose redutase), enquanto uma proteína, nomeada PRDX5 (peroxiredoxina-5) foi considerado regulado durante a maturação. Verificou-se que essas proteínas desempenham um papel importante na diferenciação dos espermatozóides e, portanto, na fecundação.

Syntin, (1996) identificou a atividade secretora das células epididimais em suínos usando estudos com técnicas *in vivo* e *in vitro* caracterizando as proteínas secretadas pelo túbulo epididimário pela técnica de eletroforese. Neste estudo demonstrou-se que 125 polipeptídios específicos são secretados no interior do lúmen epididimário permitindo

distinguir porções pela alta especificidade das proteínas em cada região. Outro experimento, conduzido por Syntin, avaliou o número de proteínas secretadas no epidídimo no período de avaliação de seis meses. Aproximadamente 48% de todas as proteínas segregadas no epidídimo de suínos adulto foram dependentes da presença de andrógenos, estimulados (33,6%) ou reprimidos (14,4%); 47% foram modulados por outros fatores, e 5% não foram regulados. No entanto, o grau de dependência androgênica varia. A regionalização da atividade secretora do epitélio epidídimo resultou em uma regulação específica para cada proteína, que foi modulada de acordo com a região de expressão e influenciada por fatores testiculares ou do epidídimo que ainda não foram identificados (SYNTIN, et al., 1999).

CAPÍTULO II

4. Artigo Científico 1

DOI: 10.21451/1984-3143-AR955

Anim. Reprod., v.14, (Suppl.1), p.1234-1244. 2017

The epididymis and its role on sperm quality and male fertility

Ana Paula Binato de Souza, Ângela Maria Schorr-Lenz, Franciele Lucca, Ivan Cunha Bustamante-Filho[1]

Laboratório de Biotecnologia, Universidade do Vale do Taquari (Univates), Lajeado, RS, Brazil.

Abstract

The epididymis is a complex organ where spermatozoa acquire motility and ability to fertilize the egg. Epididymal maturation lasts 1 or 2 weeks and exposes the immature spermatozoa to a sequentially modified milieu, promoting intense interactions with secretions by the epididymal epithelium. Sperm surface modifications in response to interactions with epididymal secretions are key steps to achieve fertility ability. However, the precise molecular mechanisms that convert an immotile and infertile gamete into a highly motile cell capable of fusion with an oocyte are still unknown. Recent data on proteomics and transcriptomics of epididymal fluid and epididymosomes brought new ideas of the physiological roles of proteins and miRNAs in epididymal maturation in spermatozoa. This review focuses on the recent discoveries on epididymal fluid composition and its role on sperm maturation and preservation, linking to their survival and fertility potential.

Keywords: epididymis, epididymosomes, spermatozoa, proteomics, sperm maturation.

Introduction

Modern livestock production systems rely on efficient reproductive management and the continuous search for maximum efficiency has demanded new methods for animal selection and semen evaluation. Our understanding of male reproductive physiology is still expanding and the role of the epididymis on sperm maturation is considered today a key factor for male fertility. To effectively identify spermatozoa fertilizing ability, it is indispensable to determine whether the sperm cells have completed their maturation process. This complex event is tightly regulated and operated mainly by proteins secreted by the testis and epididymis, and these proteins are considered potential candidates as molecular markers. Biomarker-based semen analysis can be used not only in single ejaculate evaluation but also in both sire fertility and breeding soundness assessment (Sutovsky, 2015). The goals of this new approach are to optimize and increase the use of single sire in different livestock systems. The present review will discuss aspects of epididymal physiology and bring new information learned through genomic proteomic studies, discussing how the comprehension of sperm epididymal maturation could contribute to the development of new reproductive biotechnologies.

A brief introduction to epididymal physiology

Viable spermatozoa are produced inside several biological tubes lumina, where complex processes of cell differentiation and maturation occur. Spermatogenesis takes place in the walls of the seminiferous tubules and, after spermiation, the immature spermatozoa begin interacting with a sequence of distinct luminal environments during their transition along the excurrent ducts (Hess, 2002). Seminiferous tubules connect to the rete testis, a cuboidal epithelium forming an anastomotic network that connects to the efferent ducts, a series of 4 to 20 tubules depending on the species (Robaire et al., 2006). These tubules converge to empty into the epididymis, a single coiled duct with over 1 m length in the mouse, 3 m in the rat; and 6 m in the human (reviewed by Hinton et al., 2011). It is usually divided into four anatomical regions: the initial segment, head (caput), body (corpus), and tail (cauda). Each region of the epididymis is organized into lobules separated by connective tissue septa that serve not only as internal support for the organ but also as a functional separation which allows for selective expression of genes and proteins within each individual lobule (Robaire et al., 2006; Turner et al., 2003).

Both anatomical and physiological aspects of the epididymis are hurdles to overcome when studying the epididymis. Comparing proteomic or gene expression data between regions is tricky since each region behaves differently and apparently independently. In fact, the Hinton group suggested very recently that despite being formed by one single Wolffian duct, the epididymis seems to be a series of organs placed side by side (Domeniconi et al., 2016). This compartmentalized gene expression results in segment-specific protein secretions into the luminal fluid, creating sperm microenvironments where specific modifications in spermatozoa happen. The composition of the intra luminal milieu is defined by the pseudostratified epithelium composed of six cell types possessing distinct physiological functions: narrow and apical cells found in the proximal region of the epididymis and principal cells, clear cells, machophages, dentritic cells, basal cells and halo cells found throughout the organ (Breton et al., 2016; Da Silva and Barton, 2016; Kempinas and Klinefelter, 2014; Shum et al., 2014). Each cell type contributes to the establishment and regulation of a unique luminal environment for the concentration, maturation, storage, and viability of spermatozoa.

Luminal acidification is achieved by epithelial cells that have specific roles depending on their location along the epididymis (Shum et al., 2011). The importance of luminal acidification was observed in c-ros knockout (KO) male mice, which are infertile and have an abnormally elevated epididymal luminal pH

[1]Corresponding author: ivan.bustamante@pq.cnpq.br
Received: March 30, 2017
Accepted: December 30, 2017

(Yeung et al., 2004). Similarly, a KO male mouse model for Foxi1 (a transcription factor specifically expressed in clear cells that controls the expression of proteins involved in acid secretion) presented a higher epididymal luminal pH compared with its wild type counterpart, being also infertile because of an inability of their spermatozoa to reach the oviduct and fertilize the egg (Blomqvist et al., 2006; Vidarsson et al., 2009). A practical observation of inhibition of luminal acidification is the exposure to environmental pollutants, such as tobacco smoke and heavy metals, which induce a reduction in male fertility (Shum et al., 2011).

Clear cells are present in caput, corpus and cauda regions of the epididymis and proximal vas deferens participating in the resorption of luminal content. Also, they contribute with the net proton secretion via the proton-pumping ATPase (V-ATPase), which is highly expressed in their apical plasma membrane (Beaulieu et al., 2005; Da Silva et al., 2007a; Da Silva et al., 2007b; Pastor-Soler et al., 2008; Shum et al., 2008). These cells are significantly more numerous in the cauda epididymis compared with the caput region, suggesting a major acidifying role in the distal region, where spermatozoa are stored (Shum et al., 2011).

Furthermore, clear cells of the human epididymis also express the V-ATPase (Da Silva et al., 2007a; Herak-Kramberger et al., 2001), indicating that the acidifying role of these cells occurs across species. The a4 promoter is under the control of the Foxi1 transcription factor, and several V-ATPase subunits are absent in clear cells from Foxi1 KO mice (Blomqvist et al., 2006; Vidarsson et al., 2009), indicating the importance of the V-ATPase in male fertility. Clear cells might contribute to the reestablishment of an acidic resting luminal pH following principal cell activation (Shum et al., 2011).

At alkaline luminal pH, the V-ATPase is mainly located in well-developed apical microvilli, and at acidic pH, it is actively recycling between sub-apical endosomes and the apical membrane. Intracellular production of bicarbonate (HCO_3^-) is essential for the alkaline pH-induced response and cAMP induces an apical translocation of V-ATPase identical to that induced by alkaline pH. Alkalinization of luminal pH, followed by an increase in intracellular pH in clear cells, leads to an elevation of intracellular bicarbonate concentration (Pastor-Soler et al., 2003). Bicarbonate elevation activates soluble adenylyl cyclase (sAC) and triggers cAMP production, which in turn leads to the accumulation of V-ATPase in apical microvilli. Clear cells also have the ability to respond to an increase in luminal bicarbonate concentration at constant pH, presumably due to entry of bicarbonate across the apical membrane, and subsequent elevation in intracellular bicarbonate concentration followed by sAC activation (Pastor-Soler et al., 2003).

The epididymal epithelium cells are also responsible for water removal from the lumen with three main consequences. First, there is an increase in luminal sperm concentration from 10^8 spermatozoa/mL in the rete testis fluid to 10^9 in the deferent duct. Second, there is a constant modulation in protein concentration, with a 10-fold increase from the rete testis fluid and the initial segment of the epididymis (2 to 4 mg/ml) to the distal caput (50-60 mg/ml) (Belleannee et al., 2011b; Dacheux et al., 2012; Fouchecourt et al., 2000).

The third consequence is related to osmolality, since the hypothesis that immature spermatozoa have a reduced ability to regulate their volume in osmotic challenging environments was considered (Cooper and Barfield, 2006). The increasing osmolality with which spermatozoa are confronted in the epididymis, if acting to reduce cell volume, should lead to an uptake of secreted permeant epididymal osmolytes during the process of regulatory volume increase. Recently, it was demonstrated that both caput and cauda sperm cells regulate volume, but cauda spermatozoa were more effective (Damm and Cooper, 2010). The osmotic stress is of great concern when developing sperm preservation media, like semen extenders routinely used in artificial insemination programs in livestock production. Despite all advances observed in sperm cryopreservation, some species like swine still face hurdles in post thaw sperm survival.

The development of motility by spermatozoa during epididymal transit

The remarkable biochemical changes in the epididymal sperm surroundings induces progressive and controlled modifications both biochemically and functionally. Motility is the most evident change in the epididymal sperm, with irregular and asymmetric flagella beating in the caput epididymis becoming symmetrical with propagation of waves on each side of the flagella, inducing forward motility of the spermatozoa when it reaches the cauda (Bork et al., 1988; Chevrier and Dacheux, 1992; Dacheux and Dacheux, 2014). However, such motility is only observed *in vitro* when epididymal sperm have been washed free of epididymal fluids and extended in a proper artificial medium. *In vivo*, weak beating flagella can be seen in the rete testis and efferent duct fluids, but after the increase in sperm concentration in the epididymal fluid, most of the spermatozoa maintain quiescent motility whatever its location in the epididymis (Dacheux and Dacheux, 2014).

The sperm flagellum machinery at the output of the testis is molecularly functional but inactivated *in vivo*, however the precise mechanism of activation of sperm motility in the epididymis is still unclear. This cell function is dependent on the intracellular cAMP generated by adenylyl cyclase, and on subsequent successive protein phosphorylations including protein kinase A, A-kinase anchor proteins and many other phosphorylated proteins (Esseltine and Scott, 2013; Perino et al., 2012; Turner, 2006).

Throughout the epididymal lumen, the sperm's intracellular cAMP level increases from the corpus to the cauda (Dacheux and Paquignon, 1980; Hoskins et al., 1974; Pariset et al., 1985), simultaneously with metabolic capacity and ATP production (Inskeep and

Hammerstedt, 1982). In addition, [HCO_3^-] and [Ca^{2+}] are key factors of the luminal epididymal fluid, which could directly control intracellular cAMP concentrations in the epididymal spermatozoa and consequently activate protein phosphorylation and motility (Xia et al., 2007). Calcium combined with bicarbonate ions is able to accelerate the flagellar beating of mature sperm *in vitro*, changing to symmetrical flagellar wave propagation, directly associated with the level of internal [Ca^{2+}] (Carlson et al., 2007; Lindemann et al., 1991). Instead, the removal of Ca^{2+} prevents this speeding up of flagellar beating (Carlson et al., 2003). Therefore, the low concentration of luminal and intracellular sperm [Ca^{2+}] found in the terminal part of the epididymis contributes to maintaining mature sperm motility quiescent (Dacheux and Dacheux, 2014). These findings point out that the control of the intracellular cAMP of spermatozoa and, consequently, protein phosphorylation is the key to understand the progressive acquisition of motility during epididymal transit. Determining the precise way sperm acquire motility in the epididymis could result in the development of better semen processing protocols in cases of male infertility.

Regulation of secretory activity in the epididymis

While half of the epididymal proteins are under positive or negative control by androgens, other proteins (43%) are modulated by local factors or are not influenced despite the physiological conditions (Syntin et al., 1999). The influence of lumicrine factors on the epididymis has been investigated after efferent duct ligation (EDL), avoiding testicular factors from entering the epididymis (Robaire et al., 2006). As a consequence, several phenomena were observed like epididymal gene expression changes (Hermo et al., 2000; Hinton et al., 1998; Lan et al., 1998), decreased protein synthesis and secretion (Holland et al., 1992) and apoptosis of epithelial cells of the initial segment (Abe and Takano, 1989; Fan and Robaire, 1998; Nicander et al., 1983). After EDL, secretion in the proximal caput is the most highly affected region with a 50% decrease in the specific proteins found in this region, such as RNase-Train A (Dacheux et al., 2005).

Testicular factors play a role in the control of protein secretion in the first part of the epididymis. Specific proteins of the epididymal caput, such as glutathione peroxidase (GPX) and hexosaminidase (HEX), are positively regulated by testosterone. In the distal caput and corpus, lactoferrin, Niemann–Pick type C protein also called Cholesterol Transfer Protein or HE1 (NCP2/CTP/HE1) and E-RABP are also stimulated by androgens, whereas clusterin is inhibited (Dacheux et al., 2005). Indeed, several genes have been shown to depend on testicular factors with diverse bioactivities such as gamma-glutamyl transpeptidase (Palladino and Hinton, 1994a; Palladino and Hinton, 1994b), GPX (Rigaudiere et al., 1992; Vernet et al., 1997), 5-alpha-reductase (Viger and Robaire, 1996), and ADAM7 (Cornwall and Hsia, 1997).

Also, the epididymal physiology is strongly regulated by steroid hormones. Several papers described the influence of orchiectomy and EDL in the epididymis, with dramatic changes in morphology and function (Brooks, 1976; Ezer and Robaire, 2003; Fawcett and Hoffer, 1979; Turner et al., 2007a; Turner et al., 2007b). Therefore, there is a proven dependence on testicular and circulating factors for proper epididymal function (Belleannee et al., 2011a). Testosterone produced by Leydig cells affects metabolism, ion transport, synthesis and secretion of epididymal proteins and sperm maturation, transport and storage (Bilinska et al., 2006). In rabbits, testosterone leaves the testis through the efferent ducts and is incorporated into principal cells of the epididymis by endocytosis of the complex testosterone–androgen binding protein (ABP) (Danzo et al., 1977). There, it can be quickly metabolized to dihydrotestosterone (DHT) by 5-alpha reductase, and to estradiol by aromatase P450 (Robaire and Hamzeh, 2011; Robaire et al., 2006).

In epididymal cell lines androgenic regulation of gene expression involves the androgen dependent signaling pathways MEK, ERK1/2 and CREB, (Hamzeh and Robaire, 2011). Additionally, formation of an androgen–androgen receptor (AR) complex regulates transcription of androgen response elements (AREs) containing-genes (Heinlein and Chang, 2002a; Heinlein and Chang, 2002b; Janne et al., 2000). Interestingly, like androgens, estrogens are present at a very high concentration in the testis and are generated from the aromatization of testosterone both in Leydig cells (Hess et al., 2001a; Hess et al., 2001b) and in epididymal spermatozoa (Hess et al., 1995; Joseph et al., 2011). Estrogens' biological effects are induced via interaction with ESR1 or ESR2 nuclear receptors and subsequent recognition of estrogen response elements (EREs) located in the promoters of target genes (Joseph et al., 2011).

Role of epididymal proteome in sperm maturation

The epididymal fluid is described as the most sequentially modified milieu of the body. And the most important change in this luminal fluid is induced by water reabsorption (Dacheux and Dacheux, 2014). Together with secretory activities of the tubular epithelium, these changes modulates metabolic pathways, such as second messenger and intracellular protein phosphorylation levels, energy metabolism, plasma membrane transport (Dacheux et al., 1989; Ecroyd et al., 2004; Jones et al., 2007; Saez et al., 2011; Voglmayr et al., 1985) (for review, refer to (Cornwall, 2009; Robaire et al., 2006)). This "passive" maturation is necessary because spermatozoa have no or very low capacity to synthesize new components, owing to their condensed DNA (Belleannee et al., 2012b).

The outstanding contributions of the Dacheux group to the characterization of seminal plasma and epididymal fluids of different species - including monotremes (Nixon et al., 2011), opened new roads for the study of male reproductive physiology. Hundreds of epididymal proteins have already been identified from the epididymal fluid of different species. For all these

epididymal fluids characterized, so far no more than twenty proteins are present in high concentrations, representing 80 to 90% of the total luminal proteins (Dacheux and Dacheux, 2014). Several of these proteins are common to different species such as lactoferrin, lipocalin 5, clusterin, glutathione peroxidase 5, prostaglandin D2 synthase, transferrin, Niemann-Pick disease, type C2, phosphoethanolamine binding protein 4, beta-N-acetyl-hexosaminidase, glutathione S transferase, gelsolin, actin, beta galactosidase (Dacheux and Dacheux, 2014). Specifically in man, 77% of the total luminal proteins are represented by albumin (43.8%), clusterin (7.6%), NCP2/CTP/HE1 (6%), lactoferrin (5.9%), extracellular matrix protein (3.2%), α1-antitrypsin (2.7%), prostaglandin D2 synthase (2.2%), transferrin (1.3%), and actin binding protein (1.2%) (Dacheux et al., 2006).

Significant variations among species both in concentration and in regionalization of epididymal proteins were described. For example, lactoferrin, mannosidase, prostaglandin D2 synthase, and albumin are present in high concentrations in the stallion, boar, ram, and human, respectively, but glutathione peroxidase and prostaglandin D2 synthase are virtually absent from the human and boar, respectively (Guyonnet et al., 2011).

Souza and coworkers detected 113 ± 7 spots per gel of cauda epididymal fluid from rams by means of 2D SDS-PAGE analysis (Souza et al., 2012). The most abundant proteins in these gels appeared as albumin and transferrin. These proteins corresponded to 27.3% of all spot intensities and were present as trains of multiple isoforms. Such molecular heterogeneity is linked to post translational modifications (mostly different degrees of glycosylation), which occur in the secretory cells and that induce the secretion of series of isoforms of the same protein (Dacheux et al., 2005). Other proteins identified include clusterin, alpha-1-anti-trypsin, prostaglandin D synthase, alpha-2-HS glycoprotein and actin.

In bulls, Moura et al. identified 114 ± 3 spots in the cauda epididymal fluid protein maps and the most abundant proteins were albumin (21.1%), epididymal secretory protein E1 (10.5%), prostaglandin D-synthase (7.6%) and gelsolin (6%) (Moura et al., 2010). Many proteins appeared in the CEF map as groups of isoforms, such as clusterin (11 spots), transferrin (6 spots), N-acetyl-β-glucosaminidase (6 spots), cauxin (7 spots), prostaglandin D-synthase (4 spots), gelsolin (3 spots) and glutathione peroxidase (2 spots). Other proteins identified were acidic seminal fluid protein (aSFP), aldehyde reductase, α-L-fucosidase, α-1-β-glycoprotein, apolipoprotein A-1, β actin, calmodulin, cathepsin D, cystatin E/M, α-1-antitrypsin, enolase, galectin 3- binding protein, leucine amino-peptidase and a 49-kDa nucleobindin.

In boars, the proteomic profile of the epididymal fluid also showed a very high polymorphism, both in molecular mass and p*I*, as principal characteristic of the proteins secreted in the lumen. A total of 125 epididymal proteins were identified by mass spectrometry covering 187 spots (Syntin et al., 1996). The number of isoforms secreted for a given protein varied according to the epididymal region. Additionally, post-secretory modifications such as partial proteolysis and deglycosylation may occur, thus, influencing the number of isoforms present in the lumen for a given protein as it transits along the epididymis. The secretory activity of the caput region is 6– 8 times greater than that of the caudal region (Dacheux et al., 2005). Protein secretion in the caput, corpus and cauda, thus, represents 83, 16 and 1% of the overall secretion of the epididymis, respectively. The maximum secretory activity corresponds to the maximum concentration of sperm in the fluid and a minimum volume surrounding them. The most abundant proteins are RNase-Train A, GPX, NCP2/CTP/HE1, retinoic acid binding protein (E-RABP), mannosidase, hexoaminidase, clusterin, cathepsin L, lactoferrin. Only one protein is specific for the distal corpus, train H (36–40 kDa), while two minor proteins appear in the cauda (Dacheux et al., 2005; Syntin et al., 1996).

In the stallion, the protein concentration of 35 mg/ml in the proximal caput is around 5 times higher than in rete testis fluid (Fouchécourt et al., 2000). The concentration increases to a maximum value of 60–80 mg/ml in the distal caput, and then decreases progressively toward the corpus and cauda to reach 20–30 mg/ml. A total of 324 different spots distributed throughout the epididymis were detected, corresponding to 201 isolated spots or trains of different proteins. The 5 major polymorphic proteins secreted by testicular tissue were an isoform of clusterin, an isoform of prostaglandin D-synthase (30 kDa, pI 5.5–6), train T1 (67–80 kDa, pI 4–6.2), train T2 (94 kDa, pI 6.5), and train T3 (43 kDa, pI 6.5–7.8). Trains T1, T2, and T3 were specific to the testis. The caput was the most active region, accounting for 73% of the total epididymal secretion. The corpus was the next most active, secreting 20.5%, followed by the cauda, 6.5%. Lactoferrin and clusterin were the most abundant proteins, making up 41.2% and 24.8% of the total epididymal secretion, respectively. Procathepsin D (5.2%), CTP/HE1 (3%), hexosaminidase (2.9%), prostaglandin D-synthase (2.3%), and GPX (1.4%) were the other major compounds secreted (Fouchécourt et al., 2000).

After secretion, these proteins display different fates, such as accumulation of or changes in their modifications that give rise to many different isoforms. Not all of these major secreted proteins remain in the fluid: in the boar, RNAse 10 is present in the anterior caput fluid but is reabsorbed in the next zones, and almost no protein can be found distal to the caput region (Castella et al., 2004). The same pattern was observed for chaperones belonging to the protein disulfide isomerase (PDI) family in sperm and epididymal fluid from boars (Schorr-Lenz et al., 2016).

This resorptive activity is mostly visible in the vas deferens and the proximal caput, where the fluid is mainly composed of testicular fluid and a few epididymal secreted proteins (Guyonnet et al., 2011). Most of the proteins originating from the testis, such as albumin, transferrin, and testicular clusterin, are rapidly

reabsorbed in the efferent ducts, and generally almost all testicular proteins are removed from the fluid before the posterior part of the epididymis (Clulow et al., 1994; Dacheux et al., 2009; Dacheux et al., 2003; Syntin et al., 1996; Veeramachaneni and Amann, 1991). However, some variations among species occur, such as in humans, for which albumin and transferrin remain in large quantities throughout the duct (Dacheux et al., 2006).

Today, proteomic methods became more powerful using shotgun mass spectrometer approaches, with higher sensitivity and throughput results (Amaral et al., 2013; Amaral et al., 2014). Using advanced mass spectrometry and a proteomics platform, Wang et al. (Wang et al., 2013) identified 4675 proteins from human sperm, which is about 4-fold greater than the previously estimated number, demonstrating the unexpected complexity of the human sperm protein composition. With such a large-scale sperm proteome, it is possible to analyze functional pathways in sperm, not only helping the study of sperm function, but also in the development of contraceptive drugs. Annotation of drug targets showed that 500 human sperm proteins are known targets (Wang et al., 2013). The list of sperm proteins can be a rich resource for the development contraceptive drugs. For example, the identified Angiotensin-converting enzyme (ACE) has been shown to be important for male fertility in mice (Krege et al., 1995). Thus, its inhibitors, such as enalapril and quinapril and other 13 different drugs, could be tested as part of new human contraceptive approaches (Wang et al., 2013).

Proteomic research of both sperm and seminal plasma opened doors for a better understanding of the role of specific proteins in semen quality and fertility. Despite the association of several proteins with semen traits (for example the characterization of bovine osteopontin as a seminal plasma fertility-associated protein (Cancel et al., 1997)), suggested molecular markers for sperm quality did not become part of routine ejaculate examination and semen processing. It is accepted that the current methods used in sperm quality assessment are unsatisfactory to correctly predict sperm fertility potential. Also, they do not provide enough information for diagnosing and overcoming possible clinical infertility situations (Payan-Carreira et al., 2013). Therefore, there is a significant window of opportunity for the biotechnological use of semen protein markers to select for or to improve semen quality and fertility in both in human and animal reproduction.

The crosstalk between epithelial cells and spermatozoa during epididymal transit

The acquisition of intraluminal epididymal proteins by transiting spermatozoa occurs by means of hydrophobic interactions (Cooper, 1998). Some sperm proteins acquired during maturation do not behave as coating proteins when sperm cells are experimentally submitted to different biophysical treatments (Thimon et al., 2008b). Some of them behave as integral membrane proteins, including GPI (glycosylphosphatidylinositol) anchored-proteins (Kirchhoff et al., 1996; Legare et al., 1999), while others are integrated inside sperm cell compartments during the maturational process, probably involved in sperm motility (Eickhoff et al., 2004; Eickhoff et al., 2006; Eickhoff et al., 2001).

The incorporation of epididymal proteins by spermatozoa cannot be explained by the classical secretory pathway (Cooper, 1998; Sullivan et al., 2007; Thimon et al., 2008b). Many sperm proteins acquired during the epididymal transit behave as integral membrane proteins when cells are treated with different extraction procedures. Apocrine secretion and exosomes are the main mechanism of transfer of epididymal-secreted proteins to the sperm plasma membrane (Sullivan et al., 2005). The epididymosomes are blebs released from the apical pole of principal cells, and their contents appear to be segregated; only free ribosomes, endoplasmic reticulum cisternae, and small membrane vesicles are visualized (Hermo and Jacks, 2002; Rejraji et al., 2006). The presence of these 20 nm diameter vesicles in the apical cytoplasm of cells forming blebs, as well as in the intraluminal compartment, suggests that they are liberated in the epididymal lumen once blebs detach from principal cells (Sullivan and Saez, 2013). The cholesterol:phospholipids ratio of these vesicles can be as high as 2, and sphingomyelin is the major phospholipid constituent (Sullivan et al., 2005). Epididymosomes in the epididymal fluid have been reported in rat (Eickhoff et al., 2001; Fornes et al., 1995), bovine (Fraile et al., 1996; Frenette et al., 2003; Sutovsky et al., 2001), mouse (Rejraji et al., 2002), horse (Sostaric et al., 2008) and man (Thimon et al., 2008b).

The protein composition of epididymosomes is complex and varied along the epididymis. In rams (Gatti et al., 2004; Gatti et al., 2005) and bulls (Frenette et al., 2003; Frenette et al., 2002), epididymosome protein concentration differs from fluids or spermatozoa collected in the same segment of the epididymis. The proteome of epididymosomes collected in the caput and cauda epididymis in bovine is composed of 555 and 438 proteins respectively, being that 231 proteins are common to both types of epididymosomes (Girouard et al., 2011). Proteins proposed to be involved in sperm–egg interaction and motility, as well as proteins involved in remodeling of sperm components or potentially involved in sperm protection and elimination, were shown to be associated with epididymosomes (Sullivan and Saez, 2013). The proteome of cauda epididymosomes collected from the vas deferens during surgical vasectomy reversal in men showed that epididymosomes transit along the epididymis in humans and that vesicles collected distally represent a mixed population of vesicles secreted all along the epididymis (Thimon et al., 2008a; Thimon et al., 2008b).

The fusogenic properties of bovine epididymosomes with spermatozoa were investigated by Schwarz et al. who observed that spermatozoa isolated from the epididymal caput showed a higher fusion rate

(both pH and time dependent) than those taken from the cauda (Schwarz et al., 2013). Also, the lipid and protein content in spermatozoa changed during epididymal transit and after *in vitro* fusion with epididymosomes. The authors also demonstrated the transfer of epididymis-derived PMCA4 to spermatozoa via epididymosomes.

In a recent paper from the Sullivan group, the study of epididymal sperm binding protein 1 (ELSPBP1) in dead spermatozoa shed some light in how epididymosomes transfer proteins to sperm. To date, ELSPBP1 function remains unclear but its sequence similarity with binder of sperm proteins (BSPs) suggests a role on modulation of phospholipids and cholesterol in sperm membrane (Ekhlasi-Hundrieser et al., 2007; Manjunath et al., 2007; Manjunath and Thérien, 2002). With an elegant approach, D'Amours and coworkers showed that ELSPBP1 is secreted by principal cells in association with epididymosomes, which specifically transfer ELSPBP1 only to spermatozoa already dead before incubation (D'Amours et al., 2012). This receptivity was enhanced by the presence of zinc in the incubation medium. As a result, a subpopulation is formed suggesting an underlying mechanism involved, in which ELSPBP1 could be a tag for the recognition of dead spermatozoa during epididymal transit.

In the last decade, small non-coding RNAs such as microRNAs (miRNAs) have gained attention as critical regulators of gene expression in several biological processes, including differentiation of the epididymal epithelium and acquisition of male fertility (Bjorkgren et al., 2012; Hawkins et al., 2011; Papaioannou and Nef, 2010). Consisting of about 22 nucleotides, miRNAs regulate posttranscriptional gene expression by targeting mRNAs for cleavage or translational repression (Bartel, 2009). Distinct miRNA signatures in the caput, corpus and cauda of human epididymis were found to correlate with epididymal gene expression pattern (Belleannee et al., 2012a).

The Sullivan group was the first to report the ability of epididymosomes to transport miRNAs, extending the current knowledge with regards to the role of epididymosomes in the transfer of proteins to maturing spermatozoa. In a bovine model, small RNAs were found to be threefold more abundant in epididymosomes from the proximal region compared to those in the distal region (Belleannee et al., 2013). Overall, 1645 miRNA sequences from 74 different species and 82 bovine miRNA sequences were detected with strong signal intensity in epididymosomes. Among these, 178 miRNAs were differentially detected between caput and cauda epididymosomes, including 92 miRNAs enriched in caput epididymosomes and 86 enriched in cauda epididymosomes. miRNA populations from epididymosomes did not mirror the miRNA profiles of their surrounding epithelium, suggesting that instead of being passively released by epididymal epithelial cells, subpopulations of epididymal miRNAs may employ selective and distinct biogenesis and secretion pathways that are regulated in a region-specific manner along the epididymis. Similarly, other studies proposed that the miRNA content of extracellular vesicles does not simply imitate the miRNA repertoire of the cells of origin (Guduric-Fuchs et al., 2012; Mittelbrunn et al., 2011).

Concluding remarks

During the first one or two weeks of post-testicular life, spermatozoa is incarcerated in a long and highly coiled biological tube, nevertheless experiencing different environments until ejaculation. These subtle sequential changes in the luminal milieu are a result of regionalized specialization of the epididymal epithelium. Coordinated secretions and endocytosis lead to an intense modification of the epididymal fluid protein profile, exposing the gametes to factors that will modulate sperm physiology. Moreover, apocrine secretions of principal cells produce epididymosomes that deliver target proteins, miRNAs and lipids to spermatozoa, a fundamental event for gamete recognition and fusion. Research on the molecular processes driving the vesicle-dependent maturation of spermatozoa, as well as several other luminal components, will increase the understanding of sperm maturation in the epididymis, opening doors for the discovery of new markers for semen quality and fertility.

Acknowledgements

We thank CNPq, CAPES, FAPERGS and FUVATES for funding projects in the laboratory. The authors apologize to the many scientists whose research could not be cited because of space considerations.

References

Abe K, Takano H. 1989. Cytological response of the principal cells in the initial segment of the epididymal duct to efferent duct cutting in mice. *Arch Histol Cytol*, 52:321-326.

Amaral A, Castillo J, Estanyol JM, Ballesca JL, Ramalho-Santos J, Oliva R. 2013. Human sperm tail proteome suggests new endogenous metabolic pathways. *Mol Cell Proteomics*, 12:330-342.

Amaral A, Castillo J, Ramalho-Santos J, Oliva R. 2014. The combined human sperm proteome: cellular pathways and implications for basic and clinical science. *Hum Reprod Update*, 20:40-62.

Bartel DP. 2009. MicroRNAs: target recognition and regulatory functions. *Cell*, 136:215-233.

Beaulieu V, Da Silva N, Pastor-Soler N, Brown CR, Smith PJ, Brown D, Breton S. 2005. Modulation of the actin cytoskeleton via gelsolin regulates vacuolar H+-ATPase recycling. *J Biol Chem*, 280:8452-8463.

Belleannee C, Belghazi M, Labas V, Teixeira-Gomes AP, Gatti JL, Dacheux JL, Dacheux F. 2011a. Purification and identification of sperm surface proteins and changes during epididymal maturation. *Proteomics*, 11:1952-1964.

Belleannee C, Calvo E, Caballero J, Sullivan R. 2013. Epididymosomes convey different repertoires of

microRNAs throughout the bovine epididymis. *Biol Reprod*, 89:30.

Belleannee C, Calvo E, Thimon V, Cyr DG, Legare C, Garneau L, Sullivan R. 2012a. Role of microRNAs in controlling gene expression in different segments of the human epididymis. *PloS one*, 7:e34996.

Belleannee C, Labas V, Teixeira-Gomes AP, Gatti JL, Dacheux JL, Dacheux F. 2011b. Identification of luminal and secreted proteins in bull epididymis. *J Proteomics*, 74:59-78.

Belleannee C, Thimon V, Sullivan R. 2012b. Region-specific gene expression in the epididymis. *Cell Tissue Res*, 349:717-731.

Bilinska B, Wiszniewska B, Kosiniak-Kamysz K, Kotula-Balak M, Gancarczyk M, Hejmej A, Sadowska J, Marchlewicz M, Kolasa A, Wenda-Rozewicka L. 2006. Hormonal status of male reproductive system: androgens and estrogens in the testis and epididymis. In vivo and in vitro approaches. *Reprod Biol*, 6(Suppl. 1):43-58.

Bjorkgren I, Saastamoinen L, Krutskikh A, Huhtaniemi I, Poutanen M, Sipila P. 2012. Dicer1 ablation in the mouse epididymis causes dedifferentiation of the epithelium and imbalance in sex steroid signaling. *PloS one*, 7:e38457.

Blomqvist SR, Vidarsson H, Soder O, Enerback S. 2006. Epididymal expression of the forkhead transcription factor Foxi1 is required for male fertility. *EMBO J*, 25:4131-4141.

Bork K, Chevrier C, Paquignon M, Jouannet P, Dacheux JL. 1988. [Flagellar motility amd movement of boar spermatozoa during epididymal transit]. *Reprod Nutr Dev*, 28:1307-1315.

Breton S, Ruan YC, Park YJ, Kim B. 2016. Regulation of epithelial function, differentiation, and remodeling in the epididymis. *Asian J Androl*, 18:3-9.

Brooks DE. 1976. Changes in the composition of the excurrent duct system of the rat testis during postnatal development. *J Reprod Fertil*, 46:31-38.

Cancel AM, Chapman DA, Killian GJ. 1997. Osteopontin Is the 55-Kilodalton Fertility-Associated Protein in Holstein Bull Seminal Plasma. *Biol Reprod*, 57:1293-1301.

Carlson AE, Hille B, Babcock DF. 2007. External Ca2+ acts upstream of adenylyl cyclase SACY in the bicarbonate signaled activation of sperm motility. *Dev Biol*, 312:183-192.

Carlson AE, Westenbroek RE, Quill T, Ren D, Clapham DE, Hille B, Garbers DL, Babcock DF. 2003. CatSper1 required for evoked Ca2+ entry and control of flagellar function in sperm. *Proc Natl Acad Sci U S A*, 100:14864-14868.

Castella S, Benedetti H, de Llorens R, Dacheux JL, Dacheux F. 2004. Train A, an RNase A-like protein without RNase activity, is secreted and reabsorbed by the same epididymal cells under testicular control. *Biol Reprod*, 71:1677-1687.

Chevrier C, Dacheux JL. 1992. Evolution of the flagellar waveform of ram spermatozoa in relation to the degree of epididymal maturation. *Cell Motil Cytoskeleton*, 23:8-18.

Clulow J, Jones RC, Hansen LA. 1994. Micropuncture and cannulation studies of fluid composition and transport in the ductuli efferentes testis of the rat: comparisons with the homologous metanephric proximal tubule. *Exp Physiol*, 79:915-928.

Cooper TG. 1998. Interactions between epididymal secretions and spermatozoa. *J Reprod Fertil Suppl*, 53:119-136.

Cooper TG, Barfield JP. 2006. Utility of infertile male models for contraception and conservation. *Mol Cell Endocrinol*, 250:206-211.

Cornwall GA. 2009. New insights into epididymal biology and function. *Hum Reprod Update*, 15:213-227.

Cornwall GA, Hsia N. 1997. ADAM7, a member of the ADAM (a disintegrin and metalloprotease) gene family is specifically expressed in the mouse anterior pituitary and epididymis. *Endocrinology*, 138:4262-4272.

D'Amours O, Frenette G, Bordeleau L-J, Allard N, Leclerc P, Blondin P, Sullivan R. 2012. Epididymosomes Transfer Epididymal Sperm Binding Protein 1 (ELSPBP1) to Dead Spermatozoa During Epididymal Transit in Bovine. *Biol Reprod*, 87:94, 91-11.

Da Silva N, Barton CR. 2016. Macrophages and dendritic cells in the post-testicular environment. *Cell Tissue Res*, 363:97-104.

Da Silva N, Shum WW, Breton S. 2007a. Regulation of vacuolar proton pumping ATPase-dependent luminal acidification in the epididymis. *Asian J Androl*, 9:476-482.

Da Silva N, Shum WW, El-Annan J, Paunescu TG, McKee M, Smith PJ, Brown D, Breton S. 2007b. Relocalization of the V-ATPase B2 subunit to the apical membrane of epididymal clear cells of mice deficient in the B1 subunit. *American journal of physiology Cell physiology*, 293:C199-210.

Dacheux JL, Belghazi M, Lanson Y, Dacheux F. 2006. Human epididymal secretome and proteome. *Mol Cell Endocrinol*, 250:36-42.

Dacheux JL, Belleannee C, Guyonnet B, Labas V, Teixeira-Gomes AP, Ecroyd H, Druart X, Gatti JL, Dacheux F. 2012. The contribution of proteomics to understanding epididymal maturation of mammalian spermatozoa. *Syst Biol Reprod Med*, 58:197-210.

Dacheux JL, Belleannee C, Jones R, Labas V, Belghazi M, Guyonnet B, Druart X, Gatti JL, Dacheux F. 2009. Mammalian epididymal proteome. *Mol Cell Endocrinol*, 306:45-50.

Dacheux JL, Castella S, Gatti JL, Dacheux F. 2005. Epididymal cell secretory activities and the role of proteins in boar sperm maturation. *Theriogenology*, 63:319-341.

Dacheux JL, Dacheux F. 2014. New insights into epididymal function in relation to sperm maturation. *Reproduction*, 147:R27-42.

Dacheux JL, Dacheux F, Paquignon M. 1989. Changes in sperm surface membrane and luminal protein fluid content during epididymal transit in the boar. *Biol Reprod*, 40:635-651.

Dacheux JL, Gatti JL, Dacheux F. 2003. Contribution of epididymal secretory proteins for spermatozoa maturation. *Microsc Res Tech*, 61:7-17.

Dacheux JL, Paquignon M. 1980. Relations between the fertilizing ability, motility and metabolism of epididymal spermatozoa. *Reprod Nutr Dev*, 20:1085-1099.

Damm OS, Cooper TG. 2010. Maturation of sperm volume regulation in the rat epididymis. *Asian J Androl*, 12:578-590.

Danzo BJ, Cooper TG, Orgebin-Crist MC. 1977. Androgen binding protein (ABP) in fluids collected from the rete testis and cauda epididymidis of sexually mature and immature rabbits and observations on morphological changes in the epididymis following ligation of the ductuli efferentes. *Biol Reprod*, 17:64-77.

Domeniconi RF, Souza AC, Xu B, Washington AM, Hinton BT. 2016. Is the Epididymis a Series of Organs Placed Side By Side? *Biol Reprod*, 95:10.

Ecroyd H, Asquith KL, Jones RC, Aitken RJ. 2004. The development of signal transduction pathways during epididymal maturation is calcium dependent. *Dev Biol*, 268:53-63.

Eickhoff R, Baldauf C, Koyro HW, Wennemuth G, Suga Y, Seitz J, Henkel R, Meinhardt A. 2004. Influence of macrophage migration inhibitory factor (MIF) on the zinc content and redox state of protein-bound sulphydryl groups in rat sperm: indications for a new role of MIF in sperm maturation. *Mol Hum Reprod*, 10:605-611.

Eickhoff R, Jennemann G, Hoffbauer G, Schuring MP, Kaltner H, Sinowatz F, Gabius HJ, Seitz J. 2006. Immunohistochemical detection of macrophage migration inhibitory factor in fetal and adult bovine epididymis: release by the apocrine secretion mode? *Cells Tissues Organs*, 182:22-31.

Eickhoff R, Wilhelm B, Renneberg H, Wennemuth G, Bacher M, Linder D, Bucala R, Seitz J, Meinhardt A. 2001. Purification and characterization of macrophage migration inhibitory factor as a secretory protein from rat epididymis: evidences for alternative release and transfer to spermatozoa. *Mol Med*, 7:27-35.

Ekhlasi-Hundrieser M, Schafer B, Philipp U, Kuiper H, Leeb T, Mehta M, Kirchhoff C, Topfer-Petersen E. 2007. Sperm-binding fibronectin type II-module proteins are genetically linked and functionally related. *Gene*, 392:253-265.

Esseltine JL, Scott JD. 2013. AKAP signaling complexes: pointing towards the next generation of therapeutic targets? *Trends Pharmacol Sci*, 34:648-655.

Ezer N, Robaire B. 2003. Gene expression is differentially regulated in the epididymis after orchidectomy. *Endocrinology*, 144:975-988.

Fan X, Robaire B. 1998. Orchidectomy induces a wave of apoptotic cell death in the epididymis. *Endocrinology*, 139:2128-2136.

Fawcett DW, Hoffer AP. 1979. Failure of exogenous androgen to prevent regression of the initial segments of the rat epididymis after efferent duct ligation or orchidectomy. *Biol Reprod*, 20:162-181.

Fornes WM, Sosa MA, Bertini F, Burgos MH. 1995. Vesicles in rat epididymal fluid. Existence of two populations differing in ultrastructure and enzymatic composition. *Andrologia*, 27:233-237.

Fouchécourt S, Métayer S, Locatelli A, Dacheux F, Dacheux J-L. 2000. Stallion Epididymal Fluid Proteome: Qualitative and Quantitative Characterization; Secretion and Dynamic Changes of Major Proteins. *Biol Reprod*, 62:1790-1803.

Fouchecourt S, Metayer S, Locatelli A, Dacheux F, Dacheux JL. 2000. Stallion epididymal fluid proteome: qualitative and quantitative characterization; secretion and dynamic changes of major proteins. *Biol Reprod*, 62:1790-1803.

Fraile B, Martin R, De Miguel MP, Arenas MI, Bethencourt FR, Peinado F, Paniagua R, Santamaria L. 1996. Light and electron microscopic immunohistochemical localization of protein gene product 9.5 and ubiquitin immunoreactivities in the human epididymis and vas deferens. *Biol Reprod*, 55:291-297.

Frenette G, Lessard C, Madore E, Fortier MA, Sullivan R. 2003. Aldose reductase and macrophage migration inhibitory factor are associated with epididymosomes and spermatozoa in the bovine epididymis. *Biol Reprod*, 69:1586-1592.

Frenette G, Lessard C, Sullivan R. 2002. Selected proteins of "prostasome-like particles" from epididymal cauda fluid are transferred to epididymal caput spermatozoa in bull. *Biol Reprod*, 67:308-313.

Gatti JL, Castella S, Dacheux F, Ecroyd H, Metayer S, Thimon V, Dacheux JL. 2004. Post-testicular sperm environment and fertility. *Anim Reprod Sci*, 82-83:321-339.

Gatti JL, Metayer S, Belghazi M, Dacheux F, Dacheux JL. 2005. Identification, proteomic profiling, and origin of ram epididymal fluid exosome-like vesicles. *Biol Reprod*, 72:1452-1465.

Girouard J, Frenette G, Sullivan R. 2011. Comparative proteome and lipid profiles of bovine epididymosomes collected in the intraluminal compartment of the caput and cauda epididymidis. *Int J Androl*, 34:e475-486.

Guduric-Fuchs J, O'Connor A, Camp B, O'Neill CL, Medina RJ, Simpson DA. 2012. Selective extracellular vesicle-mediated export of an overlapping set of microRNAs from multiple cell types. *BMC Genomics*, 13:357.

Guyonnet B, Dacheux F, Dacheux JL, Gatti JL. 2011. The epididymal transcriptome and proteome provide some insights into new epididymal regulations. *J Androl*, 32:651-664.

Hamzeh M, Robaire B. 2011. Androgens activate mitogen-activated protein kinase via epidermal growth factor receptor/insulin-like growth factor 1 receptor in the mouse PC-1 cell line. *J Endocrinol*, 209:55-64.

Hawkins SM, Buchold GM, Matzuk MM. 2011. Minireview: The roles of small RNA pathways in reproductive medicine. *Mol Endocrinol*, 25:1257-1279.

Heinlein CA, Chang C. 2002a. Androgen receptor (AR) coregulators: an overview. *Endocr Rev*, 23:175-200.

Heinlein CA, Chang C. 2002b. The roles of androgen receptors and androgen-binding proteins in nongenomic androgen actions. *Mol Endocrinol*, 16:2181-2187.

Herak-Kramberger CM, Breton S, Brown D, Kraus O, Sabolic I. 2001. Distribution of the vacuolar H+

atpase along the rat and human male reproductive tract. *Biol Reprod*, 64:1699-1707.

Hermo L, Jacks D. 2002. Nature's ingenuity: bypassing the classical secretory route via apocrine secretion. *Mol Reprod Dev*, 63:394-410.

Hermo L, Xiaohong S, Morales CR. 2000. Circulating and luminal testicular factors affect LRP-2 and Apo J expression in the epididymis following efferent duct ligation. *J Androl*, 21:122-144.

Hess RA. 2002. The Efferent Ductules: Structure and Functions. In: Robaire B, Hinton BT (Eds.). The Epididymis: from Molecules to Clinical Practice. New York: Kluwer Academic/Plenum Publishers. pp.49-80.

Hess RA, Bunick D, Bahr J. 2001a. Oestrogen, its receptors and function in the male reproductive tract - a review. *Mol Cell Endocrinol*, 178:29-38.

Hess RA, Bunick D, Bahr JM. 1995. Sperm, a source of estrogen. *Environ Health Perspect*, 103(Suppl 7):59-62.

Hess RA, Zhou Q, Nie R, Oliveira C, Cho H, Nakaia M, Carnes K. 2001b. Estrogens and epididymal function. *Reprod Fertil Dev*, 13:273-283.

Hinton BT, Galdamez MM, Sutherland A, Bomgardner D, Xu B, Abdel-Fattah R, Yang L. 2011. How do you get six meters of epididymis inside a human scrotum? *J Androl*, 32:558-564.

Hinton BT, Lan ZJ, Rudolph DB, Labus JC, Lye RJ. 1998. Testicular regulation of epididymal gene expression. *J Reprod Fertil Suppl*, 53:47-57.

Holland MK, Vreeburg JT, Orgebin-Crist MC. 1992. Testicular regulation of epididymal protein secretion. *J Androl*, 13:266-273.

Hoskins DD, Stephens DT, Hall ML. 1974. Cyclic adenosine 3':5'-monophosphate and protein kinase levels in developing bovine spermatozoa. *J Reprod Fertil*, 37:131-133.

Inskeep PB, Hammerstedt RH. 1982. Changes in metabolism of ram sperm associated with epididymal transit or induced by exogenous carnitine. *Biol Reprod*, 27:735-743.

Janne OA, Moilanen AM, Poukka H, Rouleau N, Karvonen U, Kotaja N, Hakli M, Palvimo JJ. 2000. Androgen-receptor-interacting nuclear proteins. *Biochem Soc Trans*, 28:401-405.

Jones RC, Dacheux JL, Nixon B, Ecroyd HW. 2007. Role of the epididymis in sperm competition. *Asian J Androl*, 9:493-499.

Joseph A, Shur BD, Hess RA. 2011. Estrogen, efferent ductules, and the epididymis. *Biol Reprod*, 84:207-217.

Kempinas WG, Klinefelter GR. 2014. Interpreting histopathology in the epididymis. *Spermatogenesis*, 4:e979114.

Kirchhoff C, Osterhoff C, Young L. 1996. Molecular cloning and characterization of HE1, a major secretory protein of the human epididymis. *Biol Reprod*, 54:847-856.

Krege JH, John SW, Langenbach LL, Hodgin JB, Hagaman JR, Bachman ES, Jennette JC, O'Brien DA, Smithies O. 1995. Male-female differences in fertility and blood pressure in ACE-deficient mice. *Nature*, 375:146-148.

Lan ZJ, Labus JC, Hinton BT. 1998. Regulation of gamma-glutamyl transpeptidase catalytic activity and protein level in the initial segment of the rat epididymis by testicular factors: role of basic fibroblast growth factor. *Biol Reprod*, 58:197-206.

Legare C, Gaudreault C, St-Jacques S, Sullivan R. 1999. P34H sperm protein is preferentially expressed by the human corpus epididymidis. *Endocrinology*, 140:3318-3327.

Lindemann CB, Gardner TK, Westbrook E, Kanous KS. 1991. The calcium-induced curvature reversal of rat sperm is potentiated by cAMP and inhibited by anti-calmodulin. *Cell Motil Cytoskeleton*, 20:316-324.

Manjunath P, Bergeron A, Lefebvre J, Fan J. 2007. Seminal plasma proteins: functions and interaction with protective agents during semen preservation. *Society of Reproduction and Fertility Supplement*, 65:217-228.

Manjunath P, Thérien I. 2002. Role of seminal plasma phospholipid-binding proteins in sperm membrane lipid modification that occurs during capacitation *J Reprod Immunol*, 53:109-119

Mittelbrunn M, Gutierrez-Vazquez C, Villarroya-Beltri C, Gonzalez S, Sanchez-Cabo F, Gonzalez MA, Bernad A, Sanchez-Madrid F. 2011. Unidirectional transfer of microRNA-loaded exosomes from T cells to antigen-presenting cells. *Nature communications*, 2:282.

Moura AA, Souza CE, Stanley BA, Chapman DA, Killian GJ. 2010. Proteomics of cauda epididymal fluid from mature Holstein bulls. *Journal of proteomics*, 73:2006-2020.

Nicander L, Osman DI, Ploen L, Bugge HP, Kvisgaard KN. 1983. Early effects of efferent ductule ligation on the proximal segment of the rat epididymis. *Int J Androl*, 6:91-102.

Nixon B, Ecroyd HW, Dacheux JL, Jones RC. 2011. Monotremes provide a key to understanding the evolutionary significance of epididymal sperm maturation. *J Androl*, 32:665-671.

Palladino MA, Hinton BT. 1994a. Developmental regulation of expression of multiple gamma-glutamyl transpeptidase mRNAs in the postnatal rat epididymis. *Biochem Biophys Res Commun*, 198:554-559.

Palladino MA, Hinton BT. 1994b. Expression of multiple gamma-glutamyl transpeptidase messenger ribonucleic acid transcripts in the adult rat epididymis is differentially regulated by androgens and testicular factors in a region-specific manner. *Endocrinology*, 135:1146-1156.

Papaioannou MD, Nef S. 2010. microRNAs in the testis: building up male fertility. *J Androl*, 31:26-33.

Pariset CC, Feinberg JM, Dacheux JL, Weinman SJ. 1985. Changes in calmodulin level and cAMP-dependent protein kinase activity during epididymal maturation of ram spermatozoa. *J Reprod Fertil*, 74:105-112.

Pastor-Soler N, Beaulieu V, Litvin TN, Da Silva N, Chen Y, Brown D, Buck J, Levin LR, Breton S. 2003. Bicarbonate-regulated adenylyl cyclase (sAC) is a sensor that regulates pH-dependent V-ATPase recycling. *J Biol Chem*, 278:49523-49529.

Pastor-Soler NM, Hallows KR, Smolak C, Gong F, Brown D, Breton S. 2008. Alkaline pH- and cAMP-

induced V-ATPase membrane accumulation is mediated by protein kinase A in epididymal clear cells. *American journal of physiology Cell physiology*, 294:C488-494.

Payan-Carreira R, Borges P, Mir F, Fontbonne A.2013. Molecular Markers in Sperm Analysis. In: Lemma A (Eds.). Success in Artificial Insemination - Quality of Semen and Diagnostics Employed: InTech.

Perino A, Ghigo A, Scott JD, Hirsch E. 2012. Anchoring proteins as regulators of signaling pathways. *Circ Res*, 111:482-492.

Rejraji H, Sion B, Prensier G, Carreras M, Motta C, Frenoux JM, Vericel E, Grizard G, Vernet P, Drevet JR. 2006. Lipid remodeling of murine epididymosomes and spermatozoa during epididymal maturation. *Biol Reprod*,74:1104-1113.

Rejraji H, Vernet P, Drevet JR. 2002. GPX5 is present in the mouse caput and cauda epididymidis lumen at three different locations. *Mol Reprod Dev*, 63:96-103.

Rigaudiere N, Ghyselinck NB, Faure J, Dufaure JP. 1992. Regulation of the epididymal glutathione peroxidase-like protein in the mouse: dependence upon androgens and testicular factors. *Mol Cell Endocrinol*, 89:67-77.

Robaire B, Hamzeh M. 2011. Androgen action in the epididymis. *J Androl*, 32:592-599.

Robaire B, Hinton BT, Orgebin-Crist M-C, Jimmy DN, Ph.D, Tony MP, Ph.D, Donald WP, Ph.D, John RGC, D.Sc, F.R.S.C, David MdK, M.D, A.O, JoAnne SR, Ph.D, Paul MW, Ph.D.2006. The EpididymisKnobil and Neill's Physiology of Reproduction (Third Edition). St Louis: Academic Press. pp.1071-1148.

Saez F, Ouvrier A, Drevet JR. 2011. Epididymis cholesterol homeostasis and sperm fertilizing ability. *Asian J Androl*, 13:11-17.

Schorr-Lenz AM, Alves J, Henckes NA, Seibel PM, Benham AM, Bustamante-Filho IC. 2016. GnRH immunization alters the expression and distribution of protein disulfide isomerases in the epididymis. *Andrology*, 4(5):957-963.

Schwarz A, Wennemuth G, Post H, Brandenburger T, Aumuller G, Wilhelm B. 2013. Vesicular transfer of membrane components to bovine epididymal spermatozoa. *Cell Tissue Res*, 353:549-561.

Shum WW, Da Silva N, McKee M, Smith PJ, Brown D, Breton S. 2008. Transepithelial projections from basal cells are luminal sensors in pseudostratified epithelia. *Cell*, 135:1108-1117.

Shum WW, Ruan YC, Da Silva N, Breton S. 2011. Establishment of cell-cell cross talk in the epididymis: control of luminal acidification. *J Androl*, 32:576-586.

Shum WW, Smith TB, Cortez-Retamozo V, Grigoryeva LS, Roy JW, Hill E, Pittet MJ, Breton S, Da Silva N. 2014. Epithelial basal cells are distinct from dendritic cells and macrophages in the mouse epididymis. *Biol Reprod*, 90:90.

Sostaric E, Aalberts M, Gadella BM, Stout TA. 2008. The roles of the epididymis and prostasomes in the attainment of fertilizing capacity by stallion sperm. *Anim Reprod Sci*, 107:237-248.

Souza CE, Rego JP, Lobo CH, Oliveira JT, Nogueira FC, Domont GB, Fioramonte M, Gozzo FC, Moreno FB, Monteiro-Moreira AC, Figueiredo JR, Moura AA. 2012. Proteomic analysis of the reproductive tract fluids from tropically-adapted Santa Ines rams. *Journal of proteomics*, 75:4436-4456.

Sullivan R, Frenette G, Girouard J. 2007. Epididymosomes are involved in the acquisition of new sperm proteins during epididymal transit. *Asian J Androl*, 9:483-491.

Sullivan R, Saez F. 2013. Epididymosomes, prostasomes, and liposomes: their roles in mammalian male reproductive physiology. *Reproduction*, 146:R21-35.

Sullivan R, Saez F, Girouard J, Frenette G. 2005. Role of exosomes in sperm maturation during the transit along the male reproductive tract. *Blood Cells Mol Dis*, 35:1-10.

Sutovsky P. 2015. New Approaches to Boar Semen Evaluation, Processing and Improvement. Reprod Domest Anim, 50(Suppl.2):11-19.

Sutovsky P, Moreno R, Ramalho-Santos J, Dominko T, Thompson WE, Schatten G. 2001. A putative, ubiquitin-dependent mechanism for the recognition and elimination of defective spermatozoa in the mammalian epididymis. *J Cell Sci*, 114:1665-1675.

Syntin P, Dacheux F, Druart X, Gatti JL, Okamura N, Dacheux JL. 1996. Characterization and identification of proteins secreted in the various regions of the adult boar epididymis. *Biol Reprod*, 55:956-974.

Syntin P, Dacheux J-L, Dacheux F. 1999. Postnatal Development and Regulation of Proteins Secreted in the Boar Epididymis. *Biol Reprod*, 61:1622-1635.

Thimon V, Calvo E, Koukoui O, Legare C, Sullivan R. 2008a. Effects of vasectomy on gene expression profiling along the human epididymis. *Biol Reprod*, 79:262-273.

Thimon V, Frenette G, Saez F, Thabet M, Sullivan R. 2008b. Protein composition of human epididymosomes collected during surgical vasectomy reversal: a proteomic and genomic approach. *Hum Reprod*, 23:1698-1707.

Turner RM. 2006. Moving to the beat: a review of mammalian sperm motility regulation. *Reprod Fertil Dev*, 18:25-38.

Turner TT, Bomgardner D, Jacobs JP, Nguyen QA. 2003. Association of segmentation of the epididymal interstitium with segmented tubule function in rats and mice. *Reproduction*, 125:871-878.

Turner TT, Johnston DS, Finger JN, Jelinsky SA. 2007a. Differential gene expression among the proximal segments of the rat epididymis is lost after efferent duct ligation. *Biol Reprod*, 77:165-171.

Turner TT, Johnston DS, Jelinsky SA, Tomsig JL, Finger JN. 2007b. Segment boundaries of the adult rat epididymis limit interstitial signaling by potential paracrine factors and segments lose differential gene expression after efferent duct ligation. *Asian J Androl*, 9:565-573.

Veeramachaneni DN, Amann RP. 1991. Endocytosis of androgen-binding protein, clusterin, and transferrin in the efferent ducts and epididymis of the ram. *J Androl*, 12:288-294.

Vernet P, Faure J, Dufaure JP, Drevet JR. 1997. Tissue and developmental distribution, dependence upon testicular factors and attachment to spermatozoa of GPX5, a murine epididymis-specific glutathione peroxidase. *Mol Reprod Dev*, 47:87-98.

Vidarsson H, Westergren R, Heglind M, Blomqvist SR, Breton S, Enerback S. 2009. The forkhead transcription factor Foxi1 is a master regulator of vacuolar H-ATPase proton pump subunits in the inner ear, kidney and epididymis. *PloS one*, 4:e4471.

Viger RS, Robaire B. 1996. The mRNAs for the steroid 5 alpha-reductase isozymes, types 1 and 2, are differentially regulated in the rat epididymis. *J Androl*, 17:27-34.

Voglmayr JK, Sawyer RF, Jr., Dacheux JL. 1985. Glycoproteins: a variable factor in surface transformation of ram spermatozoa during epididymal transit. *Biol Reprod*, 33:165-176.

Wang G, Guo Y, Zhou T, Shi X, Yu J, Yang Y, et al. 2013. In-depth proteomic analysis of the human sperm reveals complex protein compositions. *Journal of proteomics*, 79:114-122.

Xia J, Reigada D, Mitchell CH, Ren D. 2007. CATSPER channel-mediated Ca2+ entry into mouse sperm triggers a tail-to-head propagation. *Biol Reprod*, 77:551-559.

Yeung CH, Breton S, Setiawan I, Xu Y, Lang F, Cooper TG. 2004. Increased luminal pH in the epididymis of infertile c-ros knockout mice and the expression of sodium-hydrogen exchangers and vacuolar proton pump H+-ATPase. *Mol Reprod Dev*, 68:159-168.

CAPÍTULO III

5. Artigo Científico 2

Received: 25 September 2019 | Accepted: 16 July 2020

DOI: 10.1002/mrd.23408

Molecular Reproduction & Development

RESEARCH ARTICLE

Changes in porcine cauda epididymal fluid proteome by disrupting the HPT axis: Unveiling potential mechanisms of male infertility

Ana P. B. Souza[1] | Tayná N. Lopes[1] | Anna F. T. da Silva[1] | Lucélia Santi[2] | Walter O. Beys-da-Silva[2] | John R. Yates 3rd[3] | Ivan C. Bustamante-Filho[1]

[1]Laboratório de Biotecnologia, Universidade do Vale do Taquari—Univates, Lajeado, Rio Grande do Sul, Brazil

[2]Faculdade de Farmácia, Universidade Federal do Rio Grande do Sul, Porto Alegre, Rio Grande do Sul, Brazil

[3]Department of Molecular Medicine, Scripps Research, La Jolla, California

Correspondence
Dr. Ivan C. Bustamante-Filho, Laboratório de Biotecnologia, Universidade do Vale do Taquari—Univates, Rua Avelino Tallini, 171, Lajeado, RS 95914-014, Brazil.
Email: ivan.bustamante@pq.cnpq.br

Funding information
Fundação de Amparo à Pesquisa do Estado do Rio Grande do Sul, Grant/Award Number: 16/2551-0000223-1; Coordenação de Aperfeiçoamento de Pessoal de Nível Superior; Conselho Nacional de Desenvolvimento Científico e Tecnológico, Grant/Award Number: 447251/2014-7; Fundação Vale do Taquari de Educação e Desenvolvimento Social (FUVATES): 08/Reitoria/Univates/2016

Abstract

Male infertility or subfertility is frequently associated with disruption of the hypothalamic–pituitary–testis axis events, like secondary hypogonadism. However, little is known how this condition affects the proteomic composition of the epididymal fluid. In the present study, we evaluated the proteomic changes in the cauda epididymal fluid (CEF) in a swine model of secondary hypogonadism induced by anti-GnRH immunization using multidimensional protein identification technology. Seven hundred and eighteen proteins were identified in both GnRH-immunized and control groups. GnRH immunization doubled the number of proteins in the CEF, with 417 proteins being found exclusively in samples from GnRH-immunized boars. CEF from GnRH-immunized boars presented an increase in the number of proteins related to cellular and metabolic processes, with affinity to organic cyclic compounds, small molecules, and heterocyclic compounds, as well changed the enzymatic profile of the CEF. Also, a significant increase in the number of proteins associated to the ubiquitin–proteasome system was identified in CEF from GnRH-immunized animals. These results bring strong evidence of the impact of secondary hypogonadism on the epididymal environment, which is responsible for sperm maturation and storage prior ejaculation. Finally, the differently expressed proteins in the CEF are putative seminal biomarkers for testicular and epididymal disorders caused by secondary hypogonadism.

KEYWORDS

epididymis, GnRH, hypogonadism, proteomics, swine animal model

1 | INTRODUCTION

The epididymal environment is of key importance for turning immotile spermatozoa in cells with fertilizing abilities. After exiting the testis, they enter in a unique convoluted tubule with a length ranging from 1 to 7 m for rodents and primates, and to 60–70 m for domestic animals, such as porcine and equine (Dacheux et al., 2012; Hinton et al., 2011). By the end of the epididymal transit, spermatozoa are considered mature, having acquired motility and the ability to recognize and to fuse with the oocyte (Gatti, Castella, Dacheux, Ecroyd, Métayer et al., 2004).

Thirty years of proteomic studies of boar epididymis provided valuable information about the changes and possible roles of specific proteins of testicular and epididymal origins on sperm maturation (Dacheux & Dacheux, 1989; Dacheux, Castella, Gatti, & Dacheux, 2005; Feugang, Liao, Willard, & Ryan, 2018; Syntin, Dacheux, & Dacheux, 1999). In the initial segment of the epididymis, the epididymal fluid (EF) is composed of a mixture of testicular and epididymal proteins.

Most of the proteins originating from testicular secretion, such as albumin, transferrin, testicular clusterin, and prostaglandin D-synthase are reabsorbed in the efferent ducts (Clulow, Jones, & Hansen, 1994; Dacheux et al., 2009; Fouchecourt, Metayer, Locatelli, Dacheux, & Dacheux, 2000). The epididymal epithelial cells have high protein synthesis and secretion activity, with marked differences between regions. The anterior part of the epididymis is the most active. Protein secretion in the caput, corpus and cauda, thus, represents 83%, 16%, and 1% of the overall secretion of the epididymis, respectively. In addition, 70–80% of the secretome is composed of 10–20 of the major secreted proteins present in the luminal fluid (Dacheux et al., 2009).

As a biological tube, the epididymal tubule wall alters the ionic environment of the lumen (e.g., calcium, pH, HCO_3^-) and modulates the presence of specific energy substrates to maintain a low ATP concentration in spermatozoa (Battistone et al., 2019; Gatti et al., 2004; Wade, Roman, Jones, & Aitken, 2003). At the end of the maturation process, spermatozoa are stored in the cauda region, where they are kept in high cell concentration, with a low metabolic status. This quiescent state of the spermatozoa in the cauda is a result of the spatial mechanical limitations due to high sperm concentration. It is induced by the presence of specific proteins produced by the epididymis and other factors, all derived from epididymal epithelial secretions (Zhou, De Iuliis, Dun, & Nixon, 2018). At the distal part of the epididymis, spermatozoa are fully matured and capable of fertilizing. There, they are stored until ejaculation, and the cauda epididymal fluid (CEF) might be considered a natural semen preservation medium.

Pathological conditions affecting the epididymis, like epididymitis, bacterial infections, varicocele, trauma, and endocrine disorders turn the epididymis a hostile place for preserving spermatozoa (Michel, Pilatz, Hedger, & Meinhardt, 2015; Sullivan & Mieusset, 2016). Male infertility or subfertility frequently occurs in cases of disruption of the hypothalamic–pituitary–testis (HPT) axis, like secondary hypogonadism (Basaria, 2014; Dohle et al., 2015). In addition, several environmental toxins have been also associated with HPT-axis disruption with direct consequences to sperm quality (Gupta, 2012; Jeelani, Bluth, & Abu-Soud, 2016; Mostafalou & Abdollahi, 2017). Understanding how these pathologies interfere with the EF composition might shed a light on the effects of spermatozoa maturation and male fertility. Therefore, the aim of this study was to identify the proteomic changes in the CEF in a swine model of secondary hypogonadism induced by anti-GnRH immunization.

2 | RESULTS

Multidimensional protein identification technology (MudPIT) analysis of the CEF of GnRH-immunized and control boars found a total of 718 proteins. GnRH immunization doubled the number of proteins in the CEF, with 417 proteins being found exclusively in samples from testicular degenerated boars. An expressive difference was observed regarding exclusive proteins found between GnRH-immunized and control CED proteomes. Control CEF had only 15 exclusive proteins, while CEF from GnRH-immunized boars had 417 unique proteins (Figure 1). Based on spectral counts and PatternLab's TFold analysis, of the 286 proteins found in CEF of both groups, 54 proteins were significantly differentially expressed (*Q* value of 0.05, *F*-stringency of 0.04). Table 1 presents the differentially expressed proteins in the CEF with a minimum fold change of 2.0. The complete lists of identified proteins are presented as the Supporting Information Material.

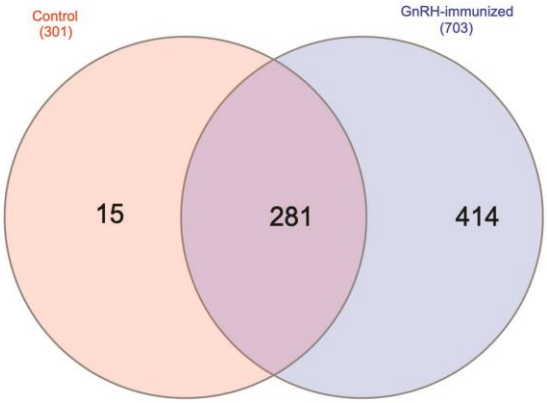

FIGURE 1 Venn diagram showing the distribution of identified proteins in cauda epididymis fluid from healthy (control) and GnRH-immunized boars

Changes in the CEF proteome as a consequence of the disruption of the HPT axis by GnRH immunization were not only quantitative but also qualitative. The comparison of the Gene Ontology (GO) terms associated with each proteome evidenced changes in all three GO classes (Figure 2a–c). CEF from GnRH-immunized boars presented an increase in the number of proteins related to cellular and metabolic processes, with affinity to organic cyclic compounds, small molecules, and heterocyclic compounds. CEF presents significant amounts of proteins related to binding activity. The analyses of GO terms associated to cellular component indicate that 80% of the CEF proteins were related to cell parts, including organelles and membrane. Proportionally, CEF from GnRH-immunized boars had fewer proteins from extracellular region. Immunization against GnRH also changed the enzymatic profile of the CEF (Figure 2d). Control samples had 6 proteins with hydrolase activity, whereas GnRH-immunized CEF presented 105 hits. Also, the amounts of oxidoreductases and transferases were increased up to 10 times.

Enrichment of prioritized genes in biological pathways and functional categories were tested using the hypergeometric test against gene sets (Figure 3). Gene enrichment analyzes resulted in 166 and 467 genes associated with control CEF proteins and GnRH-immunized CEF proteins, respectively. GnRH immunization increased the number of proteins related to gene sets associated with important hallmark pathways, such as glycolysis and spermatogenesis. Interestingly, other enriched hallmark pathways possibly involved in the testicular and epididymal disruption due to immunocastration were upregulated,

TABLE 1 Proteins differently expressed in the cauda epididymal fluid (CEF) of healthy (control) and GnRH-immunized boars

Proteins name	Accession number	Fold change	*p* Value
Proteins upregulated in the control CEF			
PREDICTED: nucleobindin-2 isoform X1	XP_003480773.1	11.33	7.91E−05
Epididymis-specific alpha-mannosidase precursor	NP_999014.1	5.70	.003069
Hemoglobin subunit beta	NP_001138313.1	5.33	.005030
PREDICTED: neprilysin isoform 1	XP_003132549.1	3.30	.043041
PREDICTED: di-*N*-acetylchitobiase, partial	XP_003356466.3	2.80	.012668
Proteins upregulated in the GnRH-immunized CEF			
Serotransferrin precursor	NP_001231582.1	−20.80	.000976
Chaperonin containing TCP1, subunit 5 (epsilon)	NP_001265708.1	−18.00	.000106
PREDICTED: thiomorpholine-carboxylate dehydrogenase	XP_003124605.2	−16.22	.030920
Cystatin-C precursor	NP_001038067.1	−15.67	.011125
Inhibitor of carbonic anhydrase precursor	NP_999012.1	−15.67	.003750
PREDICTED: acrosin-binding protein isoform X1	XP_003126581.1	−14.89	.001434
PREDICTED: triosephosphate isomerase isoform X1	XP_005652645.1	−14.00	.015937
PREDICTED: 14-3-3 protein zeta/delta isoform X1	XP_001927263.3	−12.80	.004220
PREDICTED: cystatin M-like	XP_003122555.1	−8.37	1.81E−05
PREDICTED: disintegrin and metalloproteinase domain-containing protein 20-like	XP_003128673.1	−7.80	3.51E−05
Phosphoglycerate mutase 2	NP_001128440.1	−7.38	.003460
Proepidermal growth factor precursor	NP_999185.1	−6.93	.025374
Prostaglandin-H2 D-isomerase precursor	NP_999393.1	−6.84	.000386
PREDICTED: protein CutA isoform X1	XP_001927987.2	−6.79	.000301
PREDICTED: testis-expressed sequence 101 protein isoform X6	XP_005655969.1	−6.21	.000735
PREDICTED: LOW QUALITY PROTEIN: actin, beta-like 2	XP_005674537.1	−6.13	.003522
Angiogenin precursor	NP_001038038.1	−6.06	.000116
PREDICTED: calmodulin-like	XP_003125211.1	−5.43	.011898
PREDICTED: WAP four-disulfide core domain protein 10A	XP_003134515.1	−5.35	.002611
PREDICTED: probable inactive ribonuclease-like protein 12-like isoform X1	XP_001929241.1	−5.33	.001028
ly6/PLAUR domain-containing protein 4 precursor	NP_001182280.1	−5.33	.002590
Aspartate aminotransferase, cytoplasmic	NP_999092.1	−5.33	.015937
PREDICTED: testis-expressed sequence 101 protein isoform X1	XP_003127256.3	−5.29	.000242
PREDICTED: alkaline phosphatase, tissue-nonspecific isozyme	XP_005658515.1	−5.28	.000107
PREDICTED: actin, cytoplasmic 1	XP_003124328.1	−4.29	.006455
PREDICTED: lysosomal alpha-mannosidase isoform X1	XP_003123362.1	−4.25	.002178
PREDICTED: pancreatic secretory granule membrane major glycoprotein GP2 isoform X2	XP_005662159.1	−3.89	.002590
Arylsulfatase A precursor	NP_999098.1	−3.81	.002966
Serum albumin precursor	NP_001005208.1	−3.70	8.37E−05
PREDICTED: serotransferrin isoform X2	XP_005669896.1	−3.67	.006332
Epididymal secretory protein E1 precursor	NP_999371.1	−3.40	.009715
PREDICTED: plastin-3 isoform X1	XP_001925971.3	−3.39	.001782
Heat shock protein HSP 90-alpha	NP_999138.1	−3.30	.001549
PREDICTED: legumain-like	XP_005658137.1	−3.29	.010251
Hemopexin precursor	NP_999118.1	−3.18	.001518
Epididymal secretory glutathione peroxidase precursor	NP_999051.1	−3.09	.003170
PREDICTED: carboxylesterase 5A	XP_005653315.1	−3.02	.003518
Cysteine-rich secretory protein 1 precursor	NP_001121906.1	−2.62	.001182
Aangiotensin-converting enzyme isoform 2 precursor	NP_001077410.1	−2.47	.010819
Ceruloplasmin precursor	NP_001254623.2	−2.10	.010886
Angiotensin-converting enzyme isoform 1 precursor	NP_001028187.2	−2.08	.009324

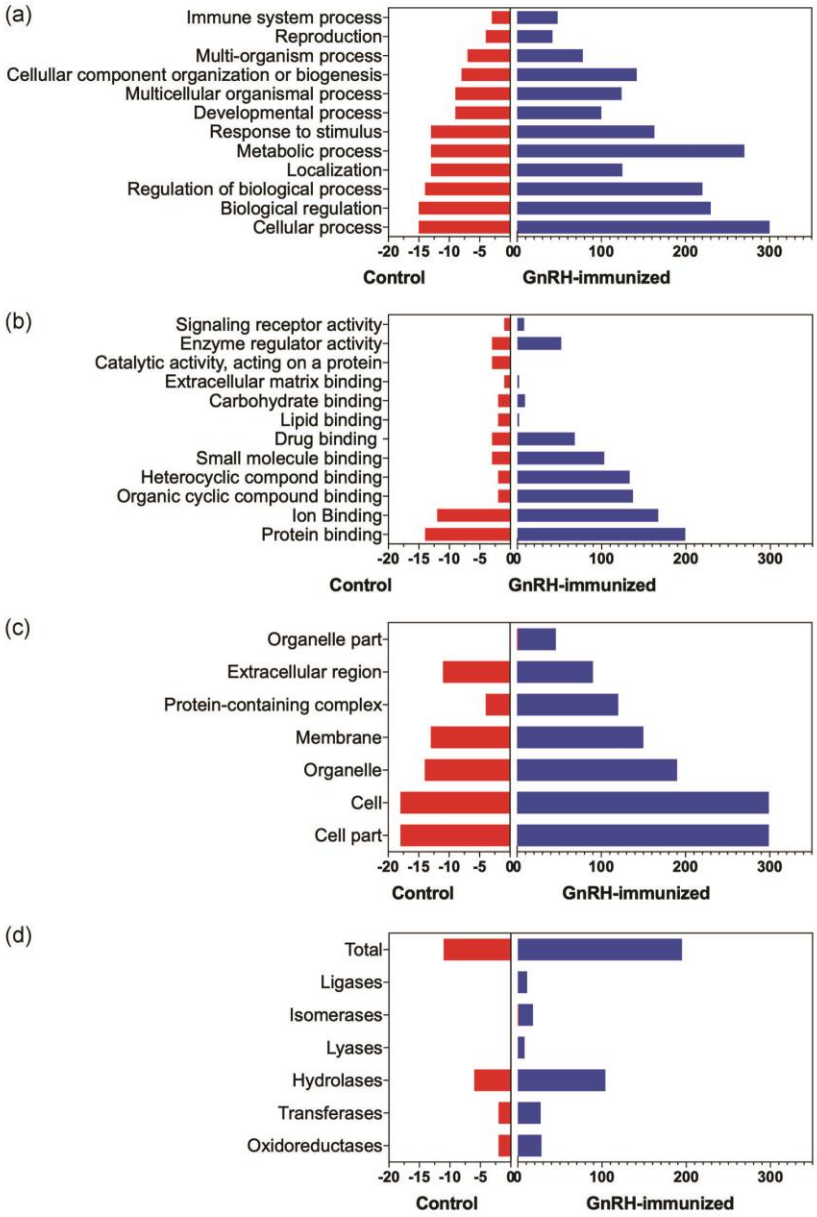

FIGURE 2 Distribution of proteins identified in cauda epididymal fluid from healthy (control) and GnRH-immunized boars according to (a) biological process, (b) molecular function, (c) cellular component, and (d) enzyme code distribution. Analysis performed using Blas2Go software

such as apoptosis, phosphoinositide 3-kinase–protein kinase B–mammalian target of rapamycin (PI3K–AKT–mTOR) and mTOR complex 1 signaling, MYC targets, oxidative stress, and proteasome (Figure 3a,b). In accordance, upregulated Kyoto Encyclopedia of Genes and Genomes (KEGG) pathways indicate changes in important metabolic routes, like glycolysis and gluconeogenesis, and metabolism of sugars, fatty acids, and amino acids. Enriched genes related to KEGG pathways directly associated to tissue organization, like "regulation of actin cytoskeleton," "focal adhesion," and "glycosaminoglycan degradation" were also significantly affected by anti-GnRH immunization (Figure 3c,d). Testis-expressed genes counted for 166 in control group and 351 in GnRH-immunized group. Tissue enrichment analysis with the GENE2FUNC tool demonstrated a high expression of the prioritized genes in testis (Figure 4a,b).

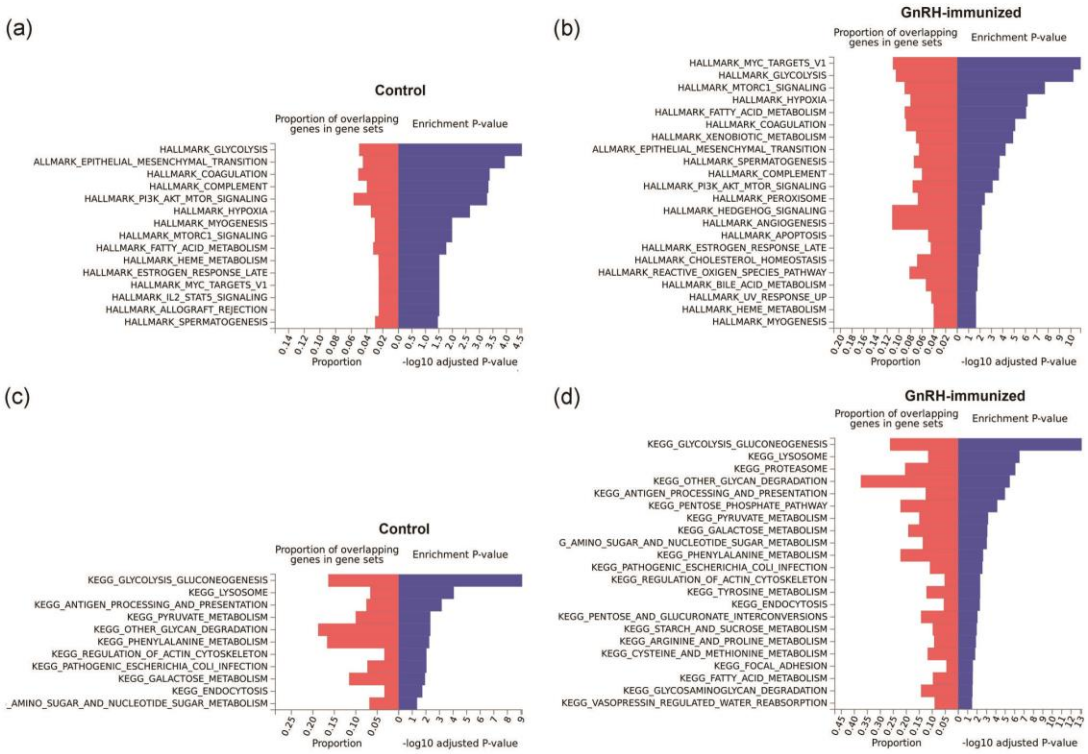

FIGURE 3 Analysis of the genes expressed in the testis related to proteins identified in the cauda epididymal fluid from control and GnRH-immunized boars. (a,b) Hallmark pathways identified using hypergeometric tests indicating overrepresentation of testis-expressed genes within gene sets from Molecular Signatures Database. (c,d) Kyoto Encyclopedia of Genes and Genomes pathway enrichment, indicating the most prevalent signaling pathways. Analysis performed using GENE2FUNC tool from Functional Mapping and Annotation of Genome-Wide Association platform

The use of GO terms classification by Functional Mapping and Annotation of Genome-Wide Association (FUMA) analysis make possible to infer which proteins are related to vesicle and exosome secretion, an important feature of epididymal cells. Thirty-four proteins were associated with vesicle transport and secretion, with 22 proteins present in both groups, and 12 proteins found exclusively in the GnRH-immunized group (Figure 5a). Protein–protein interaction (PPI) network of exosome-related proteins is presented in Figure 5b. Of the 12 proteins upregulated in CEF of immunocastrated boars, five proteins (apolipoprotein H, apolipoprotein A1, fibrinogen beta chain, plasminogen, and Ig-like domain-containing protein) presented closer interactions.

To verify how GnRH immunization would influence the expression of differentially identified proteins (fold change > 2.0) between groups, the relative expression of five genes were assessed by quantitative polymerase chain reaction (qPCR). The analysis of the genes CCT5, CST3, MAM2B2, nucleobindin-2 (NUCB2), and TF revealed little influence of their expression level. Serotranferrin gene (TF) was the only gene with different expression level, presenting a 50% reduction in the testis of GnRH-immunized boars ($p < .074$; Figure 6). Differently, some genes showed significant changes in messenger RNA (mRNA) expression levels in the epididymis, as a consequence of GnRH blocking, together with a marked regionalized gene expression (Figure 7). The MAMB2 gene showed higher relative expression in all epididymal regions between groups, with a 20-fold increase in the cauda epididymis of GnRH-immunized boars ($p = .0003$). A higher relative expression level of the TF gene was also observed in the corpus epididymis of the GnRH-immunized ($p = .0006$). The expression of the genes CCT5 and NUCB2 were downregulated in the GnRH-immunized boars. While the relative expression of CCT5 was reduced in the cauda epididymis of GnRH-immunized boars ($p = .0096$), NUCB2 expression were inferior in the caput ($p = .0255$) and corpus ($p = .0148$) of immunocastrated animals. CST3 was the only gene tested with no difference between experimental groups, presenting a higher expression in cauda in comparison to the other epididymal regions in both groups (control: $p = .0027$; GnRH-immunized: $p < .0001$).

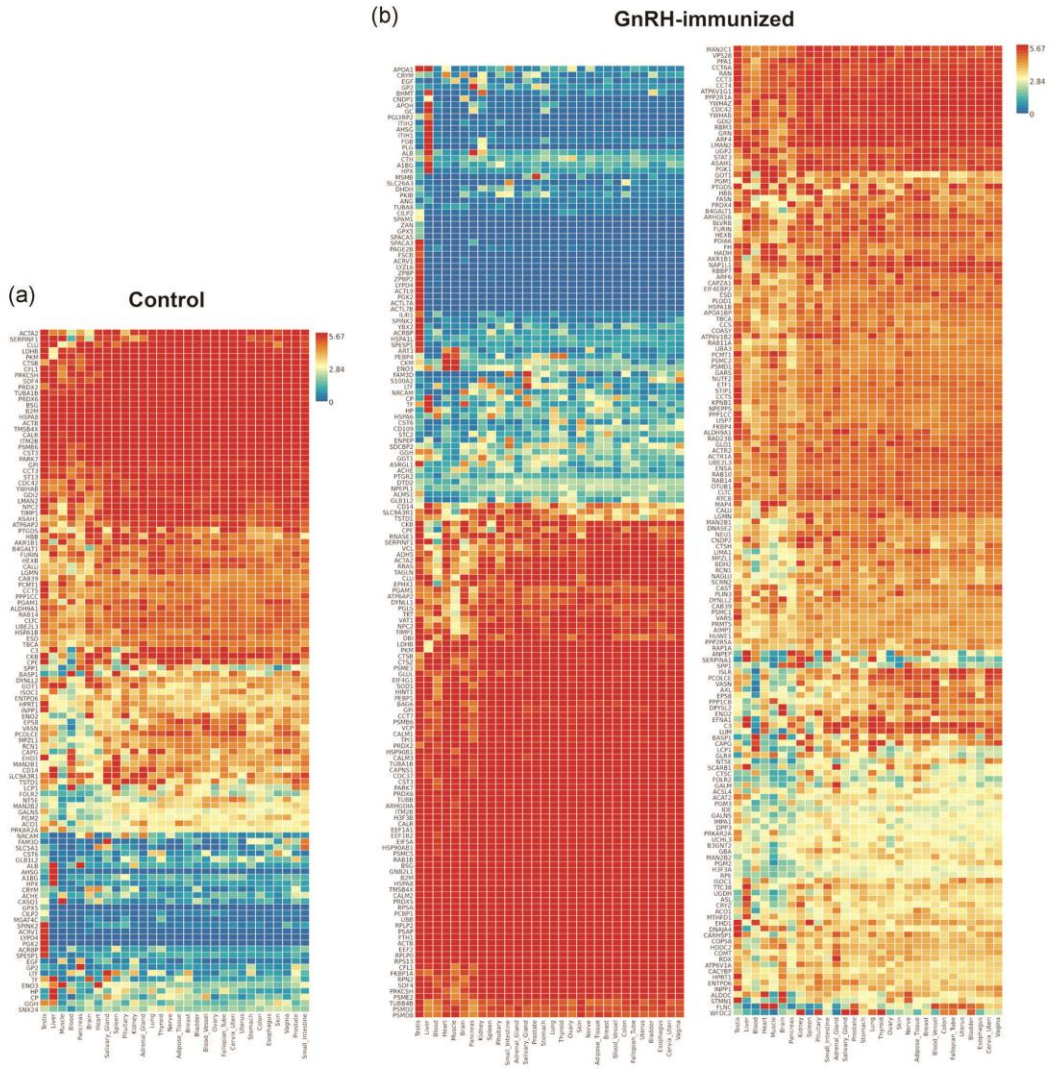

FIGURE 4 Tissue enrichment heatmaps indicating the level of expression of the genes related to cauda epididymal fluid proteins of control group (a) and GnRH-immunized group (b). Analysis performed using GENE2FUNC tool from Functional Mapping and Annotation of Genome-Wide Association platform

3 | DISCUSSION

Cauda epididymis is the final environment of mature spermatozoa before ejaculation. Its fluid is responsible for maintaining cell function and structural viability; thus, changes in this milieu could result in impaired sperm storage and decreased fertility. In the boar, several studies were published aiming to describe the epididymal proteome (Dacheux et al., 2005; Labas et al., 2015; Syntin et al., 1999, 1996) as well as the seminal plasma protein profile (Gonzalez-Cadavid et al., 2014; Perez-Patino et al., 2016, 2019; Strzezek et al., 2005) and molecular markers associated with semen quality (De Lazari et al., 2019) and freezability (Valencia, Gomez, Lopez, Mesa, & Henao, 2017; Vilagran et al., 2015). However, there is a gap in understanding how the epididymal milieu is impacted in pathological conditions, such as HPT-axis disruption. By comparing the CEF proteome of healthy and GnRH-immunized boars, a model for human secondary hypogonadism (Schorr-Lenz et al., 2016; Weber, Alves, Abujamra, & Bustamante-Filho, 2018), we observed a considerable effect in the protein composition, both quantitatively and qualitatively. Together with a better understanding of the impacts of HPT-axis disruption in the CEF, differentially expressed proteins are putative seminal biomarkers for secondary hypogonadism.

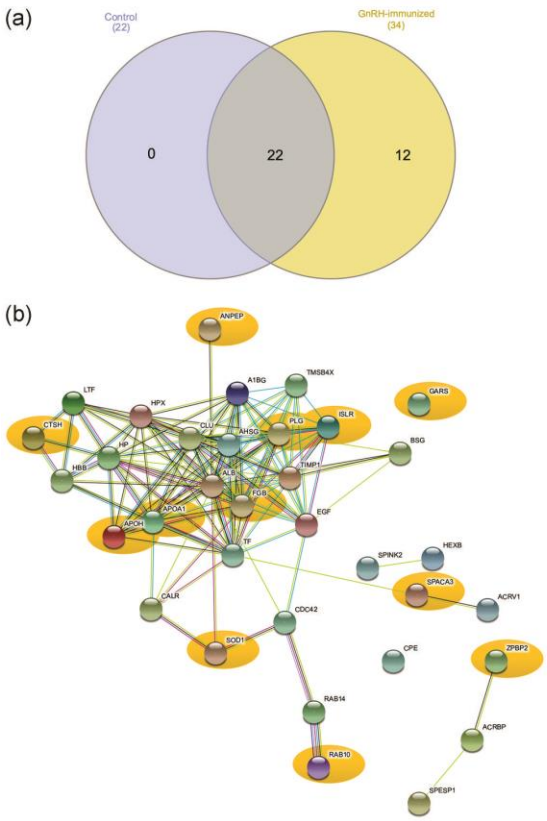

FIGURE 5 In silico analysis of the proteins classified with the gene ontology terms "vesicle" (GO:0031982) and "vesicle lumen" (GO:0031983). (a) Vesicle-related genes expressed in the testis identified in the cauda epididymal fluid (CEF) proteomes of healthy and GnRH-immunized boars, as indicated by Functional Mapping and Annotation of Genome-Wide Association analysis. (b) Protein–protein interaction network generated by string server indicating in yellow the upregulated proteins found in GnRH-immunized boars CEF

The total number of proteins identified in the CEF increased 2.3 times in animals subjected to immunocastration in comparison to control group. In fact, 58.9% ($n = 414$) of the 703 proteins found in the GnRH-immunized group were considered unique/exclusive in this group. Conversely, in the CEF proteome of control group had only 15 of 301 (5.0%) of exclusive proteins. This profound effect is a result of severe changes in the physiology of the testis and epididymis. GnRH blocking and disrupt the synthesis of steroid hormones, leading to a severe impairment of seminiferous tubuli structure. As demonstrated previously, anti-GnRH vaccination leads to a reduction of 18% of tubuli diameter due to changes ranged from mild disruption, such as spermatocyte loss and decrease in the normal number of layers of germ cells, to severe loss of germ cells (Einarsson et al., 2011). Also, vaccinated boars clearly showed a disruption in the number and morphology of Leydig cells, with loss of cytoplasmic eosinophilia and occurrence of pycnotic-like nuclei (Einarsson et al., 2011).

Other studies, using flutamide as a antiandrogen, describe that it affects the expression of junction proteins and junction complex structure, not only by inhibiting androgen receptor activity, but also by modulating protein kinase-dependent signaling in testicular cells (Chojnacka et al., 2016; Hejmej & Bilinska, 2018). As expected, the epididymis is also affected by flutamide exposure, with increased epididymal cells apoptosis, lower androgen receptor expression, concomitant with decreased Cx43 (gap junction protein connexin43; Lydka et al., 2011). These effects might explain the increase in the number of proteins usually found in the cytoplasm or organelles. Despite the important effects of flutamine in testicular and epididymal androgen action (Gorowska, Zarzycka, Chojnacka, Bilinska, & Hejmej, 2014), the role of estrogens in male reproductive organs has also to be considered. Immunocastration reduces serum estradiol levels to similar values as surgical castration (Brunius et al., 2011), and it might impact the function of efferent ductules and initial segment epididymis, regions where estrogens have a predominant role (Joseph, Shur, & Hess, 2011).

The remarkable increase in enzymes after anti-GnRH immunization, specially hydrolases and oxidoreductases, seems to turn the cauda epididymal milieu in a toxic environment for the stored spermatozoa. The abundance of active esterases, lipases, phosphatases, glycosidases, peptidases, and nucleosidases could impair sperm function and structure. Some important enzymes associated with energy metabolism, such as triosephosphate isomerase and phosphoglycerate mutase 2, were upregulated in immunized CEF (14X and 7.4X, respectively). Also, enzymes and chaperones important for the redox balance of the CEF were affected, including serotransferrin (20.8X), heat shock protein 90 (3.3X), and epididymal secretory glutathione peroxidase (3.1X). Therefore, the redox balance of the cauda epididymal milieu is altered, possibly affecting spermatozoa physiological processes, which depend on reactive oxygen species as signaling molecules (Kothari, Thompson, Agarwal, & du Plessis, 2010; Leisegang, Henkel, & Agarwal, 2017).

A number of events related to sperm fertility are potentially dependent of a proper redox environment, such the sperm nuclear condensation. During the spermatogenic process, histones are replaced by transition proteins and ultimately by protamines. While the transition proteins also play significant roles during spermatogenesis, protamines are required for adequate sperm structure and function (Fujii & Imai, 2014). Sulfoxidation of protamine cysteines residues provides chromatin with resistance against oxidative stress, which is accomplished in the epididymis (Kanippayoor, Alpern, & Moehring, 2013). The majority of the sulfoxidation in protamines occurs in the epididymis where the maturation of sperm proceeds. In mice, the spermatozoa lacking both the sperm nuclear GPX4 and the epididymal glutathione peroxidase 5 activities presented delayed and defective nuclear compaction, nuclear instability and DNA damage (Noblanc et al., 2012). Therefore, an unbalanced expression of redox enzymes, as found in GnRH-immunized CEF, would impair spermatozoa nuclear structural stability and condensation.

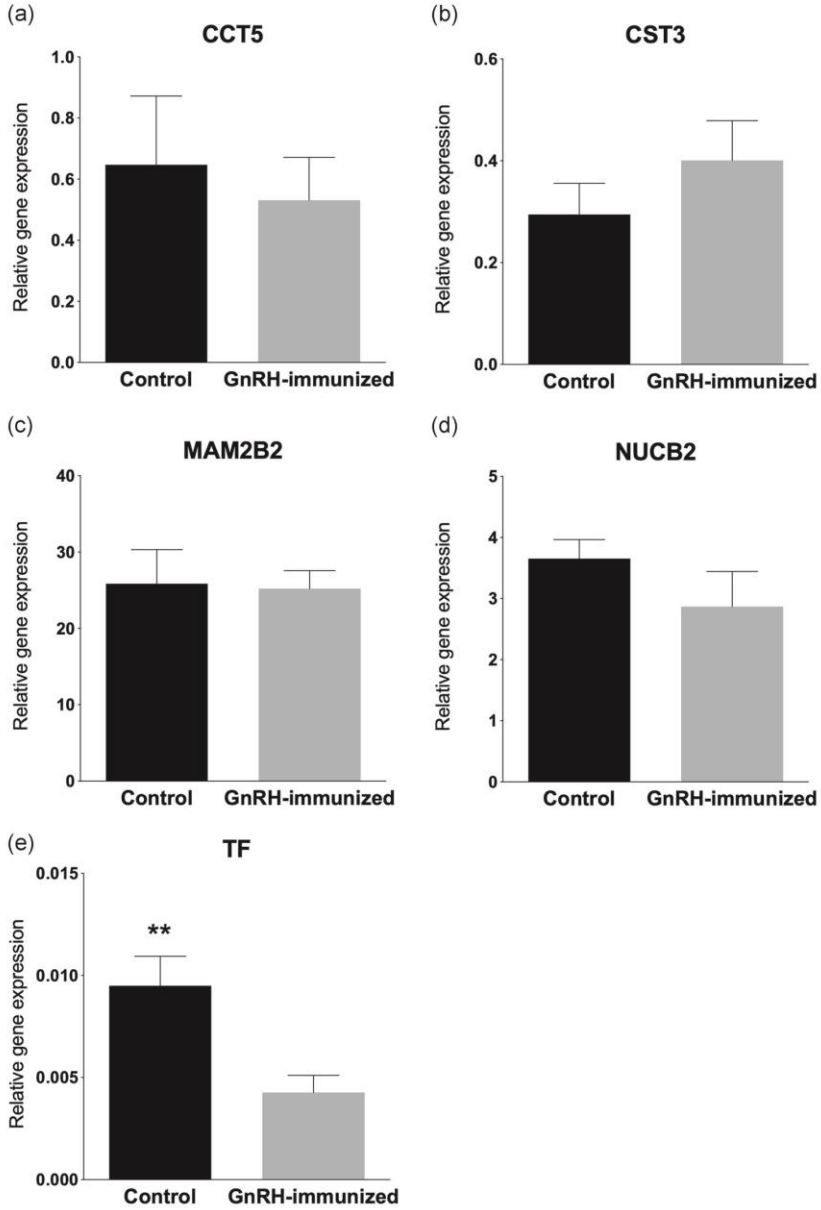

FIGURE 6 Testicular messenger RNA expression of genes related to the synthesis of the proteins (a) protein-chaperonin containing TCP1, subunit 5 (epsilon); (b) cystatin-C; (c) epididymis-specific alpha-mannosidase; (d) nucleobindin-2; and (e) serotransferrin. $^{**}p < .007$

GO and hallmark pathways analyses revealed the increase of proteins associated with key pathways for spermatogenesis. The increase of proteins associated with the PI3K/Akt/mTOR signaling pathway suggests an upregulation of these pathways, associated with suppression of autophagy and promotion of necrosis in several cell types (Ozturk, Steger, & Schagdarsurengin, 2017; Toocheck et al., 2016; Zhang et al., 2012). The testicular damage caused by anti-GnRH immunization via Sertoli and germ cells necrosis could explain the identification of more than 400 proteins exclusively present in the CEF of immunocastrated boars.

One limitation of the approach used in this study was that CEF included soluble proteins as well as extracellular vesicles (Lotvall et al., 2014). Epididymosomes are a heterogeneous population of small membrane bound extracellular vesicles that are released from

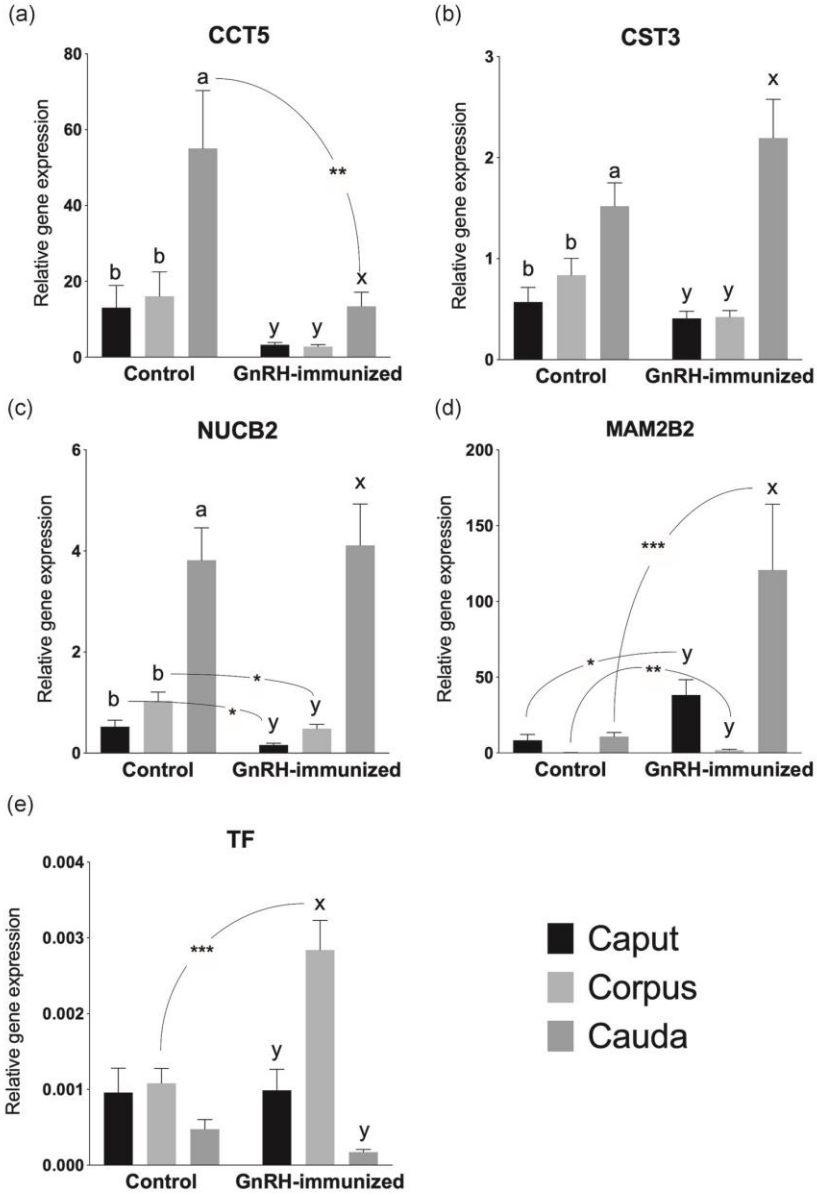

FIGURE 7 Epididymal messenger RNA expression of genes related to the synthesis of the proteins (a) protein-chaperonin containing TCP1, subunit 5 (epsilon); (b) cystatin-C; (c) epididymis-specific alpha-mannosidase; (d) nucleobindin-2; and (e) serotransferrin. Statistical differences among regions within a group are indicated by superscripts a, b and x, y, respectively ($p < .05$). Asterisks indicate difference between groups: $^{*}p < .05$; $^{**}p < .01$, $^{***}p < .001$

the epididymal epithelium via an apocrine secretory mechanism (Hermo & Jacks, 2002; Machtinger, Laurent, & Baccarelli, 2016; Nixon et al., 2019). They contribute with the alteration of the sperm proteome by delivering a diverse macromolecular payload (including proteins, lipids, micro RNAs) to spermatozoa (Mulcahy, Pink, & Carter, 2014). Despite the sample processing method used, by means of bioinformatics, it was possible to identify proteins associated with vesicles, possibly the epididymosomes. Thus, these analyses revealed 12 genes upregulated in GnRH-immunized boars in comparison to the control group. Among the identified genes, some are associated to cell binding (APOH), cholesterol efflux (APOA1), zona pellucida binding (ZPBP2), egg binding (SPACA3) antioxidant scavenging (SOD1).

Although the real effect of GnRH blocking in the proteome of the epididymosomes is currently unknown, the present results suggest that a hypogonadal condition could alter the epididymosomal protein content.

The analysis of gene expression of five CEF proteins differently expressed between groups suggests an endocrine regulation of the expression of CCT5, MAM2B2, NUCB2, and TF genes in the epididymis. Although the level of epididymal expression of NUCB2 and TF could explain the differences found in the proteome between groups, this is not true for the other genes evaluated. This observation suggests that the CEF composition is defined not only by testicular and epididymal secretion, but also the fate of the protein during epididymal transit. The contrasting results found in qPCR and proteomics results could be a related to proteolytic activities that occurs during the epididymal maturation (Baska et al., 2008).

Several proteins associates with the ubiquitin–proteasome system were identified exclusively in the GnRH-immunized CEF proteome, such as ubiquitin carboxyl-terminal hydrolase isozyme L3, ubiquitin, ubiquitin thioesterase OTUB1, E3-ubiquitin-protein ligases, ubiquitin-conjugating enzyme, ubiquitin-like modifier-activating enzyme, proteasome subunit beta type-6, 26S proteasome non-ATPase regulatory subunit, proteasome activator complex subunit 1 and 2, among others. The gene enrichment analysis of both proteomes indicates an increasing in proportion of overlapping genes in gene sets and the respective enrichment *p* values of the following canonical pathways involved with proteasome activity, autodegradation of the E3-ubiquitin ligase COP1, protein folding, antigen processing ubiquitination proteasome degradation (the Supporting Information Material). These findings indicate that an endocrine disruption in the HPT axis result in an impairment of the ubiquitin–proteasome system (UPS) in the epididymis, probably related with the drastic changes in the CEF proteome seen in this study. More than 30 different enzymes related to ubiquitination are involved in the control of spermatogenesis, being involved with some stages of sperm development (Hou & Yang, 2013). For example, Lerer-Goldshtein et al. (2010) demonstrated that a modification in gene expression or deficiency in the ubiquitin–proteasome, E3-ubiquitin ligase TATA element modulatory factor, results in defective sperm formation (head defects and coiled tails; Brohi & Huo, 2017). However, the roles of protein degradation go beyond the efferent ductules. Several publications have investigated the role of UPS and related proteins with epididymal maturation, sperm quality control, and male fertility (Sutovsky, 2003, 2015; Sutovsky et al., 2001; Thompson, Ramalho-Santos, & Sutovsky, 2003; Zigo, Jonakova, Manaskova-Postlerova, Kerns, & Sutovsky, 2019). As elegantly described by Baska et al. (2008), the activity of the ubiquitin system is not limited to the intracellular environment. Later, it was demonstrated that defective spermatozoa that have undergone proper ubiquitination are eliminated by the epididymis by the ubiquitin–proteasome pathway of the epididymis (Eskandari-Shahraki, Tavalaee, Deemeh, Jelodar, & Nasr-Esfahani, 2013). Therefore, the presence of UPS-related proteins in the epididymal milieu contributes with the role of ubiquitination as a sperm quality control process. Our findings clearly demonstrate the impact of anti-GnRH immunization in CEF proteins involved in the UPS in the swine. Thus, one may consider that man presenting secondary hypogonadism (Basaria, 2014; Giannetta, Gianfrilli, Barbagallo, Isidori, & Lenzi, 2012; Marino, Moriondo, Vighi, Pignatti, & Simoni, 2014) could also present an impairment of these events, leading to poor semen quality and infertility.

4 | MATERIALS AND METHODS

4.1 | Animals and experimental design

For this study, 20 crossbred (Large-White and Duroc) boars between 300 and 540 days old were used. All boars were fed with a corn and soy diet and water ad libitum, according to their nutritional requirements (NRC 2012). This study was conducted according to protocols approved by the Animal Experimentation Ethics Committee (CEUA/UNIVATES Protocol 001/2015). Animals assigned to the control group ($n = 10$) were orchidectomized and the epididymides collected. For the GnRH-immunized group, boars ($n = 10$) were immunized against the gonadotropin releasing hormone, 4 and 8 weeks before slaughter, following the Vivax® (Pfizer) protocol (Schorr-Lenz et al., 2016; Weber et al., 2018). Blocking GnRH results in a drastic decrease in serum testosterone and estrogen levels (Zamaratskaia et al., 2008). As consequence, boars present reduced testicular weight and diminished seminiferous tubuli diameter due to severe loss of germ cells (Einarsson et al., 2011), showing a similar pathological presentation of clinical testicular degeneration associated to HPT-axis disruption. Epididymides were then collected in a local slaughterhouse.

4.2 | Preparation of CEF protein extracts

Epididymal sections of region 9, corresponding to boar cauda epididymis (Dacheux et al., 2005) were dissected and the EF (with spermatozoa) were flushed out and collected in tubes. The suspensions were centrifuged (800*g* for 10 min), and the recovered supernatants were centrifuged (12,000*g* for 1 hr at 4°C) to remove any cell debris. Samples were stored at −80°C after the addition of protease inhibitor cocktail (Sigma-Aldrich). Bicinchoninic acid method was used to determine protein concentrations (Pierce).

CEF samples ($n = 10$) were polled in equal quantities (300 μg of total protein per sample) and then suspended in digestion buffer (8 M urea, 100 mM Tris-HCl, pH 8.5). Proteins were reduced with 5 mM Tris-2-carboxyethyl-phosphine and alkylated with 10 mM iodoacetamide. After the addition of 1 mM $CaCl_2$ (final concentration), protein digestion was done using 2 μg of trypsin (Promega, Madison, WI) by incubation at 37°C during 16 hr. Proteolysis was stopped by adding formic acid (5%). Then, samples were centrifuged at 10,000*g* for 20 min, and the supernatant was collected and stored at −80°C.

4.3 | Multidimensional protein identification technology

For peptide separation, protein digests were pressure-loaded into a 250 μm id capillary packed with 2.5 cm of 5 μm Luna strong cation exchanger (Whatman), followed by 2 cm of 3 μm Aqua C18 reversed phase (Phenomenex) with a 1 μm frit. After washing with wash buffer (95% water, 5% acetonitrile, and 0.1% formic acid), a 100 μm id capillary with a 5 μm pulled tip packed with 11 cm of 3 μm Aqua C18 resin (Phenomenex) was attached via a union. Then, the entire split-column was placed in line with an Agilent 1100 quaternary high-performance liquid chromatography (HPLC) and analyzed using a modified 12-step separation (Santi et al., 2014; Wolters, Washburn, & Yates, 2001). The following buffers were used: Buffer A (5% acetonitrile/0.1% formic acid), Buffer B (80% acetonitrile/0.1% formic acid), and Buffer C (500 mM ammonium acetate, 5% acetonitrile, and 0.1% formic acid). Step 1 consisted of a 60 min gradient from 0–100% (vol/vol) Buffer B. Steps 2–10 had different Buffer C percentages, from 10% to 100%. Finally, an additional step containing 90% (vol/vol) Buffer C and 10% (vol/vol) Buffer B was performed. Pooled samples were analyzed in triplicates.

4.4 | Mass spectrometry

Peptides eluted from the microcapillary column were electrosprayed directly into an LTQ Orbitrap XL mass spectrometer (Thermo Fisher Scientific, San Jose, CA) with the application of a distal 2.5 kV spray voltage. A cycle consisted of one full scan of the mass range (MS; 400–2,000 m/z, resolution of 60,000) followed by five data-dependent collision-induced dissociation (CID) MS/MS spectra in the LTQ. Dynamic exclusion was enabled with a repeat count of 1, a repeat duration of 30 s, an exclusion list size of 150, and exclusion duration of 180 s. The mass window for precursor ion selection was set to 400–1,600, unassigned, and charge 1 was rejected, and the normalized collision energy for CID was set on 35. Scan functions of the mass spectrometer and HPLC solvent gradients were controlled through the XCalibur data system. All MS/MS spectra were analyzed as proposed by Santi et al. (2014) and Weber et al. (2019). Briefly, protein identification and quantification analysis were done with Integrated Proteomics Pipeline (www.integratedproteomics.com/). Tandem mass spectra were extracted into ms2 files from raw files using RawExtract 1.9.9 (McDonald et al., 2004) and were searched using ProLuCID algorithm against the *Sus scrofa* reference sequence database from NCBI, downloaded on July 2015. The peptide mass search tolerance was set to 3 Da, and carboxymethylation (+57.02146 Da) of cysteine was considered to be a static modification. ProLuCID results were assembled and filtered using the DTASelect program (Tabb, McDonald, & Yates, 2002), resulting in a dataset with a false discovery rate of 1% for protein.

4.5 | Bioinformatics and data analysis

The Blast2GO 5.0 tool (Gotz et al., 2008) was used to categorize the proteins detected by GO annotation (Ashburner et al., 2000) according to biological process and molecular function. Also, the metabolic pathways were assessed using the KEGG map module. Other bioinformatics tools were used to determine the subcellular location (TargetP 1.0; cutoff > 0.9; Emanuelsson, Brunak, von Heijne, & Nielsen, 2007) and to predict transmembrane protein topology with a hidden Markov model (TMHMM 2.0; Krogh, Larsson, von Heijne, & Sonnhammer, 2001). SignalP 4.1 was used for prediction of secreted proteins (using cutoff default; Petersen, Brunak, von Heijne, & Nielsen, 2011). TargetP, TMHMM, and SignalP programs are available at http://www.cbs.dtu.dk/services.

All proteins identified by MudPIT in CEF samples were mapped in the Uniprot database using the Retrieve/ID mapping tool. This step allowed the identification of the genes related to the proteins found in CEF of control and GnRH-immunized boars. Then, tissue specificity and gene set enrichment analyses were carried out with GENE2FUNC module implemented in the FUMA studies platform (Watanabe, Taskesen, van Bochoven, & Posthuma, 2017). A first analysis (2 × 2 enrichment tests) included all genes retrieved from Uniprot setting only protein-coding genes as a background gene set. The GTEx v7 comprising 30 general tissue types dataset was used for tissue specificity analyses. Differentially expressed genes (DEGs) sets were precalculated in GENE2FUNC by means of two-sided *t* test for any one of tissues against all others. Then, expression values were normalized (zero-mean) followed by a $\log_2$ transformation of expression values (transcripts per million). After Benjamini–Hochberg correction and absolute log fold change ≥0.58, genes with $p \leq .05$ were defined as DEGs in a given tissue compared to others. Only genes expressed in the testis (epididymis data are not available in FUMA) were reanalyzed by GENE2FUNC for tissue expression, GO and hallmarks based in the Molecular Signatures Database (Liberzon et al., 2015).

An in silico approach was used to verify proteins associated to vesicles secretion and exosomes. Genes classified with GO terms "vesicle" (GO:0031982) and "vesicle lumen" (GO:0031983) were analyzed using the Search Tool for the Retrieval of Interacting Genes/Proteins database (STRING v10.5; Szklarczyk et al., 2014) to construct the PPI network associated with vesicle transport and secretion. All the interactions between proteins were resultant from high-throughput experiments and previous knowledge in curated databases at high level of confidence (sources: experiments, databases; score ≥ 0.90; Szklarczyk et al., 2014).

4.6 | Quantitative polymerase chain reaction

The expression levels of selected genes related to differently expressed proteins were assessed by qPCR. Testicular parenchyma and regions 1, 5, and 9 of the epididymides (Dacheux et al., 2005) were excised, rinsed in ice-cold phosphate-buffered saline, and treated with RNALater® (Invitrogen). Tissues were snap frozen in liquid

nitrogen and stored at −80°C until RNA extraction. Total RNA was extracted from 100 mg of tissue using the GE Healthcare Illustra Spin® Kit. Complementary DNA (cDNA) was synthesized from 1.5 μg of RNA, using M-MLV Reverse Transcriptase® (Invitrogen). The integrity of the RNA was verified by PCR followed by agarose gel electrophoresis using *ACTB* as normalizer gene.

Synthesized cDNA was used for real-time qPCR for amplification of the reference gene β-actin (ACTB; Qi, Chen, Guo, Yu, & Chen, 2009) and of five differentially expressed proteins, as follows: proteins upregulated in control CEF: NUCB2 and epididymis-specific alpha-mannosidase (MAN2B2); proteins upregulated in GnRH-immunized CEF: serotranferrin precursor (TF), chaperonin containing TCP1 subunit 5 (CCT5), and cystatin-C (CST3). Primers are presented in Table S1. SYBR Green qPCR assays were performed on cDNA samples in a StepOne Plus apparatus (Applied Biosystems). Reactions of 25 μl were done in triplicate. Each reaction contained 10 μl cDNA (diluted 1:50), 4.14 μl water, 2 μl 10X buffer (200 mM Tris-HCl [pH 8.4], 500 mM KCl), 3.31 mM $MgCl_2$, 0.11 mM dNTPs, 0.22 mM of each primer, 2 μl SYBR green (diluted 1:10,000; Molecular Probes), and 0.625 μl of Platinum Taq DNA Polimerase (5 U/μl; Invitrogen). The parameters for qPCR reaction were: 95°C for 15 min, 45 cycles with a 15 s denaturation step at 95°C, followed by a 56°C annealing step for 30 s and a 72°C extension step for 30 s and a final extension step at 72°C for 10 min. Melting curves were done with 0.3°C increase every 30 s. Fluorescence detection was performed immediately at the end of each annealing step and the specificity of the amplification was confirmed by analyzing the melting curves. A no-template control was also included in each assay. LinRegPCR software was used to calculate PCR efficiency (Ramakers, Ruijter, Deprez, & Moorman, 2003; Ruijter et al., 2009). The relative expression ratio was calculated compared to the arithmetic mean expression of ACTB (Pfaffl, 2001).

4.7 | Statistical analysis

Data were tested for normality using the Shapiro–Wilk test. To verify if immunization against GnRH influences target genes expression, Student's *t* test or Mann–Whitney test were used to compare means between groups whether data presented normal or nonnormal distribution, respectively. Differences in gene expression between epididymal regions verified by one-way analysis of variance, followed by the Tukey's post-hoc test. All analyses were performed using the GraphPad Prism 8 software and a significance level of 5% was considered to indicate statistical difference.

5 | CONCLUSION

The data obtained in the present study using a swine model for secondary hypogonadism provides novel insights into the changes in the cauda epididymis milieu and the possible implications on sperm maturation, storage and quality. Such approach allowed us to (a) understand the changes in the proteomic landscape of the CEF caused by GnRH immunological blocking and to (b) identify biomarker candidates for this condition in man. Due to anatomo-physiological aspects and obvious methodological hurdles, the study of the human epididymal content is a difficult task and, therefore, the GnRH-immunized swine is a viable animal model to investigate epididymal physiopathology and its impacts in human fertility.

ACKNOWLEDGMENTS

This study was supported by the Conselho Nacional de Desenvolvimento Científico e Tecnológico (CNPq) Grant 447251/2014-7, Fundação de Amparo à Pesquisa do Estado do Rio Grande do Sul Grant 16/2551-0000223-1, and Fundação Vale do Taquari de Educação e Desenvolvimento Social Grant 8/Reitoria/Univates/2016. Ana Paula Binato de Souza was a CAPES scholarship recipient. The authors wish to thank the Associação de Criadores de Suínos do Rio Grande do Sul, Cooperativa Languiru, and BRF for the provision of reproductive tissue samples.

CONFLICT OF INTERESTS

The authors declare that there are no conflict of interests.

ORCID

Lucélia Santi http://orcid.org/0000-0002-5698-7006
Walter O. Beys-da-Silva https://orcid.org/0000-0001-8329-7839
John R. Yates https://orcid.org/0000-0001-5267-1672
Ivan C. Bustamante-Filho http://orcid.org/0000-0002-0793-8443

REFERENCES

Ashburner, M., Ball, C. A., Blake, J. A., Botstein, D., Butler, H., Cherry, J. M., … Sherlock, G. (2000). Gene ontology: Tool for the unification of biology. The Gene Ontology Consortium. *Nature Genetics*, *25*(1), 25–29.

Basaria, S. (2014). Male hypogonadism. *Lancet*, *383*(9924), 1250–1263.

Baska, K. M., Manandhar, G., Feng, D., Agca, Y., Tengowski, M. W., Sutovsky, M., … Sutovsky, P. (2008). Mechanism of extracellular ubiquitination in the mammalian epididymis. *Journal of Cellular Physiology*, *215*(3), 684–696.

Battistone, M. A., Merkulova, M., Park, Y. J., Peralta, M. A., Gombar, F., Brown, D., & Breton, S. (2019). Unravelling purinergic regulation in the epididymis: Activation of V-ATPase-dependent acidification by luminal ATP and adenosine. *The Journal of Physiology*, *597*(7), 1957–1973.

Brohi, R. D., & Huo, L. J. (2017). Posttranslational modifications in spermatozoa and effects on male fertility and sperm viability. *OMICS*, *21*(5), 245–256.

Brunius, C., Zamaratskaia, G., Andersson, K., Chen, G., Norrby, M., Madej, A., & Lundstrom, K. (2011). Early immunocastration of male pigs with Improvac((R))—effect on boar taint, hormones and reproductive organs. *Vaccine*, *29*(51), 9514–9520.

Chojnacka, K., Hejmej, A., Zarzycka, M., Tworzydlo, W., Bilinski, S., Pardyak, L., … Bilinska, B. (2016). Flutamide induces alterations in the cell-cell junction ultrastructure and reduces the expression of Cx43 at the blood-testis barrier with no disturbance in the rat seminiferous tubule morphology. *Reproductive Biology and Endocrinology*, *14*, 14.

Clulow, J., Jones, R. C., & Hansen, L. A. (1994). Micropuncture and cannulation studies of fluid composition and transport in the ductuli efferentes testis of the rat: Comparisons with the homologous metanephric proximal tubule. *Experimental Physiology*, *79*(6), 915–928.

Dacheux, J. L., Belleannee, C., Guyonnet, B., Labas, V., Teixeira-Gomes, A. P., Ecroyd, H., … Dacheux, F. (2012). The contribution of proteomics to

understanding epididymal maturation of mammalian spermatozoa. *Systems Biology in Reproductive Medicine*, *58*(4), 197–210.

Dacheux, J. L., Belleannee, C., Jones, R., Labas, V., Belghazi, M., Guyonnet, B., … Dacheux, F. (2009). Mammalian epididymal proteome. *Molecular and Cellular Endocrinology*, *306*(1-2), 45–50.

Dacheux, J. L., Castella, S., Gatti, J. L., & Dacheux, F. (2005). Epididymal cell secretory activities and the role of proteins in boar sperm maturation. *Theriogenology*, *63*(2), 319–341.

Dacheux, F., & Dacheux, J. L. (1989). Androgenic control of antagglutinin secretion in the boar epididymal epithelium. An immunocytochemical study. *Cell and Tissue Research*, *255*(2), 371–378.

De Lazari, F. L., Sontag, E. R., Schneider, A., Moura, A. A. A., Vasconcelos, F. R., Nagano, C. S., … Bustamante-Filho, I. C. (2019). Seminal plasma proteins and their relationship with sperm motility and morphology in boars. *Andrologia*, *51*(4), e13222.

Dohle, G. R., Arver, S., Bettocchi, C., Jones, T. H., Kliesch, S., & Punab, M. (2015). *Guidelines on male hypogonadism*. European Association of Urology.

Einarsson, S., Brunius, C., Wallgren, M., Lundstrom, K., Andersson, K., Zamaratskaia, G., & Rodriguez-Martinez, H. (2011). Effects of early vaccination with Improvac((R)) on the development and function of reproductive organs of male pigs. *Animal Reproduction Science*, *127*(1-2), 50–55.

Emanuelsson, O., Brunak, S., von Heijne, G., & Nielsen, H. (2007). Locating proteins in the cell using TargetP, SignalP and related tools. *Nature Protocols*, *2*(4), 953–971.

Eskandari-Shahraki, M., Tavalaee, M., Deemeh, M. R., Jelodar, G. A., & Nasr-Esfahani, M. H. (2013). Proper ubiquitination effect on the fertilisation outcome post-ICSI. *Andrologia*, *45*(3), 204–210.

Feugang, J. M., Liao, S. F., Willard, S. T., & Ryan, P. L. (2018). In-depth proteomic analysis of boar spermatozoa through shotgun and gel-based methods. *BMC Genomics*, *19*(1), 62.

Fouchecourt, S., Metayer, S., Locatelli, A., Dacheux, F., & Dacheux, J. L. (2000). Stallion epididymal fluid proteome: Qualitative and quantitative characterization; secretion and dynamic changes of major proteins. *Biology of Reproduction*, *62*(6), 1790–1803.

Fujii, J., & Imai, H. (2014). Redox reactions in mammalian spermatogenesis and the potential targets of reactive oxygen species under oxidative stress. *Spermatogenesis*, *4*(2), e979108.

Gatti, J.-L., Castella, S., Dacheux, F., Ecroyd, H., Métayer, S., Thimon, V., & Dacheux, J.-L. (2004a). Post-testicular sperm environment and fertility. *Animal Reproduction Science*, *82–83*, 321–339.

Giannetta, E., Gianfrilli, D., Barbagallo, F., Isidori, A. M., & Lenzi, A. (2012). Subclinical male hypogonadism. *Best Practice & Research*, *26*(4), 539–550.

Gonzalez-Cadavid, V., Martins, J. A., Moreno, F. B., Andrade, T. S., Santos, A. C., Monteiro-Moreira, A. C., … Moura, A. A. (2014). Seminal plasma proteins of adult boars and correlations with sperm parameters. *Theriogenology*, *82*(5), 697–707.

Gorowska, E., Zarzycka, M., Chojnacka, K., Bilinska, B., & Hejmej, A. (2014). Postnatal exposure to flutamide affects CDH1 and CTNNB1 gene expression in adult pig epididymis and prostate and alters metabolism of testosterone. *Andrology*, *2*(2), 186–197.

Gotz, S., Garcia-Gomez, J. M., Terol, J., Williams, T. D., Nagaraj, S. H., Nueda, M. J., … Conesa, A. (2008). High-throughput functional annotation and data mining with the Blast2GO suite. *Nucleic Acids Research*, *36*(10), 3420–3435.

Gupta, P. K. (2012). Toxicity of herbicides. In R. C. Gupta (Ed.), *Veterinary toxicology: Basic and clinical principles* (pp. 631–652). New York, NY: Academic Press.

Hejmej, A., & Bilinska, B. (2018). The effects of flutamide on cell-cell junctions in the testis, epididymis, and prostate. *Reproductive Toxicology*, *81*, 1–16.

Hermo, L., & Jacks, D. (2002). Nature's ingenuity: Bypassing the classical secretory route via apocrine secretion. *Molecular Reproduction and Development*, *63*(3), 394–410.

Hinton, B. T., Galdamez, M. M., Sutherland, A., Bomgardner, D., Xu, B., Abdel-Fattah, R., & Yang, L. (2011). How do you get six meters of epididymis inside a human scrotum? *Journal of Andrology*, *32*(6), 558–564.

Hou, C. C., & Yang, W. X. (2013). New insights to the ubiquitin-proteasome pathway (UPP) mechanism during spermatogenesis. *Molecular Biology Reports*, *40*(4), 3213–3230.

Jeelani, R., Bluth, M. H., & Abu-Soud, H. M. (2016). Toxicology in reproductive endocrinology. *Clinics in Laboratory Medicine*, *36*(4), 709–720.

Joseph, A., Shur, B. D., & Hess, R. A. (2011). Estrogen, efferent ductules, and the epididymis. *Biology of Reproduction*, *84*(2), 207–217.

Kanippayoor, R. L., Alpern, J. H., & Moehring, A. J. (2013). Protamines and spermatogenesis in *Drosophila* and *Homo sapiens*: A comparative analysis. *Spermatogenesis*, *3*(2), e24376.

Kothari, S., Thompson, A., Agarwal, A., & du Plessis, S. S. (2010). Free radicals: Their beneficial and detrimental effects on sperm function. *Indian Journal of Experimental Biology*, *48*(5), 425–435.

Krogh, A., Larsson, B., von Heijne, G., & Sonnhammer, E. L. (2001). Predicting transmembrane protein topology with a hidden Markov model: Application to complete genomes. *Journal of Molecular Biology*, *305*(3), 567–580.

Labas, V., Spina, L., Belleannee, C., Teixeira-Gomes, A. P., Gargaros, A., Dacheux, F., & Dacheux, J. L. (2015). Analysis of epididymal sperm maturation by MALDI profiling and top-down mass spectrometry. *Journal of Proteomics*, *113*, 226–243.

Leisegang, K., Henkel, R., & Agarwal, A. (2017). Redox regulation of fertility in aging male and the role of antioxidants: A savior or stressor. *Current Pharmaceutical Design*, *23*(30), 4438–4450.

Lerer-Goldshtein, T., Bel, S., Shpungin, S., Pery, E., Motro, B., Goldstein, R. S., … Nir, U. (2010). TMF/ARA160: A key regulator of sperm development. *Developmental Biology*, *348*(1), 12–21.

Liberzon, A., Birger, C., Thorvaldsdottir, H., Ghandi, M., Mesirov, J. P., & Tamayo, P. (2015). The Molecular Signatures Database (MSigDB) hallmark gene set collection. *Cell Systems*, *1*(6), 417–425.

Lotvall, J., Hill, A. F., Hochberg, F., Buzas, E. I., Di Vizio, D., Gardiner, C., … Thery, C. (2014). Minimal experimental requirements for definition of extracellular vesicles and their functions: A position statement from the International Society for extracellular vesicles. *Journal of Extracellular Vesicles*, *3*, 26913.

Lydka, M., Kopera-Sobota, I., Kotula-Balak, M., Chojnacka, K., Zak, D., & Bilinska, B. (2011). Morphological and functional alterations in adult boar epididymis: Effects of prenatal and postnatal administration of flutamide. *Acta Veterinaria Scandinavica*, *53*, 12.

Machtinger, R., Laurent, L. C., & Baccarelli, A. A. (2016). Extracellular vesicles: Roles in gamete maturation, fertilization and embryo implantation. *Human Reproduction Update*, *22*(2), 182–193.

Marino, M., Moriondo, V., Vighi, E., Pignatti, E., & Simoni, M. (2014). Central hypogonadotropic hypogonadism: Genetic complexity of a complex disease. *International Journal of Endocrinology*, *2014*, 649154.

McDonald, W. H., Tabb, D. L., Sadygov, R. G., MacCoss, M. J., Venable, J., Graumann, J., … Yates, J. R., 3rd (2004). MS1, MS2, and SQT-three unified, compact, and easily parsed file formats for the storage of shotgun proteomic spectra and identifications. *Rapid Communications in Mass Spectrometry*, *18*(18), 2162–2168.

Michel, V., Pilatz, A., Hedger, M. P., & Meinhardt, A. (2015). Epididymitis: Revelations at the convergence of clinical and basic sciences. *Asian Journal of Andrology*, *17*(5), 756–763.

Mostafalou, S., & Abdollahi, M. (2017). Pesticides: An update of human exposure and toxicity. *Archives of Toxicology*, *91*(2), 549–599.

Mulcahy, L. A., Pink, R. C., & Carter, D. R. (2014). Routes and mechanisms of extracellular vesicle uptake. *Journal of Extracellular Vesicles*, *3*, 24641.

Nixon, B., De Iuliis, G. N., Hart, H. M., Zhou, W., Mathe, A., Bernstein, I. R., … Dun, M. D. (2019). Proteomic profiling of mouse epididymosomes reveals their contributions to post-testicular sperm maturation. *Molecular & Cellular Proteomics*, *18*(Suppl. 1), S91–S108.

Noblanc, A., Peltier, M., Damon-Soubeyrand, C., Kerchkove, N., Chabory, E., Vernet, P., … Kocer, A. (2012). Epididymis response partly compensates for spermatozoa oxidative defects in snGPx4 and GPx5 double mutant mice. *PLoS One*, *7*(6), e38565.

Ozturk, N., Steger, K., & Schagdarsurengin, U. (2017). The impact of autophagy in spermiogenesis. *Asian Journal of Andrology*, *19*(6), 617–618.

Perez-Patino, C., Barranco, I., Parrilla, I., Valero, M. L., Martinez, E. A., Rodriguez-Martinez, H., & Roca, J. (2016). Characterization of the porcine seminal plasma proteome comparing ejaculate portions. *Journal of Proteomics*, *142*, 15–23.

Perez-Patino, C., Parrilla, I., Li, J., Barranco, I., Martinez, E. A., Rodriguez-Martinez, H., & Roca, J. (2019). The proteome of pig spermatozoa is remodeled during ejaculation. *Molecuar & Celluar Proteomics*, *18*(1), 41–50.

Petersen, T. N., Brunak, S., von Heijne, G., & Nielsen, H. (2011). SignalP 4. 0: Discriminating signal peptides from transmembrane regions. *Nature Methods*, *8*(10), 785–786.

Pfaffl, M. W. (2001). A new mathematical model for relative quantification in real-time RT-PCR. *Nucleic Acids Research*, *29*(9), e45.

Qi, S., Chen, J., Guo, R., Yu, B., & Chen, D. (2009). β-Defensins gene expression in tissues of the crossbred and Tibetan pigs. *Journal of Livestock Science*, *123*, 161–168.

Ramakers, C., Ruijter, J. M., Deprez, R. H., & Moorman, A. F. (2003). Assumption-free analysis of quantitative real-time polymerase chain reaction (PCR) data. *Neuroscience Letters*, *339*(1), 62–66.

Ruijter, J. M., Ramakers, C., Hoogaars, W. M., Karlen, Y., Bakker, O., van den Hoff, M. J., & Moorman, A. F. (2009). Amplification efficiency: Linking baseline and bias in the analysis of quantitative PCR data. *Nucleic Acids Research*, *37*(6), e45.

Santi, L., Beys-da-Silva, W. O., Berger, M., Calzolari, D., Guimaraes, J. A., Moresco, J. J., & Yates, J. R., 3rd. (2014). Proteomic profile of *Cryptococcus neoformans* biofilm reveals changes in metabolic processes. *Journal of Proteome Research*, *13*(3), 1545–1559.

Schorr-Lenz, A. M., Alves, J., Henckes, N. A., Seibel, P. M., Benham, A. M., & Bustamante-Filho, I. C. (2016). GnRH immunization alters the expression and distribution of protein disulfide isomerases in the epididymis. *Andrology*, *4*(5), 957–963.

Strzezek, J., Wysocki, P., Kordan, W., Kuklinska, M., Mogielnicka, M., Soliwoda, D., & Fraser, L. (2005). Proteomics of boar seminal plasma—current studies and possibility of their application in biotechnology of animal reproduction. *Reproductive Biology*, *5*(3), 279–290.

Sullivan, R., & Mieusset, R. (2016). The human epididymis: Its function in sperm maturation. *Human Reproduction Update*, *22*(5), 574–587.

Sutovsky, P. (2003). Ubiquitin-dependent proteolysis in mammalian spermatogenesis, fertilization, and sperm quality control: Killing three birds with one stone. *Microscopy Research and Technique*, *61*(1), 88–102.

Sutovsky, P. (2015). New approaches to boar semen evaluation, processing and improvement. *Reproduction in Domestic Animals*, *50*(Suppl. 2), 11–19.

Sutovsky, P., Moreno, R., Ramalho-Santos, J., Dominko, T., Thompson, W. E., & Schatten, G. (2001). A putative, ubiquitin-dependent mechanism for the recognition and elimination of defective spermatozoa in the mammalian epididymis. *Journal of Cell Science*, *114*(Pt 9), 1665–1675.

Syntin, P., Dacheux, J.-L., & Dacheux, F. (1999). Postnatal development and regulation of proteins secreted in the boar epididymis. *Biology of Reproduction*, *61*(6), 1622–1635.

Syntin, P., Dacheux, F., Druart, X., Gatti, J. L., Okamura, N., & Dacheux, J. L. (1996). Characterization and identification of proteins secreted in the various regions of the adult boar epididymis. *Biology of Reproduction*, *55*(5), 956–974.

Szklarczyk, D., Franceschini, A., Wyder, S., Forslund, K., Heller, D., Huerta-Cepas, J., … von Mering, C. (2014). STRING v10: Protein–protein interaction networks, integrated over the tree of life. *Nucleic Acids Research*, *43*(D1), D447–D452.

Tabb, D. L., McDonald, W. H., & Yates, J. R., 3rd (2002). DTASelect and contrast: Tools for assembling and comparing protein identifications from shotgun proteomics. *Journal of Proteome Research*, *1*(1), 21–26.

Thompson, W. E., Ramalho-Santos, J., & Sutovsky, P. (2003). Ubiquitination of prohibitin in mammalian sperm mitochondria: Possible roles in the regulation of mitochondrial inheritance and sperm quality control. *Biology of Reproduction*, *69*(1), 254–260.

Toocheck, C., Clister, T., Shupe, J., Crum, C., Ravindranathan, P., Lee, T. K., … Walker, W. H. (2016). Mouse spermatogenesis requires classical and nonclassical testosterone signaling. *Biology of Reproduction*, *94*(1), 11.

Valencia, J., Gomez, G., Lopez, W., Mesa, H., & Henao, F. J. (2017). Relationship between HSP90a, NPC2 and L-PGDS proteins to boar semen freezability. *Journal of Animal Science and Biotechnology*, *8*, 21.

Vilagran, I., Yeste, M., Sancho, S., Castillo, J., Oliva, R., & Bonet, S. (2015). Comparative analysis of boar seminal plasma proteome from different freezability ejaculates and identification of Fibronectin 1 as sperm freezability marker. *Andrology*, *3*(2), 345–356.

Wade, M. A., Roman, S. D., Jones, R. C., & Aitken, R. J. (2003). Adenylyl cyclase isoforms in rat testis and spermatozoa from the cauda epididymidis. *Cell and Tissue Research*, *314*(3), 411–419.

Watanabe, K., Taskesen, E., van Bochoven, A., & Posthuma, D. (2017). Functional mapping and annotation of genetic associations with FUMA. *Nature Communications*, *8*(1), 1826.

Weber, A., Alves, J., Abujamra, A. L., & Bustamante-Filho, I. C. (2018). Structural modeling and mRNA expression of epididymal beta-defensins in GnRH immunized boars: A model for secondary hypogonadism in man. *Molecular Reproduction and Development*, *85*(12), 921–933.

Weber, A., Argenti, L. E., de Souza, A. P. B., Santi, L., Beys-da-Silva, W. O., Yates, J. R., & Bustamante-Filho, I. C. (2019). Ready for the journey: A comparative proteome profiling of porcine cauda epididymal fluid and spermatozoa. *Cell and Tissue Research*.

Wolters, D. A., Washburn, M. P., & Yates, J. R., 3rd. (2001). An automated multidimensional protein identification technology for shotgun proteomics. *Analytical Chemistry*, *73*(23), 5683–5690.

Zamaratskaia, G., Andersson, H. K., Chen, G., Andersson, K., Madej, A., & Lundstrom, K. (2008). Effect of a gonadotropin-releasing hormone vaccine (Improvac) on steroid hormones, boar taint compounds and performance in entire male pigs. *Reproduction in Domestic Animals*, *43*(3), 351–359.

Zhang, M., Jiang, M., Bi, Y., Zhu, H., Zhou, Z., & Sha, J. (2012). Autophagy and apoptosis act as partners to induce germ cell death after heat stress in mice. *PLoS One*, *7*(7), e41412.

Zhou, W., De Iuliis, G. N., Dun, M. D., & Nixon, B. (2018). Characteristics of the epididymal luminal environment responsible for sperm maturation and storage. *Frontiers in Endocrinology*, *9*, 59.

Zigo, M., Jonakova, V., Manaskova-Postlerova, P., Kerns, K., & Sutovsky, P. (2019). Ubiquitin-proteasome system participates in the de-aggregation of spermadhesin and DQH protein during boar sperm capacitation. *Reproduction*.

SUPPORTING INFORMATION

Additional supporting information may be found online in the Supporting Information section.

How to cite this article: Souza APB, Lopes TN, da Silva AFT, et al. Changes in porcine cauda epididymal fluid proteome by disrupting the HPT axis: Unveiling potential mechanisms of male infertility. *Mol Reprod Dev*. 2020;1–14.
https://doi.org/10.1002/mrd.23408

Table S1 – Primers used for gene expression quantification of porcine CCT5, CST3, MAN2B2, NUCB2 and TF by qPCR.

Genes	Primers sequences (5' → 3')	Acession number	Amplicon size
CCT5	GCTGGATGTGACCTCAGTAG CTAGGTTAGCGCCAGTTTC	NP_001265708.1	104
CST3	AATAGACGCGGATGTCAACG GCGACAGCTGGACTTCACC	NP_001038067.1	316
MAN2B2	CTCAAACTCAGGAGACAGGA CCTGGCTCATACGTACTGTT	NP_999014.1	148
NUCB2	ACAGGTATAGACCACCATGC GTTCCAGATCACTTGTAGCC	XP_003480773.1	121
TF	ATACCAAGGACCTCCTCTTC AGTACAGGCTTCCAGGAGTT	NP_001231582.1	149
ACTB	CATCACCATCGGCAACGAGC TAGAGGTCCTTGCGGATGTC	XM_003124280.4	141

Supplementary data
Changes in porcine cauda epididymal fluid proteome by disrupting the HPT axis: unveiling potential mechanisms of male infertility, by Souza et al.

TFOLD

Accession number	Fold Change	p-value	Description
gi|350580256|ref|XP_003480773.1|	11,33	7,91E-05	PREDICTED: nucleobindin-2 isoform X1 [Sus scrofa]
gi|47523156|ref|NP_999014.1|	5,70	0,003069	epididymis-specific alpha-mannosidase precursor [Sus scrofa]
gi|261245058|ref|NP_001138313.1|	5,33	0,005030	hemoglobin subunit beta [Sus scrofa]
gi|311269573|ref|XP_003132549.1|	3,30	0,043041	PREDICTED: neprilysin isoform 1 [Sus scrofa]
gi|545835516|ref|XP_003356466.3|	2,80	0,012668	PREDICTED: di-N-acetylchitobiase, partial [Sus scrofa]
gi|350591295|ref|XP_003483243.1|	1,90	0,030435	PREDICTED: protein FAM3D isoformX2 [Sus scrofa]
gi|350594172|ref|XP_003483854.1|	1,74	0,009070	PREDICTED: brain acid soluble protein 1 isoform 2 [Sus scrofa]
gi|47523782|ref|NP_999527.1|	1,60	0,003884	lactotransferrin precursor [Sus scrofa]
gi|194036918|ref|XP_001928194.1|	-1,68	0,043276	PREDICTED: thiosulfate sulfurtransferase/rhodanese-like domain-containing protein 1-like isoform X1 [Sus scrofa]
gi|545864333|ref|XP_005652458.1|	-1,78	0,037839	PREDICTED: ceruloplasmin isoform X1 [Sus scrofa]
gi|350587143|ref|XP_001927117.4|	-1,83	0,028749	PREDICTED: legumain isoform X1 [Sus scrofa]
gi|51592135|ref|NP_001004043.1|	-1,88	0,021600	cofilin-1 [Sus scrofa]
gi|47522648|ref|NP_999086.1|	-1,89	0,008945	beta-hexosaminidase subunit beta precursor [Sus scrofa]
gi|77627998|ref|NP_001028187.2|	-2,08	0,009324	angiotensin-converting enzyme isoform 1 precursor [Sus scrofa]
gi|406647880|ref|NP_001254623.2|	-2,10	0,010886	ceruloplasmin precursor [Sus scrofa]
gi|145279215|ref|NP_001077410.1|	-2,47	0,010819	angiotensin-converting enzyme isoform 2 precursor [Sus scrofa]
gi|190360575|ref|NP_001121906.1|	-2,62	0,001182	cysteine-rich secretory protein 1 precursor [Sus scrofa]
gi|545829772|ref|XP_005653315.1|	-3,02	0,003518	PREDICTED: carboxylesterase 5A [Sus scrofa]
gi|47523090|ref|NP_999051.1|	-3,09	0,003170	epididymal secretory glutathione peroxidase precursor [Sus scrofa]
gi|47522736|ref|NP_999118.1|	-3,18	0,001518	hemopexin precursor [Sus scrofa]
gi|545888519|ref|XP_005658137.1|	-3,29	0,010251	PREDICTED: legumain-like [Sus scrofa]
gi|47522774|ref|NP_999138.1|	-3,30	0,001549	heat shock protein HSP 90-alpha [Sus scrofa]
gi|335306431|ref|XP_001925971.3|	-3,39	0,001782	PREDICTED: plastin-3 isoformX1 [Sus scrofa]
gi|47523496|ref|NP_999371.1|	-3,40	0,009715	epididymal secretory protein E1 precursor [Sus scrofa]
gi|545864004|ref|XP_005669896.1|	-3,67	0,006332	PREDICTED: serotransferrin isoform X2 [Sus scrofa]
gi|52353352|ref|NP_001005208.1|	-3,70	8,37E-05	serum albumin precursor [Sus scrofa]
gi|47522624|ref|NP_999098.1|	-3,81	0,002966	arylsulfatase A precursor [Sus scrofa]
gi|545814700|ref|XP_005662159.1|	-3,89	0,002590	PREDICTED: pancreatic secretory granule membrane major glycoprotein GP2 isoform X2 [Sus scrofa]
gi|311248892|ref|XP_003123362.1|	-4,25	0,002178	PREDICTED: lysosomal alpha-mannosidase isoformX1 [Sus scrofa]
gi|311250866|ref|XP_003124328.1|	-4,29	0,006455	PREDICTED: actin, cytoplasmic 1 [Sus scrofa]
gi|545890279|ref|XP_005658515.1|	-5,28	0,000107	PREDICTED: alkaline phosphatase, tissue-nonspecific isozyme [Sus scrofa]
gi|350585298|ref|XP_003127256.3|	-5,29	0,000242	PREDICTED: testis-expressed sequence 101 protein isoform X1 [Sus scrofa]
gi|194038971|ref|XP_001929241.1|	-5,33	0,001028	PREDICTED: probable inactive ribonuclease-like protein 12-like isoform X1 [Sus scrofa]
gi|305855190|ref|NP_001182280.1|	-5,33	0,002590	ly6/PLAUR domain-containing protein 4 precursor [Sus scrofa]
gi|47522636|ref|NP_999092.1|	-5,33	0,015937	aspartate aminotransferase, cytoplasmic [Sus scrofa]
gi|311274943|ref|XP_003134515.1|	-5,35	0,002611	PREDICTED: WAP four-disulfide core domain protein 10A [Sus scrofa]
gi|311252670|ref|XP_003125211.1|	-5,43	0,011898	PREDICTED: calmodulin-like [Sus scrofa]
gi|113205746|ref|NP_001038038.1|	-6,06	0,000116	angiogenin precursor [Sus scrofa]
gi|545877574|ref|XP_005674537.1|	-6,13	0,003522	PREDICTED: LOW QUALITY PROTEIN: actin, beta-like 2 [Sus scrofa]
gi|545831249|ref|XP_005655969.1|	-6,21	0,000735	PREDICTED: testis-expressed sequence 101 protein isoform X6 [Sus scrofa]
gi|311260243|ref|XP_001927987.2|	-6,79	0,000301	PREDICTED: protein CutA isoformX1 [Sus scrofa]
gi|47523540|ref|NP_999393.1|	-6,84	0,000386	prostaglandin-H2 D-isomerase precursor [Sus scrofa]
gi|47522862|ref|NP_999185.1|	-6,93	0,025374	pro-epidermal growth factor precursor [Sus scrofa]
gi|201066358|ref|NP_001128440.1|	-7,38	0,003460	phosphoglycerate mutase 2 [Sus scrofa]
gi|311261284|ref|XP_003128673.1|	-7,80	3,51E-05	PREDICTED: disintegrin and metalloproteinase domain-containing protein 20-like [Sus scrofa]
gi|311247246|ref|XP_003122555.1|	-8,37	1,81E-05	PREDICTED: cystatin-M-like [Sus scrofa]
gi|350583022|ref|XP_001927263.3|	-12,80	0,004220	PREDICTED: 14-3-3 protein zeta/delta isoform X1 [Sus scrofa]
gi|545827404|ref|XP_005652645.1|	-14,00	0,015937	PREDICTED: triosephosphate isomerase isoform X1 [Sus scrofa]
gi|311256291|ref|XP_003126581.1|	-14,89	0,001434	PREDICTED: acrosin-binding protein isoform X1 [Sus scrofa]
gi|47523160|ref|NP_999012.1|	-15,67	0,003750	inhibitor of carbonic anhydrase precursor [Sus scrofa]
gi|113205858|ref|NP_001038067.1|	-15,67	0,011125	cystatin-C precursor [Sus scrofa]
gi|335284508|ref|XP_003124605.2|	-16,22	0,030920	PREDICTED: thiomorpholine-carboxylate dehydrogenase [Sus scrofa]
gi|523580068|ref|NP_001265708.1|	-18,00	0,000106	chaperonin containing TCP1, subunit 5 (epsilon) [Sus scrofa]
gi|347582654|ref|NP_001231582.1|	-20,80	0,000976	serotransferrin precursor [Sus scrofa]

Supplementary data
Changes in porcine cauda epididymal fluid proteome by disrupting the HPT axis: unveiling potential mechanisms of male infertility, by Souza et al.

EXCLUSIVE IN CONTROL

Accession number	Spec Count	Protein ID
gi|545843002|ref|XP_005666475.1|	18	PREDICTED: alpha-1-antitrypsin-like [Sus scrofa]
gi|350597193|ref|XP_003484383.1|	13	PREDICTED: LOW QUALITY PROTEIN: peptidyl-prolyl cis-trans isomerase B [Sus scrofa]
gi|48374067|ref|NP_001001537.1|	8	inter-alpha-trypsin inhibitor heavy chain H4 precursor [Sus scrofa]
gi|335278948|ref|XP_003121222.2|	8	PREDICTED: G-protein coupled receptor 126, partial [Sus scrofa]

gi|311270082|ref|XP_003132759.1|	7	PREDICTED: glutaredoxin-1-like [Sus scrofa]
gi|350593258|ref|XP_003133326.3|	6	PREDICTED: alpha-1,6-mannosylglycoprotein 6-beta-N-acetylglucosaminyltransferase A [Sus scrofa]
gi|545831678|ref|XP_005664699.1|	5	PREDICTED: epididymal sperm-binding protein 1 isoform X1 [Sus scrofa]
gi|255683521|ref|NP_001157493.1|	5	sodium/glucose cotransporter 1 [Sus scrofa]
gi|343098472|ref|NP_001230198.1|	4	calsequestrin-1 precursor [Sus scrofa]
gi|49274610|ref|NP_001001859.1|	4	alpha-1,3-mannosyl-glycoprotein 4-beta-N-acetylglucosaminyltransferase C [Sus scrofa]
gi|311265493|ref|XP_003130681.1|	4	PREDICTED: cathepsin L1-like isoform X1 [Sus scrofa]
gi|350581034|ref|XP_003123920.3|	3	PREDICTED: sorting nexin-24 isoform X1 [Sus scrofa]
gi|178056464|ref|NP_001116693.1|	3	beta-hexosaminidase subunit alpha precursor [Sus scrofa]
gi|350583750|ref|XP_003481579.1|	2	PREDICTED: hsc70-interacting protein isoform 1 [Sus scrofa]
gi|311248295|ref|XP_003123069.1|	2	PREDICTED: izumo sperm-egg fusion protein 4 isoform 1 [Sus scrofa]

Supplementary data
Changes in porcine cauda epididymal fluid proteome by disrupting the HPT axis: unveiling potential mechanisms of male infertility, by Souza et al.

EXCLUSIVE IN GnRH-IMMUNIZED

Accession number	Spec Count	Protein ID
gi|545805908|ref|XP_005660679.1|	111	PREDICTED: glutathione S-transferase P [Sus scrofa]
gi|335288480|ref|XP_001925235.3|	40	PREDICTED: LOW QUALITY PROTEIN: alpha-2-macroglobulin [Sus scrofa]
gi|47522950|ref|NP_999232.1|	39	calpastatin [Sus scrofa]
gi|545816848|ref|XP_005662521.1|	37	PREDICTED: Alstrom syndrome protein 1 isoform X1 [Sus scrofa]
gi|311270662|ref|XP_003132938.1|	35	PREDICTED: phosphatidylethanolamine-binding protein 1 [Sus scrofa]
gi|153792600|ref|NP_001093400.1|	34	fatty acid synthase [Sus scrofa]
gi|178056512|ref|NP_001116600.1|	33	heat shock 70 kDa protein 1-like [Sus scrofa]
gi|311266778|ref|XP_003131242.1|	29	PREDICTED: histone H3.3 [Sus scrofa]
gi|545843050|ref|XP_005656514.1|	28	PREDICTED: calmin (calponin-like, transmembrane) isoform X1 [Sus scrofa]
gi|47523738|ref|NP_999504.1|	27	dnaJ homolog subfamily A member 4 [Sus scrofa]
gi|545812163|ref|XP_005661680.1|	26	PREDICTED: histidine triad nucleotide-binding protein 1-like [Sus scrofa]
gi|335281298|ref|XP_003122400.2|	25	PREDICTED: tubulin beta-4B chain isoform X1 [Sus scrofa]
gi|545835769|ref|XP_005656214.1|	25	PREDICTED: phosphoglucomutase-1 isoform X1 [Sus scrofa]
gi|545847933|ref|XP_005667277.1|	24	PREDICTED: LOW QUALITY PROTEIN: N-acetylated-alpha-linked acidic dipeptidase 2 [Sus scrofa]
gi|345197236|ref|NP_001230811.1|	22	calmin (calponin-like, transmembrane) [Sus scrofa]
gi|47523636|ref|NP_999446.1|	22	complement factor H precursor [Sus scrofa]
gi|545806957|ref|XP_005674623.1|	22	PREDICTED: LOW QUALITY PROTEIN: AHNAK nucleoprotein [Sus scrofa]
gi|545808198|ref|XP_003122961.4|	21	PREDICTED: leucine zipper protein 2, partial [Sus scrofa]
gi|47523768|ref|NP_999520.1|	21	epoxide hydrolase 1 precursor [Sus scrofa]
gi|113205892|ref|NP_001038077.1|	20	tubulin beta chain [Sus scrofa]
gi|116175277|ref|NP_001070695.1|	20	ubiquitin carboxyl-terminal hydrolase isozyme L3 [Sus scrofa]
gi|194043861|ref|XP_001928233.1|	20	PREDICTED: tubulin alpha-1D chain [Sus scrofa]
gi|545806931|ref|XP_005660855.1|	20	PREDICTED: elongation factor 1-gamma [Sus scrofa]
gi|545884624|ref|XP_005657843.1|	20	PREDICTED: LOW QUALITY PROTEIN: ubiquitin-like modifier activating enzyme 1 [Sus scrofa]
gi|545891896|ref|XP_003130977.3|	19	PREDICTED: uncharacterized protein LOC100522509 [Sus scrofa]
gi|335288532|ref|XP_001925819.3|	19	PREDICTED: ubiquitin carboxyl-terminal hydrolase 5 isoform 1 [Sus scrofa]
gi|343962597|ref|NP_001230636.1|	19	cytosolic non-specific dipeptidase [Sus scrofa]
gi|545837880|ref|XP_005665717.1|	18	PREDICTED: histone H2A type 1-F-like [Sus scrofa]
gi|335284210|ref|XP_003354541.1|	18	PREDICTED: heat shock protein beta-1-like isoform 1 [Sus scrofa]
gi|348605274|ref|NP_001231762.1|	18	alcohol dehydrogenase 5 (class III), chi polypeptide [Sus scrofa]
gi|147899784|ref|NP_001090887.1|	18	elongation factor 1-alpha 1 [Sus scrofa]
gi|350593970|ref|XP_001925937.3|	18	PREDICTED: 26S proteasome non-ATPase regulatory subunit 1 [Sus scrofa]
gi|335289610|ref|XP_003355932.1|	18	PREDICTED: alpha-actinin-4 isoformX3 [Sus scrofa]
gi|545890424|ref|XP_003361362.3|	17	PREDICTED: ectonucleotide pyrophosphatase/phosphodiesterase family member 3-like, partial [Sus scrofa]
gi|47523850|ref|NP_999563.1|	17	apolipoprotein A-I preproprotein [Sus scrofa]
gi|343478174|ref|NP_001230356.1|	17	T-complex protein 1 subunit alpha [Sus scrofa]
gi|47523626|ref|NP_999445.1|	17	transitional endoplasmic reticulum ATPase [Sus scrofa]
gi|350584484|ref|XP_003126645.3|	17	PREDICTED: tubulin alpha-8 chain isoform X1 [Sus scrofa]
gi|194033405|ref|XP_001928380.1|	16	PREDICTED: acetyl-CoA acetyltransferase, cytosolic [Sus scrofa]
gi|298677090|ref|NP_001177351.1|	16	superoxide dismutase [Cu-Zn] [Sus scrofa]
gi|157427740|ref|NP_001098779.1|	16	ubiquitin [Sus scrofa]
gi|545857759|ref|XP_005657006.1|	16	PREDICTED: synaptic vesicle membrane protein VAT-1 homolog [Sus scrofa]
gi|335297787|ref|XP_003131575.2|	16	PREDICTED: puromycin-sensitive aminopeptidase isoformX1 [Sus scrofa]
gi|545807264|ref|XP_005660921.1|	15	PREDICTED: syntaxin-3 isoform X1 [Sus scrofa]
gi|311272992|ref|XP_003133677.1|	15	PREDICTED: ribulose-phosphate 3-epimerase-like isoform X1 [Sus scrofa]
gi|343183368|ref|NP_001230248.1|	15	immunoglobulin lambda-like polypeptide 5 precursor [Sus scrofa]
gi|545813941|ref|XP_005662074.1|	15	PREDICTED: T-complex protein 1 subunit zeta-like [Sus scrofa]
gi|80971510|ref|NP_001032228.1|	15	triosephosphate isomerase [Sus scrofa]
gi|194039812|ref|XP_001927727.1|	15	PREDICTED: histone H2A type 1-like [Sus scrofa]
gi|305855148|ref|NP_001182266.1|	15	peptidyl-prolyl cis-trans isomerase FKBP4 [Sus scrofa]
gi|47522678|ref|NP_999068.1|	15	inter-alpha-trypsin inhibitor heavy chain H2 precursor [Sus scrofa]

gi|545805428|ref|XP_005652802.1|	15	PREDICTED: tubulin beta-4B chain isoform X6 [Sus scrofa]
gi|194033860|ref|XP_001927901.1|	15	PREDICTED: UV excision repair protein RAD23 homolog B [Sus scrofa]
gi|545824386|ref|XP_005655529.1|	15	PREDICTED: polycystic kidney disease and receptor for egg jelly-related protein [Sus scrofa]
gi|178057067|ref|NP_001116568.1|	14	hsp90 co-chaperone Cdc37 [Sus scrofa]
gi|240851536|ref|NP_001155875.1|	14	ubiquitin thioesterase OTUB1 [Sus scrofa]
gi|346986428|ref|NP_001231362.1|	14	heat shock 90kD protein 1, beta [Sus scrofa]
gi|346644731|ref|NP_001231134.1|	14	ecto-ADP-ribosyltransferase 3 precursor [Sus scrofa]
gi|350579921|ref|XP_003353801.2|	14	PREDICTED: dipeptidyl peptidase 3-like isoformX1 [Sus scrofa]
gi|346716314|ref|NP_001231169.1|	13	Rho GDP dissociation inhibitor (GDI) beta [Sus scrofa]
gi|311252547|ref|XP_003125148.1|	13	PREDICTED: T-complex protein 1 subunit delta [Sus scrofa]
gi|311246600|ref|XP_001926112.2|	13	PREDICTED: serine/threonine-protein phosphatase 2A activator isoformX1 [Sus scrofa]
gi|178057125|ref|NP_001116576.1|	13	cathepsin Z precursor [Sus scrofa]
gi|350590718|ref|XP_003131850.3|	13	PREDICTED: bleomycin hydrolase [Sus scrofa]
gi|545818213|ref|XP_005662702.1|	13	PREDICTED: LOW QUALITY PROTEIN: xanthine dehydrogenase/oxidase [Sus scrofa]
gi|335300581|ref|XP_003358947.1|	13	PREDICTED: T-complex protein 1 subunit theta isoform 1 [Sus scrofa]
gi|335289253|ref|XP_003126970.2|	13	PREDICTED: nuclear transport factor 2-like [Sus scrofa]
gi|208610190|ref|NP_001129152.1|	12	ubiquitin carboxyl-terminal hydrolase 7 [Sus scrofa]
gi|251823933|ref|NP_001156532.1|	12	cadherin-1 precursor [Sus scrofa]
gi|545858751|ref|XP_005668985.1|	12	PREDICTED: collagen alpha-1(I) chain-like [Sus scrofa]
gi|350580562|ref|XP_003480848.1|	11	PREDICTED: actin-like protein 9 [Sus scrofa]
gi|545813944|ref|XP_005662075.1|	11	PREDICTED: T-complex protein 1 subunit zeta-like isoform X1 [Sus scrofa]
gi|148747594|ref|NP_001092068.1|	11	60S acidic ribosomal protein P0 [Sus scrofa]
gi|162952052|ref|NP_001106151.1|	11	transketolase [Sus scrofa]
gi|350586543|ref|XP_003482212.1|	11	PREDICTED: glutamate--cysteine ligase catalytic subunit isoform 2 [Sus scrofa]
gi|47523266|ref|NP_998954.1|	11	bifunctional coenzyme A synthase precursor [Sus scrofa]
gi|335280610|ref|XP_003353615.1|	11	PREDICTED: LOW QUALITY PROTEIN: talin-1 [Sus scrofa]
gi|545802170|ref|XP_005659934.1|	10	PREDICTED: 60S acidic ribosomal protein P1 isoform X2 [Sus scrofa]
gi|72535192|ref|NP_001026958.1|	10	ras-related protein Rab-11A [Sus scrofa]
gi|47522632|ref|NP_999094.1|	10	pro-cathepsin H precursor [Sus scrofa]
gi|311249251|ref|XP_003123542.1|	10	PREDICTED: 6-phosphogluconolactonase isoform X1 [Sus scrofa]
gi|194044822|ref|XP_001927404.1|	10	PREDICTED: peroxiredoxin-4 isoform X1 [Sus scrofa]
gi|350592249|ref|XP_003483427.1|	10	PREDICTED: V-type proton ATPase subunit B, brain isoform [Sus scrofa]
gi|72535168|ref|NP_001026948.1|	10	perilipin-3 [Sus scrofa]
gi|311256211|ref|XP_001925210.2|	10	PREDICTED: alpha-2-macroglobulin [Sus scrofa]
gi|147905672|ref|NP_001090963.1|	10	poliovirus receptor related 2 precursor [Sus scrofa]
gi|545884199|ref|XP_003135011.3|	10	PREDICTED: CTP synthase 2, partial [Sus scrofa]
gi|47522870|ref|NP_999189.1|	10	serine/threonine-protein phosphatase 2A 65 kDa regulatory subunit A alpha isoform [Sus scrofa]
gi|178056753|ref|NP_001116644.1|	10	glycogen phosphorylase, liver form [Sus scrofa]
gi|545890310|ref|XP_003361314.3|	10	PREDICTED: 26S proteasome non-ATPase regulatory subunit 1-like, partial [Sus scrofa]
gi|335281715|ref|XP_003122673.2|	9	PREDICTED: isoaspartyl peptidase/L-asparaginase isoform X1 [Sus scrofa]
gi|350581733|ref|XP_003124656.3|	9	PREDICTED: calcium-regulated heat stable protein 1 isoformX2 [Sus scrofa]
gi|256838111|ref|NP_001157985.1|	9	zona pellucida-binding protein 2 precursor [Sus scrofa]
gi|113205762|ref|NP_001038043.1|	9	granulins precursor [Sus scrofa]
gi|350589877|ref|XP_003482940.1|	9	PREDICTED: spermatid-associated protein isoformX2 [Sus scrofa]
gi|345441771|ref|NP_001230857.1|	9	aldolase C, fructose-bisphosphate [Sus scrofa]
gi|335285938|ref|XP_003131986.2|	9	PREDICTED: Y-box-binding protein 2 isoform X1 [Sus scrofa]
gi|545870917|ref|XP_005654198.1|	9	PREDICTED: anthrax toxin receptor-like [Sus scrofa]
gi|346421411|ref|NP_001231080.1|	9	proteasome (prosome, macropain) 26S subunit, ATPase, 1 [Sus scrofa]
gi|47522762|ref|NP_999132.1|	9	scavenger receptor class B member 1 [Sus scrofa]
gi|346716148|ref|NP_001231230.1|	9	importin-5 [Sus scrofa]
gi|47523154|ref|NP_999017.1|	8	beta-microseminoprotein precursor [Sus scrofa]
gi|190360587|ref|NP_001121909.1|	8	cysteine-rich secretory protein 2 precursor [Sus scrofa]
gi|392513715|ref|NP_001254774.1|	8	heterogeneous nuclear ribonucleoprotein K [Sus scrofa]
gi|156120148|ref|NP_001095292.1|	8	sialidase-1 precursor [Sus scrofa]
gi|545823190|ref|XP_005663542.1|	8	PREDICTED: protein prune homolog [Sus scrofa]
gi|47522776|ref|NP_999140.1|	8	ferritin heavy chain [Sus scrofa]
gi|311258478|ref|XP_003127625.1|	8	PREDICTED: procollagen-lysine,2-oxoglutarate 5-dioxygenase 1 [Sus scrofa]
gi|311259466|ref|XP_003128111.1|	8	PREDICTED: putative hydroxypyruvate isomerase isoformX1 [Sus scrofa]
gi|194038631|ref|XP_001924224.1|	8	PREDICTED: alpha-mannosidase 2C1 isoformX1 [Sus scrofa]
gi|545810172|ref|XP_005661340.1|	8	PREDICTED: long-chain-fatty-acid--CoA ligase ACSBG2 isoform X1 [Sus scrofa]
gi|545853691|ref|XP_005668202.1|	8	PREDICTED: abl interactor 1-like [Sus scrofa]
gi|350579657|ref|XP_001927830.3|	8	PREDICTED: 78 kDa glucose-regulated protein [Sus scrofa]
gi|545889661|ref|XP_005674251.1|	8	PREDICTED: desmocollin-2, partial [Sus scrofa]
gi|178056221|ref|NP_001116561.1|	8	complement C4 precursor [Sus scrofa]
gi|545885011|ref|XP_005673709.1|	8	PREDICTED: E3 ubiquitin-protein ligase HUWE1 isoform X2 [Sus scrofa]
gi|194043605|ref|XP_001925468.1|	8	PREDICTED: GTP-binding nuclear protein Ran [Sus scrofa]
gi|349501107|ref|NP_001231795.1|	7	ribosomal protein, large, P2 [Sus scrofa]
gi|47522724|ref|NP_999112.1|	7	WAP four-disulfide core domain protein 2 precursor [Sus scrofa]
gi|335283572|ref|XP_003354344.1|	7	PREDICTED: transcriptional activator protein Pur-alpha isoformX1 [Sus scrofa]
gi|346716193|ref|NP_001231245.1|	7	nucleosome assembly protein 1-like 1 [Sus scrofa]

gi|545859175|ref|XP_005669109.1|	7	PREDICTED: sperm acrosome membrane-associated protein 3 isoform X1 [Sus scrofa]
gi|545807276|ref|XP_005660925.1|	7	PREDICTED: syntaxin-3 isoform X5 [Sus scrofa]
gi|545831915|ref|XP_003127328.2|	7	PREDICTED: 17-beta-hydroxysteroid dehydrogenase 14 [Sus scrofa]
gi|350579215|ref|XP_003480558.1|	7	PREDICTED: peptidyl-prolyl cis-trans isomerase A-like [Sus scrofa]
gi|335306783|ref|XP_003360570.1|	7	PREDICTED: rab GDP dissociation inhibitor alpha isoform 1 [Sus scrofa]
gi|350580949|ref|XP_003480929.1|	7	PREDICTED: RGM domain family member B isoform X1 [Sus scrofa]
gi|346421347|ref|NP_001231022.1|	7	glucosamine-6-phosphate isomerase 1 [Sus scrofa]
gi|545807261|ref|XP_003353891.3|	7	PREDICTED: membrane-spanning 4-domains subfamily A member 14 [Sus scrofa]
gi|47522666|ref|NP_999074.1|	7	glutamine synthetase [Sus scrofa]
gi|47523724|ref|NP_999497.1|	7	guanine nucleotide-binding protein subunit beta-2-like 1 [Sus scrofa]
gi|545846764|ref|XP_005667063.1|	7	PREDICTED: osteopontin isoform X3 [Sus scrofa]
gi|47523666|ref|NP_999469.1|	7	proteasome activator complex subunit 1 [Sus scrofa]
gi|194041937|ref|XP_001928912.1|	7	PREDICTED: alpha-centractin [Sus scrofa]
gi|350586098|ref|XP_003482113.1|	7	PREDICTED: PDZ domain-containing protein GIPC2 isoformX2 [Sus scrofa]
gi|545876538|ref|XP_003133871.3|	7	PREDICTED: serine protease 40-like [Sus scrofa]
gi|545894908|ref|XP_005674702.1|	7	PREDICTED: LOW QUALITY PROTEIN: pyridoxal-dependent decarboxylase domain containing 1, partial [Sus scrofa]
gi|350587377|ref|XP_003356918.2|	7	PREDICTED: cytosol aminopeptidase-like [Sus scrofa]
gi|311245256|ref|XP_003121758.1|	7	PREDICTED: LOW QUALITY PROTEIN: protein ERGIC-53 [Sus scrofa]
gi|350586545|ref|XP_003128383.3|	7	PREDICTED: glutamate--cysteine ligase catalytic subunit isoform 1 [Sus scrofa]
gi|545833908|ref|XP_005656083.1|	7	PREDICTED: E3 ubiquitin-protein ligase UBR4-like [Sus scrofa]
gi|311264042|ref|XP_003129970.1|	7	PREDICTED: hypoxia up-regulated protein 1 isoform X1 [Sus scrofa]
gi|335281609|ref|XP_003353842.1|	7	PREDICTED: stress-induced-phosphoprotein 1 [Sus scrofa]
gi|311267179|ref|XP_003131436.1|	7	PREDICTED: alpha-N-acetylglucosaminidase [Sus scrofa]
gi|178056524|ref|NP_001116599.1|	7	heat shock 70 kDa protein [Sus scrofa]
gi|311276019|ref|XP_003135010.1|	7	PREDICTED: G-protein coupled receptor 64 [Sus scrofa]
gi|545846068|ref|XP_005666929.1|	7	PREDICTED: heat shock 70 kDa protein 4L isoform X1 [Sus scrofa]
gi|311268288|ref|XP_003131980.1|	6	PREDICTED: eukaryotic translation initiation factor 5A-1 isoformX3 [Sus scrofa]
gi|545828984|ref|XP_005653287.1|	6	PREDICTED: uncharacterized protein C16orf55 homolog [Sus scrofa]
gi|178056574|ref|NP_001116582.1|	6	ephrin-A1 precursor [Sus scrofa]
gi|545828359|ref|XP_005664319.1|	6	PREDICTED: ubiquitin-conjugating enzyme E2 N [Sus scrofa]
gi|47523832|ref|NP_999554.1|	6	glutathione S-transferase alpha M14 [Sus scrofa]
gi|311267462|ref|XP_003131581.1|	6	PREDICTED: secernin-2 [Sus scrofa]
gi|350591525|ref|XP_003132469.3|	6	PREDICTED: ubiquitin-like modifier-activating enzyme 5 [Sus scrofa]
gi|335292500|ref|XP_003128571.2|	6	PREDICTED: probable D-tyrosyl-tRNA(Tyr) deacylase 2 [Sus scrofa]
gi|47523086|ref|NP_999309.1|	6	peroxiredoxin-5, mitochondrial [Sus scrofa]
gi|80971504|ref|NP_001032223.1|	6	40S ribosomal protein SA [Sus scrofa]
gi|545844182|ref|XP_005666606.1|	6	PREDICTED: uncharacterized protein LOC100739772 [Sus scrofa]
gi|350595948|ref|XP_003135490.3|	6	PREDICTED: iduronate 2-sulfatase [Sus scrofa]
gi|545852995|ref|XP_005668089.1|	6	PREDICTED: ubiquilin-1 isoform X1 [Sus scrofa]
gi|350529411|ref|NP_001231937.1|	6	proteasome (prosome, macropain) 26S subunit, ATPase, 2 [Sus scrofa]
gi|47522792|ref|NP_999148.1|	6	26S protease regulatory subunit 8 [Sus scrofa]
gi|545882495|ref|XP_003134717.3|	6	PREDICTED: podocalyxin isoform X1 [Sus scrofa]
gi|194038534|ref|XP_001929109.1|	6	PREDICTED: prostaglandin reductase 2 isoformX1 [Sus scrofa]
gi|57527982|ref|NP_001009576.1|	6	radixin [Sus scrofa]
gi|350592016|ref|XP_003358886.2|	6	PREDICTED: LOW QUALITY PROTEIN: protein TFG [Sus scrofa]
gi|194041525|ref|XP_001927836.1|	6	PREDICTED: dihydropyrimidinase-related protein 2 isoformX2 [Sus scrofa]
gi|311247536|ref|XP_003122689.1|	6	PREDICTED: bifunctional ATP-dependent dihydroxyacetone kinase/FAD-AMP lyase (cyclizing) isoform X1 [Sus scrofa]
gi|545869109|ref|XP_005657389.1|	6	PREDICTED: disintegrin and metalloproteinase domain-containing protein 1a-like [Sus scrofa]
gi|545811613|ref|XP_005661563.1|	6	PREDICTED: IQ motif containing GTPase activating protein 2 [Sus scrofa]
gi|156120152|ref|NP_001095294.1|	6	complement factor B precursor [Sus scrofa]
gi|305855130|ref|NP_001182307.1|	6	valyl-tRNA synthetase [Sus scrofa]
gi|311261216|ref|XP_001924364.2|	6	PREDICTED: c-1-tetrahydrofolate synthase, cytoplasmic [Sus scrofa]
gi|347800709|ref|NP_001231660.1|	6	scinderin [Sus scrofa]
gi|350587056|ref|XP_003482334.1|	6	PREDICTED: LOW QUALITY PROTEIN: papilin [Sus scrofa]
gi|545808768|ref|XP_005661239.1|	6	PREDICTED: 6-phosphogluconolactonase isoform X2 [Sus scrofa]
gi|47523174|ref|NP_999006.1|	5	whey acidic protein precursor [Sus scrofa]
gi|295444982|ref|NP_001171401.1|	5	sperm acrosome-associated protein 5 precursor [Sus scrofa]
gi|335304924|ref|XP_003360068.1|	5	PREDICTED: WAP four-disulfide core domain protein 10A [Sus scrofa]
gi|147903958|ref|NP_001090965.1|	5	cystatin-B [Sus scrofa]
gi|545895092|ref|XP_003362187.2|	5	PREDICTED: programmed cell death protein 6 isoform X1 [Sus scrofa]
gi|545815590|ref|XP_005655252.1|	5	PREDICTED: TBC1 domain family member 24 [Sus scrofa]
gi|47523432|ref|NP_999339.1|	5	alpha-endosulfine [Sus scrofa]
gi|47522614|ref|NP_999101.1|	5	ribonuclease 4 precursor [Sus scrofa]
gi|545797758|ref|XP_005654435.1|	5	PREDICTED: zinc finger C2HC domain-containing protein 1B, partial [Sus scrofa]
gi|545819696|ref|XP_005674638.1|	5	PREDICTED: LOW QUALITY PROTEIN: maestro heat-like repeat family member 1 [Sus scrofa]
gi|545840970|ref|XP_005666231.1|	5	PREDICTED: transmembrane protein 202 isoform X1 [Sus scrofa]
gi|545873092|ref|XP_005671657.1|	5	PREDICTED: ly6/PLAUR domain-containing protein 6B [Sus scrofa]
gi|47523516|ref|NP_999381.1|	5	inositol monophosphatase 1 [Sus scrofa]
gi|147899312|ref|NP_001090923.1|	5	F-actin capping protein subunit alpha 1 [Sus scrofa]
gi|345199288|ref|NP_001230831.1|	5	protein phosphatase 1, regulatory (inhibitor) subunit 7 [Sus scrofa]

gi|350586350|ref|XP_003128195.3|	5	PREDICTED: GDP-mannose 4,6 dehydratase [Sus scrofa]
gi|51592133|ref|NP_001004042.1|	5	V-type proton ATPase catalytic subunit A [Sus scrofa]
gi|350584406|ref|XP_003355633.2|	5	PREDICTED: solute carrier family 2, facilitated glucose transporter member 3 [Sus scrofa]
gi|335293644|ref|XP_003357019.1|	5	PREDICTED: vitamin D-binding protein [Sus scrofa]
gi|545819718|ref|XP_005655380.1|	5	PREDICTED: speriolin, partial [Sus scrofa]
gi|312062797|ref|NP_001185848.1|	5	proactivator polypeptide precursor [Sus scrofa]
gi|335309466|ref|XP_003361648.1|	5	PREDICTED: vitamin K-dependent protein S, partial [Sus scrofa]
gi|311258421|ref|XP_003127605.1|	5	PREDICTED: 6-phosphogluconate dehydrogenase, decarboxylating [Sus scrofa]
gi|335281454|ref|XP_003122543.2|	5	PREDICTED: cathepsin F isoform X1 [Sus scrofa]
gi|148230645|ref|NP_001090982.1|	5	ADAM metallopeptidase domain 3A (cyritestin 1) precursor [Sus scrofa]
gi|47522786|ref|NP_999145.1|	5	UTP--glucose-1-phosphate uridylyltransferase [Sus scrofa]
gi|545814757|ref|XP_005662170.1|	5	PREDICTED: transmembrane channel-like 5 [Sus scrofa]
gi|350582355|ref|XP_003354851.2|	5	PREDICTED: exportin-1 [Sus scrofa]
gi|350591881|ref|XP_003358824.2|	5	PREDICTED: leishmanolysin-like peptidase isoform 2, partial [Sus scrofa]
gi|311275457|ref|XP_003134747.1|	5	PREDICTED: filamin-C isoformX1 [Sus scrofa]
gi|343432668|ref|NP_001230348.1|	5	RNA binding motif (RNP1, RRM) protein 3 [Sus scrofa]
gi|194036155|ref|XP_001929591.1|	5	PREDICTED: protein S100-A2-like isoform 1 [Sus scrofa]
gi|47523694|ref|NP_999483.1|	5	calpain small subunit 1 [Sus scrofa]
gi|49274647|ref|NP_001001866.1|	5	copper chaperone for superoxide dismutase [Sus scrofa]
gi|545839106|ref|XP_005665954.1|	5	PREDICTED: T-complex protein 11 homolog isoform X1 [Sus scrofa]
gi|545829295|ref|XP_003126924.4|	5	PREDICTED: alanine--tRNA ligase, cytoplasmic isoform X1 [Sus scrofa]
gi|545844858|ref|XP_005653628.1|	4	PREDICTED: carboxypeptidase E-like [Sus scrofa]
gi|311275477|ref|XP_003134759.1|	4	PREDICTED: staphylococcal nuclease domain-containing protein 1-like [Sus scrofa]
gi|47523046|ref|NP_999284.1|	4	acyl-CoA-binding protein [Sus scrofa]
gi|350590240|ref|XP_003483017.1|	4	PREDICTED: lysozyme-like protein 6-like [Sus scrofa]
gi|335282758|ref|XP_003123386.2|	4	PREDICTED: UV excision repair protein RAD23 homolog A isoform X1 [Sus scrofa]
gi|47523490|ref|NP_999372.1|	4	matrilysin precursor [Sus scrofa]
gi|264681466|ref|NP_001161127.1|	4	ribonuclease pancreatic precursor [Sus scrofa]
gi|545803726|ref|XP_005660307.1|	4	PREDICTED: LOW QUALITY PROTEIN: glyoxylate reductase/hydroxypyruvate reductase [Sus scrofa]
gi|311263507|ref|XP_003129712.1|	4	PREDICTED: beta-arrestin-1 isoformX1 [Sus scrofa]
gi|311266924|ref|XP_003131314.1|	4	PREDICTED: beta-2-glycoprotein 1 isoform X1 [Sus scrofa]
gi|545848645|ref|XP_005667423.1|	4	PREDICTED: cell adhesion molecule 1 isoform X1 [Sus scrofa]
gi|50979301|ref|NP_999001.1|	4	major seminal plasma glycoprotein PSP-II precursor [Sus scrofa]
gi|194035504|ref|XP_001927493.1|	4	PREDICTED: vacuolar protein sorting-associated protein 28 homolog [Sus scrofa]
gi|545826633|ref|XP_005664050.1|	4	PREDICTED: nucleosome assembly protein 1-like 1 isoform X3 [Sus scrofa]
gi|311251192|ref|XP_003124491.1|	4	PREDICTED: argininosuccinate lyase-like isoform 1 [Sus scrofa]
gi|545894517|ref|XP_005658832.1|	4	PREDICTED: V-set and immunoglobulin domain-containing protein 1-like [Sus scrofa]
gi|545809112|ref|XP_005652935.1|	4	PREDICTED: UV excision repair protein RAD23 homolog A isoform X3 [Sus scrofa]
gi|311265636|ref|XP_003130749.1|	4	PREDICTED: lysozyme-like protein 1 [Sus scrofa]
gi|545859151|ref|XP_005674660.1|	4	PREDICTED: LOW QUALITY PROTEIN: chaperonin containing TCP1, subunit 6B (zeta 2) [Sus scrofa]
gi|311247879|ref|XP_003122857.1|	4	PREDICTED: 26S protease regulatory subunit 6A isoform X1 [Sus scrofa]
gi|350589013|ref|XP_003130369.3|	4	PREDICTED: calcyclin-binding protein isoform X1 [Sus scrofa]
gi|178056588|ref|NP_001116645.1|	4	ras-related protein Rab-1B [Sus scrofa]
gi|545801828|ref|XP_005659876.1|	4	PREDICTED: beta-Ala-His dipeptidase isoform X1 [Sus scrofa]
gi|545863999|ref|XP_003358602.3|	4	PREDICTED: prostatic acid phosphatase-like [Sus scrofa]
gi|311252459|ref|XP_003125105.1|	4	PREDICTED: poly(rC)-binding protein 1 isoform X1 [Sus scrofa]
gi|335308956|ref|XP_003361437.1|	4	PREDICTED: acylamino-acid-releasing enzyme-like [Sus scrofa]
gi|545822321|ref|XP_005663227.1|	4	PREDICTED: nitrilase homolog 1 isoform X1 [Sus scrofa]
gi|545808992|ref|XP_005661285.1|	4	PREDICTED: ATP-dependent RNA helicase DDX39A isoform X2 [Sus scrofa]
gi|545859572|ref|XP_005657071.1|	4	PREDICTED: phosphatidylinositol transfer protein alpha isoform [Sus scrofa]
gi|113205776|ref|NP_001038050.1|	4	cystathionine gamma-lyase [Sus scrofa]
gi|343790858|ref|NP_001230566.1|	4	uncharacterized protein LOC100157036 [Sus scrofa]
gi|545857085|ref|XP_005668719.1|	4	PREDICTED: beta-2-glycoprotein 1 isoform X2 [Sus scrofa]
gi|264681454|ref|NP_001161122.1|	4	S-adenosylmethionine synthase isoform type-2 [Sus scrofa]
gi|335294000|ref|XP_003129333.2|	4	PREDICTED: 3-hydroxybutyrate dehydrogenase type 2-like isoform 1 [Sus scrofa]
gi|304365428|ref|NP_001182041.1|	4	protein disulfide-isomerase A3 precursor [Sus scrofa]
gi|166796059|ref|NP_001107755.1|	4	aminoacyl tRNA synthase complex-interacting multifunctional protein 1 [Sus scrofa]
gi|47523628|ref|NP_999442.1|	4	aminopeptidase N [Sus scrofa]
gi|178056556|ref|NP_001116620.1|	4	probable aminopeptidase NPEPL1 [Sus scrofa]
gi|545886252|ref|XP_003135355.3|	4	PREDICTED: collagen alpha-5(IV) chain isoform 2 [Sus scrofa]
gi|335285849|ref|XP_003125387.2|	4	PREDICTED: cytosolic 5'-nucleotidase 1B isoformX1 [Sus scrofa]
gi|350578417|ref|XP_001927580.3|	4	PREDICTED: CD109 antigen isoformX1 [Sus scrofa]
gi|545867986|ref|XP_005657299.1|	4	PREDICTED: collagen alpha-1(III) chain-like [Sus scrofa]
gi|350588694|ref|XP_003357434.2|	4	PREDICTED: plasma membrane calcium-transporting ATPase 4-like [Sus scrofa]
gi|545869001|ref|XP_005657376.1|	4	PREDICTED: kinase suppressor of Ras 2, partial [Sus scrofa]
gi|55741862|ref|NP_999548.1|	4	zonadhesin precursor [Sus scrofa]
gi|335308621|ref|XP_003361307.1|	4	PREDICTED: cAMP-dependent protein kinase inhibitor beta-like isoformX2 [Sus scrofa]
gi|194039886|ref|XP_001928622.1|	4	PREDICTED: histone H3.1-like [Sus scrofa]
gi|545823364|ref|XP_005663591.1|	4	PREDICTED: Na(+)/H(+) exchange regulatory cofactor NHE-RF3 isoform X1 [Sus scrofa]
gi|545888279|ref|XP_005674165.1|	4	PREDICTED: ruvB-like 1-like, partial [Sus scrofa]

gi|335293690|ref|XP_003129163.2|	4	PREDICTED: general vesicular transport factor p115 isoform X1 [Sus scrofa]
gi|335301996|ref|XP_001925416.3|	4	PREDICTED: insulin-degrading enzyme isoformX1 [Sus scrofa]
gi|350593938|ref|XP_003133733.3|	4	PREDICTED: cullin-3 isoform X1 [Sus scrofa]
gi|350590384|ref|XP_003131576.3|	4	PREDICTED: importin subunit beta-1 isoformX1 [Sus scrofa]
gi|545875426|ref|XP_005672192.1|	4	PREDICTED: isocitrate dehydrogenase [NADP] cytoplasmic-like isoform X1 [Sus scrofa]
gi|350595384|ref|XP_003134854.3|	4	PREDICTED: glycine--tRNA ligase isoform X1 [Sus scrofa]
gi|545824833|ref|XP_005663885.1|	4	PREDICTED: myosin-9 [Sus scrofa]
gi|348605128|ref|NP_001231714.1|	3	chromosome 7 open reading frame 41 ortholog [Sus scrofa]
gi|311271327|ref|XP_003133106.1|	3	PREDICTED: eukaryotic translation initiation factor 4E-binding protein 2 [Sus scrofa]
gi|346986485|ref|NP_001231390.1|	3	glia maturation factor beta [Sus scrofa]
gi|194040450|ref|XP_001927992.1|	3	PREDICTED: lactoylglutathione lyase isoform 1 [Sus scrofa]
gi|545840626|ref|XP_005653589.1|	3	PREDICTED: calcium and integrin-binding protein 1 [Sus scrofa]
gi|545813950|ref|XP_005662077.1|	3	PREDICTED: T-complex protein 1 subunit zeta-like isoform X3 [Sus scrofa]
gi|335297926|ref|XP_003131645.2|	3	PREDICTED: c-Jun-amino-terminal kinase-interacting protein 4 [Sus scrofa]
gi|194039824|ref|XP_001927985.1|	3	PREDICTED: histone H4-like [Sus scrofa]
gi|178056688|ref|NP_001001867.1|	3	galectin-1 [Sus scrofa]
gi|312062795|ref|NP_001185851.1|	3	mitogen-activated protein kinase 1 [Sus scrofa]
gi|545822723|ref|XP_005663365.1|	3	PREDICTED: ephrin-A1 isoform X1 [Sus scrofa]
gi|47523456|ref|NP_999349.1|	3	serine/threonine-protein phosphatase PP1-beta catalytic subunit [Sus scrofa]
gi|194043487|ref|XP_001929679.1|	3	PREDICTED: transport and Golgi organization protein 2 homolog isoformX1 [Sus scrofa]
gi|311273314|ref|XP_003133809.1|	3	PREDICTED: COP9 signalosome complex subunit 8 isoformX1 [Sus scrofa]
gi|545852754|ref|XP_005668061.1|	3	PREDICTED: aminopeptidase B [Sus scrofa]
gi|47523722|ref|NP_999496.1|	3	hydroxyacyl-coenzyme A dehydrogenase, mitochondrial precursor [Sus scrofa]
gi|350592774|ref|XP_003483533.1|	3	PREDICTED: LOW QUALITY PROTEIN: phenazine biosynthesis-like domain-containing protein [Sus scrofa]
gi|229892828|ref|NP_001153565.1|	3	protein arginine N-methyltransferase 5 [Sus scrofa]
gi|350583320|ref|XP_001926918.3|	3	PREDICTED: mucin-1 [Sus scrofa]
gi|545852104|ref|XP_005667984.1|	3	PREDICTED: melanoma inhibitory activity protein 3-like, partial [Sus scrofa]
gi|545811625|ref|XP_005661568.1|	3	PREDICTED: arylsulfatase B [Sus scrofa]
gi|118403844|ref|NP_001072142.1|	3	UB2D1 [Sus scrofa]
gi|335290008|ref|XP_003356046.1|	3	PREDICTED: ras-related protein R-Ras [Sus scrofa]
gi|194033866|ref|XP_001924388.1|	3	PREDICTED: actin-like protein 7B [Sus scrofa]
gi|194036463|ref|XP_001928684.1|	3	PREDICTED: ras-related protein Rap-1A isoform 1 [Sus scrofa]
gi|311275995|ref|XP_003135004.1|	3	PREDICTED: histone-binding protein RBBP7 isoformX1 [Sus scrofa]
gi|340007402|ref|NP_001229989.1|	3	RAB10, member RAS oncogene family [Sus scrofa]
gi|172072661|ref|NP_001116458.1|	3	tRNA-splicing ligase RtcB homolog [Sus scrofa]
gi|194033864|ref|XP_001924348.1|	3	PREDICTED: actin-like protein 7A [Sus scrofa]
gi|319401915|ref|NP_001188313.1|	3	rho GDP-dissociation inhibitor 1 [Sus scrofa]
gi|350592964|ref|XP_003483582.1|	3	PREDICTED: PDZ and LIM domain protein 1 [Sus scrofa]
gi|194034398|ref|XP_001924948.1|	3	PREDICTED: fibrous sheath CABYR-binding protein-like [Sus scrofa]
gi|335282386|ref|XP_003354050.1|	3	PREDICTED: elongation factor 2 [Sus scrofa]
gi|47522608|ref|NP_999106.1|	3	dolichyl-diphosphooligosaccharide--protein glycosyltransferase subunit 2 precursor [Sus scrofa]
gi|167908791|ref|NP_001108148.1|	3	LIM domain and actin-binding protein 1 [Sus scrofa]
gi|545797910|ref|XP_005652732.1|	3	PREDICTED: LOW QUALITY PROTEIN: ectonucleotide pyrophosphatase/phosphodiesterase family member 1 [Sus scrofa]
gi|47523020|ref|NP_999271.1|	3	zona pellucida-binding protein 1 precursor [Sus scrofa]
gi|545802100|ref|XP_005659919.1|	3	PREDICTED: LOW QUALITY PROTEIN: 60S ribosomal protein L4 [Sus scrofa]
gi|154147714|ref|NP_001093662.1|	3	serine/threonine-protein phosphatase 2A 56 kDa regulatory subunit alpha isoform [Sus scrofa]
gi|153792027|ref|NP_001093402.1|	3	phosphoglycerate kinase 1 [Sus scrofa]
gi|303227969|ref|NP_001181902.1|	3	piwi-like protein 1 [Sus scrofa]
gi|311273235|ref|XP_003133777.1|	3	PREDICTED: intestinal-type alkaline phosphatase isoform 2 [Sus scrofa]
gi|350586196|ref|XP_003482130.1|	3	PREDICTED: nardilysin isoform X2 [Sus scrofa]
gi|281427370|ref|NP_001163993.1|	3	T-complex protein 1 subunit eta [Sus scrofa]
gi|545832172|ref|XP_003481945.2|	3	PREDICTED: L-amino-acid oxidase isoform X1 [Sus scrofa]
gi|545802439|ref|XP_005660021.1|	3	PREDICTED: nidogen-2 [Sus scrofa]
gi|545867932|ref|XP_005657279.1|	3	PREDICTED: LOW QUALITY PROTEIN: exportin-7 [Sus scrofa]
gi|347582595|ref|NP_001231568.1|	3	histidine-rich glycoprotein precursor [Sus scrofa]
gi|350535040|ref|NP_001233182.1|	3	eukaryotic translation initiation factor 4 gamma 1 [Sus scrofa]
gi|350538593|ref|NP_001233247.1|	3	phosphoglucomutase-1 [Sus scrofa]
gi|545813642|ref|XP_005662027.1|	3	PREDICTED: huntingtin-interacting protein 1 [Sus scrofa]
gi|148232174|ref|NP_001090901.1|	3	interleukin-6 receptor subunit beta precursor [Sus scrofa]
gi|545824398|ref|XP_005663793.1|	3	PREDICTED: fibulin-1 isoform X2 [Sus scrofa]
gi|311259825|ref|XP_001924399.2|	3	PREDICTED: leucine-rich repeat-containing protein 16A isoform X1 [Sus scrofa]
gi|343488474|ref|NP_001230453.1|	3	elongation factor 1-beta [Sus scrofa]
gi|178056510|ref|NP_001116621.1|	3	protegrin-1 precursor [Sus scrofa]
gi|343183420|ref|NP_001230268.1|	3	lumican precursor [Sus scrofa]
gi|545852998|ref|XP_005668090.1|	3	PREDICTED: ubiquilin-1 isoform X2 [Sus scrofa]
gi|545830108|ref|XP_005653329.1|	3	PREDICTED: xaa-Pro dipeptidase-like [Sus scrofa]
gi|194036595|ref|XP_001929171.1|	3	PREDICTED: pancreatic alpha-amylase [Sus scrofa]
gi|194018722|ref|NP_001123421.1|	3	creatine kinase M-type [Sus scrofa]
gi|545863946|ref|XP_005669886.1|	3	PREDICTED: thioredoxin reductase 3, partial [Sus scrofa]
gi|350583599|ref|XP_003481550.1|	3	PREDICTED: pancreatic alpha-amylase-like [Sus scrofa]

gi|311243995|ref|XP_003121268.1|	3	PREDICTED: HD domain-containing protein 2 isoform X1 [Sus scrofa]
gi|47523420|ref|NP_999331.1|	3	trans-1,2-dihydrobenzene-1,2-diol dehydrogenase [Sus scrofa]
gi|190360643|ref|NP_001121930.1|	3	tyrosine-protein kinase receptor UFO precursor [Sus scrofa]
gi|335280098|ref|XP_003121779.2|	3	PREDICTED: immunoglobulin superfamily DCC subclass member 4 [Sus scrofa]
gi|47522638|ref|NP_999089.1|	3	inter-alpha-trypsin inhibitor heavy chain H1 precursor [Sus scrofa]
gi|223950621|ref|NP_001138854.1|	3	large proline-rich protein BAG6 [Sus scrofa]
gi|545862076|ref|XP_005669546.1|	3	PREDICTED: microtubule-associated protein futsch-like isoform X1 [Sus scrofa]
gi|311249900|ref|XP_003123855.1|	3	PREDICTED: peptidyl-glycine alpha-amidating monooxygenase isoformX2 [Sus scrofa]
gi|305855063|ref|NP_001182293.1|	2	P antigen family, member 2B [Sus scrofa]
gi|311260957|ref|XP_003128592.1|	2	PREDICTED: NEDD8 isoform X1 [Sus scrofa]
gi|545875478|ref|XP_005672209.1|	2	PREDICTED: ribulose-phosphate 3-epimerase-like isoform X3 [Sus scrofa]
gi|350591216|ref|XP_003483230.1|	2	PREDICTED: inter-alpha-trypsin inhibitor heavy chain H4-like [Sus scrofa]
gi|298104120|ref|NP_001177123.1|	2	V-type proton ATPase subunit G 1 [Sus scrofa]
gi|305855180|ref|NP_001182259.1|	2	catechol O-methyltransferase [Sus scrofa]
gi|47523632|ref|NP_999444.1|	2	proteasome activator complex subunit 2 [Sus scrofa]
gi|114326183|ref|NP_001041537.1|	2	ADP-ribosylation factor 4 [Sus scrofa]
gi|545834322|ref|XP_005665169.1|	2	PREDICTED: stathmin isoform X1 [Sus scrofa]
gi|335288272|ref|XP_003355570.1|	2	PREDICTED: GLIPR1-like protein 1 [Sus scrofa]
gi|335289705|ref|XP_003355965.1|	2	PREDICTED: flavin reductase (NADPH) [Sus scrofa]
gi|545808200|ref|XP_005661126.1|	2	PREDICTED: leucine zipper protein 2-like [Sus scrofa]
gi|545830024|ref|XP_005655861.1|	2	PREDICTED: programmed cell death protein 5 [Sus scrofa]
gi|158819038|ref|NP_001103643.1|	2	stanniocalcin-2 precursor [Sus scrofa]
gi|545841030|ref|XP_003128554.4|	2	PREDICTED: E3 ubiquitin-protein ligase ARIH1 [Sus scrofa]
gi|118403828|ref|NP_001072145.1|	2	ADP-ribosylation factor 6 [Sus scrofa]
gi|545810915|ref|XP_005661466.1|	2	PREDICTED: receptor expression-enhancing protein 3-like [Sus scrofa]
gi|311250234|ref|XP_003124023.1|	2	PREDICTED: eukaryotic peptide chain release factor subunit 1 isoform X1 [Sus scrofa]
gi|348605266|ref|NP_001231758.1|	2	ribosomal protein S13 [Sus scrofa]
gi|346644699|ref|NP_001231019.1|	2	protein SET [Sus scrofa]
gi|545830235|ref|XP_005664544.1|	2	PREDICTED: glyceraldehyde-3-phosphate dehydrogenase, testis-specific [Sus scrofa]
gi|343887407|ref|NP_001230604.1|	2	thiopurine S-methyltransferase [Sus scrofa]
gi|350587964|ref|XP_003482524.1|	2	PREDICTED: PDZ and LIM domain protein 5 isoformX2 [Sus scrofa]
gi|335301749|ref|XP_001925115.3|	2	PREDICTED: inorganic pyrophosphatase [Sus scrofa]
gi|194332494|ref|NP_001123720.1|	2	chloride anion exchanger [Sus scrofa]
gi|350578376|ref|XP_001924454.2|	2	PREDICTED: phosphoacetylglucosamine mutase isoform X1 [Sus scrofa]
gi|350587966|ref|XP_003482525.1|	2	PREDICTED: PDZ and LIM domain protein 5 isoformX3 [Sus scrofa]
gi|545842604|ref|XP_005656491.1|	2	PREDICTED: LOW QUALITY PROTEIN: sterile alpha motif domain-containing protein 15 [Sus scrofa]
gi|47523356|ref|NP_998903.1|	2	N-acetylmuramoyl-L-alanine amidase precursor [Sus scrofa]
gi|545818958|ref|XP_005662797.1|	2	PREDICTED: ATP-dependent RNA helicase DDX1-like [Sus scrofa]
gi|545801578|ref|XP_005659850.1|	2	PREDICTED: aldehyde dehydrogenase family 1 member A3-like [Sus scrofa]
gi|194044045|ref|XP_001927367.1|	2	PREDICTED: N(4)-(beta-N-acetylglucosaminyl)-L-asparaginase isoform 1 [Sus scrofa]
gi|343478283|ref|NP_001230406.1|	2	proteasome (prosome, macropain) 26S subunit, non-ATPase, 2 [Sus scrofa]
gi|335292947|ref|XP_001928857.3|	2	PREDICTED: serpin A3-8 [Sus scrofa]
gi|545859496|ref|XP_005669161.1|	2	PREDICTED: uncharacterized protein LOC100521041 [Sus scrofa]
gi|47523758|ref|NP_999515.1|	2	1-phosphatidylinositol 4,5-bisphosphate phosphodiesterase zeta-1 [Sus scrofa]
gi|545886298|ref|XP_005673876.1|	2	PREDICTED: long-chain-fatty-acid--CoA ligase 4 isoform X1 [Sus scrofa]
gi|545894948|ref|XP_005659027.1|	2	PREDICTED: echinoderm microtubule-associated protein-like 2, partial [Sus scrofa]
gi|190360619|ref|NP_001121905.1|	2	solute carrier family 2, facilitated glucose transporter member 4 [Sus scrofa]
gi|113205806|ref|NP_001038055.1|	2	plasminogen precursor [Sus scrofa]
gi|329744607|ref|NP_001193278.1|	2	inter-alpha-trypsin inhibitor heavy chain H3 precursor [Sus scrofa]
gi|545812261|ref|XP_005661711.1|	2	PREDICTED: heat shock 70 kDa protein 4 [Sus scrofa]
gi|311273021|ref|XP_003133690.1|	2	PREDICTED: fibronectin isoformX2 [Sus scrofa]
gi|83921635|ref|NP_001033089.1|	2	FKBP1A-like [Sus scrofa]
gi|545858510|ref|XP_005654022.1|	2	PREDICTED: ubiquitin-conjugating enzyme E2 Z-like [Sus scrofa]
gi|545865410|ref|XP_005670141.1|	2	PREDICTED: uncharacterized protein LOC100156975, partial [Sus scrofa]
gi|545894027|ref|XP_005658538.1|	2	PREDICTED: vesicle-associated membrane protein-associated protein A [Sus scrofa]
gi|343887448|ref|NP_001230626.1|	2	sulfotransferase family, cytosolic, 2B, member 1 [Sus scrofa]
gi|349585363|ref|NP_001231792.1|	2	syndecan binding protein (syntenin) 2 [Sus scrofa]
gi|545879911|ref|XP_005672867.1|	2	PREDICTED: syndecan binding protein (syntenin) 2 isoform X1 [Sus scrofa]
gi|197251934|ref|NP_001127826.1|	2	actin-related protein 2 [Sus scrofa]
gi|545835301|ref|XP_005665378.1|	2	PREDICTED: calcium-binding tyrosine phosphorylation-regulated protein isoform X2 [Sus scrofa]
gi|194038688|ref|XP_001928209.1|	2	PREDICTED: immunoglobulin superfamily containing leucine-rich repeat protein-like isoformX1 [Sus scrofa]
gi|113205780|ref|NP_001038049.1|	2	quinone oxidoreductase [Sus scrofa]
gi|545825997|ref|XP_005655696.1|	2	PREDICTED: proliferation-associated protein 2G4-like [Sus scrofa]
gi|54020970|ref|NP_001005730.1|	2	glucosylceramidase precursor [Sus scrofa]
gi|346421409|ref|NP_001231079.1|	2	transgelin [Sus scrofa]
gi|311263676|ref|XP_003129789.1|	2	PREDICTED: dipeptidyl peptidase 1 [Sus scrofa]
gi|346421314|ref|NP_001231042.1|	2	fibrinogen beta chain precursor [Sus scrofa]
gi|335293373|ref|XP_003356947.1|	2	PREDICTED: UDP-glucose 6-dehydrogenase isoform 1 [Sus scrofa]
gi|346986445|ref|NP_001231372.1|	2	NSFL1 (p97) cofactor (p47) [Sus scrofa]
gi|350583690|ref|XP_003125999.3|	2	PREDICTED: tetratricopeptide repeat protein 38 [Sus scrofa]

gi|545830671|ref|XP_005664641.1|	2	PREDICTED: 26S proteasome non-ATPase regulatory subunit 8 [Sus scrofa]
gi|311269142|ref|XP_001924412.2|	2	PREDICTED: NEDD8-activating enzyme E1 catalytic subunit isoformX1 [Sus scrofa]
gi|311246134|ref|XP_003122092.1|	2	PREDICTED: acyl-coenzyme A amino acid N-acyltransferase 2-like [Sus scrofa]
gi|545844095|ref|XP_005666593.1|	2	PREDICTED: prominin-1 isoform X1 [Sus scrofa]
gi|335285409|ref|XP_003125160.2|	2	PREDICTED: UDP-GlcNAc:betaGal beta-1,3-N-acetylglucosaminyltransferase 2 [Sus scrofa]
gi|47523866|ref|NP_999571.1|	2	aldose 1-epimerase [Sus scrofa]
gi|545868232|ref|XP_005670524.1|	2	PREDICTED: serine protease 55 isoform X1 [Sus scrofa]
gi|113205774|ref|NP_001038045.1|	2	signal transducer and activator of transcription 3 [Sus scrofa]
gi|317681941|ref|NP_001186971.1|	2	betaine--homocysteine S-methyltransferase 1 [Sus scrofa]
gi|346986355|ref|NP_001231329.1|	2	rab9 effector protein with kelch motifs [Sus scrofa]
gi|545812395|ref|XP_005661738.1|	2	PREDICTED: LOW QUALITY PROTEIN: polycystic kidney disease 2-like 2 protein [Sus scrofa]
gi|47522618|ref|NP_999099.1|	2	vinculin [Sus scrofa]
gi|545845436|ref|XP_005666819.1|	2	PREDICTED: general vesicular transport factor p115 isoform X2 [Sus scrofa]
gi|47522856|ref|NP_999182.1|	2	glutamyl aminopeptidase [Sus scrofa]
gi|545799434|ref|XP_005659493.1|	2	PREDICTED: collagen alpha-1(XII) chain [Sus scrofa]
gi|545860373|ref|XP_003483154.2|	2	PREDICTED: myosin-10, partial [Sus scrofa]

CAPÍTULO IV

6. Artigo Científico 3

CSIRO PUBLISHING

Reproduction, Fertility and Development
https://doi.org/10.1071/RD20017

How does secondary hypogonadism affect the spermatozoa proteome? Lessons from a porcine animal model

Ana P. B. Souza[A], *Tayná N. Lopes*[A], *Anna F. T. Silva*[A], *Lucélia Santi*[B], *Walter O. Beys-da-Silva*[B], *John R. Yates, 3rd*[C] *and Ivan C. Bustamante-Filho*[A,D]

[A]Laboratório de Biotecnologia, Universidade do Vale do Taquari, Rua Avelino Tallini, 171, Lajeado, RS 9514-014, Brazil.
[B]Faculdade de Farmácia, Universidade Federal do Rio Grande do Sul, Avenida Ipiranga, 2752, Porto Alegre, RS 90610-000, Brazil.
[C]Scripps Research Institute, SR11, Department of Molecular Medicine, 10550 North Torrey Pines Road, La Jolla, CA 92037, USA.
[D]Corresponding author. Email: ivan.bustamante@pq.cnpq.br

Abstract. Secondary hypogonadism is a consequence of congenital or acquired diseases that affect the hypothalamus and/or pituitary gland, impairing secretion of gonadotrophin-releasing hormone (GnRH). Androgen deficiency resulting from reduced GnRH secretion is likely to have disrupting effects in epididymal epithelial cells, impairing the sperm maturation process. The aim of this study was to describe changes in the proteome of epididymal spermatozoa in a porcine model of secondary hypogonadism. Cauda epididymal spermatozoa were obtained from 10 boars previously immunised against GnRH (Vivax; Pfizer) and from 10 healthy boars. Protein extracts were analysed by multidimensional protein identification technology. In all, 1322 unique proteins were identified in the protein extracts of cauda epididymal spermatozoa, with significant changes in the abundance of key proteins involved in sperm metabolism (enolase, pyruvate dehydrogenase), acrosome reaction and capacitation (oxoprolinase, acrosomal protein SP-10, dihydrolipoyl dehydrogenase) and sperm–oocyte interactions (zona pellucida-binding protein, zonadhesin, sperm adhesion molecule 1). In addition, the abundance of mitochondrial proteins was severely affected, with significant changes in proteins of Complex I and II, as well as ATPase of the oxidative phosphorylation chain. The proteins identified in this study are potential sperm biomarkers of testicular and epididymal dysfunction related to disruption of the hypothalamus–pituitary–testis axis.

Additional keywords: epididymis, fertility, spermatozoa.

Received 15 January 2020, accepted 30 June 2020, published online 4 August 2020

Introduction

Hypogonadism in men is characterised by impaired testicular function, with possible effects on spermatogenesis and androgen synthesis. Although it is a common endocrine disorder, the exact prevalence of hypogonadism is unknown (Fraietta *et al.* 2013). Primary hypogonadism is characterised by low testosterone production and elevated concentrations FSH and LH. In contrast, secondary or hypogonadotrophic hypogonadism is a consequence of congenital or acquired diseases that affect the hypothalamus and/or pituitary gland, impairing gonadotrophin-releasing hormone (GnRH) secretion (Darby and Anawalt 2005).

Secondary hypogonadism is an underdiagnosed and undertreated medical condition (Katz *et al.* 2012) that has been estimated to affect up to 5 million men in the US, although >90% remain untreated (Araujo *et al.* 2007). The symptoms of secondary hypogonadism can include decreased libido, impaired erectile function, muscle weakness, increased adiposity, depressed mood and decreased vitality (Fraietta *et al.* 2013). Infertility is often associated with secondary hypogonadism (Basaria 2014; Kruljac *et al.* 2020). Normal spermatogenesis depends on the secretion of GnRH and LH, which are responsible for testosterone synthesis (Verhoeven *et al.* 2007). Intratesticular testosterone concentrations are 50- to 100-fold higher than serum concentrations, but when intratesticular testosterone drops to below 20 ng mL^{-1}, spermatogenesis can be significantly affected (Zirkin *et al.* 1989; Ho and Tan 2013). Nonetheless, other consequences of androgen deficiency must also be considered, especially in the epididymis.

Epididymal sperm maturation includes the acquisition of progressive and sustained sperm motility and the development of fertilisation capacity (Yeung and Cooper 2002). These functional changes occur during epididymal transit, whereby the sperm plasma membrane undergoes constant remodelling, with the sequential attachment and secretion of proteins that requires precise timing and order of epididymal gene expression in different segments of the epididymis (Sipilä *et al.* 2011;

Perobelli *et al.* 2013). These different stages have been shown to be essential for the acquisition of motility and fertility by male gametes (Belleannee *et al.* 2011; Belleannée *et al.* 2012).

Endogenous androgens exert most of their effects by binding to androgen receptor (AR), regulating androgen-responsive gene transcription in target cells (Patrão *et al.* 2009; Perobelli *et al.* 2013). Lumicrine interaction between androgens and ARs involves the transport of testicular testosterone bound to androgen-binding protein (ABP) in the proximal epididymis. There, the testosterone–ABP complexes are taken up into the cytoplasm of epithelial cells, where 5α-reductase converts testosterone into dihydrotestosterone, the main androgen involved in the modulation of epididymal function (Robaire and Hamzeh 2011; Perobelli *et al.* 2013).

Little is known about the consequences of secondary hypogonadism in the epididymis. Based on the role of androgens in epididymal physiology (Robaire and Hamzeh 2011), androgen deficiency resulting from reduced GnRH secretion would have disrupting effects in epididymal epithelial cells, impairing the sperm maturation process (Scheer and Robaire 1980; Hamzeh and Robaire 2011; Robaire and Hamzeh 2011). Because investigating epididymal spermatozoa in men has several practical hurdles, an animal model can be used to investigate how these cells are affected in secondary hypogonadism. Our group has been working with a pig model for male human secondary hypogonadism based on immunisation against GnRH, which disrupts the hypothalamic–pituitary–testis (HPT) axis. Using this model, we have described significant changes in the epididymal expression of important proteins associated with fertilisation-related events, such as the members of the protein disulfide isomerase family (Schorr-Lenz *et al.* 2016) and β-defensins (Weber *et al.* 2018). Because of the importance of strict endocrine control of spermatogenesis and epididymal maturation, we believe that a hypogonadal state will disrupt the expression of a significant number of sperm proteins, impairing fertility. Thus, to determine the broader effects of GnRH inhibition on the proteome of epididymal spermatozoa, this study investigated changes in the proteome of spermatozoa harvested from the cauda epididymidis of boars immunised against GnRH.

Materials and methods

Animals, experimental groups and sample preparation

Twenty sexually mature healthy boars (Large White), routinely used as semen donors for AI, were used in the study. Animals were between 300 and 540 days of age, were housed in a boar stud and were normally fed with a commercial corn–soybean meal diet and water *ad libitum* according to the nutritional requirement guidelines for adult boars (National Research Council 2012). Boars assigned to the control group ($n = 10$) were surgically castrated, and the testes and epididymides were immediately dissected to obtain epididymal fluid samples. In the anti-GnRH-immunised group, boars ($n = 10$) were immunised twice against GnRH, 4 and 8 weeks before they were killed in a local abattoir, following the Vivax (Pfizer) protocol (Schorr-Lenz *et al.* 2016; Weber *et al.* 2018). Anti-GnRH immunisation blocks the secretion of GnRH, resulting in a rapid decrease in serum testosterone and oestrogen concentrations (Zamaratskaia *et al.* 2008; Bilskis *et al.* 2012). After immunisation of boars against GnRH, testicular weight is decreased and the diameter of the seminiferous tubules is reduced diameter due to the severe loss of germ cells (Einarsson *et al.* 2011), which is a comparable pathological presentation of clinical testicular degeneration associated with disruption of the HPT axis. The testes and epididymides of anti-GnRH-immunised boars were dissected out for epididymal fluid collection.

All animal experiments described herein conformed to the Guide for Care and Use of Laboratory Animals (National Research Council 2011) and the experimental procedures were approved by the Animal Experimentation Ethics Committee of the Universidade do Vale do Taquari (Protocol no. 001/2015).

The testes and epididymides were transported under refrigeration to the laboratory for processing and arrived within 30 min. Cauda epididymal sections (Region 9; Dacheux *et al.* 2005) were cannulated with a 25-G needle connected to 10-mL syringe containing 2 mL Dulbecco's phosphate-buffered saline (DPBS; composition (mM): NaCl, 136.89; KCl, 2.68; Na_2HPO_4, 8.1; $CaCl_2 \cdot 2H_2O$, 1.46 mM) at room temperature. Epididymal fluid with spermatozoa was then flushed out and collected in a Petri dish. The recovered sperm mass was placed in 5 mL DPBS warmed to room temperature and transferred to microtubes. An aliquot (500 µL) was obtained for sperm analysis; the samples were then centrifuged (800*g*, 10 min, 4°C) and the resulting pellets containing spermatozoa ($\sim 1 \times 10^7$) were washed three times with 1 mL ice-cold phosphate-buffered saline (PBS; composition (mM): NaCl, 140; KCl, 15; Na_2HPO_4, 7; KH_2PO_4, 1.5, pH 7.4), centrifuged (800*g*, 10 min, 4°C) and resuspended in 0.5 mL RIPA buffer (composition: 25 mM Tris-HCl (pH 7.6), 150 mM NaCl, 1% Nonidet P-40, 1% (w/v) sodium deoxycholate, 0.1% (w/v) sodium dodecyl sulfate) with protease inhibitors for cell lysis. The suspension was gently stirred, lysed via mechanical shearing using a 27 G needle and centrifuged at 12 000*g* for 1 h at 4°C. The total protein content of cauda epididymal spermatozoa (CESperm) protein extracts was quantified using the Pierce BCA Protein Assay Kit.

Epididymal sperm analysis

To assess sperm motility, cauda epididymal fluid was extended in DPBS at room temperature. For motility analysis, a 3.0-µL aliquot was placed into a chamber slide (chamber depth 20 µm; Leja) and sperm motility was assessed using a computer-aided sperm analysis (CASA) system (AndroVison version 1.1.4; Minitüb) under phase contrast microscopy (×200 magnification; Axio Scope A1; Zeiss). The settings for cell detection were head size from 10 to 80 μm^2 and form factor from 1.2 to 5. Progressive motility was defined as curvilinear velocity (VCL) >40 µm s^{-1} and straight line velocity (VSL) >10 µm s^{-1}. Sperm cells with an amplitude of lateral head displacement (ALH) <1 µm and VCL <24 µm s^{-1} were considered immotile. For sperm morphology, extended CESperm samples were fixed in a formalin–citrate solution (2.94%). Analyses were performed under a phase contrast microscope at a magnification of ×1000, evaluating 200 spermatozoa per sample. Sperm abnormalities included acrosome defect, abnormal head, abnormal midpiece, attached proximal cytoplasmic droplets, bent tail or

coiled tail. In the boar, CESperm typically have retained distal droplets (Kaplan *et al.* 1984; Kato *et al.* 1996; Kuster and Althouse 2003); therefore, in the present study this characteristic was not considered a defect.

Processing of protein extracts and protein digestion

CESperm protein extracts from the 10 control boars were pooled, as were extracts the 10 anti-GnRH-immunised boars. For pooling, 300 µg total protein from each sample was used and the pooled samples were then suspended in digestion buffer (8 M urea, 100 mM Tris-HCl, pH 8.5). Proteins were reduced with 5 mM tris-2-carboxyethyl-phosphine for 20 min at room temperature, followed by alkylation with 10 mM iodoacetamide at room temperature in the dark for 15 min. After the addition of 1 mM $CaCl_2$ (final concentration), proteins were digested using 2 µg trypsin (Promega) by incubation at 37°C for 16 h. After the incubation, formic acid was added to the samples at a final concentration of 5% to stop proteolysis. The samples were the centrifuged at 10 000*g* for 20 min at 4°C, and the supernatant was collected and stored at –80°C until analysis.

Multidimensional protein identification technology

The protein digest was pressure loaded into a 250-µm ID capillary packed with 2.5 cm of 5-µm Luna strong cation exchanger (Whatman), followed by 2 cm of 3-m Aqua C18 reverse phase (Phenomenex) with a 1 µm frit. The column was washed with buffer containing 95% water, 5% acetonitrile (ACN) and 0.1% formic acid. Immediately after washing, a 100-µm ID capillary (5 µm pulled tip packed with 11 cm of 3-µm Aqua C18 resin; Phenomenex) was attached via a union and placed in line with an Agilent 1100 quaternary HPLC. A modified 12-step separation was used (Wolters *et al.* 2001; Weber *et al.* 2020). The buffer solutions used were as follows: Buffer A, 5% ACN/0.1% formic acid; Buffer B, 80% ACN/0.1% formic acid; and Buffer C, 500 mM ammonium acetate, 5% ACN, and 0.1% formic acid. Step 1 consisted of a 60-min gradient from 0% to 100% (v/v) Buffer B. Steps 2–10 had different percentages of Buffer C, ranging from 10% to 100%. An additional step containing 90% (v/v) Buffer C and 10% (v/v) Buffer B was used at the end. Three technical replicates were performed for each group.

Mass spectrometry

After the HPLC step, eluted peptides were electro-sprayed directly into a linear trap quadrupole (LTQ) Orbitrap XL mass spectrometer (Thermo Fisher Scientific) with the application of a distal 2.5-kV spray voltage. A cycle consisted of one full scan of the mass range (400–2000 *m/z*, resolution of 60 000) followed by five data-dependent collision-induced dissociation (CID) tandem mass spectrometry (MS/MS) spectra in the LTQ. Dynamic exclusion was enabled with a repeat count of 1, a repeat duration of 30 s, an exclusion list size of 150 and an exclusion duration of 180 s. In addition, the mass window for precursor ion selection was set to 400–1600, unassigned, charge 1 was rejected and the normalised collision energy for CID was 35. Mass spectrometer scan functions and HPLC solvent gradients were controlled through the XCalibur data system (ThermoFisher Scientific). All MS/MS spectra were analysed using the software analysis protocol proposed by Santi *et al.* (2014). Briefly, protein identification and quantification analyses were done using the Integrated Proteomics Pipeline (www.integratedproteomics.com/, accessed 15 July 2015). RawExtract 1.9.9.2 (http://fields.scripps.edu/download/RawXtract1_9_9_2.zip, accessed 15 July 2015) was used to extract MS/MS spectra into ms2 files from raw files (McDonald *et al.* 2004) and peptides were searched using ProLuCID (http://fields.scripps.edu/yates/wp/?page_id=821, accessed in 15 jul 2015) (Xu *et al.* 2006) against the *Sus scrofa* reference sequence database from National Center for Biotechnology Information (NCBI), downloaded in July 2015. The peptide mass search tolerance was set to 3 Da, and carboxymethylation (+57.02146 Da) of cysteine was considered to be a static modification. ProLuCID results were assembled and filtered using the DTASelect program (http://fields.scripps.edu/yates/wp/?page_id=816, accessed 15 July 2015) (Tabb *et al.* 2002), resulting in a dataset with a false discovery rate (FDR) of 1% for protein. In addition, as a filtering criterion, a minimum of two peptides per hit was considered and only proteins identified in at least two of the three multidimensional protein identification technology (MudPIT) runs were considered for statistical analysis. Abundance estimates for protein quantitation from MS data were based on counting the total number of fragmentation spectra that map to peptides of a given protein (spectral count (SC); Liu *et al.* 2004; Lundgren *et al.* 2010).

Data analysis and bioinformatics

Venn diagrams were generated using the PatternLab for Proteomics platform module (http://www.patternlabforproteomics.org/, accessed 15 July 2015) (Carvalho *et al.* 2016). Proteins were grouped by maximum parsimony and the presence of proteins in at least two replicates was required for each condition. Volcano plots were generated by comparison between two semen sample groups using the TFold module in the PatternLab for Proteomics platform. Proteins were grouped by maximum parsimony, and the normalised spectral abundance factor (NSAF) was used to normalise SC data. The Benjamin–Hochberg (BH) Q-value was set at 0.05. A variable fold-change cut-off for each individual protein was calculated according to the *t*-test *P*-value using an F-stringency automatically optimised by the TFold software (Carvalho *et al.* 2012). Proteins with low abundance were removed using an L-stringency value of 0.4 (Carvalho *et al.* 2010).

The Blast2GO 5 tool (https://www.blast2go.com/, accessed 23 March 2017) (Conesa *et al.* 2005) was used to categorise the proteins detected by Gene Ontology (GO) annotation (Ashburner *et al.* 2000) according to biological process and molecular function. Metabolic pathways were assessed using the Kyoto Encyclopedia of Genes and Genomes (KEGG) map module. In addition, the subcellular localisation of proteins was identified using the SignalP 5.0 server (http://www.cbs.dtu.dk/services/SignalP/, accessed 13 December 2019) (Almagro Armenteros *et al.* 2019).

In addition to protein data analysis, the GENE2FUNC module of the Functional Mapping and Annotation of Genome-Wide Association Studies (FUMA) platform (https://fuma.ctglab.nl/, accessed 12 October 2018) (Watanabe *et al.* 2017) was used to verify tissue specificity and gene set

enrichment analyses. All proteins identified were mapped in the Uniprot database using the Retrieve/ID mapping tool (https://www.uniprot.org/uploadlists/, accessed 12 October 2018). This step allowed identification of the genes related to the proteins found in sperm protein extracts. An initial analysis (2×2 enrichment tests) included all the genes retrieved from Uniprot, setting only protein-coding genes as a background gene set. The GTEx v7 30 general tissue types dataset was used for tissue specificity analyses. Differentially expressed gene (DEG) sets were precalculated in the GENE2FUNC by means of two-sided *t*-tests for any one of the tissues against all others. For this, expression values were normalised (zero-mean) following a $\log_2$ transformation of expression values (transcripts per million). After BH correction and absolute $\log_2$(fold-change) ≥ 0.58, genes with $P \leq 0.05$ were defined as DEGs in a given tissue compared with others. Genes related to the identified proteins were reanalysed by GENE2FUNC for tissue expression, GO and hallmarks based on the Molecular Signatures Database (MSigDB; Liberzon *et al.* 2015).

Protein interaction networks were generated and analysed using exclusive and upregulated proteins. The String v.11 server (https://string-db.org/, accessed 12 October 2018), a large database of known and predicted protein interactions, was used identify physical and functional interactions among proteins, also considering relevant GO terms (Szklarczyk *et al.* 2015). In addition, the STITCH v.5 tool (http://stitch.embl.de/, accessed 12 October 2018) allowed the creation of a protein network based on the interaction with small molecules. Such analysis provides an overview of the potential effects of chemicals on their interaction partners (Szklarczyk *et al.* 2016).

Expression of testicular and epididymal genes related to proteins identified in CESperm

To investigate whether immunisation against GnRH affected gene expression in the testis and epididymis, genes related to proteins that were differentially expressed between control and anti-GnRH-immunised CESperm groups were selected for expression analysis by quantitative polymerase chain reaction (qPCR). Samples from testicular parenchyma and Regions 1, 5 and 9 of the epididymides were excised, rinsed in ice-cold PBS and treated with RNAlater (Invitrogen). Tissues were quickly frozen in liquid nitrogen and stored at –80°C until RNA extraction. Total RNA was extracted from 100 mg tissue using the GE Healthcare Illustra Spin kit. M-MLV Reverse Transcriptase (Invitrogen) was used for cDNA synthesis from 1.5 µg total RNA. The integrity of the RNA was verified by PCR followed by agarose gel electrophoresis. SYBR Green qPCR assays were performed in a StepOne Plus thermocycler (Applied Biosystems) to evaluate the expression of the *calreticulin* (*CALR*), enolase 3 (*ENO3*), epididymal-specific lipocalin-5 (*LCN5*), epididymis-specific alpha mannosidase (*MAN2B2*) and prostaglandin-H2 D-isomerase (*PTGDS*) genes. The primers used are provided in Table S1, available as Supplementary Material to this paper. The qPCR reaction mixture consisted of 10 µL cDNA (diluted 1 : 100), 4.14 µL water, 2.2 µL of 10× Buffer (200 mM Tris-HCl, pH 8.4, 500 mM KCl), 3.31 mM $MgCl_2$, 0.45 mM dNTPs, 0.044 mM each primer, 2.2 µL SYBR green (diluted 1 : 10 000; Molecular Probes) and 0.05 µL Platinum Taq DNA Polymerase (5 U μL^{-1}; Invitrogen). The final reaction volume was 20 µL and each sample was analysed in quadruplicate. The reaction parameters were as follows: a prerun at 95°C for 15 min, followed by 45 cycles of denaturation at 95°C for 15 s, annealing at 58°C for 30 s and extension at 72°C for 30 s, with a final extension step at 72°C for 10 min. Melting curves were performed with a 0.3°C increase every 30 s. Fluorescence was detected immediately at the end of each annealing step, and the specificity of the amplification was confirmed by analysing the melting curves. As an internal control, a no-template reaction was included in each assay. PCR efficiency was assessed using LinRegPCR software (https://www.genetargetsolutions.com.au/qpcr/linregpcr-and-factor-qpcr/, accessed 14 January 2017) (Ramakers *et al.* 2003; Ruijter *et al.* 2009). The relative expression ratio for each gene was calculated by comparison against the arithmetic mean expression of the reference gene β-actin (*ACTB*), as described previously (Pfaffl 2001).

Statistical analysis

The normal distribution of data was accessed using the D'Agostino–Pearson test. CESperm parameters were compared using Student's *t*-test. The significance of differences in gene expression between the testis and epididymal regions was determined by one-way analysis of variance (ANOVA), followed by Tukey's post hoc test. All calculations were performed in GraphPad Prism 6 software and significance was set at two-tailed $P < 0.05$.

Results

Data regarding the motility and morphology of CESperm are summarised in Table 1. Anti-GnRH immunisation induced a severe loss of total and progressive motility ($P < 0.0001$) and a significant increase in abnormal spermatozoa ($P < 0.0001$). The increase in head abnormalities and proximal droplets ($P < 0.0001$) and the reduction in distal droplets ($P < 0.0001$) suggest impairment of epididymal maturation.

Using shotgun proteomics, a total of 1322 unique CESperm proteins were identified, with a marked prevalence of low-abundance proteins (893 proteins with SC <100). The highest SC was obtained for heat shock protein 70 kDa protein 1-like (4563), whereas 28 proteins had SCs between 2000 and 500. Another 185 proteins had SCs between 499 and 100. The proteomes of CESperm from control and anti-GnRH-immunised animals had 1202 and 1208 unique proteins respectively, indicating that the immunisation against GnRH had, at least in numerical terms, little effect on the sperm proteome.

Nonetheless, the occurrence of proteins exclusively in one of the experimental groups and the differential expression of several proteins present in both conditions revealed that HPT disruption indeed changes the proteome of CESperm. Of all proteins identified, 17.7% were found exclusively in control or anti-GnRH-immunised samples (Fig. 1*a*). Most proteins were identified in both groups, but only 101 proteins (9.2%) were found to be differentially expressed between experimental groups (Fig. 1*b*). Table 2 presents the differentially expressed proteins with a minimum $\log_2$(fold-change) of 2.0 (Q-value = 0.05, F-stringency = 0.04). The complete list of identified proteins is provided in Table S2.

Table 1. Effects of immunisation of boars against gonadotrophin-releasing hormone (GnRH) on cauda epididymal sperm motility and morphology
Data are the mean ± s.d. ($n = 10$ in each group). CI, confidence interval

	Control	GnRH-immunized	95% CI	*P*-value
Total motility (%)	69.8 ± 7.7	13.8 ± 3.2	−74.57, −68.83	<0.0001
Progressive motility (%)	52.3 ± 5.3	5.2 ± 1.3	−62.73, −51.87	<0.0001
Normal spermatozoa (%)	70 ± 2.9	6.4 ± 2.7	−66.24, −60.96	<0.0001
Head defects (%)	9.8 ± 1.5	28.4 ± 2.8	16.48, 20.72	<0.0001
Acrosome defects (%)	4.0 ± 1.3	4.2 ± 1.6	−1.194, 1.594	0.7665
Tail defects (%)	3.8 ± 1.3	3.9 ± 1.4	−1.201, 1.401	0.8735
Proximal droplet (%)	12.4 ± 1.8	85.3 ± 5.5	69.07, 76.73	<0.0001
Distal droplet[A] (%)	82.9 ± 3.7	4.7 ± 3.0	−81.37, −75.03	<0.0001

[A]Distal droplets were not considered a sperm defect in boar spermatozoa from the cauda epididymidis.

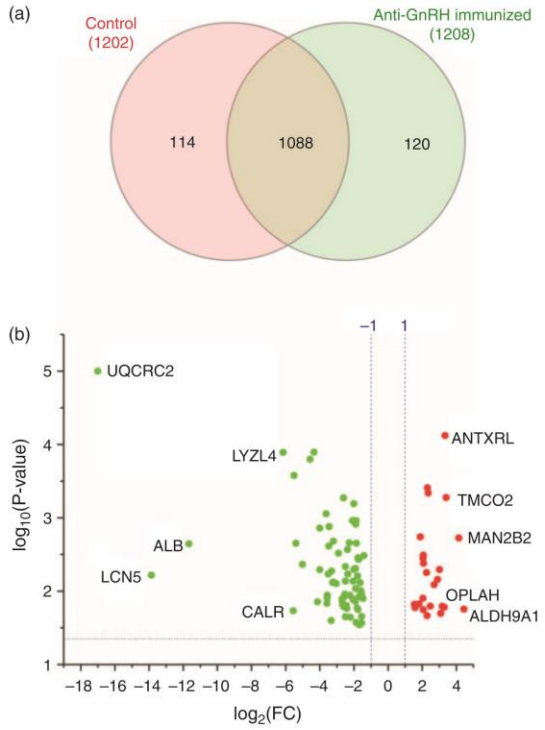

Fig. 1. Comparison of the proteomes of cauda epididymal spermatozoa (CESperm) between healthy (control) boars and boars immunised against gonadotrophin-releasing hormone (GnRH). (*a*) Venn diagram showing the distribution of identified proteins in CESperm of control and anti-GnRH-immunised boars (generated by InteractVenn (http://www.interactivenn.net/, accessed 13 March 2016) Heberle *et al.* 2015( ).*b*) Volcano plot of differentially expressed proteins with $\log_2$(fold changes) (FCs) greater than 1 and less than –1 and *P*-values >0.05. The top five most abundant proteins found in control (FC >1; red dots) and in anti-GnRH-immunised (FC < –1; green dots) groups are indicated. ALB, serum albumin precursor; ALDH9A1, 4-trimethylaminobutyraldehyde dehydrogenase; ANTXRL, anthrax toxin receptor-like; CALR, calreticulin; LCN5, lipocalin-5; LYZL4, lysozyme-like protein 4 isoform 1; MAN2B2, α-mannosidase; OPLAH, 5-oxoprolinase, partial; TMCO2, transmembrane and coiled-coil domain-containing protein 2; UQCRC2, cytochrome b–c_1 complex subunit 2.

As mentioned above, the effects of changes in the proteome cannot be evaluated merely by numbers. Functional analyses of differences between sperm proteomes showed mild variations. Using Blast2GO (BioBam), comparisons of GO terms related with each CESperm proteome show that there was little or no variation in the number of proteins related to cellular and metabolic process, or cellular localisation (Fig. 2*a*–*c*). However, the enzyme profile exhibited more significant changes, with an increase in the number of hits in five of the six enzyme classes evaluated, especially for oxidoreductase and hydrolases (Fig. 2*d*).

The enrichment analysis performed using the GENE2FUNC module of the FUMA platform retrieved 339 genes related to CESperm proteins (Fig. 3*a*). Tissue enrichment revealed a significant difference in regionalised expression of several genes encoding for CESperm proteins. Of all genes analysed, the expression of 23% was higher in the testis compared with other tissues (Fig. 3*b*). Important metabolic pathways were identified in the KEGG analysis, indicating a higher proportion of overlapping genes for glycolysis and gluconeogenesis, pyruvate metabolism, amino acid degradation, fatty acid metabolism, oxidative phosphorylation and glycosaminoglycan and other glycan degradation pathways (Fig. 4*a*). Analysis of hallmark gene sets based on MSigDB collections indicated that anti-GnRH immunisation enhanced the expression of genes encoding components of peroxisome, genes upregulated in response to ultraviolet (UV) radiation, genes upregulated during adipocyte differentiation, genes regulated by MYC and genes encoding proteins involved in the processing of drugs and other xenobiotics (Fig. 5).

Analysis of interactions among proteins (Fig. 6) and small molecules (Fig. 7) confirmed the upregulation of mitochondrial proteins involved in sperm energy metabolism (glycolysis, gluconeogenesis and the tricarboxylic acid (TCA) cycle). In addition, interactions were demonstrated with citric acid, oxaloacetate and coenzyme A, important metabolites directly involved in these pathways. An interaction with thiamine pyrophosphate, a vitamin B_1 derivate and cofactor of several biochemical reactions, was also shown.

The effects of anti-GnRH immunisation on testicular and epididymal gene expression were assessed through the genes encoding the proteins that were differently expressed in anti-GnRH-immunised CESperm. Epididymal levels of *PTGDS*,

Table 2. Differentially expressed proteins in cauda epididymal spermatozoa of healthy boars and boars immunised against gonadotrophin-releasing hormone (GnRH)

Negative $\log_2$(fold change) (FC) values indicate overexpression in control samples, whereas positive $\log_2$(FC) values indicate overexpression in samples from anti-GnRH-immunised boars. The spectral count (SC) is the sum of the total number of spectra identified for a protein in all replicates of control and anti-GnRH-immunised samples. The subcellular localisation of proteins was determined using the SignalP 5.0 server, whereas gene ontology (GO) results were obtained from Blast2GO (BioBam Bioinformatics). ER, endoplasmic reticulum; MHC, major histocompatibility complex; SR, sarcoplasmic reticulum; ZP, zona pellucida

Accession no.	Name	Gene symbol	SC	$\log_2$(FC)	*P*-value	Subcellular localisation	GO (cellular component)
XP_005663205.1	4-Trimethylaminobutyraldehyde dehydrogenase	*ALDH9A1*	136	−4.44	0.01767		
NP_999014.1	Epididymis-specific α-mannosidase precursor	*MAN2B2*	67	−4.15	0.00189		Extracellular region; vacuolar membrane
XP_005655383.1	5-Oxoprolinase-like	*LOC100515137*	44	−3.40	0.00053		
XP_003125520.3	5-Oxoprolinase, partial	*OPLAH*	44	−3.40	0.00053		
XP_005654198.1	Anthrax toxin receptor-like	*ANTXRL*	52	−3.33	0.00008		Integral component of membrane
XP_003356376.2	Transmembrane and coiled-coil domain-containing protein 2	*TMCO2*	43	−3.30	0.01662		Integral component of membrane
XP_005662522.1	Alstrom syndrome protein 1 isoform X2	*ALMS1*	219	−3.18	0.01614		
XP_001928380.1	Acetyl-CoA acetyltransferase, cytosolic	*ACAT2*	49	−3.08	0.02021		Cytosol; nucleolus
NP_999227.1	Dihydrolipoyl dehydrogenase, mitochondrial precursor	*DLD*	313	−3.01	0.00508	Mitochondrion; nucleus; flagellum; acrosome	Acrosomal vesicle; cell; mitochondrial matrix; mitochondrion; motile cilium; nucleus; oxoglutarate dehydrogenase complex
XP_005662521.1	Alstrom syndrome protein 1 isoform X1	*ALMS1*	269	−2.90	0.00696		Centriole; centrosome; cytosol
XP_005673709.1	E3 ubiquitin–protein ligase HUWE1 isoform X2	*HUWE1*	89	−2.71	0.00819		Cytoplasm; cytosol; nucleoplasm; nucleus
XP_005655919.1	Hormone-sensitive lipase isoform X1	*LIPE*	198	−2.47	0.01605		
XP_003361852.2	L-Lactate dehydrogenase A-like 6B-like, partial	*LOC100625752*	678	−2.36	0.00046		
XP_001926443.2	L-Lactate dehydrogenase A-like 6B-like isoform X1	*LOC100153697*	701	−2.31	0.00039		
NP_001182704.1	L-Lactate dehydrogenase C chain	*LDHC*	92	−2.29	0.02162	Cytoplasm	Cytoplasm
NP_001038049.1	Quinone oxidoreductase	*CRYZ*	117	−2.25	0.00560		Cytosol
NP_001037992.1	β-Enolase	*ENO3*	1097	−2.08	0.00417	Cytoplasm	Phosphopyruvate hydratase complex
XP_005657006.1	Synaptic vesicle membrane protein VAT-1 homologue	*VAT1*	92	−2.07	0.01797		Phosphopyruvate hydratase complex
NP_001163991.1	T-Complex protein 1 subunit β	*CCT2*	279	−2.07	0.00324	Cytoplasm	Cell body; chaperonin-containing T-complex; microtubule; ZP receptor complex
NP_001177351.1	Superoxide dismutase [Cu–Zn]	*SOD1*	195	−2.05	0.01253	Cytoplasm; nucleus	Axon cytoplasm; cell; cytoplasm; cytoplasmic vesicle; cytosol; dendrite cytoplasm; extracellular region; extracellular space; mitochondrion; neuronal cell body; nucleoplasm; nucleus; peroxisome; plasma membrane; protein-containing complex
XP_005652652.1	γ-Enolase	*ENO2*	1080	−2.04	0.00355		Perikaryon; phosphopyruvate hydratase complex; photoreceptor inner segment; plasma membrane
XP_003124603.2	Cytochrome b–c_1 complex subunit 2, mitochondrial-like	*UQCRC2*	72	17.00	1.00E-05		
XP_003122377.1	Epididymal-specific lipocalin-5	*LCN5*	109	13.87	0.00605		

NP_001005208.1	Serum albumin precursor	*ALB*	38	11.67	0.00227		Cytoplasm; extracellular space; protein-containing complex
XP_003132179.1	Lysozyme-like protein 4 isoform 1	*LYZL4*	150	6.14	0.00013		Acrosomal vesicle; extracellular space; sperm flagellum
NP_001167604.1	Calreticulin precursor	*CALR*	59	5.56	0.01859	ER lumen; SR lumen; perinuclear region; membrane	Cytosol; ER membrane; ER quality control compartment; external side of plasma membrane; extracellular space; MHC Class I peptide loading complex; nuclear envelope; perinuclear region of cytoplasm; polysome; SR lumen
XP_003130749.1	Lysozyme-like protein 1	*LOC100517051*	293	5.51	0.00027		
NP_999393.1	Prostaglandin H_2 D-isomerase precursor	*PTGDS*	64	5.40	0.00223	Rough ER; nucleus membrane; Golgi apparatus; perinuclear region; secreted	Extracellular region; Golgi apparatus; nuclear membrane; perinuclear region of cytoplasm; rough ER
XP_005653969.1	Zona pellucida-binding protein 2 isoform X1	*ZPBP2*	469	5.01	0.00431		acrosomal vesicle; cell body; extracellular region; ZP receptor complex
XP_003483017.1	Lysozyme-like protein 6-like	*LYZL6*	117	4.57	0.00016		Sperm midpiece; sperm plasma membrane
XP_003130113.2	Protein FAM118B isoform X1	*FAM118B*	48	4.33	0.00013		Cytoplasm
XP_001926294.2	Dynein light chain 1, axonemal	*DNAL1*	41	4.13	0.01401		
NP_001231327.1	Pyruvate dehydrogenase E1 component subunit β, mitochondrial	*PDHB*	60	4.00	0.00139		
NP_999086.1	β-Hexosaminidase subunit β precursor	*HEXB*	80	4.00	0.00510	Lysosome	Acrosomal vesicle; azurophil granule; cell; extracellular space; membrane
XP_001929445.2	ATP synthase subunit β, mitochondrial	*ATP5B*	347	3.63	0.00088		
NP_999131.1	Long-chain 3-ketoacyl-CoA thiolase	*HADHB*	87	3.58	0.01471		
XP_005667535.1	Acrosomal protein SP-10 isoform X3	*ACRV1*	228	3.56	0.01135		
NP_001231762.1	Alcohol dehydrogenase 5 (Class III), chi polypeptide	*ADH5*	41	3.56	0.01236		Cytosol
XP_005667534.1	Acrosomal protein SP-10 isoform X2	*ACRV1*	302	3.51	0.00586		
XP_005655375.1	Maestro heat-like repeat-containing protein family member 1-like isoform X1	*LOC100511504*	201	3.47	0.00243		
NP_999176.1	Sperm adhesion molecule 1	*SPAM-1* *SPAM1*	209	3.45	0.00132		
NP_001152784.1	Sperm-associated antigen 6	*SPAG6*	60	3.33	0.02518		Microtubule cytoskeleton
XP_003124136.1	Casein kinase I isoform α isoformX1	*CSNK1A1*	56	3.31	0.00532		
XP_005667533.1	Acrosomal protein SP-10 isoform X1	*ACRV1*	369	3.24	0.00764		
XP_001925814.4	Putative phospholipase B-like 2 isoform 1	*PLBD2*	42	3.20	0.00209		
XP_005674638.1	Low-quality protein: maestro heat-like repeat family member 1	*MROH1*	147	3.20	0.00754		
NP_001182249.1	Acrosomal protein SP-10 precursor	*ACRV1*	391	3.03	0.00790		Acrosomal vesicle
NP_999527.1	Lactotransferrin precursor	*LTF*	199	2.90	0.00303	Cytoplasmic granule	Extracellular space; specific granule
NP_001231167.1	Sulfide:quinone oxidoreductase, mitochondrial	*SQOR*	96	2.69	0.01320		Mitochondrion
NP_999147.1	Leucocyte surface antigen CD47 precursor	*CD47*	70	2.68	0.01278	Cell membrane; multipass membrane protein	Extracellular exosome; integral component of plasma membrane
XP_003483583.1	Phosphoglycerate mutase 1	*PGAM1*	55	2.67	0.01521		Cytosol
XP_005665011.1	Membrane metallo-endopeptidase-like 1	*MMEL1*	137	2.61	0.00054		
XP_005656305.1	Isocitrate dehydrogenase [NAD] subunit α, mitochondrial isoform X3	*IDH3A*	61	2.59	0.01638		

(*Continued*)

Table 2. (Continued)

Accession no.	Name	Gene symbol	SC	Log_2(FC)	*P*-value	Subcellular localisation	GO (cellular component)
XP_001927373.3	Isocitrate dehydrogenase [NAD] subunit α, mitochondrial isoform X1	*IDH3A*	61	2.59	0.01638		Mitochondrion
XP_001929699.1	Protein MENT	*C4H1orf56*	121	2.56	0.01191		
NP_001230149.1	Lon peptidase 1, mitochondrial	*LONP1*	53	2.53	0.01102		
XP_003135545.1	Isocitrate dehydrogenase [NAD] subunit gamma, mitochondrial isoformX1	*IDH3G*	56	2.50	0.00463		
NP_001121906.1	Cysteine-rich secretory protein 1 precursor	*CRISP1*	49	2.50	0.00732		Extracellular region
XP_001929208.1	Methylmalonate-semialdehyde dehydrogenase [acylating], mitochondrial isoform X1	*ALDH6A1*		2.49	0.02240		
NP_001231558.1	Phospholipase B-like 1 precursor	*PLBD1*	62	2.44	0.01569		
XP_003360859.1	Inactive ribonuclease-like protein 9-like	*LOC100626159*	92	2.41	0.01716		
XP_003480848.1	Actin-like protein 9	*ACTL9*	226	2.37	0.00272		
NP_999548.1	Zonadhesin precursor	*ZAN*	516	2.35	0.00584	Cell membrane; single-pass Type I membrane protein	Integral component of membrane; plasma membrane
NP_001171401.1	Sperm acrosome-associated protein 5 precursor	*SPACA5*	98	2.27	0.00220		
XP_005661563.1	IQ motif containing GTPase activating protein 2	*IQGAP2*	68	2.24	0.01132		
XP_005664116.1	Phospholipase B-like 1-like	*LOC100739094*	45	2.21	0.02265		
XP_003128111.1	Putative hydroxypyruvate isomerase isoformX1	*HYI*	80	2.08	0.00110		
NP_001183950.1	Hydroxysteroid dehydrogenase-like protein 2	*HSDL2*	61	2.05	0.00732		
NP_001038025.1	Protein phosphatase 1 catalytic subunit gamma isoform	*PPP1CC*	201	2.05	0.01298		Protein phosphatase type 1 complex
NP_999441.1	Citrate synthase, mitochondrial precursor	*CS*	424	2.01	0.00064	Mitochondrial matrix	
NP_999217.1	1-Phosphatidylinositol 4,5-bisphosphate phosphodiesterase delta-4	*PLCD4*	66	2.00	0.00506	Membrane; peripheral membrane protein; nucleus; cytoplasm; ER	Cell; ER; membrane; nucleus
XP_005672249.1	1-Phosphatidylinositol 4,5-bisphosphate phosphodiesterase delta-4 isoform X7	*PLCD4*	66	2.00	0.00506		

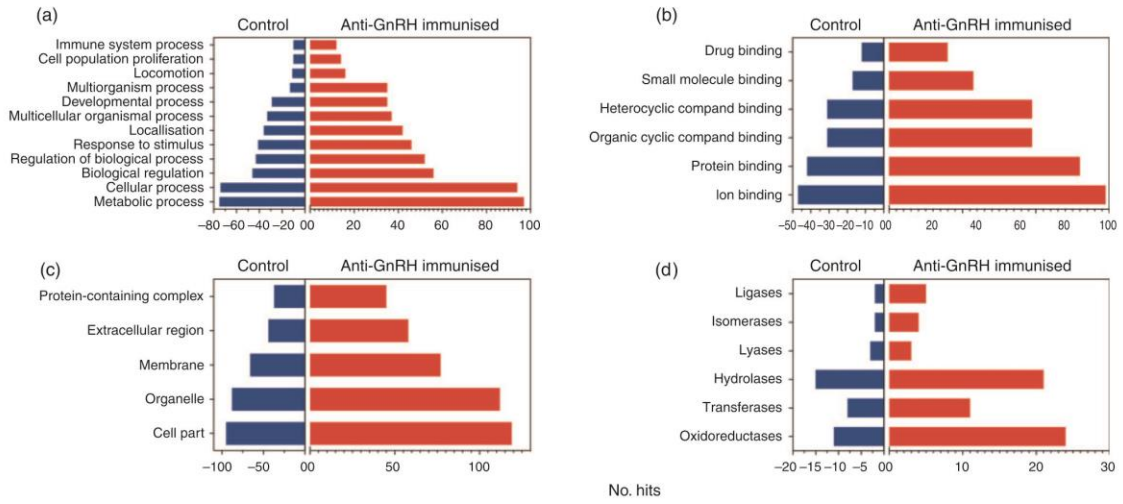

Fig. 2. Distribution of proteins identified in cauda epididymal fluid from healthy (control) boars and boars immunised against gonadotrophin-releasing hormone (GnRH) according to (*a*) biological process, (*b*) molecular function, (*c*) cellular components and (*d*) enzymes. Analyses were performed using Blas2Go5 software (BioBam).

LCN5 and *MAN2B2* mRNA were clearly affected by blocking the secretion of GnRH (Fig. 8). Expression of *PTGD5* and *LCN5* was reduced in immunised animals ($P < 0.05$), whereas *MAN2B2* expression increased ($P < 0.001$). Although there were marked differences in the expression of *CALR* and *ENO3* mRNA between epididymal regions, there was no significant difference in expression between the control and anti-GnRH-immunised groups. There were no significant differences in testicular gene expression between the two groups (Fig. 9).

Discussion

This study represents the first report based on MudPIT to examine the effects of immunisation against GnRH on the proteome of CESperm in a porcine model on men with secondary hypogonadism. As such, it provides a more complete picture of how the protein profile is changed in secondary hypogonadism, serving as a reference to better understand possible molecular mechanisms of infertility in hypogonadal men.

In all, 1322 unique proteins were identified, with fewer than 20% being exclusive in one of the experimental conditions or exhibiting differential expression. This was a surprising result because immunocastration abruptly decreases androgens and oestrogen concentrations, impairing spermatogenesis with severe disruption of the histoarchitecture of the testis and atrophy (Brunius *et al.* 2011; Einarsson *et al.* 2011; Han *et al.* 2017). Although a bigger discrepancy between proteomes was expected, possible explanations for the present results may include: (1) the method of HPT disruption; and (2) the nature of the protein composition of the spermatozoa.

The protocol for immunisation against GnRH in boars comprises two doses administered 1 month apart, with boars killed 30 days after the second dose. With this protocol, serum testosterone concentrations drop to below 0.05 μg mL^{-1} (Zamaratskaia *et al.* 2008; Einarsson *et al.* 2011), with severe consequences for the testes and epididymides. One must consider that spermatogenesis in the boar lasts 40 days, with a spermatogenic cycle length of 8.6–9.0 days. In addition, sperm transit through the epididymis takes approximately 10 days (França *et al.* 2005). Thus, the population of spermatozoa collected from cauda epididymidis of immunised males could be formed by different subpopulations of cells produced under and exposed to different endocrine conditions. In this scenario, spermatozoa that were differently affected by HPT axis disruption could mask a greater effect of immunisation against GnRH on the sperm proteome. Nevertheless, significant decreases in sperm motility and an increase in the number of cells with structural defects were observed after immunocastration in the present study, with similar values as reported previously (Einarsson *et al.* 2011).

The complexity of the swine sperm proteome may also explain the small difference in the CESperm proteome between healthy (control) and anti-GnRH-immunised boars. Most (67.5%) proteins identified had an SC of ≤100 and only 29 proteins were highly abundant (SC >500). In addition, 52 of the 72 differentially expressed proteins had an SC <200 (i.e. proteins with lower abundance in the total sperm proteome). Other studies using shotgun approaches also found a majority of low-abundance proteins in the pig sperm proteome (Perez-Patiño *et al.* 2019*a*, 2019*b*, 2019*c*; Weber *et al.* 2020). Interestingly, data from human spermatozoa are similar. Over 6000 proteins have been described in human spermatozoa, also with a great number of proteins present in lower quantities (Baker *et al.* 2007; Wang *et al.* 2013; Holland and Ohlendieck 2015). In addition, differential proteomics studies found that few proteins differed when sperm proteins were compared between normospermic, fertile patients and normospermic but infertile patients

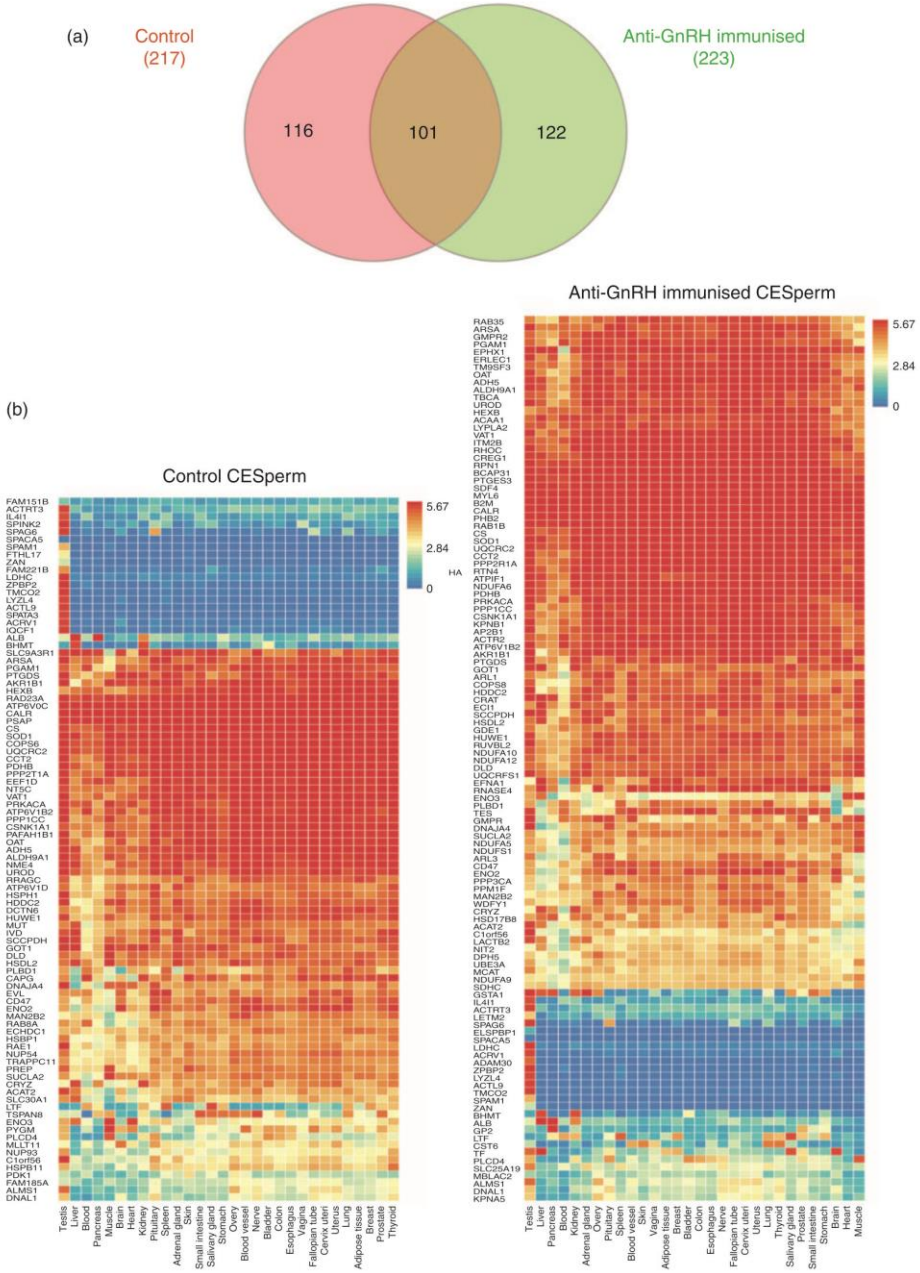

Fig. 3. Enrichment analysis performed using the GENE2FUNC module of the Functional Mapping and Annotation of Genome-Wide Association Studies (FUMA) platform (https://fuma.ctglab.nl/, accessed 12 October 2018). (*a*) Venn diagram showing the distribution of genes related to the proteomes of cauda epididymidis spermatozoa (CESperm) from control boars and boars immunised against gonadotrophin-releasing hormone (GnRH). (*b*) Tissue enrichment heat maps showing the level of expression of genes related to CESperm proteins from healthy (control) and anti-GnRH-immunised boars in another 30 tissues.

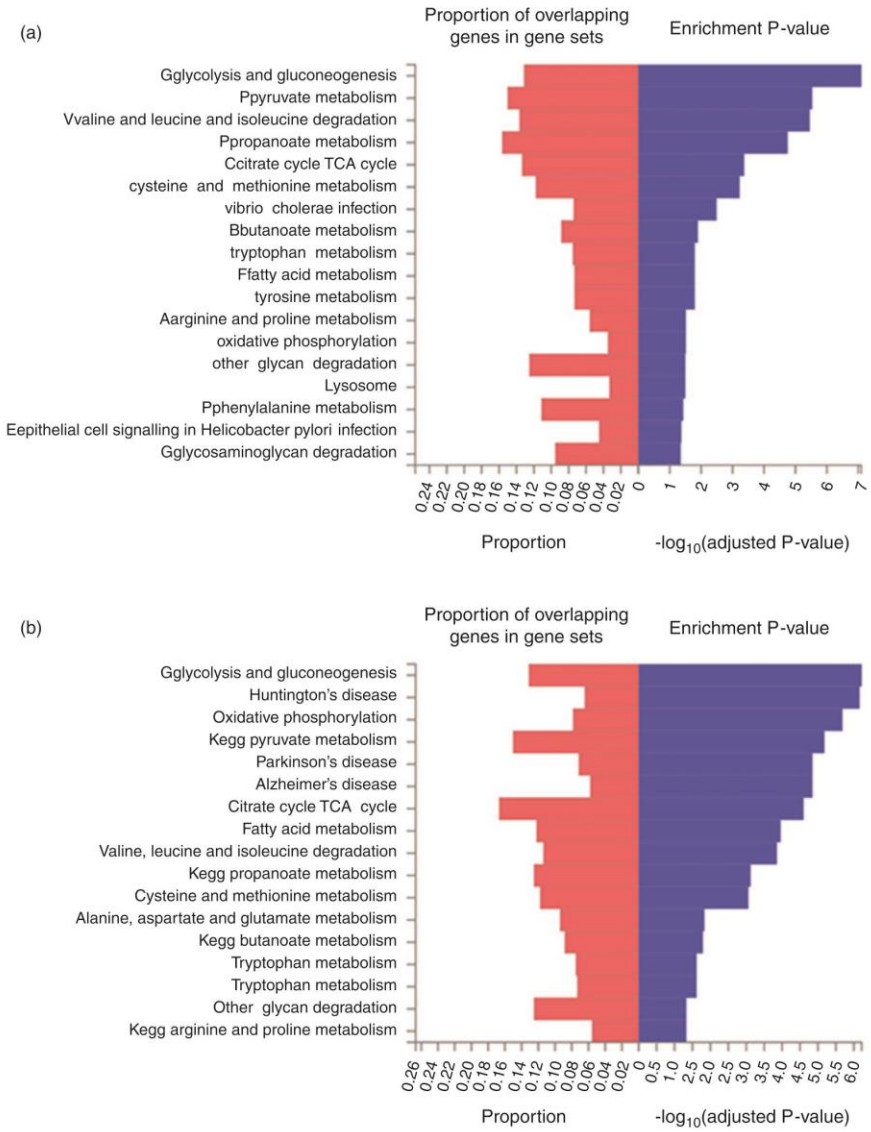

Fig. 4. Kyoto Encyclopedia of Genes and Genomes (KEGG) pathway enrichment, indicating the most prevalent signalling pathways associated with the proteome of cauda epididymidis spermatozoa from (*a*) control boars and (*b*) boars immunised against gonadotrophin-releasing hormone (GnRH). Analyses were performed using the Functional Mapping and Annotation of Genome-Wide Association Studies (FUMA) platform (https://fuma.ctglab.nl/, accessed 12 October 2018).

(Hamada *et al.* 2012; Frapsauce *et al.* 2014), as well as in spermatozoa with oxidative damage (Sharma *et al.* 2013) and those with DNA fragmentation (Intasqui *et al.* 2013).

Although immunisation did not alter gene expression of *CALR*, *ENO3*, *PTGDS*, *LCN5* and *MAN2B2* in the testis, some modification in regional expression patterns was identified in the epididymis. Nonetheless, the changes observed at the mRNA level alone do not explain the abundance of differentially expressed proteins. The following events that may occur during sperm transit through the epididymis may have contributed to the observed results: protein shedding (Tulsiani 2003; Thimon *et al.* 2006), protein degradation through the

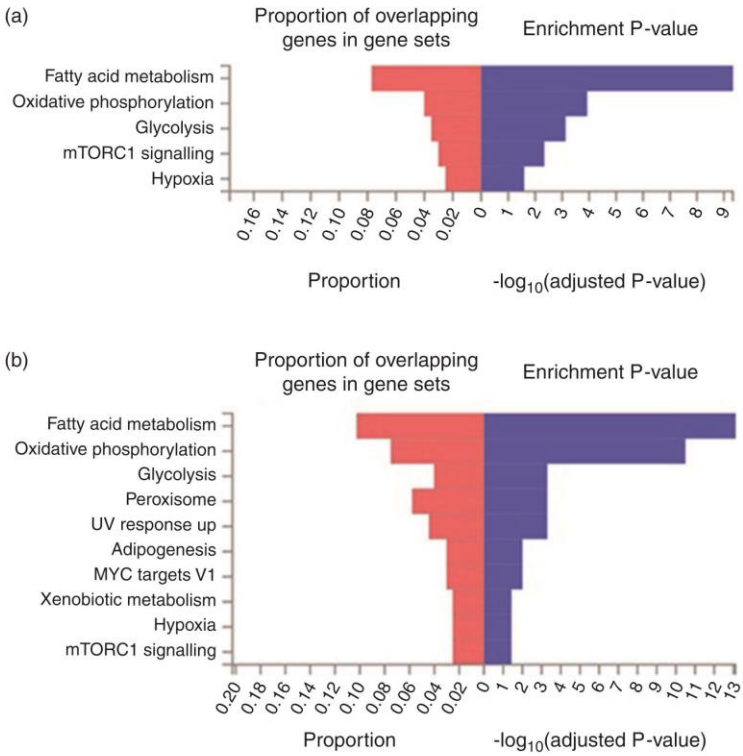

Fig. 5. Hallmark pathways identified using hypergeometric tests indicating over-representation of testis-expressed genes within gene sets from the Molecular Signatures Database. Genes were retrieved from the proteins in cauda epididymidis spermatozoa from (*a*) control boars and (*b*) boars immunised against gonadotrophin-releasing hormone (GnRH). Analyses were performed using the Functional Mapping and Annotation of Genome-Wide Association Studies (FUMA) platform (https://fuma.ctglab.nl/, accessed 12 October 2018) . mTORC1, mammalian target of rapamycin complex 1; UV, ultraviolet.

ubiquitin–proteasome system (Sutovsky 2018; Zigo *et al.* 2019) and sperm protein removal and incorporation by epididymosomes (Akintayo *et al.* 2015).

As noted above, although the quantitative effect of immunisation against GnRH on the proteome was mild, proteins that were only found in or were absent from spermatozoa from immunised males, as well proteins that were up- or down-regulated, have important roles in sperm metabolism and fertility potential (Fig. 10). The following discussed the most relevant proteins according to their role in sperm physiology and possible contribution to fertility outcome.

Proteins involved in sperm metabolism

More than 90 proteins associated with sperm metabolic processes were identified. Successful fertilisation depends on sperm functions, which are high energy-requiring events, like motility and hyperactivation. Spermatozoa from anti-GnRH-immunised boars had a different protein profile regarding metabolism-related proteins, such as an increase in enzymes involved in the glycolytic pathway (γ-enolase, β-enolase, pyruvate dehydrogenase) and subunits of the protein complexes, which form the oxidative phosphorylation chain. The most upregulated protein in CESperm from anti-GnRH-immunised boars was the cytochrome b–c_1 complex subunit 2 (UQCRC2), which was increased 17-fold. Cytochrome b–c_1 complexes are intrinsic membrane proteins that catalyse the oxidation of ubihydroquinone and the reduction of cytochrome c in mitochondrial respiratory chain (Complex II). These changes in mitochondrial function may be directly associated with the impaired sperm motility and morphology found in epididymal spermatozoa from anti-GnRH-immunised boars (Amaral *et al.* 2013; Nakamura *et al.* 2013; Gu *et al.* 2019).

The cytochrome b–c_1 complex operates through a Q-cycle mechanism that couples electron transfer to generation of the proton gradient that drives ATP synthesis (Crofts 2004). The increase in UQCRC2 suggests mitochondrial dysfunction and a possible increase in reactive oxygen species production (Aguilera-Aguirre *et al.* 2009) that may originate from the disrupted spermatogenesis. UQCRC2 has already been investigated in swine reproduction: it was highly expressed after

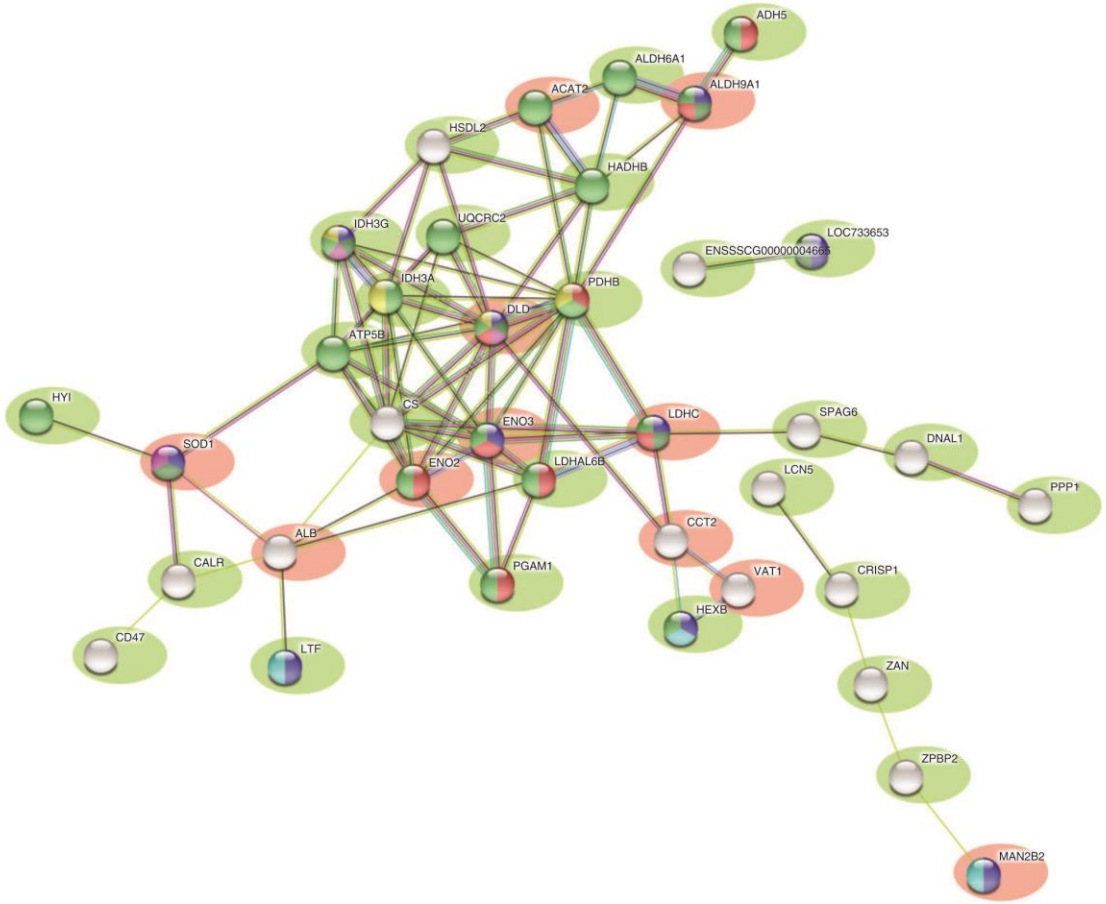

Fig. 6. Protein–protein interaction network in cauda epididymidis spermatozoa generated using the String V.11 server (https://string-db.org/, accessed 12 October 2018). Each node represents one protein. Green ellipses indicate proteins upregulated in boars immunised against gonadotrophin-releasing hormone (GnRH); pink ellipses indicate proteins upregulated in control samples. Within nodes, different colours represent different gene ontology classifications and terms (i.e. molecular function and cellular components), as well as Kyoto Encyclopedia of Genes and Genomes (KEGG) pathways.

capacitation in spermatozoa resulting in high litter sizes, whereas UQCRC1 was highly expressed after capacitation in spermatozoa resulting in low litter sizes (Kwon *et al.* 2015). Other studies have reported that UQCRC2 expression is correlated with male fertility, with high expression in spermatozoa of low-fertility bulls (Park *et al.* 2012) and mice (Shukla *et al.* 2013).

In addition, several subunits of the mitochondrial membrane respiratory chain NADH dehydrogenase (Complex I) were identified (NADH-ubiquinone oxidoreductase 75 kDa subunit, subunit 5, subunit 6, subunit 9 and subunit 10). The enzymes necessary for glycolysis are primarily associated with the fibrous sheath located in the principal piece of the tail. In contrast, oxidative phosphorylation occurs in the mitochondrial gyres located in the midpiece. Oxidative phosphorylation is a significantly more efficient method of ATP production than glycolysis, but spermatozoa from most heavily researched species depend predominantly on glycolysis for ATP production (Gibb and Aitken 2016). Interestingly, ATP synthase subunit β was overexpressed in CESperm from boars immunised against GnRH, also suggesting mitochondrial dysfunction (Guan *et al.* 2015), which could be associated with the impairment of spermatogenesis after administration of the anti-GnRH vaccine. The 17-fold increase in the abundance of UQCRC2 in anti-GnRH-immunised CESperm also suggests an association with the occurrence of mitochondria-related cell death events, such as oxidative stress and apoptosis (Bollwein and Bittner 2018).

An unbalanced redox state is an expected scenario in the testes and epididymides of androgen-deficient boars. A reduction in sperm superoxide dismutase after anti-GnRH-immunisation suggests that the spermatozoa are more susceptible to oxidative damage while still in the male reproductive tract. Similarly, oxoprolinase, an important enzyme involved in

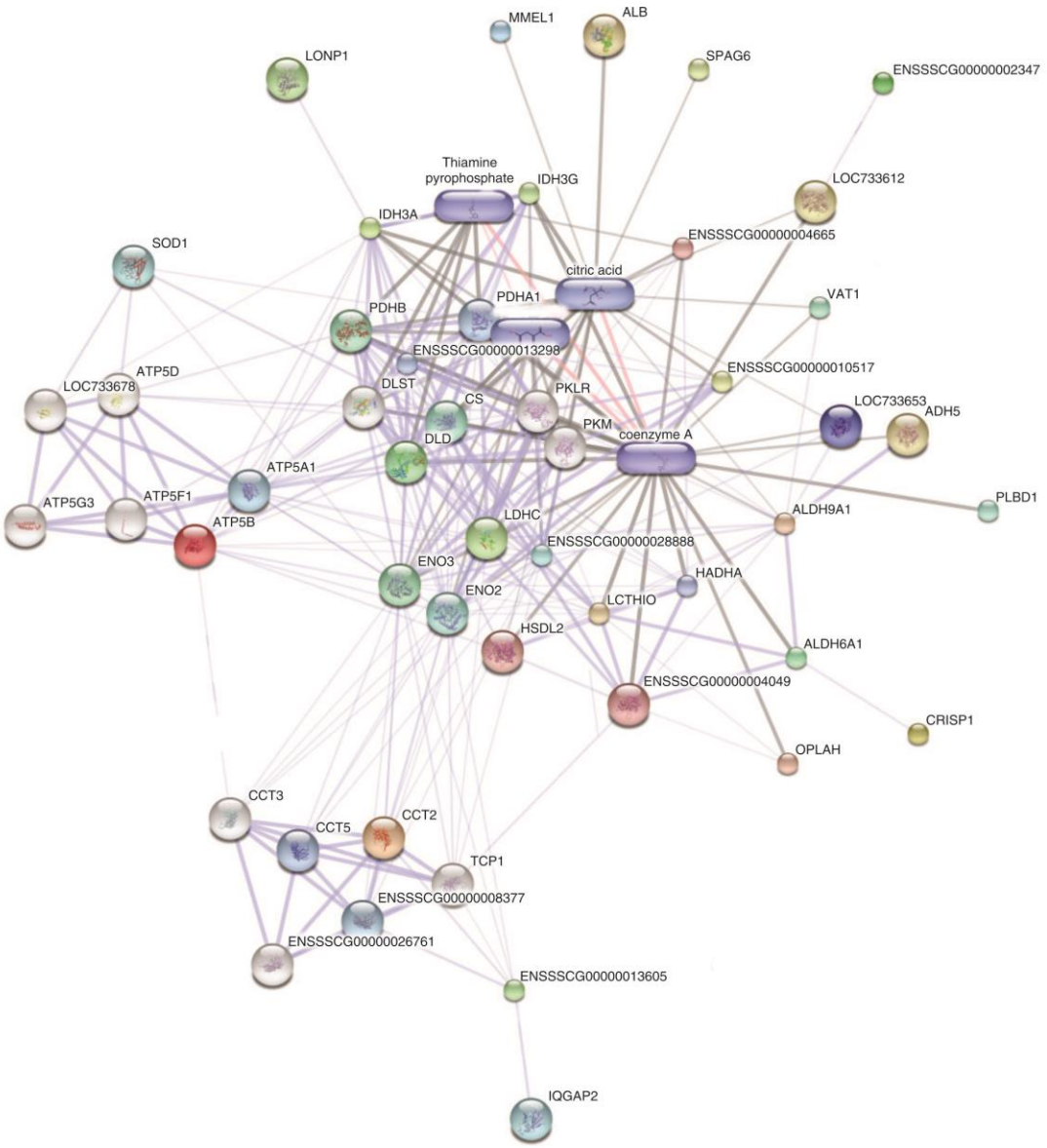

Fig. 7. Network representing interactions between cauda epididymidis sperm proteins and small molecules (metabolites or xenobiotics), generated using the STITCH v.5 server (http://stitch.embl.de/, accessed 12 October 2018). Each circular node represents a protein and each pill-shaped icon denotes a small molecule. The interaction network is formed by three clusters interconnected with a strong interaction with important molecules involved in sperm energy metabolism.

glutathione (GSH) metabolism is downregulated in CESperm from immunised boars. The glutathione pathway is connected to amino acid metabolic pathways (e.g. cysteine, methionine, glutamate; Weber *et al.* 2020), but is also an important antioxidant system. Severe impairment of sperm GSH levels was associated with a higher incidence of sperm defects (Garrido *et al.* 2004). The role of GSH in the proliferation and differentiation of spermatogenic cells may explain the abnormal sperm morphology (Li *et al.* 1989). Using human epididymal cell homogenates, Montiel *et al.* (2003) did not find any significant

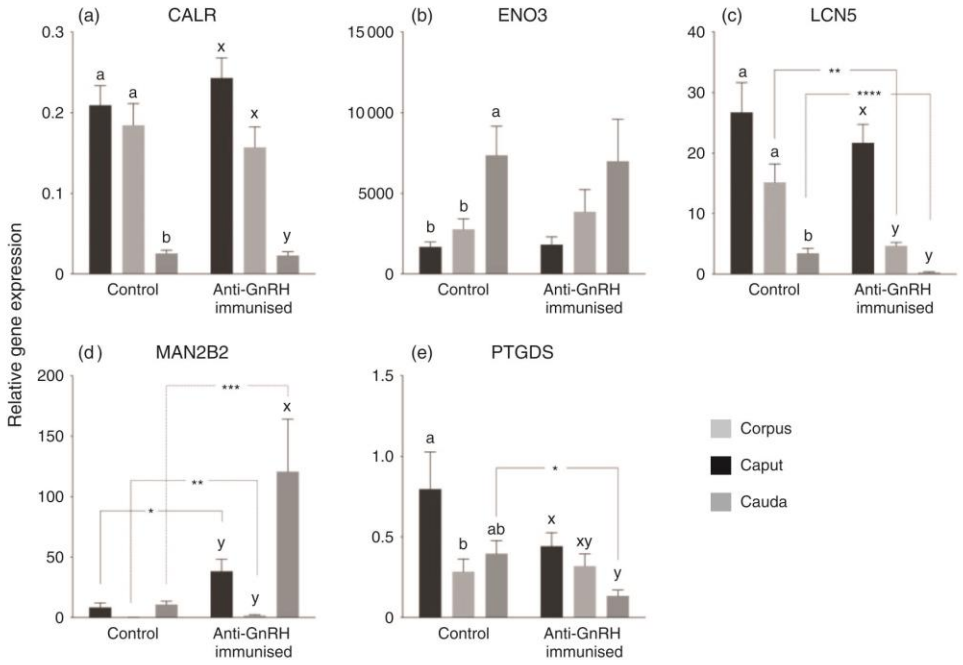

Fig. 8. Effects of immunisation of boars against gonadotrophin-releasing hormone (GnRH) on the epididymal mRNA expression of genes related to the synthesis of the proteins (*a*) calreticulin (*CALR*( ),*b*) enolase 3 (*ENO3*( ),*c*) epididymal specific lipocalin-5 (*LCN5*( ),*d*) epididymis-specific α-mannosidase (*MAN2B2*) and (*e*) prostaglandin D synthase (*PTGDS*). Data are the mean ± s.d. ($n = 10$ per group). Within groups (control or anti-GnRH immunised), different letters above columns indicate significant differences ($P < 0.05$). *$P < 0.05$, **$P < 0.01$, ***$P < 0.001$.

differences in γ-glutamyl transpeptidase and glutathione *S*-transferase activity, or cellular GSH levels, among epididymal regions and in the presence of different concentrations of dihydrotestosterone. Thus, how androgen deficiency could impair GSH metabolism in the epididymis remains unclear. Nevertheless, the importance of sperm GSH goes beyond oxidative protection, because the addition of 10 μg mL^{-1} GSH to IVF medium improved sperm penetration rates of semen samples from asthenozoospermic and infertile men (Meybodi *et al.* 2012). New studies would confirm a direct clinical association between testicular and sperm GSH metabolism and hypogonadism in men.

Downregulation in the abundance of dihydrolipoyl dehydrogenase (DLD) was identified in CESperm from anti-GnRH-immunised boars. Found in the mitochondria matrix, DLD is a flavoprotein disulfide oxidoreductase, and is the E3 component of α-ketoacid dehydrogenase multienzyme complexes. Intriguingly, DLD was also localised in the acrosome and principal piece of the sperm flagella, along with its host complex, pyruvate dehydrogenase complex (PDHc; Mitra *et al.* 2005). The non-canonical localisations of metabolic enzymes raise the possibility of an extramitochondrial energy production centre. The use of ATP generated after glycolysis in tyrosine phosphorylation reactions during capacitation of mouse spermatozoa (Travis *et al.* 2001) strengthens this possibility. A post-pyruvate metabolic enzyme such as DLD is important in hamster sperm hyperactivation and acrosome reaction (Mitra and Shivaji 2004). It was observed that inhibition of sperm PDHc and DLD leads to a 'lactic acidosis-like condition' in spermatozoa (Mitra and Shivaji 2004). A common source of energy, lactate becomes unfavourable when levels exceed optimal limits, affecting sperm intracellular pH and calcium metabolism. These results highlight the importance of pyruvate metabolism and lactate–pyruvate equilibrium during capacitation in the maintenance of sperm pH, calcium and fertility. Modifications in the expression and activity of enzymes associated with these pathways may explain fertilisation failure in human assisted reproductive technologies (Siva *et al.* 2014).

Proteins involved in fertilisation

As expected, the expression of key proteins for acrosome reaction and sperm–egg interaction was affected by disruption of the HPT axis. These results show that in a hypogonadal condition, spermatozoa not only have structural defects, but also have an altered composition of key proteins necessary for fertilisation. Proteins on the sperm surface are primary candidate partners for interaction with the zona pellucida (ZP). Many studies have shown that both ejaculated and capacitated spermatozoa are able to bind to the ZP, but only a capacitated spermatozoon is able to fertilise an ovum (Bedford 1983;

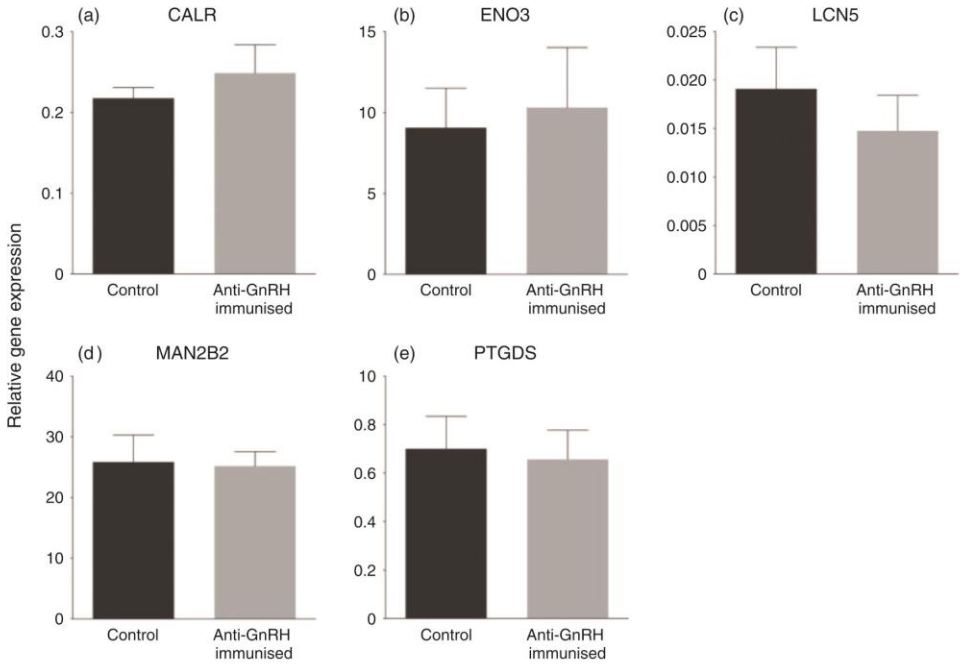

Fig. 9. Effects of immunisation of boars against gonadotrophin-releasing hormone (GnRH) on testicular mRNA expression of genes related to the synthesis of the proteins (*a*) calreticulin (*CALR*( ),*b*) enolase 3 (*ENO3*( ),*c*) epididymal specific lipocalin-5 (*LCN5*( ),*d*) epididymis-specific α-mannosidase (*MAN2B2*) and (*e*) prostaglandin D-synthase (*PTGDS*). Data are the mean ± s.d. ($n = 10$ per group).

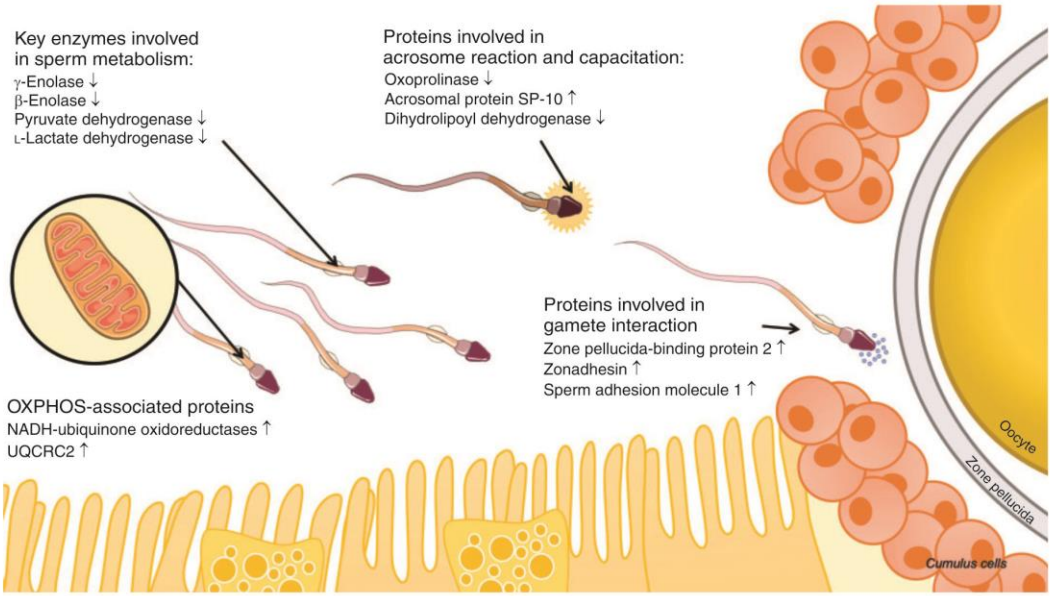

Fig. 10. Schematic representation of selected proteins differentially expressed in cauda epididymal spermatozoa (CESperm) from boars immunised against gonadotrophin-releasing hormone (GnRH). Arrows pointing up and down indicate higher and lower abundance of the proteins respectively in CESperm from immunised animals relative to control. OXPHOS, oxidative phosphorylation; UQCRC2, cytochrome b–c_1 complex subunit 2.

Erickson *et al.* 2007; Landim-Alvarenga *et al.* 2004; Aguiar *et al.* 2019; Leemans *et al.* 2019). In the present study, an increase in the abundance of several proteins associated with the sperm–egg interaction reveals a disturbance in the preparation of the mature sperm membrane. In fact, an increase in ZP-binding protein 2 in spermatozoa was associated with spermatogenic dysfunction caused by high-intensity exercise (Guo *et al.* 2019). Studies have shown that long-term, high-intensity exercise can lead to neurological–endocrine disorders, resulting in exercise-induced low blood testosterone concentrations and decreases in spermatogenesis and sperm quality (Griffith *et al.* 1990; Arce *et al.* 1993; Vaamonde *et al.* 2018).

Also upregulated in CESperm from anti-GnRH-immunised boars, zonadhesin (Zan) is a sperm transmembrane protein that binds directly and in a species-specific manner to the ZP (Hardy and Garbers 1994). Similar to species-specific egg recognition proteins of abalone and sea urchin spermatozoa, Zan is an acrosomal protein (Bi *et al.* 2003; Olson *et al.* 2004) that is exposed during fertilisation (Tardif *et al.* 2010). A study in a Zan-knockout mouse model showed that $Zan^{-/-}$ males are fertile, showing similar IVF results compared with wild-type mice (Tardif *et al.* 2010). Interestingly, loss of Zan increased adhesion of mouse spermatozoa to heterologous ZP (pig, cow and rabbit) but not mouse ZP. Zan is produced in the testis as a precursor protein that is subsequently proteolytically processed (Hardy and Garbers 1995; Gao and Garbers 1998). Zan binds the ZP after the acrosome reaction has been initiated and may be one of the proteins that anchors the acrosomal shroud to the ZP, thereby allowing the spermatozoa to continue penetration and fertilisation to proceed (Lea *et al.* 2001).

Three different isoforms of acrosomal protein SP-10, a well-established capacitation marker, were found to be upregulated (more than threefold) in the spermatozoa of immunised boars. SP-10 was first identified in human sperm acrosome, being later detected in several mammalian species, including the pig (Herr *et al.* 1990; Foster *et al.* 1994). The different isoforms of acrosomal protein SP-10 are the result alternative splicing, and they may play important roles in sperm capacitation and spontaneous acrosome reaction (Choi *et al.* 2008). The *SP10* gene is testis specific and is expressed in round spermatids. The differentiation marker SP-10 serves as a useful indicator to elucidate the regulation of round spermatid-specific gene transcription and acrosome biogenesis (Reddi *et al.* 2002). The testicular tissue disruption caused by anti-GnRH immunisation (Brunius *et al.* 2011; Einarsson *et al.* 2011) may explain the increase in acrosomal protein SP-10 in this group in the present study. Further studies are needed to verify whether acrosomal protein SP-10 is a suitable sperm marker for testicular atrophy as a consequence of hypogonadism.

Conclusion

Overall, the results of this study indicate significant changes in the CESperm proteome in a porcine model of human secondary hypogonadism. The abundance of several proteins involved in sperm metabolism, energy production, capacitation, acrosome reaction and sperm–egg interaction was altered, which may negatively affect fertility outcomes. Secondary hypogonadism in men is commonly associated with infertility. However, not every patient has seminal alterations, such as oligospermia and decreased sperm motility. Such clinical presentation poses an obstacle to diagnosis and treatment. Therefore, some of the proteins identified herein may be potential candidate sperm biomarkers for testicular and epididymal dysfunction related to disruption of the HPT axis.

Conflicts of interest

The authors declare no conflicts of interest.

Acknowledgements

This work was supported by grants from Conselho Nacional de Desenvolvimento Científico e Tecnológico (CNPq; 447251/2014-7), Fundação de Amparo à Pesquisa do Estado do Rio Grande do Sul (FAPERGS; 16/2551-0000223-1) and Fundação Vale do Taquari de Educação e Desenvolvimento Social (FUVATES; 08/Reitoria/Univates/2016). Ana Paula Binato de Souza was the recipient of an academic scholarship from CAPES.

References

Aguiar, G. B., Caldas-Bussiere, M. C., Maciel, V. L., Jr, Carvaho, C. S. P., and Souza, C. L. M. (2019). Association of L-arginine with heparin on the sperm capacitation improves *in vitro* embryo production in bovine. *Anim. Reprod.* **16**, 938–944. doi:10.21451/1984-3143-AR2019-0022

Aguilera-Aguirre, L., Bacsi, A., Saavedra-Molina, A., Kurosky, A., Sur, S., and Boldogh, I. (2009). Mitochondrial dysfunction increases allergic airway inflammation. *J. Immunol.* **183**, 5379–5387. doi:10.4049/JIMMUNOL.0900228

Akintayo, A., Legare, C., and Sullivan, R. (2015). Dicarbonyl L-xylulose reductase (DCXR), a 'moonlighting protein' in the bovine epididymis. *PLoS One* **10**, e0120869. doi:10.1371/JOURNAL.PONE.0120869

Almagro Armenteros, J. J., Tsirigos, K. D., Sonderby, C. K., Petersen, T. N., Winther, O., Brunak, S., von Heijne, G., and Nielsen, H. (2019). SignalP 5.0 improves signal peptide predictions using deep neural networks. *Nat. Biotechnol.* **37**, 420–423. doi:10.1038/S41587-019-0036-Z

Amaral, A., Lourenco, B., Marques, M., and Ramalho-Santos, J. (2013). Mitochondria functionality and sperm quality. *Reproduction* **146**, R163–R174. doi:10.1530/REP-13-0178

Araujo, A. B., Esche, G. R., Kupelian, V., O'Donnell, A. B., Travison, T. G., Williams, R. E., Clark, R. V., and McKinlay, J. B. (2007). Prevalence of symptomatic androgen deficiency in men. *J. Clin. Endocrinol. Metab.* **92**, 4241–4247. doi:10.1210/JC.2007-1245

Arce, J. C., De Souza, M. J., Pescatello, L. S., and Luciano, A. A. (1993). Subclinical alterations in hormone and semen profile in athletes. *Fertil. Steril.* **59**, 398–404. doi:10.1016/S0015-0282(16)55684-2

Ashburner, M., Ball, C. A., Blake, J. A., Botstein, D., Butler, H., Cherry, J. M., Davis, A. P., Dolinski, K., Dwight, S. S., Eppig, J. T., Harris, M. A., Hill, D. P., Issel-Tarver, L., Kasarskis, A., Lewis, S., Matese, J. C., Richardson, J. E., Ringwald, M., Rubin, G. M., and Sherlock, G. (2000). Gene ontology: tool for the unification of biology. The Gene Ontology Consortium. *Nat. Genet.* **25**, 25–29. doi:10.1038/75556

Baker, M. A., Reeves, G., Hetherington, L., Muller, J., Baur, I., and Aitken, R. J. (2007). Identification of gene products present in Triton X-100 soluble and insoluble fractions of human spermatozoa lysates using LC-MS/MS analysis. *Proteomics Clin. Appl.* **1**, 524–532. doi:10.1002/PRCA.200601013

Basaria, S. (2014). Male hypogonadism. *Lancet* **383**, 1250–1263. doi:10.1016/S0140-6736(13)61126-5

Bedford, J. M. (1983). Significance of the need for sperm capacitation before fertilization in eutherian mammals. *Biol. Reprod.* **28**, 108–120. doi:10.1095/BIOLREPROD28.1.108

Belleannee, C., Belghazi, M., Labas, V., Teixeira-Gomes, A. P., Gatti, J. L., Dacheux, J. L., and Dacheux, F. (2011). Purification and identification of sperm surface proteins and changes during epididymal maturation. *Proteomics* **11**, 1952–1964. doi:10.1002/PMIC.201000662

Belleannée, C., Thimon, V., and Sullivan, R. (2012). Region-specific gene expression in the epididymis. *Cell Tissue Res.* **349**, 717–731. doi:10.1007/S00441-012-1381-0

Bi, M., Hickox, J. R., Winfrey, V. P., Olson, G. E., and Hardy, D. M. (2003). Processing, localization and binding activity of zonadhesin suggest a function in sperm adhesion to the zona pellucida during exocytosis of the acrosome. *Biochem. J.* **375**, 477–488. doi:10.1042/BJ20030753

Bilskis, R., Sutkeviciene, N., Riskeviciene, V., Januskauskas, A., and Zilinskas, H. (2012). Effect of active immunization against GnRH on testosterone concentration, libido and sperm quality in mature AI boars. *Acta Vet. Scand.* **54**, 33. doi:10.1186/1751-0147-54-33

Bollwein, H., and Bittner, L. (2018). Impacts of oxidative stress on bovine sperm function and subsequent *in vitro* embryo development. *Anim. Reprod.* **15**, 703–710. doi:10.21451/1984-3143-AR2018-0041

Brunius, C., Zamaratskaia, G., Andersson, K., Chen, G., Norrby, M., Madej, A., and Lundstrom, K. (2011). Early immunocastration of male pigs with Improvac® – effect on boar taint, hormones and reproductive organs. *Vaccine* **29**, 9514–9520. doi:10.1016/J.VACCINE.2011.10.014

Carvalho, P. C., Yates III, J. R., and Barbosa, V. C. (2010). Analyzing shotgun proteomic data with PatternLab for proteomics. *Curr. Protoc. Bioinform.* **30**, 13.13.1–13.13.15. doi:10.1002/0471250953.BI1313S30

Carvalho, P. C., Yates, J. R., 3rd, and Barbosa, V. C. (2012). Improving the TFold test for differential shotgun proteomics. *Bioinformatics* **28**, 1652–1654. doi:10.1093/BIOINFORMATICS/BTS247

Carvalho, P. C., Lima, D. B., Leprevost, F. V., Santos, M. D. M., Fischer, J. S. G., Aquino, P. F., Moresco, J. J., Yates, J. R., 3rd, and Barbosa, V. C. (2016). Integrated analysis of shotgun proteomic data with PatternLab for proteomics 4.0. *Nat. Protoc.* **11**, 102–117. doi:10.1038/NPROT.2015.133

Choi, Y. J., Uhm, S. J., Song, S. J., Song, H., Park, J. K., Kim, T., Park, C., and Kim, J. H. (2008). Cytochrome *c* upregulation during capacitation and spontaneous acrosome reaction determines the fate of pig sperm cells: linking proteome analysis. *J. Reprod. Dev.* **54**, 68–83. doi:10.1262/JRD.19116

Conesa, A., Gotz, S., Garcia-Gomez, J. M., Terol, J., Talon, M., and Robles, M. (2005). Blast2GO: a universal tool for annotation, visualization and analysis in functional genomics research. *Bioinformatics* **21**, 3674–3676. doi:10.1093/BIOINFORMATICS/BTI610

Crofts, A. R. (2004). The cytochrome bc_1 complex: function in the context of structure. *Annu. Rev. Physiol.* **66**, 689–733. doi:10.1146/ANNUREV.PHYSIOL.66.032102.150251

Dacheux, J. L., Castella, S., Gatti, J. L., and Dacheux, F. (2005). Epididymal cell secretory activities and the role of proteins in boar sperm maturation. *Theriogenology* **63**, 319–341. doi:10.1016/J.THERIOGENOLOGY.2004.09.015

Darby, E., and Anawalt, B. D. (2005). Male hypogonadism: an update on diagnosis and treatment. *Treat. Endocrinol.* **4**, 293–309. doi:10.2165/00024677-200504050-00003

Einarsson, S., Brunius, C., Wallgren, M., Lundstrom, K., Andersson, K., Zamaratskaia, G., and Rodriguez-Martinez, H. (2011). Effects of early vaccination with Improvac® on the development and function of reproductive organs of male pigs. *Anim. Reprod. Sci.* **127**, 50–55. doi:10.1016/J.ANIREPROSCI.2011.06.006

Erickson, D. W., Way, A. L., Bertolla, R. P., Chapman, D. A., and Killian, G. J. (2007). Influence of osteopontin, casein and oviductal fluid on bovine sperm capacitation. *Anim. Reprod.* **4**, 103–112.

Foster, J. A., Klotz, K. L., Flickinger, C. J., Thomas, T. S., Wright, R. M., Castillo, J. R., and Herr, J. C. (1994). Human SP-10: acrosomal distribution, processing, and fate after the acrosome reaction. *Biol. Reprod.* **51**, 1222–1231. doi:10.1095/BIOLREPROD51.6.1222

Fraietta, R., Zylberstejn, D. S., and Esteves, S. C. (2013). Hypogonadotropic hypogonadism revisited. *Clinics (São Paulo)* **68**, 81–88. doi:10.6061/CLINICS/2013(SUP01)09

França, L. R., Avelar, G. F., and Almeida, F. F. (2005). Spermatogenesis and sperm transit through the epididymis in mammals with emphasis on pigs. *Theriogenology* **63**, 300–318. doi:10.1016/J.THERIOGENOLOGY.2004.09.014

Frapsauce, C., Pionneau, C., Bouley, J., Delarouziere, V., Berthaut, I., Ravel, C., Antoine, J. M., Soubrier, F., and Mandelbaum, J. (2014). Proteomic identification of target proteins in normal but nonfertilizing sperm. *Fertil. Steril.* **102**, 372–380. doi:10.1016/J.FERTNSTERT.2014.04.039

Gao, Z., and Garbers, D. L. (1998). Species diversity in the structure of zonadhesin, a sperm-specific membrane protein containing multiple cell adhesion molecule-like domains. *J. Biol. Chem.* **273**, 3415–3421. doi:10.1074/JBC.273.6.3415

Garrido, N., Meseguer, M., Alvarez, J., Simon, C., Pellicer, A., and Remohi, J. (2004). Relationship among standard semen parameters, glutathione peroxidase/glutathione reductase activity, and mRNA expression and reduced glutathione content in ejaculated spermatozoa from fertile and infertile men. *Fertil. Steril.* **82**, 1059–1066. doi:10.1016/J.FERTNSTERT.2004.04.033

Gibb, Z., and Aitken, R. J. (2016). The impact of sperm metabolism during *in vitro* storage: the stallion as a model. *BioMed Res. Int.* **2016**, 9380609. doi:10.1155/2016/9380609

Griffith, R. O., Dressendorfer, R. H., Fullbright, C. D., and Wade, C. E. (1990). Testicular function during exhaustive endurance training. *Phys. Sportsmed.* **18**, 54–64. doi:10.1080/00913847.1990.11710041

Gu, N. H., Zhao, W. L., Wang, G. S., and Sun, F. (2019). Comparative analysis of mammalian sperm ultrastructure reveals relationships between sperm morphology, mitochondrial functions and motility. *Reprod. Biol. Endocrinol.* **17**, 66. doi:10.1186/S12958-019-0510-Y

Guan, S. S., Sheu, M. L., Wu, C. T., Chiang, C. K., and Liu, S. H. (2015). ATP synthase subunit-beta down-regulation aggravates diabetic nephropathy. *Sci. Rep.* **5**, 14561. doi:10.1038/SREP14561

Guo, Y., Wang, A., Liu, X., and Li, E. (2019). Effects of resveratrol on reducing spermatogenic dysfunction caused by high-intensity exercise. *Reprod. Biol. Endocrinol.* **17**, 42. doi:10.1186/S12958-019-0486-7

Hamada, A., Esteves, S. C., Nizza, M., and Agarwal, A. (2012). Unexplained male infertility: diagnosis and management. *Int. Braz J Urol* **38**, 576–594. doi:10.1590/S1677-55382012000500002

Hamzeh, M., and Robaire, B. (2011). Androgens activate mitogen-activated protein kinase via epidermal growth factor receptor/insulin-like growth factor 1 receptor in the mouse PC-1 cell line. *J. Endocrinol.* **209**, 55–64. doi:10.1530/JOE-10-0223

Han, X., Zhou, Y., Zeng, Y., Sui, F., Liu, Y., Tan, Y., Cao, X., Du, X., Meng, F., and Zeng, X. (2017). Effects of active immunization against GnRH versus surgical castration on hypothalamic-pituitary function in boars. *Theriogenology* **97**, 89–97. doi:10.1016/J.THERIOGENOLOGY.2017.04.038

Hardy, D. M., and Garbers, D. L. (1994). Species-specific binding of sperm proteins to the extracellular matrix (zona pellucida) of the egg. *J. Biol. Chem.* **269**, 19000–19004.

Hardy, D. M., and Garbers, D. L. (1995). A sperm membrane protein that binds in a species-specific manner to the egg extracellular matrix is homologous to von Willebrand factor. *J. Biol. Chem.* **270**, 26025–26028. doi:10.1074/JBC.270.44.26025

Heberle, H., Meirelles, G. V., da Silva, F. R., Telles, G. P., and Minghim, R. (2015). InteractiVenn: a web-based tool for the analysis of sets through Venn diagrams. *BMC Bioinformatics* **16**, 169. doi:10.1186/S12859-015-0611-3

Herr, J. C., Wright, R. M., John, E., Foster, J., Kays, T., and Flickinger, C. J. (1990). Identification of human acrosomal antigen SP-10 in primates and pigs. *Biol. Reprod.* **42**, 377–382. doi:10.1095/BIOLREPROD42.2.377

Ho, C. C., and Tan, H. M. (2013). Treatment of the hypogonadal infertile male – a review. *Sex. Med. Rev.* **1**, 42–49. doi:10.1002/SMRJ.4

Holland, A., and Ohlendieck, K. (2015). Comparative profiling of the sperm proteome. *Proteomics* **15**, 632–648. doi:10.1002/PMIC.201400032

Intasqui, P., Camargo, M., Del Giudice, P. T., Spaine, D. M., Carvalho, V. M., Cardozo, K. H., Cedenho, A. P., and Bertolla, R. P. (2013). Unraveling the sperm proteome and post-genomic pathways associated with sperm nuclear DNA fragmentation. *J. Assist. Reprod. Genet.* **30**, 1187–1202. doi:10.1007/S10815-013-0054-6

Kaplan, M., Russell, L. D., Peterson, R. N., and Martan, J. (1984). Boar sperm cytoplasmic droplets: their ultrastructure, their numbers in the epididymis and at ejaculation and their removal during isolation of sperm plasma membranes. *Tissue Cell* **16**, 455–468. doi:10.1016/0040-8166(84)90063-6

Kato, S., Shibukawa, T., Harayama, H., and Kannan, Y. (1996). The timing of shedding and disintegration of cytoplasmic droplets from boar and goat. *J. Reprod. Dev.* **42**, 237–241. doi:10.1262/JRD.42.237

Katz, D. J., Nabulsi, O., Tal, R., and Mulhall, J. P. (2012). Outcomes of clomiphene citrate treatment in young hypogonadal men. *BJU Int.* **110**, 573–578. doi:10.1111/J.1464-410X.2011.10702.X

Kruljac, M., Finnbogadóttir, H., Bobjer, J., Giraldi, A., Fugl-Meyer, K., and Giwercman, A. (2020). Symptoms of sexual dysfunction among men from infertile couples: prevalence and association with testosterone deficiency. *Andrology* **8**, 160–165. doi:10.1111/ANDR.12678

Kuster, C. E., and Althouse, G. C. (2003). A technique for preserving retained distal cytoplasmic droplets *in situ* for immunofluorescence evaluation of ejaculated porcine spermatozoa. *Prep. Biochem. Biotechnol.* **33**, 301–310. doi:10.1081/PB-120025372

Kwon, W. S., Rahman, M. S., Ryu, D. Y., Park, Y. J., and Pang, M. G. (2015). Increased male fertility using fertility-related biomarkers. *Sci. Rep.* **5**, 15654. doi:10.1038/SREP15654

Landim-Alvarenga, F. C., Graham, J. K., Alvarenga, M. A., and Squires, E. L. (2004). Calcium influx into equine and bovine spermatozoa during *in vitro* capacitation. *Anim. Reprod.* **1**, 96–105.

Lea, I. A., Sivashanmugam, P., and O'Rand, M. G. (2001). Zonadhesin: characterization, localization, and zona pellucida binding. *Biol. Reprod.* **65**, 1691–1700. doi:10.1095/BIOLREPROD65.6.1691

Leemans, B., Stout, T. A. E., De Schauwer, C., Heras, S., Nelis, H., Hoogewijs, M., Van Soon, A., and Gadella, B. M. (2019). Update on mammalian sperm capacitation: how much does the horse differ from other species? *Reproduction* **157**, R181–R197. doi:10.1530/REP-18-0541

Li, L. Y., Seddon, A. P., Meister, A., and Risley, M. S. (1989). Spermatogenic cell–somatic cell interactions are required for maintenance of spermatogenic cell glutathione. *Biol. Reprod.* **40**, 317–331. doi:10.1095/BIOLREPROD40.2.317

Liberzon, A., Birger, C., Thorvaldsdottir, H., Ghandi, M., Mesirov, J. P., and Tamayo, P. (2015). The Molecular Signatures Database (MSigDB) hallmark gene set collection. *Cell Syst.* **1**, 417–425. doi:10.1016/J.CELS.2015.12.004

Liu, H., Sadygov, R. G., and Yates, J. R., 3rd (2004). A model for random sampling and estimation of relative protein abundance in shotgun proteomics. *Anal. Chem.* **76**, 4193–4201. doi:10.1021/AC0498563

Lundgren, D. H., Hwang, S. I., Wu, L., and Han, D. K. (2010). Role of spectral counting in quantitative proteomics. *Expert Rev. Proteomics* **7**, 39–53. doi:10.1586/EPR.09.69

McDonald, W. H., Tabb, D. L., Sadygov, R. G., MacCoss, M. J., Venable, J., Graumann, J., Johnson, J. R., Cociorva, D., and Yates, J. R., 3rd (2004). MS1, MS2, and SQT-three unified, compact, and easily parsed file formats for the storage of shotgun proteomic spectra and identifications. *Rapid Commun. Mass Spectrom.* **18**, 2162–2168. doi:10.1002/RCM.1603

Meybodi, A. M., Mozdarani, H., Moradi, Sh. Z., and Akhoond, M. R. (2012). Importance of sperm gluthatione treatment in ART. *J. Assist. Reprod. Genet.* **29**, 625–630. doi:10.1007/S10815-012-9755-5

Mitra, K., and Shivaji, S. (2004). Novel tyrosine-phosphorylated post-pyruvate metabolic enzyme, dihydrolipoamide dehydrogenase, involved in capacitation of hamster spermatozoa. *Biol. Reprod.* **70**, 887–899. doi:10.1095/BIOLREPROD.103.022780

Mitra, K., Rangaraj, N., and Shivaji, S. (2005). Novelty of the pyruvate metabolic enzyme dihydrolipoamide dehydrogenase in spermatozoa: correlation of its localization, tyrosine phosphorylation, and activity during sperm capacitation. *J. Biol. Chem.* **280**, 25743–25753. doi:10.1074/JBC.M500310200

Montiel, E. E., Huidobro, C. C., and Castellon, E. A. (2003). Glutathione-related enzymes in cell cultures from different regions of human epididymis. *Arch. Androl.* **49**, 95–105. doi:10.1080/01485010390129296-1

Nakamura, N., Dai, Q., Williams, J., Goulding, E. H., Willis, W. D., Brown, P. R., and Eddy, E. M. (2013). Disruption of a spermatogenic cell-specific mouse enolase 4 (*eno4*) gene causes sperm structural defects and male infertility. *Biol. Reprod.* **88**, 90. doi:10.1095/BIOLREPROD.112.107128

National Research Council (2011). 'Guide for the Care and Use of laboratory Animals.' 8th edn. (The National Academies Press: Washington, DC.)

National Research Council (2012). 'Nutrient Requirements of Swine.' 11th edn. (The National Academies Press: Washington, DC.)

Olson, G. E., Winfrey, V. P., Bi, M., Hardy, D. M., and NagDas, S. K. (2004). Zonadhesin assembly into the hamster sperm acrosomal matrix occurs by distinct targeting strategies during spermiogenesis and maturation in the epididymis. *Biol. Reprod.* **71**, 1128–1134. doi:10.1095/BIOLREPROD.104.029975

Park, Y. J., Kwon, W. S., Oh, S. A., and Pang, M. G. (2012). Fertility-related proteomic profiling bull spermatozoa separated by percoll. *J. Proteome Res.* **11**, 4162–4168. doi:10.1021/PR300248S

Patrão, M. T., Silva, E. J., and Avellar, M. C. (2009). Androgens and the male reproductive tract: an overview of classical roles and current perspectives. *Arq. Bras. Endocrinol. Metabol* **53**, 934–945. doi:10.1590/S0004-27302009000800006

Perez-Patiño, C., Barranco, I., Li, J., Padilla, L., Martinez, E. A., Rodriguez-Martinez, H., Roca, J., and Parrilla, I. (2019*a*). Cryopreservation differentially alters the proteome of epididymal and ejaculated pig spermatozoa. *Int. J. Mol. Sci.* **20**, 1791. doi:10.3390/IJMS20071791

Perez-Patiño, C., Li, J., Barranco, I., Martinez, E. A., Rodriguez-Martinez, H., Roca, J., and Parrilla, I. (2019*b*). The proteome of frozen–thawed pig spermatozoa is dependent on the ejaculate fraction source. *Sci. Rep.* **9**, 705. doi:10.1038/S41598-018-36624-5

Perez-Patiño, C., Parrilla, I., Li, J., Barranco, I., Martinez, E. A., Rodriguez-Martinez, H., and Roca, J. (2019*c*). The proteome of pig spermatozoa is remodeled during ejaculation. *Mol. Cell. Proteomics* **18**, 41–50. doi:10.1074/MCP.RA118.000840

Perobelli, J. E., Patrao, M. T., Fernandez, C. D., Sanabria, M., Klinefelter, G. R., Avellar, M. C., and Kempinas, W. D. (2013). Androgen deprivation from pre-puberty to peripuberty interferes in proteins expression in pubertal and adult rat epididymis. *Reprod. Toxicol.* **38**, 65–71. doi:10.1016/J.REPROTOX.2013.03.004

Pfaffl, M. W. (2001). A new mathematical model for relative quantification in real-time RT-PCR. *Nucleic Acids Res.* **29**, e45. doi:10.1093/NAR/29.9.E45

Ramakers, C., Ruijter, J. M., Deprez, R. H., and Moorman, A. F. (2003). Assumption-free analysis of quantitative real-time polymerase chain reaction (PCR) data. *Neurosci. Lett.* **339**, 62–66. doi:10.1016/S0304-3940(02)01423-4

Reddi, P. P., Shore, A. N., Acharya, K. K., and Herr, J. C. (2002). Transcriptional regulation of spermiogenesis: insights from the study of the gene encoding the acrosomal protein SP-10. *J. Reprod. Immunol.* **53**, 25–36. doi:10.1016/S0165-0378(01)00104-8

Robaire, B., and Hamzeh, M. (2011). Androgen action in the epididymis. *J. Androl.* **32**, 592–599. doi:10.2164/JANDROL.111.014266

Ruijter, J. M., Ramakers, C., Hoogaars, W. M., Karlen, Y., Bakker, O., van den Hoff, M. J., and Moorman, A. F. (2009). Amplification efficiency: linking baseline and bias in the analysis of quantitative PCR data. *Nucleic Acids Res.* **37**, e45. doi:10.1093/NAR/GKP045

Santi, L., Beys-da-Silva, W. O., Berger, M., Calzolari, D., Guimaraes, J. A., Moresco, J. J., and Yates, J. R., 3rd (2014). Proteomic profile of *Cryptococcus neoformans* biofilm reveals changes in metabolic processes. *J. Proteome Res.* **13**, 1545–1559. doi:10.1021/PR401075F

Scheer, H., and Robaire, B. (1980). Steroid delta 4–5 alpha-reductase and 3 alpha-hydroxysteroid dehydrogenase in the rat epididymis during development. *Endocrinology* **107**, 948–953. doi:10.1210/ENDO-107-4-948

Schorr-Lenz, A. M., Alves, J., Henckes, N. A., Seibel, P. M., Benham, A. M., and Bustamante-Filho, I. C. (2016). GnRH immunization alters the expression and distribution of protein disulfide isomerases in the epididymis. *Andrology* **4**, 957–963. doi:10.1111/ANDR.12205

Sharma, R., Agarwal, A., Mohanty, G., Hamada, A. J., Gopalan, B., Willard, B., Yadav, S., and du Plessis, S. (2013). Proteomic analysis of human spermatozoa proteins with oxidative stress. *Reprod. Biol. Endocrinol.* **11**, 48. doi:10.1186/1477-7827-11-48

Shukla, K. K., Kwon, W. S., Rahman, M. S., Park, Y. J., You, Y. A., and Pang, M. G. (2013). Nutlin-3a decreases male fertility via UQCRC2. *PLoS One* **8**, e76959. doi:10.1371/JOURNAL.PONE.0076959

Sipilä, P., Krutskikh, A., Pujianto, D. A., Poutanen, M., and Huhtaniemi, I. (2011). Regional expression of androgen receptor coregulators and androgen action in the mouse epididymis. *J. Androl.* **32**, 711–717. doi:10.2164/JANDROL.110.012914

Siva, A. B., Panneerdoss, S., Sailasree, P., Singh, D. K., Kameshwari, D. B., and Shivaji, S. (2014). Inhibiting sperm pyruvate dehydrogenase complex and its E3 subunit, dihydrolipoamide dehydrogenase affects fertilization in Syrian hamsters. *PLoS One* **9**, e97916. doi:10.1371/JOURNAL.PONE.0097916

Sutovsky, P. (2018). Review: sperm–oocyte interactions and their implications for bull fertility, with emphasis on the ubiquitin–proteasome system. *Animal* **12**, s121–s132. doi:10.1017/S1751731118000253

Szklarczyk, D., Franceschini, A., Wyder, S., Forslund, K., Heller, D., Huerta-Cepas, J., Simonovic, M., Roth, A., Santos, A., Tsafou, K. P., Kuhn, M., Bork, P., Jensen, L. J., and von Mering, C. (2015). STRING v10: protein–protein interaction networks, integrated over the tree of life. *Nucleic Acids Res.* **43**, D447–D452. doi:10.1093/NAR/GKU1003

Szklarczyk, D., Santos, A., von Mering, C., Jensen, L. J., Bork, P., and Kuhn, M. (2016). STITCH 5: augmenting protein–chemical interaction networks with tissue and affinity data. *Nucleic Acids Res.* **44**, D380–D384. doi:10.1093/NAR/GKV1277

Tabb, D. L., McDonald, W. H., and Yates, J. R., 3rd (2002). DTASelect and Contrast: tools for assembling and comparing protein identifications from shotgun proteomics. *J. Proteome Res.* **1**, 21–26. doi:10.1021/PR015504Q

Tardif, S., Wilson, M. D., Wagner, R., Hunt, P., Gertsenstein, M., Nagy, A., Lobe, C., Koop, B. F., and Hardy, D. M. (2010). Zonadhesin is essential for species specificity of sperm adhesion to the egg zona pellucida. *J. Biol. Chem.* **285**, 24863–24870. doi:10.1074/JBC.M110.123125

Thimon, V., Belghazi, M., Dacheux, J. L., and Gatti, J. L. (2006). Analysis of furin ectodomain shedding in epididymal fluid of mammals: demonstration that shedding of furin occurs *in vivo*. *Reproduction* **132**, 899–908. doi:10.1530/REP-06-0077

Travis, A. J., Jorgez, C. J., Merdiushev, T., Jones, B. H., Dess, D. M., Diaz-Cueto, L., Storey, B. T., Kopf, G. S., and Moss, S. B. (2001). Functional relationships between capacitation-dependent cell signaling and compartmentalized metabolic pathways in murine spermatozoa. *J. Biol. Chem.* **276**, 7630–7636. doi:10.1074/JBC.M006217200

Tulsiani, D. R. (2003). Glycan modifying enzymes in luminal fluid of rat epididymis: are they involved in altering sperm surface glycoproteins during maturation? *Microsc. Res. Tech.* **61**, 18–27. doi:10.1002/JEMT.10313

Vaamonde, D., Algar-Santacruz, C., Abbasi, A., and Garcia-Manso, J. M. (2018). Sperm DNA fragmentation as a result of ultra-endurance exercise training in male athletes. *Andrologia* **50**, e12793. doi:10.1111/AND.12793

Verhoeven, G., Denolet, E., Swinnen, J. V., Willems, A., Saunders, P. T. K., Sharpe, R. M., and Gendt, K. D. (2007). The role of androgens in the control of spermatogenesis: lessons from transgenic models involving a Sertoli cell-selective knockout of the androgen receptor. *Anim. Reprod.* **4**, 3–14.

Wang, G., Guo, Y., Zhou, T., Shi, X., Yu, J., Yang, Y., Wu, Y., Wang, J., Liu, M., Chen, X., Tu, W., Zeng, Y., Jiang, M., Li, S., Zhang, P., Zhou, Q., Zheng, B., Yu, C., Zhou, Z., Guo, X., and Sha, J. (2013). In-depth proteomic analysis of the human sperm reveals complex protein compositions. *J. Proteomics* **79**, 114–122. doi:10.1016/J.JPROT.2012.12.008

Watanabe, K., Taskesen, E., van Bochoven, A., and Posthuma, D. (2017). Functional mapping and annotation of genetic associations with FUMA. *Nat. Commun.* **8**, 1826. doi:10.1038/S41467-017-01261-5

Weber, A., Alves, J., Abujamra, A. L., and Bustamante-Filho, I. C. (2018). Structural modeling and mRNA expression of epididymal beta-defensins in GnRH immunized boars: a model for secondary hypogonadism in man. *Mol. Reprod. Dev.* **85**, 921–933. doi:10.1002/MRD.23069

Weber, A., Argenti, L. E., de Souza, A. P. B., Santi, L., Beys-da-Silva, W. O., Yates, J. R., and Bustamante-Filho, I. C. (2020). Ready for the journey: a comparative proteome profiling of porcine cauda epididymal fluid and spermatozoa. *Cell Tissue Res.* **379**, 389–405. doi:10.1007/S00441-019-03080-0

Wolters, D. A., Washburn, M. P., and Yates, J. R., 3rd (2001). An automated multidimensional protein identification technology for shotgun proteomics. *Anal. Chem.* **73**, 5683–5690. doi:10.1021/AC010617E

Xu, T., Venable, J. D., Park, S. K., Cociorva, D., Lu, B., Liao, L., Wohlschlegel, J., Hewel, J., and Yates, J. R. (2006). ProLuCID, a fast and sensitive tandem mass spectra-based protein identification program. *Mol. Cell. Proteomics* **5**, S174.

Yeung, C. H., and Cooper, T. G. (2002) Acquisition and development of sperm motility upon maturation in the epididymis. In 'The Epididymis – From Molecules To Clinical Practice'. Vol. 1. (Eds B. Robaire and B. T. Hinton.) pp. 417–434. (Kluwer Academic/Plenum Press: New York.)

Zamaratskaia, G., Andersson, H. K., Chen, G., Andersson, K., Madej, A., and Lundstrom, K. (2008). Effect of a gonadotropin-releasing hormone vaccine (Improvac) on steroid hormones, boar taint compounds and performance in entire male pigs. *Reprod. Domest. Anim.* **43**, 351–359. doi:10.1111/J.1439-0531.2007.00914.X

Zigo, M., Jonakova, V., Manaskova-Postlerova, P., Kerns, K., and Sutovsky, P. (2019). Ubiquitin–proteasome system participates in the de-aggregation of spermadhesins and DQH protein during boar sperm capacitation. *Reproduction* **157**, 283. doi:10.1530/REP-18-0413

Zirkin, B. R., Santulli, R., Awoniyi, C. A., and Ewing, L. L. (1989). Maintenance of advanced spermatogenic cells in the adult rat testis: quantitative relationship to testosterone concentration within the testis. *Endocrinology* **124**, 3043–3049. doi:10.1210/ENDO-124-6-3043

Handling Editor: Jessica E. M. Dunleavy

Supplementary

Table 2 - Complete list of proteins identified in the cauda epididymal spermatozoa proteome using MudPIT. Part of the manuscript by Souza et al.

Accession number	Fold Change	pValue	Description
gi|545822151|ref|XP_005663205.1|	4,44	0,01766539	PREDICTED: 4-trimethylaminobutyraldehyde dehydrogenase [Sus scrofa]
gi|47523156|ref|NP_999014.1|	4,153846154	0,001888656	epididymis-specific alpha-mannosidase precursor [Sus scrofa]
gi|545819737|ref|XP_005655383.1|	3,4	0,000528782	PREDICTED: 5-oxoprolinase-like [Sus scrofa]
gi|350582850|ref|XP_003125520.3|	3,4	0,000528782	PREDICTED: 5-oxoprolinase, partial [Sus scrofa]
gi|545870917|ref|XP_005654198.1|	3,333333333	7,55E-05	PREDICTED: anthrax toxin receptor-like [Sus scrofa]
gi|545835029|ref|XP_003356376.2|	3,3	0,016615629	PREDICTED: transmembrane and coiled-coil domain-containing protein 2 [Sus scrofa]
gi|545816851|ref|XP_005662522.1|	3,175438596	0,016135231	PREDICTED: Alstrom syndrome protein 1 isoform X2 [Sus scrofa]
gi|194033405|ref|XP_001928380.1|	3,083333333	0,020207522	PREDICTED: acetyl-CoA acetyltransferase, cytosolic [Sus scrofa]
gi|47522940|ref|NP_999227.1|	3,012820513	0,00508361	dihydrolipoyl dehydrogenase, mitochondrial precursor [Sus scrofa]
gi|545816848|ref|XP_005662521.1|	2,898550725	0,006957031	PREDICTED: Alstrom syndrome protein 1 isoform X1 [Sus scrofa]
gi|545885011|ref|XP_005673709.1|	2,708333333	0,008185029	PREDICTED: E3 ubiquitin-protein ligase HUWE1 isoform X2 [Sus scrofa]
gi|545831021|ref|XP_005655919.1|	2,473684211	0,016048551	PREDICTED: hormone-sensitive lipase isoform X1 [Sus scrofa]
gi|545891899|ref|XP_003361852.2|	2,356435644	0,000461327	PREDICTED: L-lactate dehydrogenase A-like 6B-like, partial [Sus scrofa]
gi|335278864|ref|XP_001926443.2|	2,306603774	0,000390575	PREDICTED: L-lactate dehydrogenase A-like 6B-like isoform X1 [Sus scrofa]
gi|307746886|ref|NP_001182704.1|	2,285714286	0,021622045	L-lactate dehydrogenase C chain [Sus scrofa]
gi|113205780|ref|NP_001038049.1|	2,25	0,005598836	quinone oxidoreductase [Sus scrofa]
gi|113205498|ref|NP_001037992.1|	2,081460674	0,004172717	beta-enolase [Sus scrofa]
gi|545857759|ref|XP_005657006.1|	2,066666667	0,017968713	PREDICTED: synaptic vesicle membrane protein VAT-1 homolog [Sus scrofa]
gi|281427374|ref|NP_001163991.1|	2,065934066	0,003241953	T-complex protein 1 subunit beta [Sus scrofa]
gi|298677090|ref|NP_001177351.1|	2,046875	0,01253165	superoxide dismutase [Cu-Zn] [Sus scrofa]
gi|545827421|ref|XP_005652652.1|	2,042253521	0,003548795	PREDICTED: gamma-enolase [Sus scrofa]
gi|311248983|ref|XP_003123401.1|	1,893129771	0,001828052	PREDICTED: cAMP-dependent protein kinase catalytic subunit alpha isoformX1 [Sus scrofa]
gi|343478174|ref|NP_001230356.1|	1,811428571	0,01490915	T-complex protein 1 subunit alpha [Sus scrofa]
gi|335285628|ref|XP_003354908.1|	1,581395349	0,016847973	PREDICTED: tetratricopeptide repeat protein 39B-like [Sus scrofa]
gi|545798018|ref|XP_005659270.1|	1,545454545	0,015159835	PREDICTED: HD domain-containing protein 2 isoform X2 [Sus scrofa]
gi|311243995|ref|XP_003121268.1|	1,545454545	0,015159835	PREDICTED: HD domain-containing protein 2 isoform X1 [Sus scrofa]
gi|545810181|ref|XP_005661343.1|	-1,415584416	0,003278076	PREDICTED: long-chain-fatty-acid--CoA ligase ACSBG2 isoform X4 [Sus scrofa]
gi|545832172|ref|XP_003481945.2|	-1,472440945	0,01259076	PREDICTED: L-amino-acid oxidase isoform X1 [Sus scrofa]
gi|359811347|ref|NP_001241645.1|	-1,543859649	0,022170701	60 kDa heat shock protein, mitochondrial [Sus scrofa]
gi|350589263|ref|XP_003130553.2|	-1,548387097	0,027387628	PREDICTED: isoleucine--tRNA ligase, mitochondrial [Sus scrofa]
gi|350592249|ref|XP_003483427.1|	-1,558139535	0,011197103	PREDICTED: V-type proton ATPase subunit B, brain isoform [Sus scrofa]
gi|47522636|ref|NP_999092.1|	-1,571428571	0,010249068	aspartate aminotransferase, cytoplasmic [Sus scrofa]
gi|47522624|ref|NP_999098.1|	-1,603448276	0,009865566	arylsulfatase A precursor [Sus scrofa]
gi|350594254|ref|XP_003133959.3|	-1,631067961	0,007658576	PREDICTED: HEAT repeat family member 7B2, partial [Sus scrofa]
gi|545883750|ref|XP_003134939.4|	-1,674418605	0,028899916	PREDICTED: LOW QUALITY PROTEIN: 2-oxoglutarate dehydrogenase, mitochondrial [Sus scrofa]
gi|311260358|ref|XP_001924974.2|	-1,674698795	0,003565205	PREDICTED: dynein heavy chain 8, axonemal isoform X1 [Sus scrofa]
gi|545877574|ref|XP_005674537.1|	-1,70212766	0,011809083	PREDICTED: LOW QUALITY PROTEIN: actin, beta-like 2 [Sus scrofa]
gi|545839370|ref|XP_005652693.1|	-1,730769231	0,003696404	PREDICTED: dynein heavy chain 8, axonemal isoform X8 [Sus scrofa]
gi|317681941|ref|NP_001186971.1|	-1,75862069	0,0035108	betaine--homocysteine S-methyltransferase 1 [Sus scrofa]
gi|346986328|ref|NP_001231318.1|	-1,76	0,017822316	saccharopine dehydrogenase-like oxidoreductase [Sus scrofa]
gi|48374071|ref|NP_001001539.1|	-1,781456954	0,006222296	aldose reductase [Sus scrofa]
gi|47522870|ref|NP_999189.1|	-1,807692308	0,016996064	serine/threonine-protein phosphatase 2A 65 kDa regulatory subunit A alpha isoform [Sus scrofa]
gi|335299885|ref|XP_003358716.1|	-1,849315068	0,002223012	PREDICTED: actin-related protein T3 [Sus scrofa]

gi|349732258|ref|NP_001231869.1|	-1,875	0,001096065	uroporphyrinogen decarboxylase [Sus scrofa]
gi|47523738|ref|NP_999504.1|	-1,875	0,026738531	dnaJ homolog subfamily A member 4 [Sus scrofa]
gi|350584746|ref|XP_003481817.1|	-1,894117647	0,009240981	PREDICTED: cullin-associated NEDD8-dissociated protein 1 [Sus scrofa]
gi|311255888|ref|XP_003126410.1|	-1,894117647	0,009240981	PREDICTED: cullin-associated NEDD8-dissociated protein 1 [Sus scrofa]
gi|350582836|ref|XP_003481371.1|	-1,895833333	0,001222338	PREDICTED: maestro heat-like repeat-containing protein family member 1-like [Sus scrofa]
gi|297591979|ref|NP_001172070.1|	-1,906976744	0,004909317	ornithine aminotransferase, mitochondrial [Sus scrofa]
gi|311266259|ref|XP_003131022.1|	-1,92	0,013750211	PREDICTED: succinyl-CoA ligase [ADP-forming] subunit beta, mitochondrial [Sus scrofa]
gi|47522920|ref|NP_999217.1|	-2	0,005063657	1-phosphatidylinositol 4,5-bisphosphate phosphodiesterase delta-4 [Sus scrofa]
gi|545875603|ref|XP_005672249.1|	-2	0,005063657	PREDICTED: 1-phosphatidylinositol 4,5-bisphosphate phosphodiesterase delta-4 isoform X7 [Sus scrofa]
gi|47523618|ref|NP_999441.1|	-2,007092199	0,00064186	citrate synthase, mitochondrial precursor [Sus scrofa]
gi|113205694|ref|NP_001038025.1|	-2,045454545	0,012975941	protein phosphatase 1 catalytic subunit gamma isoform [Sus scrofa]
gi|308081427|ref|NP_001183950.1|	-2,05	0,007315526	hydroxysteroid dehydrogenase-like protein 2 [Sus scrofa]
gi|311259466|ref|XP_003128111.1|	-2,076923077	0,001096065	PREDICTED: putative hydroxypyruvate isomerase isoformX1 [Sus scrofa]
gi|545827237|ref|XP_005664116.1|	-2,214285714	0,02265373	PREDICTED: phospholipase B-like 1-like [Sus scrofa]
gi|545811613|ref|XP_005661563.1|	-2,238095238	0,011323	PREDICTED: IQ motif containing GTPase activating protein 2 [Sus scrofa]
gi|295444982|ref|NP_001171401.1|	-2,266666667	0,002204322	sperm acrosome-associated protein 5 precursor [Sus scrofa]
gi|55741862|ref|NP_999548.1|	-2,350649351	0,00584241	zonadhesin precursor [Sus scrofa]
gi|350580562|ref|XP_003480848.1|	-2,373134328	0,002719232	PREDICTED: actin-like protein 9 [Sus scrofa]
gi|335307492|ref|XP_003360859.1|	-2,407407407	0,017162277	PREDICTED: inactive ribonuclease-like protein 9-like [Sus scrofa]
gi|347543795|ref|NP_001231558.1|	-2,444444444	0,015687867	phospholipase B-like 1 precursor [Sus scrofa]
gi|311277183|ref|XP_003135545.1|	-2,5	0,004630848	PREDICTED: isocitrate dehydrogenase [NAD] subunit gamma, mitochondrial isoformX1 [Sus scrofa]
gi|190360575|ref|NP_001121906.1|	-2,5	0,007315526	cysteine-rich secretory protein 1 precursor [Sus scrofa]
gi|194038542|ref|XP_001929208.1|	-2,5	0,022403316	PREDICTED: methylmalonate-semialdehyde dehydrogenase [acylating], mitochondrial isoform X1 [Sus scrofa]
gi|342349346|ref|NP_001230149.1|	-2,533333333	0,011015214	lon peptidase 1, mitochondrial [Sus scrofa]
gi|194036261|ref|XP_001929699.1|	-2,558823529	0,011908458	PREDICTED: protein MENT [Sus scrofa]
gi|545840224|ref|XP_005656305.1|	-2,588235294	0,016382971	PREDICTED: isocitrate dehydrogenase [NAD] subunit alpha, mitochondrial isoform X3 [Sus scrofa]
gi|335292262|ref|XP_001927373.3|	-2,588235294	0,016382971	PREDICTED: isocitrate dehydrogenase [NAD] subunit alpha, mitochondrial isoform X1 [Sus scrofa]
gi|545833287|ref|XP_005665011.1|	-2,605263158	0,000535049	PREDICTED: membrane metallo-endopeptidase-like 1 [Sus scrofa]
gi|350592969|ref|XP_003483583.1|	-2,666666667	0,015212269	PREDICTED: phosphoglycerate mutase 1 [Sus scrofa]
gi|47522790|ref|NP_999147.1|	-2,684210526	0,012781482	leukocyte surface antigen CD47 precursor [Sus scrofa]
gi|346644830|ref|NP_001231167.1|	-2,692307692	0,013197235	sulfide:quinone oxidoreductase, mitochondrial [Sus scrofa]
gi|47523782|ref|NP_999527.1|	-2,901960784	0,003027994	lactotransferrin precursor [Sus scrofa]
gi|305855186|ref|NP_001182249.1|	-3,030927835	0,007896531	acrosomal protein SP-10 precursor [Sus scrofa]
gi|350592508|ref|XP_001925814.4|	-3,2	0,002090536	PREDICTED: putative phospholipase B-like 2 isoform 1 [Sus scrofa]
gi|545819696|ref|XP_005674638.1|	-3,2	0,007543071	PREDICTED: LOW QUALITY PROTEIN: maestro heat-like repeat family member 1 [Sus scrofa]
gi|545849138|ref|XP_005667533.1|	-3,24137931	0,00764191	PREDICTED: acrosomal protein SP-10 isoform X1 [Sus scrofa]
gi|311250475|ref|XP_003124136.1|	-3,307692308	0,005318314	PREDICTED: casein kinase I isoform alpha isoformX1 [Sus scrofa]
gi|226533703|ref|NP_001152784.1|	-3,333333333	0,025180425	sperm-associated antigen 6 [Sus scrofa]
gi|47522848|ref|NP_999176.1|	-3,446808511	0,001318816	sperm adhesion molecule 1 [Sus scrofa]
gi|545819702|ref|XP_005655375.1|	-3,466666667	0,002428699	PREDICTED: maestro heat-like repeat-containing protein family member 1-like isoform X1 [Sus scrofa]
gi|545849140|ref|XP_005667534.1|	-3,507462687	0,005860353	PREDICTED: acrosomal protein SP-10 isoform X2 [Sus scrofa]
gi|348605274|ref|NP_001231762.1|	-3,555555556	0,012364241	alcohol dehydrogenase 5 (class III), chi polypeptide [Sus scrofa]
gi|545849142|ref|XP_005667535.1|	-3,56	0,011347385	PREDICTED: acrosomal protein SP-10 isoform X3 [Sus scrofa]
gi|47522760|ref|NP_999131.1|	-3,578947368	0,014707131	long-chain 3-ketoacyl-CoA thiolase [Sus scrofa]
gi|545826025|ref|XP_001929445.2|	-3,626666667	0,000882976	PREDICTED: ATP synthase subunit beta, mitochondrial [Sus scrofa]

gi|346986351|ref|NP_001231327.1|	-4	0,001386558	pyruvate dehydrogenase E1 component subunit beta, mitochondrial [Sus scrofa]
gi|47522648|ref|NP_999086.1|	-4	0,005104756	beta-hexosaminidase subunit beta precursor [Sus scrofa]
gi|335292766|ref|XP_001926294.2|	-4,125	0,014008894	PREDICTED: dynein light chain 1, axonemal [Sus scrofa]
gi|335295111|ref|XP_003130113.2|	-4,333333333	0,000127608	PREDICTED: protein FAM118B isoform X1 [Sus scrofa]
gi|350590240|ref|XP_003483017.1|	-4,571428571	0,000159243	PREDICTED: lysozyme-like protein 6-like [Sus scrofa]
gi|545858201|ref|XP_005653969.1|	-5,012820513	0,004307831	PREDICTED: zona pellucida-binding protein 2 isoform X1 [Sus scrofa]
gi|47523540|ref|NP_999393.1|	-5,4	0,002228688	prostaglandin-H2 D-isomerase precursor [Sus scrofa]
gi|311265636|ref|XP_003130749.1|	-5,511111111	0,000265255	PREDICTED: lysozyme-like protein 1 [Sus scrofa]
gi|291622246|ref|NP_001167604.1|	-5,555555556	0,018590614	calreticulin precursor [Sus scrofa]
gi|311268718|ref|XP_003132179.1|	-6,142857143	0,00012838	PREDICTED: lysozyme-like protein 4 isoform 1 [Sus scrofa]
gi|52353352|ref|NP_001005208.1|	-11,66666667	0,002271487	serum albumin precursor [Sus scrofa]
gi|311246884|ref|XP_003122377.1|	-13,86666667	0,006050765	PREDICTED: epididymal-specific lipocalin-5 [Sus scrofa]
gi|335284501|ref|XP_003124603.2|	-17	1,00E-05	PREDICTED: cytochrome b-c1 complex subunit 2, mitochondrial-like [Sus scrofa]

#These identifications were filtered out by the L-stringency and so deserve further experimentation to verify if they are indeed differentially expressed			
gi|113205688|ref|NP_001038026.1|	2	1,00E-05	sperm flagellar protein 2 [Sus scrofa]
gi|545854115|ref|XP_005668301.1|	-2,142857143	0,000661948	PREDICTED: isopentenyl-diphosphate Delta-isomerase 1 isoform X1 [Sus scrofa]
gi|347658971|ref|NP_001231613.1|	-4,444444444	0,001412907	ATP synthase, H+ transporting, mitochondrial Fo complex, subunit d [Sus scrofa]
gi|343790977|ref|NP_001230537.1|	-3,25	0,001562795	phospholysine phosphohistidine inorganic pyrophosphate phosphatase [Sus scrofa]
gi|213021241|ref|NP_001132944.1|	-3,571428571	0,001562795	proteasome subunit alpha type-6 [Sus scrofa]
gi|545840801|ref|XP_005666204.1|	-3,666666667	0,001886008	PREDICTED: cytochrome c oxidase subunit 5A, mitochondrial-like [Sus scrofa]
gi|335300872|ref|XP_001928827.3|	-2,666666667	0,002237439	PREDICTED: methylglutaconyl-CoA hydratase, mitochondrial isoform X1 [Sus scrofa]
gi|545855658|ref|XP_005653884.1|	-3,4	0,002910343	PREDICTED: CLYBL protein, partial [Sus scrofa]
gi|311275228|ref|XP_003134621.1|	-2,666666667	0,003380068	PREDICTED: glutathione S-transferase kappa 1 isoform 1 [Sus scrofa]
gi|335299818|ref|XP_003358693.1|	-2,25	0,003380068	PREDICTED: retinoic acid receptor responder protein 1 isoform 1 [Sus scrofa]
gi|545894062|ref|XP_005658550.1|	-6,25	0,003507771	PREDICTED: selenide, water dikinase 1 [Sus scrofa]
gi|545890279|ref|XP_005658515.1|	-2,416666667	0,004602944	PREDICTED: alkaline phosphatase, tissue-nonspecific isozyme [Sus scrofa]
gi|350587377|ref|XP_003356918.2|	-6	0,005452352	PREDICTED: cytosol aminopeptidase-like [Sus scrofa]
gi|311258421|ref|XP_003127605.1|	-3	0,0056775	PREDICTED: 6-phosphogluconate dehydrogenase, decarboxylating [Sus scrofa]
gi|350595555|ref|XP_003360292.2|	-3,111111111	0,005731216	PREDICTED: pyruvate dehydrogenase E1 component subunit alpha, somatic form, mitochondrial isoform 1 [Sus scrofa]
gi|350595557|ref|XP_003484129.1|	-3,111111111	0,005731216	PREDICTED: pyruvate dehydrogenase E1 component subunit alpha, somatic form, mitochondrial isoform 2 [Sus scrofa]
gi|329755341|ref|NP_001193330.1|	-2,357142857	0,005731216	dnaJ homolog subfamily C member 5B [Sus scrofa]
gi|335305197|ref|XP_003360150.1|	-2,4	0,006153776	PREDICTED: probable inactive serine protease 37-like isoform X1 [Sus scrofa]
gi|350594412|ref|XP_003359865.2|	-5,333333333	0,00755087	PREDICTED: ubiquitin domain-containing protein 2 [Sus scrofa]
gi|335298275|ref|XP_003131863.2|	-2,333333333	0,008065045	PREDICTED: glyoxalase domain-containing protein 4 [Sus scrofa]
gi|545799960|ref|XP_005659559.1|	1,8	0,008065045	PREDICTED: casein kinase I isoform gamma-1 isoform X1 [Sus scrofa]
gi|157427738|ref|NP_001098778.1|	-2	0,008626406	NAD-dependent deacetylase sirtuin-5 [Sus scrofa]
gi|350595384|ref|XP_003134854.3|	-4	0,011001434	PREDICTED: glycine--tRNA ligase isoform X1 [Sus scrofa]
gi|194036265|ref|XP_001929700.1|	-2,428571429	0,012055055	PREDICTED: protein FAM63A isoform X1 [Sus scrofa]
gi|113205746|ref|NP_001038038.1|	-3,666666667	0,013498651	angiogenin precursor [Sus scrofa]
gi|47523848|ref|NP_999562.1|	-1,833333333	0,015233146	dihydrolipoyllysine-residue succinyltransferase component of 2-oxoglutarate dehydrogenase complex, mitochondrial precursor [Sus scrofa]
gi|349732201|ref|NP_001231854.1|	-6	0,015233146	dpy-30 homolog [Sus scrofa]
gi|48675943|ref|NP_001001640.1|	-1,65	0,015937098	amine oxidase [flavin-containing] A [Sus scrofa]
gi|545803558|ref|XP_005654580.1|	2,416666667	0,016252686	PREDICTED: transmembrane protein ENSP00000340100 homolog [Sus scrofa]
gi|113205776|ref|NP_001038050.1|	-2,285714286	0,016735872	cystathionine gamma-lyase [Sus scrofa]

gi|545805333|ref|XP_005652779.1|	-2,363636364	0,017631438	PREDICTED: 14 kDa phosphohistidine phosphatase isoform X2 [Sus scrofa]
gi|311265232|ref|XP_003130551.1|	-2,666666667	0,018874776	PREDICTED: 3'(2'),5'-bisphosphate nucleotidase 1 isoformX1 [Sus scrofa]
gi|545803468|ref|XP_003480587.2|	-2,7	0,018953058	PREDICTED: vacuolar protein sorting-associated protein 13A [Sus scrofa]
gi|335281070|ref|XP_003353729.1|	-2,1	0,0189983	PREDICTED: serine/threonine-protein phosphatase 2A activator isoformX2 [Sus scrofa]
gi|545823808|ref|XP_005663640.1|	-3,222222222	0,019014648	PREDICTED: glutathione S-transferase Mu 3-like isoform X1 [Sus scrofa]
gi|349732254|ref|NP_001231868.1|	-3,222222222	0,019014648	glutathione S-transferase Mu 3-like [Sus scrofa]
gi|545865987|ref|XP_005670247.1|	2,5	0,021829735	PREDICTED: uncharacterized protein C3orf30 homolog isoform X1 [Sus scrofa]
gi|350595403|ref|XP_003134876.3|	-3,5	0,021962476	PREDICTED: probable 3-hydroxyisobutyrate dehydrogenase, mitochondrial-like [Sus scrofa]
gi|346986249|ref|NP_001231282.1|	1,571428571	0,023710328	proteasome subunit beta type-1 [Sus scrofa]
gi|311260243|ref|XP_001927987.2|	-2,153846154	0,024771377	PREDICTED: protein CutA isoformX1 [Sus scrofa]
gi|311269387|ref|XP_003132466.1|	2,571428571	0,025687215	PREDICTED: LOW QUALITY PROTEIN: dnaJ homolog subfamily C member 13 [Sus scrofa]
gi|311270444|ref|XP_001927636.2|	-3,111111111	0,026650293	PREDICTED: disintegrin and metalloproteinase domain-containing protein 29 isoform X1 [Sus scrofa]
gi|350591295|ref|XP_003483243.1|	-3,666666667	0,026681361	PREDICTED: protein FAM3D isoformX2 [Sus scrofa]
gi|311249900|ref|XP_003123855.1|	-2,333333333	0,026681361	PREDICTED: peptidyl-glycine alpha-amidating monooxygenase isoformX2 [Sus scrofa]
gi|545836103|ref|XP_003356508.2|	2,333333333	0,026681361	PREDICTED: nucleoporin NDC1 isoform 1 [Sus scrofa]
gi|311255405|ref|XP_003126221.1|	2,333333333	0,026681361	PREDICTED: keratin, type II cytoskeletal 5 isoform X1 [Sus scrofa]
gi|194034801|ref|XP_001925712.1|	2,333333333	0,026681361	PREDICTED: normal mucosa of esophagus-specific gene 1 protein isoform 1 [Sus scrofa]
gi|349585085|ref|NP_001231804.1|	3,833333333	0,027387628	RAB11B, member RAS oncogene family [Sus scrofa]
gi|194034199|ref|XP_001928042.1|	-1,545454545	0,027520304	PREDICTED: proteasome subunit alpha type-3 isoform 2 [Sus scrofa]
gi|113205878|ref|NP_001038072.1|	-2	0,027827239	delta(3,5)-Delta(2,4)-dienoyl-CoA isomerase, mitochondrial [Sus scrofa]
gi|194042318|ref|XP_001928917.1|	-2,666666667	0,028834443	PREDICTED: putative hexokinase HKDC1 [Sus scrofa]
gi|545836657|ref|XP_005656250.1|	-1,866666667	0,030024066	PREDICTED: putative hydroxypyruvate isomerase isoform X3 [Sus scrofa]
gi|311259468|ref|XP_003128112.1|	-1,866666667	0,030024066	PREDICTED: putative hydroxypyruvate isomerase isoformX2 [Sus scrofa]
gi|335287577|ref|XP_003126100.2|	2,5	0,030084923	PREDICTED: 85/88 kDa calcium-independent phospholipase A2 isoform X1 [Sus scrofa]

#PatternLab's TFold analyzer

#Parameters used:

#F-stringency :0.05, Q-value:0.05 FDR:0.05

Supplementary
List of proteins exclusive in control identified in the cauda epididymal spermatozoa

Accession number	Spec count	Protein ID
gi|545803518|ref|XP_005654565.1|	102	PREDICTED: transitional endoplasmic reticulum ATPase isoform X1 [Sus scrofa]
gi|545803675|ref|XP_005660289.1|	20	PREDICTED: protein FAM221B isoform X2 [Sus scrofa]
gi|545812805|ref|XP_005661857.1|	16	PREDICTED: casein kinase I isoform alpha isoform X5 [Sus scrofa]
gi|545894758|ref|XP_005658946.1|	11	PREDICTED: SH3 domain-containing protein 21-like, partial [Sus scrofa]
gi|545880593|ref|XP_005672990.1|	10	PREDICTED: ral GTPase-activating protein subunit beta-like, partial [Sus scrofa]
gi|545836915|ref|XP_005656255.1|	9	PREDICTED: schlafen-like protein 1 [Sus scrofa]
gi|311275253|ref|XP_003134650.1|	9	PREDICTED: single-stranded DNA-binding protein, mitochondrial isoformX1 [Sus scrofa]
gi|194038441|ref|XP_001928349.1|	9	PREDICTED: V-type proton ATPase subunit D [Sus scrofa]
gi|545797521|ref|XP_005659178.1|	9	PREDICTED: ezrin [Sus scrofa]
gi|350595679|ref|XP_003135171.3|	8	PREDICTED: putative G antigen family E member 3-like isoform X1 [Sus scrofa]
gi|545829008|ref|XP_003481823.2|	8	PREDICTED: acyl-CoA synthetase family member 3, mitochondrial-like [Sus scrofa]
gi|545831576|ref|XP_005664680.1|	8	PREDICTED: radial spoke head protein 6 homolog A, partial [Sus scrofa]
gi|545809109|ref|XP_005652934.1|	7	PREDICTED: UV excision repair protein RAD23 homolog A isoform X2 [Sus scrofa]
gi|219522010|ref|NP_001137192.1|	7	nucleoside diphosphate kinase, mitochondrial [Sus scrofa]
gi|350592774|ref|XP_003483533.1|	7	PREDICTED: LOW QUALITY PROTEIN: phenazine biosynthesis-like domain-containing protein [Sus scrofa]
gi|157427722|ref|NP_001098769.1|	7	COP9 signalosome complex subunit 6 [Sus scrofa]
gi|545815258|ref|XP_005655164.1|	7	PREDICTED: nucleoside diphosphate kinase, mitochondrial isoform X2 [Sus scrofa]
gi|545838663|ref|XP_005653518.1|	7	PREDICTED: uncharacterized protein C6orf10-like isoform X1 [Sus scrofa]
gi|335302639|ref|XP_003133385.2|	7	PREDICTED: trafficking protein particle complex subunit 11 isoform X1 [Sus scrofa]
gi|346421413|ref|NP_001231081.1|	7	nuclear pore complex protein Nup93 [Sus scrofa]
gi|47522880|ref|NP_999195.1|	7	gamma-glutamyltranspeptidase 1 [Sus scrofa]
gi|545884199|ref|XP_003135011.3|	7	PREDICTED: CTP synthase 2, partial [Sus scrofa]
gi|350588230|ref|XP_003129648.3|	7	PREDICTED: nuclear pore complex protein Nup98-Nup96 [Sus scrofa]
gi|335282758|ref|XP_003123386.2|	6	PREDICTED: UV excision repair protein RAD23 homolog A isoform X1 [Sus scrofa]
gi|264681442|ref|NP_001161116.1|	6	dynactin subunit 6 [Sus scrofa]
gi|350587673|ref|XP_003129166.3|	6	PREDICTED: nucleoporin p54 isoform 1 [Sus scrofa]
gi|47523864|ref|NP_999570.1|	6	methylmalonyl-CoA mutase, mitochondrial precursor [Sus scrofa]
gi|350591922|ref|XP_003358841.2|	6	PREDICTED: coiled-coil domain-containing protein 58 [Sus scrofa]
gi|335297237|ref|XP_003357980.1|	6	PREDICTED: nuclear protein localization protein 4 homolog [Sus scrofa]
gi|545869909|ref|XP_005654161.1|	6	PREDICTED: coiled-coil domain-containing protein 74B isoform X1 [Sus scrofa]
gi|178056470|ref|NP_001116694.1|	6	alpha-N-acetylgalactosaminidase precursor [Sus scrofa]
gi|148225750|ref|NP_001090973.1|	6	heat shock protein 105 kDa [Sus scrofa]
gi|545889631|ref|XP_005658331.1|	6	PREDICTED: LOW QUALITY PROTEIN: coiled-coil domain-containing protein 33 [Sus scrofa]
gi|335279372|ref|XP_003121421.2|	5	PREDICTED: LOW QUALITY PROTEIN: myristoylated alanine-rich C-kinase substrate [Sus scrofa]
gi|545894465|ref|XP_005658807.1|	5	PREDICTED: 14-3-3 protein epsilon-like [Sus scrofa]
gi|311252243|ref|XP_003124996.1|	5	PREDICTED: macrophage-capping protein isoformX2 [Sus scrofa]
gi|311260957|ref|XP_003128592.1|	5	PREDICTED: NEDD8 isoform X1 [Sus scrofa]
gi|219522018|ref|NP_001137196.1|	5	Na(+)/H(+) exchange regulatory cofactor NHE-RF1 [Sus scrofa]
gi|335299132|ref|XP_003358502.1|	5	PREDICTED: IQ domain-containing protein F1 [Sus scrofa]
gi|545837033|ref|XP_005665588.1|	5	PREDICTED: serpin peptidase inhibitor, clade B (ovalbumin), member 1 isoform X2 [Sus scrofa]
gi|218664471|ref|NP_001136304.1|	5	methionine adenosyltransferase 2 subunit beta [Sus scrofa]
gi|311259277|ref|XP_003128022.1|	5	PREDICTED: HEAT repeat containing 8 isoform X1 [Sus scrofa]
gi|545893209|ref|XP_005658117.1|	5	PREDICTED: ral GTPase-activating protein subunit alpha-1, partial [Sus scrofa]
gi|311262208|ref|XP_003129067.1|	4	PREDICTED: serine protease inhibitor Kazal-type 2 [Sus scrofa]
gi|311246872|ref|XP_003122373.1|	4	PREDICTED: epididymal-specific lipocalin-12 [Sus scrofa]
gi|312062793|ref|NP_001185849.1|	4	spermatogenesis-associated protein 3 [Sus scrofa]
gi|335307380|ref|XP_003360817.1|	4	PREDICTED: oxidation resistance protein 1-like isoform 2 [Sus scrofa]
gi|545820058|ref|XP_005662904.1|	4	PREDICTED: protein EFR3 homolog A-like [Sus scrofa]
gi|51592147|ref|NP_001004050.1|	4	prolyl endopeptidase [Sus scrofa]
gi|227430392|ref|NP_001153080.1|	4	[Pyruvate dehydrogenase [lipoamide]] kinase isozyme 1, mitochondrial [Sus scrofa]
gi|350581083|ref|XP_003123977.2|	4	PREDICTED: AF4/FMR2 family member 4, partial [Sus scrofa]
gi|545814710|ref|XP_005662160.1|	4	PREDICTED: dynein heavy chain 3, axonemal-like [Sus scrofa]
gi|545890644|ref|XP_003361460.2|	3	PREDICTED: cytosolic non-specific dipeptidase-like [Sus scrofa]
gi|347446663|ref|NP_001231536.1|	3	protein AF1q [Sus scrofa]
gi|148233298|ref|NP_001090954.1|	3	heat shock factor-binding protein 1 [Sus scrofa]
gi|545853086|ref|XP_005668111.1|	3	PREDICTED: dynein intermediate chain 1, axonemal-like [Sus scrofa]
gi|311257436|ref|XP_003127119.1|	3	PREDICTED: succinate dehydrogenase assembly factor 1, mitochondrial [Sus scrofa]
gi|335291454|ref|XP_003356506.1|	3	PREDICTED: heat shock protein beta-11 isoform X1 [Sus scrofa]
gi|264681456|ref|NP_001161107.1|	3	isovaleryl-CoA dehydrogenase, mitochondrial [Sus scrofa]
gi|545888750|ref|XP_003360867.2|	3	PREDICTED: lipoma-preferred partner-like, partial [Sus scrofa]
gi|545852501|ref|XP_005668034.1|	3	PREDICTED: uncharacterized protein LOC100518090, partial [Sus scrofa]
gi|335287845|ref|XP_003126234.2|	3	PREDICTED: UPF0160 protein MYG1, mitochondrial-like isoform X1 [Sus scrofa]
gi|545826559|ref|XP_005664037.1|	3	PREDICTED: tetraspanin-8 isoform X1 [Sus scrofa]
gi|545867564|ref|XP_003359029.3|	3	PREDICTED: putative protein TPRXL-like isoform 1, partial [Sus scrofa]
gi|335283572|ref|XP_003354344.1|	3	PREDICTED: transcriptional activator protein Pur-alpha isoformX1 [Sus scrofa]
gi|350585179|ref|XP_003481897.1|	3	PREDICTED: serine--tRNA ligase, mitochondrial [Sus scrofa]
gi|311248634|ref|XP_003123221.1|	3	PREDICTED: coiled-coil domain-containing protein 159 isoformX1 [Sus scrofa]

gi|190360615|ref|NP_001121917.1|	3	monocarboxylate transporter 1 [Sus scrofa]
gi|545879862|ref|XP_005672856.1|	3	PREDICTED: tyrosine-protein phosphatase non-receptor type substrate 1-like isoform X4 [Sus scrofa]
gi|545856463|ref|XP_005668661.1|	3	PREDICTED: dynein heavy chain 17, axonemal-like, partial [Sus scrofa]
gi|311258922|ref|XP_003127849.1|	3	PREDICTED: ras-related GTP-binding protein C isoform X1 [Sus scrofa]
gi|545804525|ref|XP_005660504.1|	3	PREDICTED: tetratricopeptide repeat protein 16 [Sus scrofa]
gi|335292272|ref|XP_003356696.1|	3	PREDICTED: fumarylacetoacetase [Sus scrofa]
gi|311277165|ref|XP_003135525.1|	3	PREDICTED: plasma membrane calcium-transporting ATPase 3 isoformX2 [Sus scrofa]
gi|545888706|ref|XP_005674205.1|	3	PREDICTED: plasma membrane calcium-transporting ATPase 2 [Sus scrofa]
gi|545832060|ref|XP_005664790.1|	3	PREDICTED: aldehyde dehydrogenase family 16 member A1 isoform X3 [Sus scrofa]
gi|545879186|ref|XP_005672752.1|	3	PREDICTED: 1-phosphatidylinositol 4,5-bisphosphate phosphodiesterase beta-1 [Sus scrofa]
gi|350583594|ref|XP_001928611.4|	3	PREDICTED: netrin-G1 isoformX2 [Sus scrofa]
gi|545833908|ref|XP_005656083.1|	3	PREDICTED: E3 ubiquitin-protein ligase UBR4-like [Sus scrofa]
gi|350596908|ref|XP_003361803.2|	3	PREDICTED: IST1 homolog [Sus scrofa]
gi|312062797|ref|NP_001185848.1|	3	proactivator polypeptide precursor [Sus scrofa]
gi|545886462|ref|XP_005673916.1|	2	PREDICTED: homeobox protein ESX1-like [Sus scrofa]
gi|545891896|ref|XP_003130977.3|	2	PREDICTED: uncharacterized protein LOC100522509 [Sus scrofa]
gi|545823023|ref|XP_005663479.1|	2	PREDICTED: sperm mitochondrial-associated cysteine-rich protein isoform X1 [Sus scrofa]
gi|545884396|ref|XP_001924726.5|	2	PREDICTED: ferritin heavy chain-like [Sus scrofa]
gi|311251856|ref|XP_003124792.1|	2	PREDICTED: V-type proton ATPase 16 kDa proteolipid subunit [Sus scrofa]
gi|545824511|ref|XP_005663828.1|	2	PREDICTED: postacrosomal sheath WW domain-binding protein-like isoform X1 [Sus scrofa]
gi|311261749|ref|XP_003128841.1|	2	PREDICTED: glutathione S-transferase A4-like [Sus scrofa]
gi|545856737|ref|XP_003131260.2|	2	PREDICTED: 5'(3')-deoxyribonucleotidase, cytosolic type isoform X1 [Sus scrofa]
gi|346421372|ref|NP_001231060.1|	2	ferritin, light polypeptide [Sus scrofa]
gi|350592333|ref|XP_003359097.2|	2	PREDICTED: mitochondrial peptide methionine sulfoxide reductase [Sus scrofa]
gi|311246888|ref|XP_003122378.1|	2	PREDICTED: epididymal-specific lipocalin-6 isoform 1 [Sus scrofa]
gi|545819748|ref|XP_005653148.1|	2	PREDICTED: elongation factor 1-delta isoform X4 [Sus scrofa]
gi|350593685|ref|XP_003133572.3|	2	PREDICTED: nucleoporin NUP53-like [Sus scrofa]
gi|545894790|ref|XP_005658960.1|	2	PREDICTED: LOW QUALITY PROTEIN: ribonuclease inhibitor, partial [Sus scrofa]
gi|335298113|ref|XP_003358202.1|	2	PREDICTED: fibronectin type III domain-containing protein 8 [Sus scrofa]
gi|545865248|ref|XP_005670120.1|	2	PREDICTED: lipoma-preferred partner [Sus scrofa]
gi|545835376|ref|XP_003482101.2|	2	PREDICTED: trafficking protein particle complex subunit 8 [Sus scrofa]
gi|350578155|ref|XP_003121262.3|	2	PREDICTED: ethylmalonyl-CoA decarboxylase isoform X1 [Sus scrofa]
gi|545857977|ref|XP_003131452.2|	2	PREDICTED: heat shock protein beta-9 [Sus scrofa]
gi|311249779|ref|XP_003123798.1|	2	PREDICTED: protein FAM151B isoform X1 [Sus scrofa]
gi|213021239|ref|NP_001132942.1|	2	zinc transporter 1 [Sus scrofa]
gi|47523580|ref|NP_999415.1|	2	platelet-activating factor acetylhydrolase IB subunit alpha [Sus scrofa]
gi|350586098|ref|XP_003482113.1|	2	PREDICTED: PDZ domain-containing protein GIPC2 isoformX2 [Sus scrofa]
gi|545839188|ref|XP_001929450.5|	2	PREDICTED: LOW QUALITY PROTEIN: peptidyl-prolyl cis-trans isomerase FKBP5 [Sus scrofa]
gi|350581899|ref|XP_003124791.3|	2	PREDICTED: LOW QUALITY PROTEIN: putative N-acetylglucosamine-6-phosphate deacetylase [Sus scrofa]
gi|348041218|ref|NP_001231706.1|	2	Ena-vasodilator stimulated phosphoprotein [Sus scrofa]
gi|311264679|ref|XP_003130280.1|	2	PREDICTED: protein FAM185A-like isoform X1 [Sus scrofa]
gi|311252942|ref|XP_003125344.1|	2	PREDICTED: uncharacterized protein C2orf53 homolog isoform 1 [Sus scrofa]
gi|157427748|ref|NP_001098766.1|	2	mRNA export factor [Sus scrofa]
gi|545860194|ref|XP_005669282.1|	2	PREDICTED: mucin-1-like [Sus scrofa]
gi|335281566|ref|XP_003122636.2|	2	PREDICTED: glycogen phosphorylase, muscle form isoformX1 [Sus scrofa]
gi|162139823|ref|NP_001104727.1|	2	prelamin-A/C [Sus scrofa]
gi|545826341|ref|XP_003355550.3|	2	PREDICTED: LOW QUALITY PROTEIN: protein MON2 homolog isoform 3, partial [Sus scrofa]
gi|345090993|ref|NP_001230731.1|	2	RAB8A, member RAS oncogene family [Sus scrofa]
gi|545893261|ref|XP_005658131.1|	2	PREDICTED: NEDD4-like E3 ubiquitin-protein ligase WWP2-like [Sus scrofa]
gi|545845674|ref|XP_005666888.1|	2	PREDICTED: LPS-responsive vesicle trafficking, beach and anchor containing, partial [Sus scrofa]

Supplementary
List of proteins exclusive in GnRH-immunized identified in the cauda epididymal spermatozoa

Accession number	Spec count	Protein ID
gi|545829772|ref|XP_005653315.1|	65	PREDICTED: carboxylesterase 5A [Sus scrofa]
gi|545814562|ref|XP_005653087.1|	31	PREDICTED: cytochrome b-c1 complex subunit 2, mitochondrial-like [Sus scrofa]
gi|311257294|ref|XP_003127050.1|	24	PREDICTED: cytochrome b-c1 complex subunit Rieske, mitochondrial-like [Sus scrofa]
gi|194043348|ref|XP_001929405.1|	18	PREDICTED: glutathione S-transferase theta-1 [Sus scrofa]
gi|311273371|ref|XP_003133833.1|	15	PREDICTED: NADH dehydrogenase [ubiquinone] 1 alpha subcomplex subunit 10, mitochondrial [Sus scrofa]
gi|545831678|ref|XP_005664699.1|	15	PREDICTED: epididymal sperm-binding protein 1 isoform X1 [Sus scrofa]
gi|47522614|ref|NP_999101.1|	15	ribonuclease 4 precursor [Sus scrofa]
gi|347582654|ref|NP_001231582.1|	15	serotransferrin precursor [Sus scrofa]
gi|545844155|ref|XP_005666604.1|	14	PREDICTED: cytosol aminopeptidase [Sus scrofa]
gi|343168793|ref|NP_001230220.1|	14	ras-related protein Rab-35 [Sus scrofa]
gi|223976081|ref|YP_002600779.1|	13	cytochrome c oxidase subunit I (mitochondrion) [Sus scrofa domesticus]
gi|350585834|ref|XP_003356325.2|	11	PREDICTED: importin subunit alpha-7 isoform X1 [Sus scrofa]
gi|545868067|ref|XP_005670494.1|	11	PREDICTED: disintegrin and metalloproteinase domain-containing protein 7 [Sus scrofa]
gi|311272935|ref|XP_003133651.1|	11	PREDICTED: NADH-ubiquinone oxidoreductase 75 kDa subunit, mitochondrial isoformX1 [Sus scrofa]
gi|335287187|ref|XP_003355292.1|	11	PREDICTED: ATP synthase subunit b, mitochondrial [Sus scrofa]
gi|545798187|ref|XP_005654449.1|	11	PREDICTED: importin subunit alpha-6 isoform X2 [Sus scrofa]
gi|47523160|ref|NP_999012.1|	11	inhibitor of carbonic anhydrase precursor [Sus scrofa]
gi|163915141|ref|NP_001106518.1|	10	carnitine O-acetyltransferase [Sus scrofa]
gi|545840440|ref|XP_005666170.1|	10	PREDICTED: LOW QUALITY PROTEIN: IQ motif containing GTPase activating protein 1 [Sus scrofa]
gi|47523060|ref|NP_999293.1|	9	serine/threonine-protein phosphatase 2B catalytic subunit alpha isoform [Sus scrofa]
gi|342187276|ref|NP_001230112.1|	9	AP-2 complex subunit beta [Sus scrofa]
gi|311274943|ref|XP_003134515.1|	9	PREDICTED: WAP four-disulfide core domain protein 10A [Sus scrofa]
gi|545862962|ref|XP_005669733.1|	9	PREDICTED: filamin-B [Sus scrofa]
gi|311254575|ref|XP_003125894.1|	8	PREDICTED: rho-related GTP-binding protein RhoC [Sus scrofa]
gi|47523726|ref|NP_999498.1|	8	dolichyl-diphosphooligosaccharide--protein glycosyltransferase subunit 1 precursor [Sus scrofa]
gi|47522782|ref|NP_999143.1|	7	beta-2-microglobulin precursor [Sus scrofa]
gi|350594989|ref|XP_003360077.2|	7	PREDICTED: protein WFDC11-like [Sus scrofa]
gi|108796070|ref|NP_001035834.1|	7	integral membrane protein 2B [Sus scrofa]
gi|311256688|ref|XP_003126763.1|	7	PREDICTED: NADH dehydrogenase [ubiquinone] 1 alpha subcomplex subunit 12 isoform 1 [Sus scrofa]
gi|545870343|ref|XP_005671094.1|	7	PREDICTED: probable E3 ubiquitin-protein ligase HERC4-like [Sus scrofa]
gi|545860373|ref|XP_003483154.2|	7	PREDICTED: myosin-10, partial [Sus scrofa]
gi|297747277|ref|NP_001172107.1|	6	NADH dehydrogenase (ubiquinone) 1 alpha subcomplex, 6, 14kDa [Sus scrofa]
gi|335286553|ref|XP_003355117.1|	6	PREDICTED: mitochondrial pyruvate carrier 2 isoform X1 [Sus scrofa]
gi|545838652|ref|XP_005653515.1|	6	PREDICTED: cylicin-2-like [Sus scrofa]
gi|148222591|ref|NP_001090955.1|	6	ATPase inhibitor, mitochondrial precursor [Sus scrofa]
gi|345110630|ref|NP_001230796.1|	6	RuvB-like 2 [Sus scrofa]
gi|195539468|ref|NP_001124202.1|	6	estradiol 17-beta-dehydrogenase 8 [Sus scrofa]
gi|545871476|ref|XP_005671423.1|	6	PREDICTED: transmembrane 9 superfamily member 3 [Sus scrofa]
gi|350590384|ref|XP_003131576.3|	6	PREDICTED: importin subunit beta-1 isoformX1 [Sus scrofa]
gi|311275515|ref|XP_003134775.1|	5	PREDICTED: NADH dehydrogenase [ubiquinone] 1 alpha subcomplex subunit 5 isoform X1 [Sus scrofa]
gi|545880895|ref|XP_005673031.1|	5	PREDICTED: WAP four-disulfide core domain protein 3 isoform X3 [Sus scrofa]
gi|311247401|ref|XP_003122628.1|	5	PREDICTED: peptidyl-prolyl cis-trans isomerase FKBP2 isoformX1 [Sus scrofa]
gi|335286616|ref|XP_003125707.2|	5	PREDICTED: succinate dehydrogenase cytochrome b560 subunit, mitochondrial isoform X1 [Sus scrofa]
gi|343780941|ref|NP_001230485.1|	5	prohibitin 2 [Sus scrofa]
gi|545833899|ref|XP_005656080.1|	5	PREDICTED: E3 ubiquitin-protein ligase UBR4-like [Sus scrofa]
gi|335281655|ref|XP_003353857.1|	5	PREDICTED: 4F2 cell-surface antigen heavy chain isoform X1 [Sus scrofa]
gi|223976089|ref|YP_002600787.1|	5	NADH dehydrogenase subunit 5 (mitochondrion) [Sus scrofa domesticus]
gi|335290033|ref|XP_003127407.2|	5	PREDICTED: izumo sperm-egg fusion protein 2 isoform X1 [Sus scrofa]
gi|545832241|ref|XP_005664826.1|	5	PREDICTED: izumo sperm-egg fusion protein 2 isoform X2 [Sus scrofa]
gi|194018714|ref|NP_001123449.1|	4	sperm associated antigen 11 [Sus scrofa]
gi|311261747|ref|XP_003128840.1|	4	PREDICTED: glutathione S-transferase A1-like [Sus scrofa]
gi|545874724|ref|XP_005672027.1|	4	PREDICTED: calcium-binding mitochondrial carrier protein Aralar1-like, partial [Sus scrofa]
gi|545884310|ref|XP_005674521.1|	4	PREDICTED: LOW QUALITY PROTEIN: apolipoprotein O [Sus scrofa]
gi|545823500|ref|XP_005655469.1|	4	PREDICTED: sperm-associated antigen 17, partial [Sus scrofa]
gi|553727064|ref|NP_001272902.1|	4	enoyl-CoA delta isomerase 1 [Sus scrofa]
gi|343887418|ref|NP_001230608.1|	4	diphthine synthase [Sus scrofa]
gi|47523768|ref|NP_999520.1|	4	epoxide hydrolase 1 precursor [Sus scrofa]
gi|350579469|ref|XP_003480616.1|	4	PREDICTED: fibronectin type III and SPRY domain containing 1-like isoformX2 [Sus scrofa]
gi|545874097|ref|XP_005671827.1|	4	PREDICTED: LETM1 domain-containing protein LETM2, mitochondrial [Sus scrofa]
gi|178056876|ref|NP_001116672.1|	4	testin [Sus scrofa]
gi|545830909|ref|XP_003355956.2|	4	PREDICTED: LOW QUALITY PROTEIN: mitochondrial import inner membrane translocase subunit TIM50 [Sus scrofa]
gi|194042130|ref|XP_001927430.1|	4	PREDICTED: sideroflexin-4 [Sus scrofa]
gi|148235351|ref|NP_001090944.1|	4	NADH dehydrogenase ubiquinone flavoprotein 2 [Sus scrofa]
gi|545859491|ref|XP_005669160.1|	4	PREDICTED: EF-hand calcium-binding domain-containing protein 5-like [Sus scrofa]
gi|350581138|ref|XP_003124036.3|	4	PREDICTED: catenin alpha-1 isoformX1 [Sus scrofa]
gi|335284522|ref|XP_003124619.2|	4	PREDICTED: pancreatic secretory granule membrane major glycoprotein GP2 isoform X1 [Sus scrofa]
gi|343887351|ref|NP_001230576.1|	4	WD repeat and FYVE domain-containing protein 1 [Sus scrofa]

gi|545823536|ref|XP_001927341.4|	4	PREDICTED: sperm-associated antigen 17, partial [Sus scrofa]
gi|343432650|ref|NP_001230339.1|	4	beta-lactamase-like protein 2 [Sus scrofa]
gi|194038855|ref|XP_001928049.1|	3	PREDICTED: GMP reductase 2 isoform X1 [Sus scrofa]
gi|350580865|ref|XP_003123779.3|	3	PREDICTED: tubulin-specific chaperone A [Sus scrofa]
gi|346421386|ref|NP_001231066.1|	3	ATP synthase subunit g, mitochondrial [Sus scrofa]
gi|311273314|ref|XP_003133809.1|	3	PREDICTED: COP9 signalosome complex subunit 8 isoformX1 [Sus scrofa]
gi|545892437|ref|XP_005653221.1|	3	PREDICTED: CD9 antigen-like [Sus scrofa]
gi|194042701|ref|XP_001924805.1|	3	PREDICTED: uncharacterized protein C10orf107 homolog isoform X1 [Sus scrofa]
gi|350579954|ref|XP_003480723.1|	3	PREDICTED: Sjoegren syndrome/scleroderma autoantigen 1-like [Sus scrofa]
gi|255683363|ref|NP_001157469.1|	3	myosin light polypeptide 6 [Sus scrofa]
gi|545834207|ref|XP_003356251.2|	3	PREDICTED: acyl-protein thioesterase 2 isoform X1 [Sus scrofa]
gi|197251934|ref|NP_001127826.1|	3	actin-related protein 2 [Sus scrofa]
gi|545893523|ref|XP_003360983.2|	3	PREDICTED: ubiquitin-conjugating enzyme E2 R1 [Sus scrofa]
gi|350586418|ref|XP_001929155.3|	3	PREDICTED: GMP reductase 1 isoform X1 [Sus scrofa]
gi|194036808|ref|XP_001929021.1|	3	PREDICTED: protein CREG1 isoform 2 [Sus scrofa]
gi|178056588|ref|NP_001116645.1|	3	ras-related protein Rab-1B [Sus scrofa]
gi|350590415|ref|XP_003131608.3|	3	PREDICTED: prohibitin isoform X1 [Sus scrofa]
gi|346716265|ref|NP_001231271.1|	3	omega-amidase NIT2 [Sus scrofa]
gi|350578792|ref|XP_003480452.1|	3	PREDICTED: calcineurin B homologous protein 1-like isoformX1 [Sus scrofa]
gi|256838113|ref|NP_001157986.1|	3	mitochondrial thiamine pyrophosphate carrier [Sus scrofa]
gi|163915149|ref|NP_001106522.1|	3	battenin [Sus scrofa]
gi|335290365|ref|XP_003356156.1|	3	PREDICTED: LOW QUALITY PROTEIN: 45 kDa calcium-binding protein [Sus scrofa]
gi|311268663|ref|XP_003132151.1|	3	PREDICTED: 3-ketoacyl-CoA thiolase A, peroxisomal isoform 1 [Sus scrofa]
gi|350581678|ref|XP_003354637.2|	3	PREDICTED: glycerophosphodiester phosphodiesterase 1 [Sus scrofa]
gi|545850843|ref|XP_005667827.1|	3	PREDICTED: LOW QUALITY PROTEIN: cullin-1 [Sus scrofa]
gi|545799721|ref|XP_005654488.1|	3	PREDICTED: NAD-dependent malic enzyme, mitochondrial [Sus scrofa]
gi|335288570|ref|XP_003126608.2|	3	PREDICTED: NADH dehydrogenase [ubiquinone] 1 alpha subcomplex subunit 9, mitochondrial [Sus scrofa]
gi|194036353|ref|XP_001926597.1|	3	PREDICTED: disintegrin and metalloproteinase domain-containing protein 30 [Sus scrofa]
gi|47523192|ref|NP_998993.1|	3	IgG heavy chain precursor [Sus scrofa]
gi|350592295|ref|XP_001924211.4|	3	PREDICTED: disintegrin and metalloproteinase domain-containing protein 28 isoform X1 [Sus scrofa]
gi|311274506|ref|XP_003134351.1|	3	PREDICTED: cystatin-13-like isoform X1 [Sus scrofa]
gi|335306675|ref|XP_003135528.2|	3	PREDICTED: B-cell receptor-associated protein 31 isoform X1 [Sus scrofa]
gi|545857309|ref|XP_005653957.1|	3	PREDICTED: uncharacterized protein LOC100516640 [Sus scrofa]
gi|311247246|ref|XP_003122555.1|	2	PREDICTED: cystatin-M-like [Sus scrofa]
gi|545812766|ref|XP_005661844.1|	2	PREDICTED: serine protease inhibitor Kazal-type 14-like [Sus scrofa]
gi|545852041|ref|XP_005656839.1|	2	PREDICTED: 3'(2'),5'-bisphosphate nucleotidase 1 isoform X4 [Sus scrofa]
gi|335288032|ref|XP_001929448.3|	2	PREDICTED: prostaglandin E synthase 3 isoformX1 [Sus scrofa]
gi|545895251|ref|XP_005659146.1|	2	PREDICTED: acylpyruvase FAHD1, mitochondrial, partial [Sus scrofa]
gi|72535186|ref|NP_001026955.1|	2	ADP-ribosylation factor-like protein 3 [Sus scrofa]
gi|72535184|ref|NP_001026954.1|	2	ADP-ribosylation factor-like protein 1 [Sus scrofa]
gi|194018686|ref|NP_001123435.1|	2	reticulon-4 [Sus scrofa]
gi|545836201|ref|XP_005665488.1|	2	PREDICTED: thioredoxin domain-containing protein 12-like isoform X1 [Sus scrofa]
gi|545894515|ref|XP_005658831.1|	2	PREDICTED: phenylalanine--tRNA ligase, mitochondrial-like [Sus scrofa]
gi|335301484|ref|XP_001926892.2|	2	PREDICTED: protein phosphatase 1F [Sus scrofa]
gi|311254963|ref|XP_003126026.1|	2	PREDICTED: malonyl-CoA-acyl carrier protein transacylase, mitochondrial isoform X1 [Sus scrofa]
gi|335302026|ref|XP_003359352.1|	2	PREDICTED: LOW QUALITY PROTEIN: cytochrome P450 2C18 [Sus scrofa]
gi|194036227|ref|XP_001929678.1|	2	PREDICTED: selenium-binding protein 1 [Sus scrofa]
gi|311249830|ref|XP_003123828.1|	2	PREDICTED: metallo-beta-lactamase domain-containing protein 2 [Sus scrofa]
gi|350594272|ref|XP_003359820.2|	2	PREDICTED: LOW QUALITY PROTEIN: embigin-like [Sus scrofa]
gi|335287489|ref|XP_003355368.1|	2	PREDICTED: tubulin tyrosine ligase-like family, member 12 isoform X1 [Sus scrofa]
gi|545847078|ref|XP_005667113.1|	2	PREDICTED: serine/threonine-protein kinase 33-like isoform X2 [Sus scrofa]
gi|311252641|ref|XP_003125195.1|	2	PREDICTED: endoplasmic reticulum lectin 1 isoformX1 [Sus scrofa]
gi|335299974|ref|XP_003358745.1|	2	PREDICTED: methylcrotonoyl-CoA carboxylase subunit alpha, mitochondrial [Sus scrofa]
gi|545839102|ref|XP_005656282.1|	2	PREDICTED: UHRF1-binding protein 1 [Sus scrofa]
gi|545861485|ref|XP_005669420.1|	2	PREDICTED: LOW QUALITY PROTEIN: solute carrier family 22 member 14 [Sus scrofa]
gi|350590863|ref|XP_003358315.2|	2	PREDICTED: dynein heavy chain 2, axonemal-like, partial [Sus scrofa]
gi|178056574|ref|NP_001116582.1|	2	ephrin-A1 precursor [Sus scrofa]
gi|384871692|ref|NP_001230110.2|	2	ubiquitin-protein ligase E3A isoform 1 [Sus scrofa]

CAPÍTULO V

7. DISCUSSÃO GERAL

A presente tese buscou apontar caminhos inovadores no estudo do epidídimo não só em termos técnicos, como também em estratégia de investigação científica. No capítulo 2, apresentou-se uma revisão atual dos estudos do epidídimo em mamíferos, com ênfase nas abordagens proteômicas. Resultados significativos de importantes grupos de pesquisa do Brasil e do mundo foram reunidos e discutidos a luz das possíveis aplicações práticas de marcadores proteicos seminais.

Enzima de conversão da angiotensina associadas à fertilidade em camundongos (KREGE, et al.,1995) demonstrou um importante marcador para o desenvolvimento de fármacos, com abordagem contraceptiva em humanos (WANG et al., 2013). O estudo da proteína 1 de ligação ao espermatozoide epididimal (ELSPBP1) a qual é secretada por células principais em associação com epididimossomas, revelou a transferência específica de ELSPBP1 para espermatozoides já mortos antes da incubação (D'AMOURS et al., 2012). Sugerindo um mecanismo subjacente envolvido, no qual ELSPBP1 poderia ser um marcador para o reconhecimento de espermatozoides mortos durante o trânsito epididimal.

O capítulo 3 apresentou os resultados do estudo que buscou identificar quais proteínas estavam alteradas no fluido epididimario de cachaços imunizados contra o GnRH. Neste estudo, buscou-se consolidar o suíno tratado com a vacina da imunocastração como um modelo de estudo das consequências do hipogonadismo secundário humano para a função testicular. De fato, muitas proteínas estão relacionadas a processos celulares e metabólicos quando os animais foram imunizados, consequência do dano testicular devido ao aumento de proteínas associadas a espermatogênese. O aumento de proteínas associadas ao sistema ubiquitina-proteassoma, em animais imunizados, sugere a inibição desse mecanismo em decorrência ao dano celular. Vesículas extracelulares como os epididimossomas altera o proteoma , porem a transferência e interação de proteínas com os espermatozoides durante a maturação e transporte é ainda desconhecida. Nosso estudo permite explorar as proteínas associadas a estas vesículas quando há desregulação endócrina, já que foram identificados alguns genes de ligação celular (APOH), fluxo de

colesterol (APOA1), ligação à zona pelúcida (ZPBP2), ligação ao oócito (SPACA3) e eliminação de antioxidantes (SOD1).

Uma vez identificadas as alterações no ambiente espermático na cauda do epidídimo, questinou-se que alterações proteômicas do espermatozoide nas mesmas condições. Salienta-se a importância das secreções epididimarias para a transferência de proteínas para o espermatozoide durante o transito epididimário. Tais transferências, conferem ao esprmatozoide a habilidade de tornar-se fértil. Assim, no capitulo 4 foram apresentadas os efeitos espermáticos da imunização do suíno contra GnRH. Observou-se mudanças significativas na abundância de proteínas envolvidas no metabolismo do esperma (enolase, piruvato desidrogenase), reação do acrossomo e capacitação (oxoprolinase, proteína acrossomal SP-10, diidrolipoil desidrogenase) e interações espermatozoides-oócitos (proteína de ligação à zona pelúcida , zonadesina , molécula de adesão de espermatozoides). Tais mudanças levam a redução na qualidade da produção de mitocôndrias e reorganização celular durante as divisões celulares que compreendem as fases da espermatogênese. Essas alterações deve-se pelo aumento da proteína do complexo citocromo b-c1 sub 2 (UQCRC2) em animais imunizados contra GnRH e possível aumento na produção de ROS (AGUILERA-AGUIRE et al. 2009). Essas mudanças na função mitocondrial estão diretamente associadas à prejuízos na motilidade e morfologia espermática, encontrada em espermatozóides epididimários de suínos imunizados com anti-GnRH (AMARAL et al., 2013 ; NAKAMURA et al., 2013 ; GU et al., 2019).

O hipogonadismo secundário é uma condição clinica que compromete o eixo hipotálamo-hipofise-testículo inibindo a secreção de GnRH e prejudicando a função testicular. Com base nos estudos no modelo suíno apresentados nesta tese, a infertilidade associada ao hipogonadismo secundário no homem pode ter consequências significativas no perfil proteômico do espermatozoide. A diminuição ou redução de proteínas chave para a motilidade espermática, interação com o trato reprodutivo feminino e interação espermatozoide-oocito compromete significativamente a fertilidade no homem. Estes resultados apontam proteínas que podem ser estudadas no homem, a fim de validar seus uso como biomarcadores.

No contexto da reprodução de suínos, o presente estudo por associar a expressão de proteínas epididimarias com a condição hormonal, aponta para oportunidades de novos estudos em puberdade e precocidade em machos reprodutores. Como varias proteínas

mostraram-se possivelmente reguladas endocrinamente, especula-se se um painel de proteínas seminais poderia auxiliar na melhor compreensão da puberdade no cachaço. A implementação de marcadores moleculares seminais em machos em inicio de treinamentos em centrais de produção de doses para IA poderia ser uma realidade, buscando a otimização do manejo de reprodutores.

Como modelo animal para o hipogonadismo secundário no homem, estes resultados indicam alterações bioquímicas que podem explicar a redução de fertilidade em pacientes acometidos com esta condição clínica. Os resultados de proteômica diferencial e a extensa análise de bioinformática realizada com os dados gerados, revelaram alterações nas funções celulares fundamentais para manutenção, viabilidade e função espermática.

As proteínas exploradas não apenas são potenciais biomarcadores para esta condição, mas também abrem portas para intervenções farmacológicas que possam corrigir as mudanças fisiológicas observadas.

8. CONCLUSÃO

Observou-se que o modelo suíno é um modelo adequado para o estudo da infertilidade em masculina em humanos associado ao hipogonadismo secundário. A imunização antiGnRH alterou proteínas no fluído epididimário destacando aquelas associadas a ubiquitinização e proteínas que compõe os epididimossomas. Nos espermatozoides a alteração de proteínas mitocondriais indicam alterações bioquímicas que podem explicar a redução de fertilidade em pacientes acometidos com esta condição clínica, além disso podem predizer a qualidade da espermatogênese.

Assim, o compilado de estudos baseado no relatório proteômico por MudPIT apresenta claramente os impactos na cauda do epidídimo de suínos motivado pela imunização anti-GnRH. Os mecanismos de diferenciação em vesículas epididimais ainda não foram elucidados, porém a presente tese abre portas para a investigação desse microambiente. A validação de proteínas associadas a qualidade e fertilidade poderão ser utilizados em futuras aplicações biotecnológicas a fim de indicar um marcadores moleculares para fertilidade masculina associadas ao hipogonadismo secundário.

9. REFERÊNCIAS BIBLIOGRÁFICAS

AGARWAL, A.; MAKKER, K.; SHARMA, R. Clinical relevance of oxidative stress in male factor infertility: an update. **American journal of reproductive immunology**, v. 59, n. 1, p. 2-11, 2008.

ARRIGHI, S. Are the basal cells of the mammalian epididymis still an enigma? **Reproduction, fertility, and development,** v. 26, n. 8, p. 1061-71, Oct 2014

BAKER, M. A. Proteomics of post-translational modifications of mammalian spermatozoa. **Cell and tissue research,** v. 363, n. 1, p. 279-87, Jan 2016.

BASSOLS J, BONET S, BELGHAZI M, DACHEUX F, DACHEUX JL. Proteomic study of the establishment of boar epididymal cell cultures. **Theriogenology**, v. 68, n. 1, p. 76-86, 2007.

BASSOLS J., KADAR E., BRIZ M., PINART E., SANCHO S., GARCIA-GIL N., BADIA E., PRUNEDA A., BUSSALLEU E., YESTE M., CASAS I., BONET S. Migration of the cytoplasmic droplet in epididymal cultures of sus scrofa**. Reproduction Domestic Animal** 41(4):322, 2006(a).

BASSOLS J., KADAR E., BRIZ M., PINART E., SANCHO S., GARCIA-GIL N., BADIA E., PRUNEDA A., BUSSALLEU E., YESTE M., CASAS I., BONET S. Effect of culture conditions on the obtention of boar epididymal epithelial cell monolayers. **Reproduction Domestic Animal.** 95(3–4):262–272, 2006(b).

BELLEANNEE, C., BELGHAZI, M., LABAS, V., TEIXEIRA-GOMES, A. P., GATTI, J. L., DACHEUX, J. L., AND DACHEUX, F. Purification and identification of sperm surface proteins and changes during epididymal maturation. **Proteomics**, v. 11, n. 10, p. 1952-1964, 2011.

BELLEANNÉE, C.; THIMON, V.; SULLIVAN, R. Region-specific gene expression in the epididymis. Cell and tissue research, v. 349, n. 3, p. 717-731, 2012.

BHASIN, Shalender et al. Testosterone therapy in adult men with androgen deficiency syndromes: an endocrine society clinical practice guideline. **The Journal of Clinical Endocrinology & Metabolism**, v. 91, n. 6, p. 1995-2010, 2006.

BILIŃSKA, Barbara et al. Hormonal status of male reproductive system: androgens and estrogens in the testis and epididymis. In vivo and in vitro approaches. **Reprod. Biol.**, v. 6, n. Suppl. 1, p. 43-58, 2006.

BRIZ M, FRADERA A, BONET S, PINART E. Analysis of the seminal ‘characteristics of a boar with impaired fertility. **Scientia Gerundensis** 19:53–60, 1993.

BROWN, DENNIS; SMITH, P. J.; BRETON, SYLVIE. Role of V-ATPase-rich cells in acidification of the male reproductive tract. **Journal of Experimental Biology**, v. 200, n. 2, p. 257-262, 1997.

CABALLERO, I., PARRILLA, I., ALMIÑANA, C., DEL OLMO, D., ROCA, J., MARTÍNEZ, E. A., & VÁZQUEZ, J. M. Seminal plasma proteins as modulators of the sperm function and their application in sperm biotechnologies. **Reproduction in Domestic Animals**, v. 47, p. 12-21, 2012.

CHENG, C. Y.; MRUK, D. D. The blood-testis barrier and its implications for male contraception. **Pharmacological reviews,** v. 64, n. 1, p. 16-64, Jan 2012.

CLARKE, I. et al. Related food safety of a hormone (GnRH) vaccine synthetic gonadotropin releasing to control boar taint in entire male pigs. Intern. **Journal of Applied Research in Veterinary Medicine**, v. 6, p. 7-14, 2008.

COOPER, TG. Sperm maturation in the epididymis: a new look at an old problem. **Asian Journal of Andrology**, 9 (4): 533–539, 2007.

CORNWALL, Gail A. New insights into epididymal biology and function. **Human reproduction update**, v. 15, n. 2, p. 213-227, 2009.

COWAN, A. E.; MYLES, D. G. Biogenesis of surface domains during spermiogenesis in the guinea pig. **Developmental biology,** v. 155, n. 1, p. 124-33, Jan 1993.

DA ROS, V. G. et al. From the epididymis to the egg: participation of CRISP proteins in mammalian fertilization. **Asian journal of andrology**, v. 17, n. 5, p. 711, 2015.

DACHEUX JL, BELGHAZI M, LANSON Y, DACHEUX F. Human epididymal secretome and proteome. **Molecular and cellular endocrinology**, v. 250, n. 1-2, p. 36-42, 2006.

DACHEUX, J. L. et al. Epididymal cell secretory activities and the role of proteins in boar sperm maturation. **Theriogenology,** v. 63, n. 2, p. 319-41, Jan 15 2005.

DACHEUX, J. L. et al. The contribution of proteomics to understanding epididymal maturation of mammalian spermatozoa. **Systems biology in reproductive medicine,** v. 58, n. 4, p. 197-210, Aug 2012.

DACHEUX, J.L.; BELLEANNÉE, C.; JONES, R.; LABAS, V.; BELGHAZI, M.; GUYONNET, B.; DRUART, X.; GATTI, J.L.; DACHEUX, F. Mammalian epididymal proteome. **Molecular and Cellular Endocrinology**, v.306, p.45–50. 2009.

DACHEUX, J-L; GATTI, JL; DACHEUX, F. Contribution of epididymal secretory proteins for spermatozoa maturation. **Microscopy Research and Technique**, 61: 7–17, 2003.

DARBY, E.; ANAWALT, B. D. Male hypogonadism. **Treatments in endocrinology**, v. 4, n. 5, p. 293-309, 2005

DOHLE, G. R., ARVER, S., BETTOCCHI, C., JONES, T. H., KLIESCH, S., & PUNAB, M. Guidelines on male hypogonadism. European Association of Urology. 2015.

DUNSHEA, F. R. et al. Vaccination of boars with a GnRH vaccine (Improvac) eliminates boar taint and increases growth performance. **Journal of animal science,** v. 79, n. 10, p. 2524-35, Oct 2001.

EINARSSON, Stig et al. Effects of early vaccination with Improvac® on the development and function of reproductive organs of male pigs. **Animal reproduction science**, v. 127, n. 1, p. 50-55, 2011.

ENG, J., MCCORMACK, A. L. AND YATES III, J. R. 'An approach to correlate tandem mass spectral data of peptides with amino acid sequences in a protein database', **Journal of the American Society for Mass Spectrometry**, Vol. 5, pp. 976–989, 1994.

FRAIETTA, R.; ZYLBERSTEJN, D. S.; ESTEVES, S.C. Hypogonadotropic hypogonadism revisited. **Clinics**., v. 68, p. 81-8, 2013.

FRANÇA, L.R.; CARDOSO, F.M. Duration of spermatogenesis and sperm transit time through the epididymis in the Piau boar. **Tissue Cell**, v. 30, n. 5, p. 573-582, 1998.

GARTNER, L. P.; HIATT, J. L. Tratado de Histologia. Editora Guanabara Koogan S. A., Rio de Janeiro, 1999.

GATTI, J-L; CASTELLA, S; DACHEUX, F; ECROYD, H; MÉTAYER, S; THIMON, V; DACHEUX, J-L. Post-testicular sperm environment and fertility. **Animal Reproduction Science**, 82–83: 321–339, 2004.

GONZÁLEZ-CADAVID, Verónica et al. Seminal plasma proteins of adult boars and correlations with sperm parameters. **Theriogenology**, v. 82, n. 5, p. 697-707, 2014.

GRANDE, G. et al. Quantitative Analysis of the Seminal Plasma Proteome in Secondary Hypogonadism. Journal of Clinical Medicine, v. 8, n. 12, p. 2128, 2019.

GREGORY, M.; CYR, D. G. The blood-epididymis barrier and inflammation. **Spermatogenesis,** v. 4, n. 2, p. e979619, May-Aug 2014

HAMZEH, M; ROBAIRE, B. Effect of testosterone on epithelial cell proliferation in the regressed rat epididymis. **Journal of Andrology**, vol. 30, nº. 2, March/April, 2009.

HESS, R. A. et al. A role for oestrogens in the male reproductive system. **Nature**. v, 4, p. 509-12, 1997.

HINTON BT, GALDAMEZ MM, SUTHERLAND A, BOMGARDNER D, XU B, ABDEL-FATTAH R, YANG L. How do you get six meters of epididymis inside a human scrotum?. **Journal of andrology**, v. 32, n. 6, p. 558-564, 2011.

HINTON, B. T. Future of andrology. **Journal of andrology,** v. 21, n. 2, p. 339, Mar-Apr 2000.

HOLT W.V., VAN LOOK K.J.W. Concepts in sperm heterogeneity, sperm selection and sperm competition as biological foundations for laboratory tests of semen quality. **Reproduction** 127: 527–35, 2004.

HOTALING, J.; CARRELL, D. T. Clinical genetic testing for male factor infertility: current applications and future directions. **Andrology**, v. 2, n. 3, p. 339-350, 2014.

JODAR M, SOLER-VENTURA A, OLIVA R; Semen proteomics and male infertility. Journal of proteomics, v. 162, p. 125-134, 2017.

KATZ, D. J., NABULSI, O., TAL, R., AND MULHALL, J. P. Outcomes of clomiphene citrate treatment in young hypogonadal men. **BJU international**, v. 110, n. 4, p. 573-578, 2012.

KILLIAN, Gary J.; CHAPMAN, David A.; ROGOWSKI, Lee A. Fertility-associated proteins in Holstein bull seminal plasma. **Biology of reproduction**, v. 49, n. 6, p. 1202-1207, 1993.

MANN, Matthias; JENSEN, Ole N. Proteomic analysis of post-translational modifications. **Nature biotechnology**, v. 21, n. 3, p. 255-261, 2003.

MITAL, P.; HINTON, B. T.; DUFOUR, J. M. The blood-testis and blood-epididymis barriers are more than just their tight junctions. **Biology of reproduction,** v. 84, n. 5, p. 851-8, May 2011.

MOSTAFA, T. et al. Varicocelectomy reduces reactive oxygen species levels and increases antioxidant activity of seminal plasma from infertile men with varicocele. **International Journal of Andrology**, v. 24, n. 5, p. 261-265, 2001.

MOURA, A. A. et al. Proteínas do plasma seminal, funções espermáticas e marcadores moleculares da fertilidade. **Revista Brasileira de Reprodução Animal, Belo Horizonte**, v. 35, n. 2, p. 139-144, 2011.

MOURA, A. A.; SOUZA, C. E.; STANLEY, B. A.; CHAPMAN, D. A.; KILLIAN, G. J. Proteomics of cauda epididymal fluid from mature Holstein bulls. **J Proteomics**, v. 73, n. 10, p. 2006-2020, 2010.

NONOGAKI T., NODA Y., NARIMOTO K., SHIOTANI M., MORI T., MATSUDA T., YOSHIDA O. Localization of CuZn-superoxide dismutase in the human male genital organs. **Human Reproduction** 7:81–85, 1992.

PARK, Y. J., KWON, W. S., OH, S. A., PANG, M. G. Fertility-related proteomic profiling bull spermatozoa separated by percoll. **Journal of proteome research**, v. 11, n. 8, p. 4162-4168, 2012.

PENA, S., JR. et al. Oviduct binding ability of porcine spermatozoa develops in the epididymis and can be advanced by incubation with caudal fluid. **Theriogenology,** v. 83, n. 9, p. 1502-13, Jun 2015.

PEREZ-PATINO, Cristina et al. Characterization of the porcine seminal plasma proteome comparing ejaculate portions. Journal of proteomics, v. 142, p. 15-23, 2016.

PETAK S.M., NANKIN H.R., SPARK R.F., SWERDLOFF R.S., RODRIGUEZ-RIGAU L.J. American Association of Clinical Endocrinologists American Association of Clinical Endocrinologists Medical Guidelines for clinical practice for the evaluation and treatment of hypogonadism in adult male patients—2002 update. Endocr. Pract. 2002;8:440–456. [PubMed] [Google Scholar]

PRIMIANI, N; GREGORY, M; DUFRESNE, J; SMITH, CE; LIU, YL; BARTLES, JR; CYR, DG; HERMO, L. Microvillar Size and Espin Expression in Principal Cells of the Adult Rat Epididymis Are Regulated by Androgens. **Journal of Andrology**, vol. 28, nº. 5, September/October, 2007.

PRUNEDA, A.; YEUNG, C.H.; BONET, S.; PINART, E.; COOPER, T.G. Concentration of glutamate and myo-inositol in epididymal fluid and spermatozoa from boars. **Reproduction in Domestic Animals**, v.40, n.4, p.369. 2005.

ROBAIRE B, HINTON B. (2015) The Epididymis. In: Knobil and Neill's Physiology of Reproduction. (**A. Zeleznik and A. Plant eds.)** Ch. 17. Elsevier, New York, pp. 691-771, 2015.

ROBAIRE, B., & HENDERSON, N. A. Actions of 5α-reductase inhibitors on the epididymis. **Molecular and Cellular Endocrinology**, v. 250, n. 1-2, p. 190-195, 2006.

ROBAIRE, B.; HINTON, B.; ORGEBIN-CRIST, M.-C. (Ed.). **The Epididymis: From Molecules to Clinical Practice: From Molecules to Clinical Practice: a Comprehensive Survey of the Efferent Ducts, the Epididymis and the Vas Deferens.** Springer Science & Business Media, 2002.

ROBAIRE, B; HINTON, BT. The Epididymis: from molecules to clinical practice: a comprehensive survey of the efferent ducts, the epididymis, and the vas deferens. **Kluwer Academic/Plenum Publishers**, New York, 2002.

ROBAIRE, B; VIGER, RS. Regulation of epididymal epithelial cell functions. **Biology of Reproduction**, 52, 226-23, 1995.

ROBAIRE, R; HINTON, BT; ORGEBIN-CRIST, M-C. The epididymis. In: Knobil. **Knobil and Neill's physiology of reproduction**. Cambridge: Elsevier, p. 1071-1148, 2006.

RODRÍGUEZ-VILLAMIL, P. et al. Purification of binder of sperm protein 1 (BSP1) and its effects on bovine in vitro embryo development after fertilization with ejaculated and epididymal sperm. **Theriogenology**, v. 85, n. 3, p. 540-554, 2016.

SANCHO S, VILAGRAN I. The boar ejaculate: sperm function and seminal plasma analyses. In Boar reproduction. Eds Bonet S, Casas I, Holt WV, Yeste M. Springer: Berlin, Heidelberg, pp.471-516, 2013.

SCHORR-LENZ, A. M., ALVES, J., HENCKES, N. A., SEIBEL, P. M., BENHAM, A. M., BUSTAMANTE-FILHO, I. C.GnRH immunization alters the expression and distribution of protein disulfide isomerases in the epididymis. **Andrology**, v. 4, n. 5, p. 957-963, 2016.

SEILER P., COOPER T.G., YEUNG C.H., NIESCHLAG E. Regional variation in macrophage antigen expression by murine epididymal basal cells and their regulation by testicular factors. **Journal of Andrology** 20:738–746, 1999.

SENGER, P. L. Pathways to pregnancy and parturition. **Journal Reproduction Fertility,** v. 111, p. 183-1902, 2003.

SHARPE, R. Falling sperm counts in men – Is there an endocrine cause? **Journal of Endocrinology**, v. 137, p. 357-360, 1993

STRZEZEK, J. et al. Proteomics of boar seminal plasma–current studies and possibility of their application in biotechnology of animal reproduction. **Reprod Biol**, v. 5, n. 3, p. 279-290, 2005.

SULLIVAN, R. Male fertility markers, myth or reality. **Animal reproduction science**, v. 82, p. 341-347, 2004.

SULLIVAN, R; SAEZ, F; GIROUARD, J; FRENETTE, G. Role of exosomes in sperm maturation during the transit along the male reproductive tract. **Blood Cells, Molecules, and Diseases**, 35: 1 – 10, 2005.

SULLIVAN, Robert; MIEUSSET, Roger. The human epididymis: its function in sperm maturation. **Human reproduction update**, v. 22, n. 5, p. 574-587, 2016.

SYNTIN P., DACHEUX J., DACHEUX F. Postnatal development and regulation of proteins secreted in the boar epididymis. **Biology of reproduction**, v. 61, n. 6, p. 1622-1635, 1999.

SYNTIN, P., DACHEUX, F., DRUART, X., GATTI, J. L., OKAMURA, N., & DACHEUX, J. L. Characterization and identification of proteins secreted in the various regions of the adult boar epididymis. **Biology of reproduction**, v. 55, n. 5, p. 956-974, 1996.

TOSHIMORI, K. Maturation of mammalian spermatozoa: modifications of the acrosome and plasma membrane leading to fertilization. **Cell and Tissue Research**, 293: 177-187, 1998.

TURNER T.T., BOMGARDNER D., JACOBS J.P., NGUYEN Q.A. Association of segmentation of the epididymal interstitium with segmented tubule function in rats and mice. **REPRODUCTION-CAMBRIDGE-**, v. 125, n. 6, p. 871-878, 2003..

TURNER TT, JOHNSTON DS, FINGER JN, JELINSKY SA.Differential gene expression among the proximal segments of the rat epididymis is lost after efferent duct ligation. **Biology of reproduction**, v. 77, n. 1, p. 165-171, 2007a.

TURNER TT, JOHNSTON DS, JELINSKY SA, TOMSIG JL, FINGER JN. Segment boundaries of the adult rat epididymis limit interstitial signaling by potential paracrine factors and segments lose differential gene expression after efferent duct ligation. **Asian journal of andrology**, v. 9, n. 4, p. 565-573, 2007b.

VERI J.P., HERMO L., ROBAIRE B. Immunocytochemical localization of the Yf subunit of glutathione S-transferase P shows regional variation in the staining of epithelial cells of the testis, efferent ducts, and epididymis of the male rat. **Journal of Andrology** 14:23–44, 1993.

WASHBURN, M. P., WOLTERS, D. AND YATES III, J. R. (), 'Large-scale analysis of the yeast proteome by multidimensional protein identification technology', **Nature Biotechnology**., Vol. 19, pp. 242–247, 2001.

WEBER, A., ALVES, J., ABUJAMRA, A. L., AND BUSTAMANTE-FILHO, I. C. (2018). Structural modeling and mRNA expression of epididymal β-defensins in GnRH immunized boars: A model for secondary hypogonadism in man. **Molecular reproduction and development**, v. 85, n. 12, p. 921-933, 2018.

WEBER, A., ARGENTI, L. E., DE SOUZA, A. P. B., SANTI, L., BEYS-DA-SILVA, W. O., YATES, J. R., AND BUSTAMANTE-FILHO, I. C. (2020). Ready for the journey: A comparative proteome profiling of porcine cauda epididymal fluid and spermatozoa. **Cell and Tissue Research**, v. 379, n. 2, p. 389-405, 2020.

WILKINS, Marc R. et al. Progress with proteome projects: why all proteins expressed by a genome should be identified and how to do it. **Biotechnology and genetic engineering reviews**, v. 13, n. 1, p. 19-50, 1996. ANDERSON, N. Leigh et al. The effects of peroxisome proliferators on protein abundances in mouse liver. **Toxicology and applied pharmacology**, v. 137, n. 1, p. 75-89, 1996.

WOLTERS, D. A., WASHBURN, M. P. AND YATES III, J. R. ‘An automated multidimensional protein identification technology for shotgun proteomics’, **Analytical Chemistry** Vol. 73, pp. 5683–5690, 2001.

YESTE, M.; SANCHO, S.; BRIZ, M.; PINART, E.; BUSSALLEU, E.; BONET, S. Diet supplemented with L-carnitine improves the sperm quality of Piétrain but not of Duroc and Large White boars when photoperiod and temperature increase. **Theriogenology**, v.73, p.577-86. 2010.

YEUNG C.H., NASHAN D., SORG C., OBERPENNING F., SCHULZE H., NIESCHLAG E., COOPER T.G. Basal cells of the human epididymis-antigenic and ultrastructural similarities to tissue-fixed macrophages. **Biology of Reproduction,** 50:917–926, 1994.

YOSHINAGA, K., & TOSHIMORI, K. Organização e modificações das moléculas acrossomais dos espermatozoides durante a espermatogênese e a maturação epididimal. **Pesquisa e técnica microscópica** , v. 61, n. 1, pág. 39-45, 2003.

ZAMARATSKAIA, G., ANDERSSON, H. K., CHEN, G., ANDERSSON, K., MADEJ, A., AND LUNDSTROM, K.Effect of a Gonadotropin-releasing Hormone Vaccine (ImprovacTM) on Steroid Hormones, Boar Taint Compounds and Performance in Entire Male Pigs. **Reproduction in Domestic Animals**, v. 43, n. 3, p. 351-359, 2008.

ZHOU, W., DE IULIIS, G. N., DUN, M. D., & NIXON, B. Characteristics of the epididymal luminal environment responsible for sperm maturation and storage. **Frontiers in endocrinology**, v. 9, p. 59, 2018.

ZIRKIN, B. R. Spermatogenesis: its regulation by testosterone and FSH. **Seminars in cell & developmental biology** , v. 9, n. 4, p. 417-421, 1998.

ZOETIS. Informações de bula - Vivax ®. 2015. Disponível em: <http://www.improvac.com/br/informa%C3%A7%C3%B5es-de-bula.aspx>.